



Fiber-Optic Communications

Pierre Lecoy

ISTE

 **WILEY**

This page intentionally left blank

Fiber-Optic Communications

This page intentionally left blank

Fiber-Optic Communications

Pierre Lecoy

ISTE

 WILEY

Published in France in 2007 by Hermes Science/Lavoisier entitled "Télécoms sur fibres optiques"
(3^e Éd. revue et augmentée)

First published in Great Britain and the United States in 2008 by ISTE Ltd and John Wiley & Sons, Inc.

Apart from any fair dealing for the purposes of research or private study, or criticism or review, as permitted under the Copyright, Designs and Patents Act 1988, this publication may only be reproduced, stored or transmitted, in any form or by any means, with the prior permission in writing of the publishers, or in the case of reprographic reproduction in accordance with the terms and licenses issued by the CLA. Enquiries concerning reproduction outside these terms should be sent to the publishers at the undermentioned address:

ISTE Ltd
27-37 St George's Road
London SW19 4EU
UK

www.iste.co.uk

John Wiley & Sons, Inc.
111 River Street
Hoboken, NJ 07030
USA

www.wiley.com

© ISTE Ltd, 2008

© LAVOISIER, 2007

© Hermes Science, 1992, 1997

The rights of Pierre Lecoy to be identified as the author of this work have been asserted by him in accordance with the Copyright, Designs and Patents Act 1988.

Library of Congress Cataloging-in-Publication Data

Lecoy, Pierre.

[Télécoms sur fibres optiques. English]

Fiber-optic communications / Pierre Lecoy.

p. cm.

Includes bibliographical references and index.

ISBN 978-1-84821-049-3

1. Optical fiber communication. I. Title.

TK5103.592.F52L4313 2008

621.382'75--dc22

2008019705

British Library Cataloguing-in-Publication Data

A CIP record for this book is available from the British Library

ISBN: 978-1-84821-049-3

Printed and bound in Great Britain by Antony Rowe Ltd, Chippenham, Wiltshire.



Mixed Sources
Product group from well-managed
forests and other controlled sources

Cert no. SGS-COC-2953
www.fsc.org
© 1996 Forest Stewardship Council

To Jean-Pierre NOBLANC, who was first my professor, then my colleague at Ecole Centrale Paris and my lab Director at France Telecom, who conveyed his passion for optical fibers and optoelectronics.

This page intentionally left blank

Table of Contents

Foreword.	xvii
Introduction.	xxi
Chapter 1. Multimode Optical Fibers.	1
1.1. Overview of optics	1
1.1.1. Introduction	1
1.1.2. Propagation of harmonic plane waves.	1
1.1.3. Light rays	3
1.1.4. Dielectric diopter	4
1.1.5. Reflection of a plane wave on a diopter.	6
1.1.6. Reflection coefficient	7
1.1.7. Total reflection	8
1.2. Dielectric waveguide	10
1.2.1. Planar dielectric waveguide model.	10
1.2.2. Notion of propagation modes.	11
1.2.3. Case of the asymmetric guide.	13
1.2.4. Dispersion	14
1.3. Multimode optical fibers	15
1.3.1. Definition	15
1.3.2. Multimode step-index fiber	15
1.3.3. Multimode graded-index fiber	17
1.4. Propagation in multimode optical fibers	18
1.4.1. Ray paths.	18
1.4.2. Propagation equation resolution	19
1.4.3. Different ray types	20
1.4.3.1. Meridional rays	20
1.4.3.2. Skew rays	21
1.4.4. Modes of propagation	22

1.5. Dispersion in multimode optical fibers	23
1.5.1. Intermodal dispersion	23
1.5.2. Pulse broadening calculation	23
1.5.2.1. In step-index fibers	23
1.5.2.2. In graded-index fibers	25
1.5.3. Chromatic dispersion.	26
1.5.4. Time-domain response of multimode fibers	27
1.5.5. Multimode fiber bandwidth	28
1.5.6. Mode coupling	29
1.5.7. Modal noise	31
1.6. Appendix: detail of calculation in section 1.4.2	31
Chapter 2. Single-Mode Optical Fibers.	33
2.1. Fiber optic field calculation	33
2.1.1. Electromagnetic equations	33
2.1.2. Solution for step-index fiber optics	35
2.1.2.1. General form	35
2.1.2.2. Transverse components	35
2.1.3. Mode calculation method	36
2.1.4. Nature of modes.	37
2.1.4.1. Transverse modes.	37
2.1.4.2. Hybrid modes	37
2.1.5. Cut-off frequency.	38
2.1.6. Aspect of modes	40
2.2. Single-mode fiber characteristics	42
2.2.1. Single-mode propagation condition	42
2.2.2. Gaussian single-mode fiber model.	42
2.2.3. Single-mode fiber parameters.	44
2.3. Dispersion in single-mode fibers	44
2.3.1. Chromatic dispersion.	44
2.3.2. Practical calculation	46
2.3.3. Cancellation of chromatic dispersion	47
2.3.4. Depressed inner cladding fibers	48
2.3.5. Different types of single-mode fibers	49
2.3.5.1. Standard fiber	49
2.3.5.2. Dispersion shifted fiber	50
2.3.5.3. Non-zero dispersion shifted fiber	50
2.3.6. Chromatic dispersion compensation.	51
2.4. Polarization effects in single-mode fibers	51
2.4.1. Birefringence of optical fibers	51
2.4.2. Induced birefringence	52
2.4.3. Polarization dispersion.	53
2.5. Non-linear effects in optical fibers	54

2.5.1. Introduction	54
2.5.2. Raman scattering	55
2.5.3. Brillouin scattering	56
2.5.4. Kerr effect	57
2.5.5. Consequences of the Kerr effect	58
2.5.6. Soliton propagation.	59
2.5.6.1. Description.	59
2.5.6.2. Soliton equation.	59
2.5.6.3. Soliton transmission systems	60
2.6. Microstructured (photonic) optical fibers	61
2.6.1. Introduction	61
2.6.2. Photonic bandgap	63
2.6.3. Photonic waveguides.	64
2.6.4. Photonic crystal fibers	65
2.6.5. Hollow fibers	66
Chapter 3. Fiber Optics Technology and Implementation	69
3.1. Optical fiber materials and attenuation.	69
3.1.1. Different types of optical fibers	69
3.1.2. Intrinsic attenuation of silica fibers	69
3.1.3. Plastic fibers	72
3.1.4. Other materials	73
3.1.5. Transmission windows.	74
3.2. Manufacturing of optical fibers	76
3.2.1. Principles.	76
3.2.2. Manufacturing of preforms by MCVD process	77
3.2.3. Preform manufacturing by external deposit	78
3.2.4. Drawing	79
3.2.5. Mechanical resistance	80
3.3. Optical fiber cables and connections	81
3.3.1. Principle of optical fiber cables.	81
3.3.2. Different cable types	81
3.3.2.1. Tight structure cables	81
3.3.2.2. Free structure cables	82
3.3.2.3. Compact structure cables	83
3.3.2.4. Aerial cables.	83
3.3.2.5. Submarine cables	83
3.3.3. Connection of optical fibers.	84
3.3.4. Optical connectors	85
3.3.4.1. Description.	85
3.3.4.2. Anti-reflection connectors.	86
3.3.4.3. Different connector types	87
3.4. Extrinsic fiber optic losses	88

3.4.1. Losses by bending	88
3.4.2. Losses at connections	89
3.4.2.1. Causes of losses	89
3.4.2.2. Calculation in multimode fibers	90
3.4.2.3. Calculation in single-mode fibers	91
3.4.3. Fiber optics optimization	91
3.5. Optical fiber measurements	93
3.5.1. Classification	93
3.5.2. Geometric measurements for multimode fibers	93
3.5.3. Measurements of single-mode fibers parameters	94
3.5.4. Spectral attenuation measurement	94
3.5.5. Reflectometry measurement	95
3.5.5.1. Principle	95
3.5.5.2. Power received	96
3.5.5.3. Reflectometry curve interpretation.	97
3.5.5.4. Dynamics	98
3.5.6. Bandwidth measurement	99
3.5.7. Chromatic dispersion measurement	100
3.5.8. Polarization measurements	101
Chapter 4. Integrated Optics	103
4.1. Principles	103
4.1.1. Introduction: classification of components	103
4.1.2. Technologies used	103
4.1.3. Integrated optics planar guides	105
4.1.4. Lateral guiding	105
4.1.5. Losses in guides.	107
4.2. Mode coupling and its applications.	107
4.2.1. Formalization	108
4.2.2. Coupling within a single guide	108
4.2.3. Coupling between matched guides.	110
4.2.4. Coupling between mismatched guides	111
4.3. Diffraction gratings	112
4.3.1. Principle	112
4.3.2. Operation.	113
4.3.3. Application to light coupling in a guide.	114
4.3.4. Bragg grating principle	116
4.3.5. Bragg gratings in integrated optics.	116
4.3.6. Photo-inscribed Bragg gratings in optical fibers.	118
4.3.6.1. Principle	118
4.3.6.2. Bragg grating filters	118
4.3.6.3. Chirped Bragg gratings	119

Chapter 5. Optical Components	121
5.1. Passive non-selective optical components	121
5.1.1. Definitions	121
5.1.2. Optical couplers	122
5.1.3. Isolators and circulators	124
5.1.4. Optical attenuators	125
5.2. Wavelength division multiplexers	125
5.2.1. Different types of wavelength division multiplexing	125
5.2.2. Filter multiplexers	126
5.2.3. Coupler-type multiplexers	127
5.2.4. Dense wavelength division multiplexing	127
5.2.5. Add-drop multiplexing	129
5.3. Active optical components	129
5.3.1. Principles	129
5.3.2. Electro-optic effect	130
5.3.3. Directional electro-optic coupler	131
5.3.4. Electro-optic modulator	133
5.3.5. Electro-absorption modulator	134
5.4. Fiber optic switches	135
5.4.1. Functions	135
5.4.2. Switching technologies	136
5.4.3. Example of micro electro-mechanical switching matrices	137
5.4.4. Reconfigurable optical add-drop multiplexers (ROADM)	139
Chapter 6. Optoelectronic Transmitters	141
6.1. Principles of optoelectronic components	141
6.1.1. Electroluminescence principle	141
6.1.2. Electroluminescent material	143
6.1.3. Photodetection principle	145
6.1.4. Heterojunction use	146
6.1.5. Quantum well structures	147
6.1.6. Optical amplification principles	148
6.2. Light-emitting diodes (LED)	150
6.2.1. Structure	150
6.2.2. Main light emitting diode characteristics	151
6.2.3. Light-emitting diode transmitters	152
6.2.4. Other types of light emitting diodes	152
6.3. Laser diodes	152
6.3.1. Principle	152
6.3.2. Fabry-Pérot structure laser diodes	154
6.3.3. DFB laser diodes	155
6.3.4. Lateral guiding in laser diodes	156
6.3.5. Wavelength-tunable laser diodes	157

6.3.6. Vertical cavity surface emitting lasers (VCSEL)	159
6.4. Optical transmitter interface	160
6.4.1. Description.	160
6.4.2. Laser diode characteristic	160
6.4.3. Laser diode modulation	161
6.4.4. Transmitter noise	162
6.4.5. Laser diode emission module	163
6.4.5.1. Control	163
6.4.5.2. Mounting in the optical head	163
6.5. Comparison between optoelectronic emitters	165
Chapter 7. Optoelectronic Receivers	167
7.1. Photodetectors	167
7.1.1. PIN photodiode	167
7.1.2. Photodiode characteristics.	168
7.1.3. Avalanche photodiode	169
7.1.4. Materials used in photodetection.	171
7.1.5. Phototransistor	173
7.2. Optical receiving interface	174
7.2.1. Structure	174
7.2.2. Photodiode noise	175
7.2.2.1. In PIN photodiodes.	175
7.2.2.2. In avalanche photodiodes	175
7.2.3. Optical receiver modeling.	176
7.2.4. Noise current calculation	177
7.2.5. Calculation of the signal-to-noise ratio	179
7.2.6. Optimization of the signal-to-noise ratio	180
7.3. Other photodetection schemas.	182
7.3.1. Heterodyne detection.	182
7.3.2. Balanced detection	183
Chapter 8. Optical Amplification	185
8.1. Optical amplification in doped fiber	185
8.1.1. Introduction	185
8.1.2. Optical amplification principle in erbium-doped fibers	186
8.1.3. Optical amplification gain.	187
8.1.4. Amplified signal power	188
8.1.5. Optical amplification noise	190
8.2. Erbium-doped fiber amplifiers	191
8.2.1. Description.	191
8.2.2. Characteristics.	192
8.2.3. Gain parameters of an optical amplifier.	193

8.2.4. Amplified bandwidth	194
8.2.5. Noise figure	195
8.3. Noise calculation in amplified links	195
8.3.1. Input noise in the presence of an optical amplifier	195
8.3.2. Case of an optical preamplifier receiver	197
8.3.3. Noise calculation over long links	198
8.4. Other types of optical amplifiers	199
8.4.1. Semiconductor optical amplifiers (SCOA)	199
8.4.2. Other SCOA applications	200
8.4.3. Amplifier comparison	201
8.4.4. Raman amplification	201
Chapter 9. Fiber-Optic Transmission Systems	203
9.1. Structure of a fiber-optic digital link	203
9.1.1. Different systems	203
9.1.2. Long-haul links over optical fibers	204
9.1.3. Line terminals	205
9.1.4. Line codes	206
9.1.5. Coherent optical transmissions	207
9.2. Digital link design	209
9.2.1. Filtering	209
9.2.2. Choice of fiber bandwidth	209
9.2.3. Calculation of the error probability	210
9.2.4. Calculation of the average power required in reception	212
9.2.5. Quantum limit	213
9.2.6. Loss budget	214
9.3. Digital link categories	215
9.3.1. Point-to-point, non-amplified lines	215
9.3.2. Optically amplified links	217
9.3.3. Wavelength division multiplexed links	218
9.3.4. Dispersion effects	219
9.3.5. New modulation formats	221
9.3.5.1. Duobinary modulations	221
9.3.5.2. Phase modulations	222
9.3.6. Fiber-optic submarine links	223
9.4. Fiber-optic analog transmissions	225
9.4.1. Analog baseband transmission	225
9.4.1.1. Principle	225
9.4.1.2. Link calculation	226
9.4.2. Transmission by frequency modulation of a sub-carrier	227
9.4.3. Transmission of measurement signals	227

9.5 Microwave over fiber optics links	228
9.5.1. Principle and applications	228
9.5.2. Different processes	229
9.5.3. Single-side band transmission	230
Chapter 10. Fiber-Optic Networks	233
10.1. Computer networks	233
10.1.1. Introduction	233
10.1.2. Passive optical networks	234
10.1.3. Design of a passive network	235
10.1.4. Ethernet local area networks	236
10.1.4.1. Introduction to Ethernet	236
10.1.4.2. Fiber optic Ethernet	237
10.1.4.3. Ethernet architectures	237
10.1.5. FDDI network	239
10.1.6. Fiber Channel	240
10.2. Access networks	242
10.2.1. Overview	242
10.2.2. Different FTTx architectures	243
10.2.3. Passive optical networks (PON)	245
10.2.4. PON operation	246
10.3. Wide area networks	247
10.3.1. SDH/SONET hierarchy systems	247
10.3.2. Constitution of synchronous digital hierarchy frames	249
10.3.3. SDH rings	251
10.3.4. Optical cross-connect	252
10.3.5. Optical transport network (OTN)	253
10.3.6. The optical OTN layer	255
10.4. Toward all optical networks	256
10.4.1. Wavelength division multiplexed networks	256
10.4.2. Wavelength routing	256
10.4.3. All optical network architectures	258
10.4.4. MPLS protocols	259
10.4.5. Trends	261
Chapter 11. Fiber-Optic Sensors and Instrumentation	263
11.1. Fiber optics in instrumentation	263
11.1.1. Introduction	263
11.1.2. Use of fiber optics in instrumentation	264
11.1.3. Fiber-optic measurement instrumentation	264
11.1.4. Fiber-optic sensor classification	266
11.2. Non-coherent fiber-optic sensors	266
11.2.1. Geometric and mechanical size sensors	266

11.2.2. Bending or micro-bending sensors	268
11.2.3. Temperature extrinsic sensors.	268
11.2.4. Intrinsic non-coherent sensors.	269
11.3. Interferometric sensors	270
11.3.1. Overview	270
11.3.2. Two arm interferometers.	270
11.3.2.1. Mach-Zehnder interferometer.	270
11.3.2.2. Michelson interferometer	271
11.3.3. Intermodal interferometry	272
11.3.4. One fiber interferometers	273
11.3.4.1. Fabry-Pérot interferometer	273
11.3.4.2. Bragg grating sensor	273
11.3.5. Ring (or Sagnac) interferometers	274
11.3.5.1. Optical fiber gyroscope	274
11.3.5.2. Fiber-optic current sensor	275
11.3.6. Polarimetric sensors	275
11.4. Fiber optic sensor networks	276
11.4.1. Distributed sensors	276
11.4.2. Time-division multiplexing	277
11.4.3. Wavelength division multiplexing	278
11.4.4. Coherence multiplexing	278
Exercises	281
Bibliography	325
Index	329

This page intentionally left blank

Foreword

At home, the quadruple play: digital television, radio, high speed Internet, landline and cell phones ... At work, multiple and diverse computer applications combining voice, data and images ... We conduct our business as if it is completely natural to exchange and receive all this information, but how does this transmission of information happen? This is what Pierre Lecoy, author of this book, skillfully and clearly explains, and reminds us of all the levels of creativity, mathematical calculations and technical magic that had to happen in order for a simple fiber glass cable, the optical fiber to be able to transport digital information at speeds that today exceed a dozen terabits per second or 10,000 billion bits per second on a single fiber!

Pierre offers his experience in the field of fiber optics telecommunications based on his double expertise acquired, on the one hand, within large manufacturing groups and, on the other hand, as a professor instructing generations of engineers. The combination of these two qualities is not exceptional because engineers frequently teach, but in essence, it is this combination which makes this book so interesting, especially as Pierre illustrates the importance of developing theoretical knowledge based on the development of applications and concrete accomplishments.

You will discover the professional competence of an industrialist as Pierre demonstrates a rich experience of several years in this field. He alternatively presents all the elements inherent to fiber-optic connections by focusing on the applications, their constraints and especially on choice criteria for solutions offered by technologies available on the market. Without going into too much detail, I will cite such examples as soliton propagation, micro-structured fiber optics, the principle of fiber bragg gratings in fibers, etc.

Pierre uses his competence as a professor and takes advantage of it by explaining the equations and different laws governing these fields in good company with Bessel, Laplace, Maxwell, Rayleigh and others (Fabry or Pérot). This is where Pierre's experience comes in handy: when he describes and breaks down light propagation mechanisms through fibers and the different components of networks. The reader will thus learn or rediscover the different dispersions in an optical fiber, the calculation of pulse widening as well as non-linear effect processing such as Raman scattering, Brillouin scattering and the Kerr effect. Pierre also presents the principles controlling the production of fiber optics, the different types of cables, connections and associated measurements. In addition, he explains the different wavelength division multiplexing, modulation, switching technologies and so much more.

This is why I strongly invite you to delve into this book, the fruit of patient research and compilation work of all you can find on fiber optics. I greatly recommend it as, even though this book is rigorously scientific, it is an easy read. This book is certainly very meticulous but it is also practical with concrete examples, making it easy to understand.

In this way, the novice reader will be able to follow each chapter, reading about the construction of fiber-optic connections and understand all about multimode fibers, single-mode fibers, the different types of cables, optical components, optoelectronic transmitters and receivers, optical amplification, analog and digital transmissions over fiber optics, the different types of optics – from local area to operator – with an eye on the optical future, and finally, a complete chapter is dedicated to fiber optics in instrumentation as well as optical fiber sensors.

As for you, informed reader, the structure of this book in clearly delimited chapters will enable you to go directly to the heart of the subject most interesting to you.

Lastly, Pierre puts his professor hat back on and his long teaching practice by proposing 35 exercises, thankfully with their answers! A bibliography and website addresses successfully complete this project.

What more is there to say to you, dear reader, except maybe to insist on the triple application of fiber-optic telecommunications: at home, at work and in social relations. Currently at home there are over 25 million subscribers worldwide using fiber optics providing them with 100 Mbit/s and already in Japan, several thousand users can use throughputs of 1 Gbit/s enabling them to simultaneously receive several high definition television channels while having access to hyper-realistic online video. At work, high throughput digital data, combined with video telephony, ensure rapid circulation of large volumes of data, their storage and their query in relational database management systems simultaneously. As for the social aspect,

much interest is based on the development of e-government, e-training, e-medicine and other type relations. Another significant advantage of these social evolutions resulting from fiber-optic telecommunications involves environmental protection by greatly decreasing the movement of people.

That is why I thank Pierre on your behalf for this body of work that he has successfully achieved in order to offer you these very interesting pages. Through his analysis, the fruit of deep thought processes sourced from his professional and diversified life, Pierre has shared his knowledge in this field with us. Finally, while remaining prudent and realistic, this book is part of the future with the evolution of SDH/Sonet networks toward all optical transport networks (OTN – *Optical Transport Network*) including a new optical layer, wavelength routing and multi-protocol label switching (MPLS) for packet transmission. As former director of training at Tyco Electronics and as current honorary president of Club optique, I can only applaud this methodology. Tomorrow is happening today.

Jean-Michel Mur
Honorary President of Club optique

This page intentionally left blank

Introduction

Overview

Although the first optical information transmission experiments date back to late in the 19th century, a way has to be found to correctly direct or guide the light before thinking of its application to telecommunications. The emergence of *lasers*, around 1960, led to transmission experiments in the atmosphere. However, propagation instability problems (mainly caused by air index variations) have led researchers to abandon this solution. It is now reserved for short distance communications (infrared remote control, indoor communications, infrared laser link between two buildings), even though it is now being considered again for direct links between satellites.

Optical fibers are very thin angel hair type transparent glass and use the well-known principle of fountains of light. They were used in decorative applications before being used in a more useful way (lighting, endoscopy, remote optical measures). Their application in the field of telecommunications, although considered by theoreticians (Charles Kao) as soon as 1966, was made possible in the 1970s because of the progress in silica fiber-optic production technology, allowing a very light attenuation and an adequate mechanical resistance. It was also enabled by the availability of semiconductor laser diodes, which combine laser performance with electronic component ease of use, in particular because of the progress of III-V compound semiconductors. The development of efficient cables, connectors and passive components, and the availability of industrial connection processes, have also been essential for the development of the first commercial links around 1980.

The 1990s were significant in the development of optical amplification followed by wavelength division multiplexing, leading to an explosion of capabilities in response to new requirements caused by the growth of the Internet. The next revolution should be all-optical networks. Inaugurated by the emergence of the first

all-optical switches in 2000, they were only prototypes and this concept remains to be clarified, particularly with standardization of protocols.

With approximately 100 million kilometers produced each year, and despite production activity fluctuations in this field which shows a strongly cyclic characteristic, optical fibers have become a mature technology present in increasingly wide application fields.

Fiber optics advantages

Transmission performance

Very low attenuation, very large bandwidth, possible multiplexing (in wavelength) of numerous signals and users on the same fiber, provide much higher range (over 100 km between transmitter and receiver) and capacity (bitrates of several Tbit/s are possible over a single fiber) systems than with copper wires or radio. However, depending on the considered use, other advantages can be decisive.

Implementation advantages

Including the light weight, very small size, high fiber flexibility, noticeable in telecommunications as well as for cabling in aeronautics, information technology, medicine, manufacturing, home automation, etc.

The most important practical advantage remains electrical (total insulation between terminals, possible use in explosive atmosphere, under high pressure, in medical applications) and electromagnetic safety (the fiber is not sensitive to parasites and does not create them either).

Conversely, the optical power used is weak and not dangerous. We can add total (or almost) invulnerability: it is not possible to hear the signal on an optical fiber without being spotted.

Economic advantage

Contrary to common belief, the global fiber-optic system cost (taking its installation and necessary equipment into account) is, in many cases, lower than the cost of a copper wire system (in particular with the recent increase in the price of copper), and its implementation, notably concerning connections, has become much easier and cheaper than with the first applications.

Fields of use

The main field of use is obviously telecommunications, but fiber optics easily overflow this field and work with a large number of manufacturing applications.

Telecommunications

The two main fields of use, related to network needs, have been urban links, with large capabilities and working without intermediate amplification or remote power-feeding, and submarine links such as trans-oceanic links, or coastal links without repeaters (exceeding 200 km, and over 300 km with optical amplification in terminals). Then, stimulated by the arrival of new operators, regional, national and international terrestrial connections have seen a very strong growth. They are at the base of the ATM network infrastructure.

In the early days of fiber optics, several experiments were carried out in the field of access networks for video communications and broadband service users. Direct fiber optics access or FTTH (fiber to the home) did not spread as expected in the 1980s because of economic constraints and the increase of possible throughputs with twisted pairs (available through ADSL). Intermediate solutions were then developed where the fiber was relayed, at the front end, by existing cables or radio contact. However, the need for increasingly high throughputs has reenergized this market; this movement started in Japan and Sweden and has spread to now represent a large part of the activity for manufacturers, operators and regulation authorities.

Data networks and links

Even for short distances, the use of fiber optics in the information technology field has rapidly progressed, particularly for electric insulation and insensitivity to electromagnetic disruptions. Fiber optics also enable development of multi-terminal networks and high bitrate networks, such as Fiber Channel or 1 Gbit/s (and now up to 10 Gbit/s) Ethernet, were designed for fiber optics from the start. Networks now reach “metropolitan” sizes and work together with railway networks or electricity transport without technical problems.

Industrial systems

There are various applications (telemetry, remote controls, video monitoring, field bus) where fiber insensitivity to parasites and its insulating character are essential advantages.

The massive parallelism of electronic and information technology architectures, the constant increase of frequencies on buses and the resulting electromagnetic accounting problems influence the increasing use of optical support (fibers or planar guides) to interconnect the different computer or embedded system cards (“optical backplane” concept), followed by the different chips from multiprocessor architecture, and even the different parts of a single chip in the future, in a SoC (system on chip) design.

Instrumentation and sensors

Fibers are more and more present in optical instrumentation, where they make it possible to carry out remote measurements in hard to access points. *Sensors* use fiber optics as a sensitive element and transmission support. However, their use remains limited, especially when material integration or total electromagnetic immunity is required. These applications are discussed in Chapter 11.

Finally, optical fibers still play a role in light transportation. Traditional applications (lighting, visualization, endoscopy) or more recent applications (laser beam transportation for industry, measurement, medicine) have seen their performance improve, and their cost decrease, thanks to the development of fiber-optic technologies.

Elements of a fiber-optic transmission system

Interfaces

In a point-to-point link as well as in a network, we find (see Figure 1):

- the optical transmitter interface which transforms the electric signal into optical signal. It mainly includes the optoelectronic transmission component, which can be a light-emitting diode (LED) or a laser diode (LD), components studied in Chapter 6. The interface also contains adaptation and protection circuits; it is connected to the cable by a connector or by an optical fiber pigtail that needs to be connected. Modulation is generally a light intensity modulation obtained by modulation of current going through the transmission diode or, at a very high bitrate, by an external modulation;
- the optical receiver interface containing a photodiode which converts the received optical signal into an electric signal. It is followed by a head amplifier, which must be carefully designed as its noise is generally the one limiting the minimum optical power that can be detected, and thus the range of the system (see

Chapter 7). According to the application, we then find filtering or digital reshaping circuits.

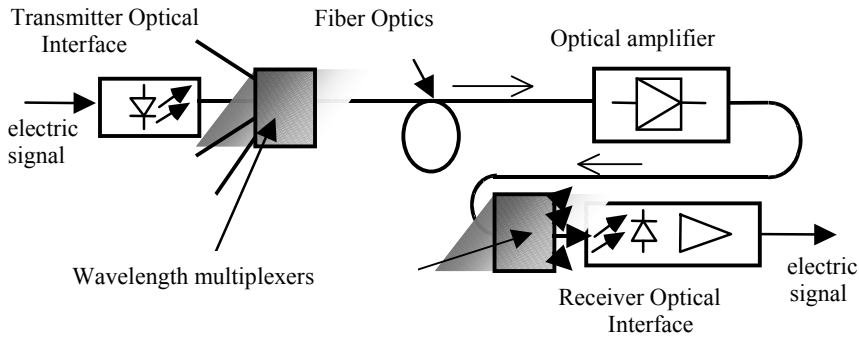


Figure 1. *Point-to-point fiber-optic link*

Repeaters

When the link length requires it, one or several *repeaters* are inserted. Ancient link repeaters (installed prior to 1995) contained receiving and transmission interfaces, linked by amplification and regeneration circuits for digital transmissions, leading to signal interruption. Nowadays, terrestrial and submarine links use erbium-doped fiber amplifiers (see Chapter 8), and are entirely optical over distances exceeding 10,000 km.

Wavelength division multiplexing

Wavelength division multiplexing (WDM) enables the multiplexing of several signals in the same fiber-optic, even if they are from geographically different origins or in opposite direction. If wavelengths are close, they can be amplified by the same optical amplifier.

This was first used in local area networks or user links, as well as in sensor networks. It now increases even already installed optical cable capabilities significantly.

Dozens, and even hundreds of Gbit/s per fiber are reached in commercial links. Achieved in the laboratory ten years ago, the Tbit/s (10^{12} bit/s!) now corresponds to

long distance infrastructure requirements; the last laboratory benchmarks have exceeded 10 Tbit/s and the theoretical limit has not yet been reached.

Fiber-optic networks

All optical networks can be developed which are not simple point-to-point links combinations interconnected by electric nodes. Optical network nodes can be passive (splitters, multi-branch couplers, wavelength division multiplexers) or active (switches, time-division multiplexers) components using integrated optics or micro-technologies (MEMS).

The development of large scale optical switching is one of the major issues today. In fact, the speed of optical transmissions is such that the bottleneck is now located in the network node electronics. However, specific architectures and protocols for optical routing must be developed.

Transmitted signals

The vast majority of applications (telecommunications, information technology) consist of digital transmissions, with bitrates from a few kbit/s to more than 10 Gbit/s. However, analog applications still subsist in video and telemetry fields.

There are more particular cases, such as retransmission over fiber optics of carrier microwave frequencies to 30 GHz, or even modulating a laser diode. This technique (already used for producing active antennae, notably for radars) is beginning to be used in satellite telecommunications stations or for retransmission of microwave signals in future access networks combining fiber and radio.

Fiberless infrared connections

Even though this book is mainly dedicated to fiber-optic telecommunications, we can mention the development of infrared wave use for line-of-sight communications at very short distance: remote control, hi-fi accessories, mobile robotics, which are traditional applications, as well as wireless local area networks. While benefiting from the practical advantages of “wireless”, infrared can transport high throughputs and resolve certain disruption and confidentiality problems raised by radio links. They are well adapted to indoor propagation (within a building, not going outside). Different protocols were defined, with the most well known being IrDA for interfacing PCs and various peripherals to 4 Mbit/s.

Direct links between buildings with $0.8\text{ }\mu\text{m}$ laser beams have recently been developed, used as microwave point-to-point beams. These free space optics (FSO) systems avoid the cost and delay of cabling. These beams are very directional because of a telescope system (lens), and work at low power (a few mW), but can be interrupted by strong fog. Very high (2.5 Gbit/s or more) bitrates can be transported over a few kilometers with no obstacles, interferences or a need for a license, contrary to radio. Important development in these systems is expected.

There are also link projects between satellites by laser beams in spatial vacuum over thousands of kilometers, obviously requiring great precision in the orientation of transmitters.

This page intentionally left blank

Chapter 1

Multimode Optical Fibers

1.1. Overview of optics

1.1.1. *Introduction*

We can begin studying light propagation in optical fibers and guides by light ray propagation in the sense of traditional geometric optics.

However, this hypothesis is only valid if the guide's transverse dimensions are much larger than the wavelength λ . The optical fiber is then considered multimode, which means that for a given wavelength, several light rays can propagate.

Transmission performances are not optimal, but this type of fiber has a certain economic advantage compared to single-mode fibers, which have a much smaller core.

1.1.2. *Propagation of harmonic plane waves*

As we know, a ray is not a real model because the light cannot remain concentrated on a very small line because of diffraction. It can, however, be approached using the plane wave model, which is a harmonic wave propagating without divergence in the z direction (see Figure 1.1):

$$E_x = E_0 \exp j(\omega t - kz), E_y = E_z = 0 \text{ and } H_y = H_0 \exp j(\omega t - kz), H_x = H_z = 0$$

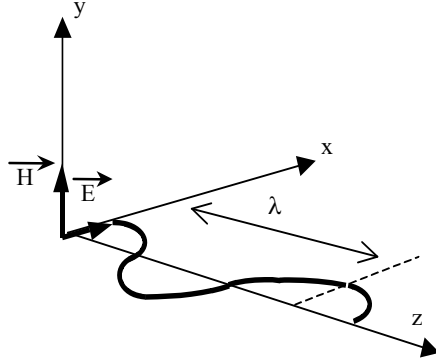


Figure 1.1. *Harmonic plane wave*

This wave is a solution for the propagation equation (this topic will be addressed in the next chapter) for a sine wave of angular frequency ω :

$$\Delta \vec{E} = -k^2 \vec{E} \text{ and } \Delta \vec{H} = -k^2 \vec{H} \text{ with } k^2 = \mu\epsilon\omega^2$$

as long as the wave width is infinite (\vec{E} and \vec{H} have the same value, in amplitude and phase, in every point on a plane parallel to xOy, or *phase plane*). In practice, its width must be much larger than the wavelength. This is the case, for example, for beams radiated by gas lasers that have a width in the order of millimeters:

k is the wave number: $k = 2\pi/\lambda$;

$v_\phi = \frac{\omega}{k} = 1/\sqrt{\mu\epsilon}$ is the phase velocity, which is the phase front propagation velocity;

$$Z = \frac{E_0}{H_0} = \sqrt{\mu/\epsilon} \text{ is the material impedance;}$$

$$\text{In the vacuum: } v_\phi = \frac{1}{\sqrt{\mu_0\epsilon_0}} = c = 3.10^8 \text{ m/s; } Z = Z_0 = \sqrt{\mu_0/\epsilon_0} = 377 \, \Omega;$$

$k = k_0 = 2\pi/\lambda_0$ where λ_0 is the wavelength in the vacuum.

In dielectric material, we have:

$\mu = \mu_0$ magnetic permeability of the vacuum;

$\epsilon = \epsilon_0 n^2$ where n is the refraction index.

We will only consider dielectrics which are perfectly transparent where index n is real. The previous relations then become:

$$v_\phi = \frac{1}{\sqrt{\mu\epsilon}} = \frac{c}{n}$$

the light velocity being divided by the refraction index:

$$Z = \sqrt{\mu/\epsilon} = \frac{Z_0}{n}; k = k_0 n; \lambda = \frac{\lambda_0}{n}$$

In what follows, we will only use the vacuum wavelength, which we will note as λ .

The power transported by this wave is equal to the Poynting vector flow, noted as: $\vec{P} = \vec{E} \wedge \vec{H}^*$, and is co-linear to \vec{k} in isotropic mediums.

1.1.3. Light rays

We can locally assimilate a light ray to a plane wave if the field variation on a distance similar to the wavelength is negligible; we can then note:

$$\vec{E}(P) = \vec{E}_0(P) \exp j(\omega t - \vec{k} \cdot \vec{OP})$$

where \vec{k} is the wave vector with a direction that is tangent to the light ray and its module is equal to:

$$k = k_0 n = \frac{2\pi}{\lambda} n, \text{ where } n \text{ is the local refraction index.}$$

In the geometric optics hypothesis, and in the case of isotropic mediums, the “light ray” path (see Figure 1.2) can be calculated by ray equation:

$$\frac{\partial}{\partial s} \left(n \frac{\partial \vec{r}}{\partial s} \right) = \text{grad } n$$

with $\frac{\partial \vec{r}}{\partial s}$ unitary vector tangent to the path and s being the curvilinear abscissa.

We can also note this as:

$$\frac{\partial \vec{k}}{\partial s} = k_0 \text{ grad } n$$

Light rays lean towards increasing indices. They can therefore be guided into a high index level, which is well known in atmospheric propagation of light or radio frequency (mirage effect) rays. This guidance mode is used in graded-index optical fibers.

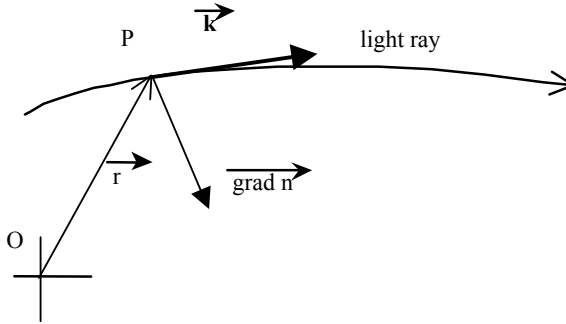


Figure 1.2. *Light ray propagation*

1.1.4. Dielectric diopter

In Figure 1.3 we illustrate a plane diopter between two perfect dielectric mediums, i.e. with real n_1 and n_2 indices. These indices become complex in the case of a partially absorbing medium. This issue will not be addressed here.

An incident plane wave (i indexed) arriving in the diopter with an angle of incidence θ_i will split into a reflected wave (indexed r) with θ_r angle of reflection and a transmitted wave (t indexed) θ_t angle of refraction. We represent a path for the wave, traditionally called the “light ray”, but we must not forget that the wave spreads on both sides of this ray.

Since there are neither charges nor currents in the dielectric, there is phase continuity of the electromagnetic field, hence continuity of phase fronts on both sides of the interface, which is written as:

$$\lambda_z = \frac{\lambda_1}{\sin \theta_i} = \frac{\lambda_1}{\sin \theta_r} = \frac{\lambda_2}{\sin \theta_t} \quad \text{or} \quad \lambda_j = \frac{\lambda}{n_j}$$

where:

$$n_1 \cdot \sin \theta_i = n_1 \cdot \sin \theta_r = n_2 \cdot \sin \theta_t \text{ (Snell-Descartes laws)}$$

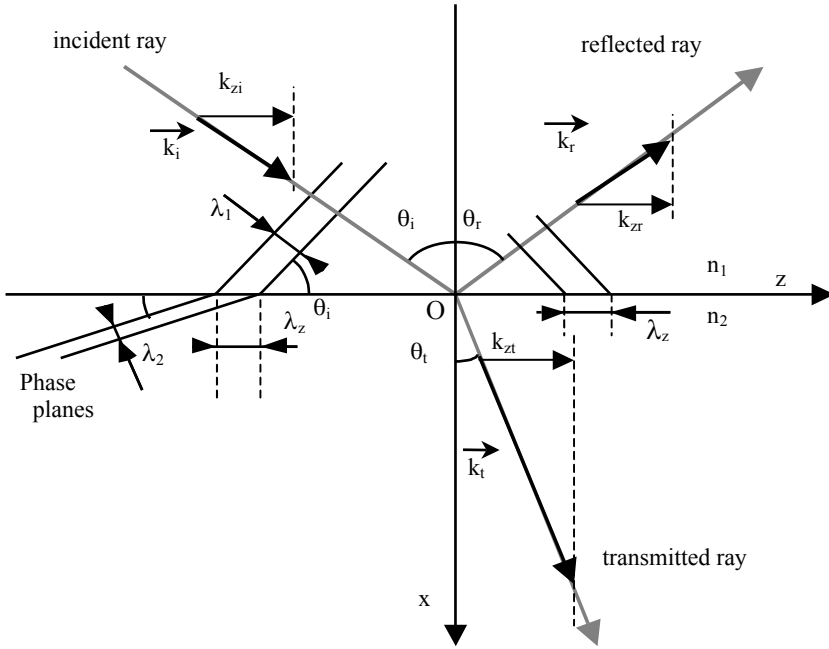


Figure 1.3. *Plane dielectric diopter*

Since the wavenumbers in the three mediums are characterized by: $k_j = k_0 \cdot n_j$, we see that Oz components of the three wave vectors are equal:

$$k_{zi} = k_{zt} = k_{zr} = \beta$$

which means that they will propagate together in the direction of axis z while remaining in-phase between each other and that the resulting field will take the form:

$$\vec{E}(x, y, z, t) = \vec{E}(x, y) \exp j(\omega t - \beta z)$$

1.1.5. Reflection of a plane wave on a diopter

The above relations give wave directions, but not the distribution of energy between them. We must conduct an electromagnetic analysis to determine it. To do this, we must split the incident wave into a component TE (\vec{E} parallel to the diopter) and a component TM (\vec{H} parallel to the diopter). These two cases are represented in Figure 1.4.

Due to field continuity at the interface between both mediums:

$$\vec{E}_i + \vec{E}_r = \vec{E}_t \text{ and } \vec{H}_i + \vec{H}_r = \vec{H}_t$$

This continuity is an essential property of dielectric guides, and a fundamental difference from the metallic wave guide.

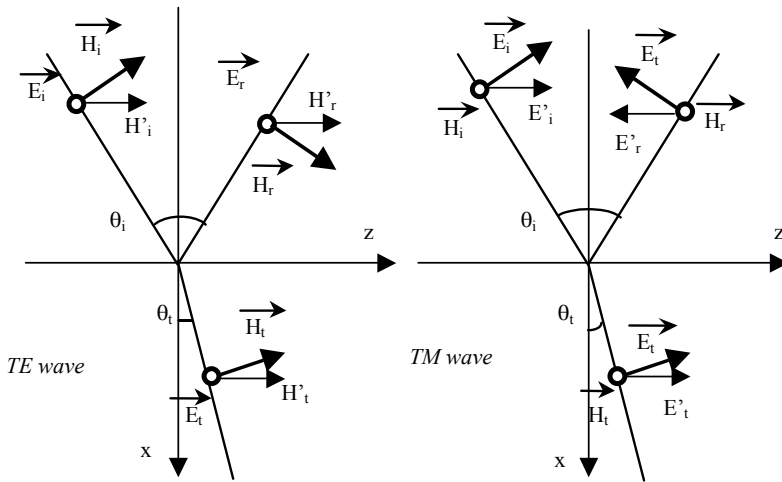


Figure 1.4. Reflection of a plane wave on a dielectric diopter

We can bring all cases down to the reflection of a wave perpendicular to the diopter by splitting field vectors and by noting E' and H' as their components parallel to the diopter.

For magnetic fields, sign conventions between incident and reflected waves are reversed because of the reversal of propagation direction. We then write:

$$E'_i + E'_r = E'_t \text{ and } H'_i - H'_r = H'_t \text{ where } Z'_1 (E'_i + E'_r) = Z'_2 E'_t$$

1.1.6. Reflection coefficient

The reflection coefficient in complex amplitudes is defined by:

$$\rho = \frac{E_r}{E_i} = \frac{E'_r}{E'_i} = \frac{H_r}{H_i} = \frac{H'_r}{H'_i} \text{ where we deduce: } \rho = \frac{Z'_2 - Z'_1}{Z'_2 + Z'_1}$$

which is equivalent to the reflection, at the end of an electric line, over an unmatched impedance. This depends on polarization (TE or TM).

The reflection of any θ_i incidence wave then becomes equal to the reflection of a zero incidence wave between two mediums of impedance:

$$Z'_1 = \frac{E_i}{H_i} = Z_1 / \cos \theta_i \text{ and } Z'_2 = \frac{E_t}{H_t} = Z_2 / \cos \theta_t \text{ for a TE wave}$$

and:

$$Z'_1 = \frac{E_i}{H_i} = Z_1 \cdot \cos \theta_i \text{ and } Z'_2 = \frac{E_t}{H_t} = Z_2 \cdot \cos \theta_t \text{ for a TM wave}$$

Because of the previous expressions, we can calculate the reflection coefficient according to the angle of incidence. For normal incidence ($\theta_i = 0$), we have:

$$\rho = \frac{Z_2 - Z_1}{Z_2 + Z_1} = \frac{n_1 - n_2}{n_1 + n_2}$$

There is phase reversal if $n_2 > n_1$.

If $n_2 > n_1$, $|\rho| \rightarrow 1$ in oblique incidence ($\cos \theta_i = 0$) whereas if $n_2 < n_1$, it is the case at limit refraction ($\cos \theta_t = 0$). In both cases, there is an angle for which $\rho = 0$ for TM waves: this is the Brewster angle, deduced from: $n_1 \cos \theta_t = n_2 \cos \theta_i$. A wave arriving with this incidence in a dielectric diopter (glass, water, etc.) results in a polarized reflected wave TE (see Figure 1.5). This well-known phenomenon is used in photography (for filtering reflections) and in polarizers, for example in lasers.

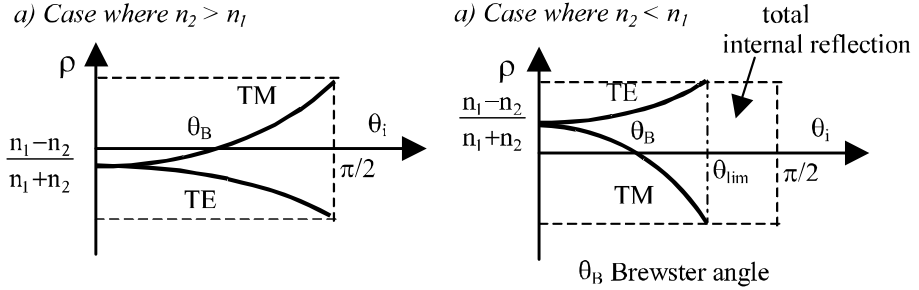


Figure 1.5. Reflection coefficient versus the angle of incidence:
a) case where $n_2 > n_1$; b) case where $n_2 < n_1$

For zero (or low) incidences, the reflection coefficient in power equals:

$$R = |\rho|^2 = \left(\frac{n_1 - n_2}{n_1 + n_2} \right)^2$$

giving 4% for the air ($n \approx 1$) – glass ($n \approx 1.5$) interface.

This Fresnel reflection is one of the causes of fiber-optic access and connection losses, and especially of integrated and optoelectronic optical components, where the indices are much higher. This is remedied by antireflection layers (dielectric layer stacking for an index adaptation at the wavelength used).

1.1.7. Total reflection

If $n_2 < n_1$, there is total reflection for $\theta_i > \theta_{\text{lim}}$, angle of limit refraction given by:

$$\sin \theta_{\text{lim}} = \frac{n_2}{n_1} \quad \text{where} \quad \sin \theta_t = \frac{n_1}{n_2} \quad \sin \theta_{\text{lim}} > 1 \quad \text{and} \quad \cos \theta_t = \pm j \sqrt{\frac{n_1^2}{n_2^2} \sin^2 \theta_i - 1}$$

The medium 2 impedance, which is in $\cos \theta_t$ or $1/\cos \theta_t$ depending on its polarization, then becomes completely imaginary.

This is the equivalent of an electric line loaded by reactive impedance. The reflection coefficient becomes imaginary and is written as:

$$\rho = \frac{Z'_2 - Z'_1}{Z'_2 + Z'_1} = \frac{1 + j\bar{z}}{1 - j\bar{z}} \text{ with } -j\bar{z} = \frac{Z'_1}{Z'_2}$$

depending on incidence and polarization.

– $|\rho| = 1$: we do have total reflection, all the energy is found in the reflected ray, but this reflection is accompanied by a *phase shift*.

– $\phi = 2 \arctg \bar{z}$ which depends on wave incidence and its polarization. It is zero at limit refraction, and leans toward $\pi/2$ in oblique incidence.

We then observe in medium 2 a non-homogenous wave; the wave vector's components are:

- in z: $k_{zi} = k_{zt} = k_0 n_1 \sin \theta_i = \beta$, real;
- in x: $k_{xi} = k_{xt} = k_0 n_2 |\cos \theta_t| = -j\gamma$, purely imaginary.

This wave's field is then written as:

$$\vec{E}_t(x, z, t) = \vec{E}_{t0} \exp j(\omega t - \beta z) \cdot \exp(-j\gamma x)$$

This wave presents a wave profile that is progressive in direction z, in phase with the progressive wave in medium 1, and an exponential profile decreasing in direction x. It is called an evanescent wave.

Its Poynting vector is purely imaginary; the energy of its wave is therefore purely reactive and does not modify reflected wave energy, as long as medium 2 is perfectly transparent (otherwise there is partial wave absorption).

The field of this evanescent wave, or field plays a very important role. It explains the interactions that can occur between medium 1 (an optical guide for example) and medium 2 at a certain distance, as long as it is not large compared to the penetration depth given by $\delta = 1/\gamma$.

These interactions are used in guided optics for splitters, as well as in optical near field microscopy.

1.2. Dielectric waveguide

1.2.1. Planar dielectric waveguide model

The planar guide is a 2D model (infinite in lateral direction y) in which the $2a$ thickness and n_1 index guide is surrounded by mediums of lower indices n_2 and n'_2 (see Figure 1.6).

These mediums must have an infinite thickness, or a thickness that is large compared to the penetration depth of the evanescent field.

We start with the case of the symmetric waveguide, with $n_2 = n'_2$. The case of asymmetric guides, where these indices are different, will be studied in section 1.2.3.

We will study this guide in geometric optics. A light ray propagating with an angle θ with Oz axis is guided by total reflection if: $\cos \theta > n_2/n_1$.

θ is the angle complementary to the angle of incidence θ_i previously used.

By splitting all three wave vectors according to Ox and Oz, we note:

$$\text{incident ray: } \vec{k}_1 = \begin{pmatrix} \alpha \\ \beta \end{pmatrix}; \text{ reflected ray: } \vec{k}'_1 = \begin{pmatrix} -\alpha \\ \beta \end{pmatrix}$$

with $\alpha = k_0 n_1 \sin \theta$ and $\beta = k_0 n_1 \cos \theta$, then $\alpha^2 = k_0^2 n_1^2 - \beta^2$:

$$\text{transmitted "ray" (evanescent field): } \vec{k}_2 = \begin{pmatrix} -j\gamma \\ \beta \end{pmatrix} \text{ with } \gamma^2 = \beta^2 - k_0^2 n_2^2$$

The sign of the quantity $k_0^2 n^2 - \beta^2$ determines the progressive (if positive) or evanescent (if negative) character of a wave in the n index medium. The ray therefore remains guided in the n_1 index medium on the condition that:

$$k_0 n_1 > \beta > k_0 n_2$$

and we define its effective index $n_a = \beta/k_0$.

The three waves have the same longitudinal β propagation constant. They will therefore progress in direction Oz by remaining phased between each other. The resulting field will take the form:

$$E(x,z,t) = E(x) \cdot \exp j(\omega t - \beta z)$$

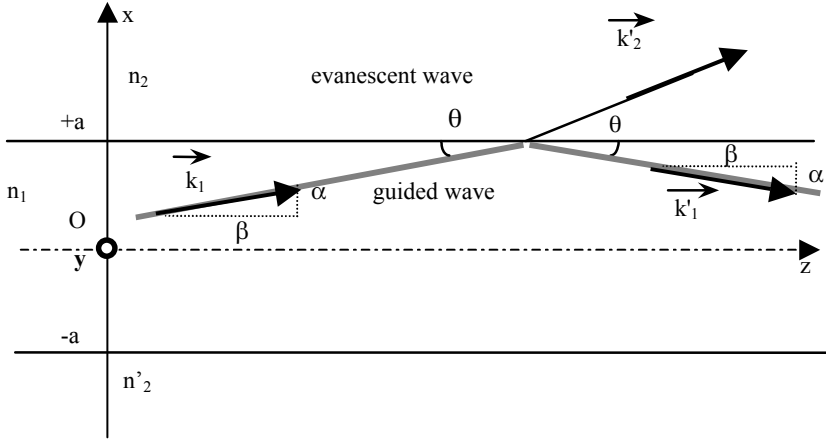


Figure 1.6. Plane dielectric wave guide

1.2.2. Notion of propagation modes

Distribution $E(x)$ of field Ox is determined by conditions at limits. In fact, in order to observe a stationary wave on a guide section, which is called a propagation mode, the wave must be in phase after a round trip between both diopeters. The phase shift: $4a.\alpha + 2\phi$ must then be a multiple integer of 2π .

The first term of this phase shift is caused by propagation in Ox direction, and the second by phase shift ϕ at the total reflection which can be calculated according to section 1.1.7 since its expression is slightly different for TE and TM waves.

This wave phase shift can be interpreted as a longer trip, or as wave reflection on a fictional metallic plane located beyond the dielectric diopter. This apparent guide widening is called the Goos-Hanchen effect (see Figure 1.7). It explains that, in a symmetric dielectric guide, the fundamental mode ($m = 0$) is always guided, contrary to the metallic guide.

The phase adaptation equation can be graphically solved and deduce α , β and γ can be deduced by introducing the normalized variables:

$$u = a.\alpha, v = a.\gamma \text{ and } V = a.k_0.\sqrt{n_1^2 - n_2^2} \text{ normalized frequency}$$

We must in fact resolve: $v = u \operatorname{tg}(u - m\pi/2)$ for modes TE, where:

$$v = \frac{n_2^2}{n_1^2} u \operatorname{tg}(u - m\pi/2) \text{ for modes TM, and } V^2 = u^2 + v^2$$

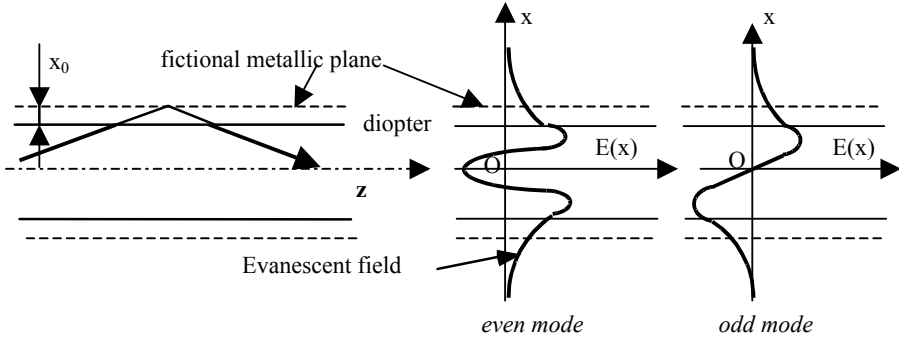


Figure 1.7. Goos-Hanchen effect and field pattern in the guide

The values of u and v , where we find β and field distribution, graphically correspond to intersections of $V = \text{constant}$ circles and equation $v(u)$ curves above, resulting in a field distribution in $\cos \alpha x$ for even modes and $\sin \alpha x$ for odd modes (see Figure 1.7). There are m field zeros along Ox (including the fundamental mode, for $m = 0$, which does not cancel out anywhere in the guide).

Modes are orthogonal between each other, i.e. the fields of both modes i and j are bound by the relation:

$$\iint [E_i(x, y) \cdot E_j^*(x, y)] dx \cdot dy = 0 \text{ over a section perpendicular to } Oz$$

The number of solutions, or modes, is completely determined by the value of V . The m -order mode exists if $V > m\pi/2$, its cut-off frequency being given by:

$$f_c(m) = m \cdot f_c \text{ with } f_c = \frac{c}{4a\sqrt{n_1^2 - n_2^2}} = \frac{c}{\lambda_c}$$

The cut-off wavelength of the m -order mode is λ_c/m . It means that this mode can only be guided at a lower wavelength (then at higher frequency), otherwise it is refracted. These results are the result of the geometric optics approximation, which is only valid if $V \gg 1$; they are therefore not rigorous if there are few modes. The cut-off frequency of 0-order mode is zero, which means that it is guided regardless

of the wavelength. This is obviously theoretical and does not consider infrared matter absorption.

1.2.3. Case of the asymmetric guide

This case is frequent in integrated optics where the guide, thin layer of n_1 index, is inserted between a substrate of slightly lower index n'_2 , and a coating of index n_2 lower than n'_2 . Again in geometric optics, the phase matching condition, therefore existence condition, of the m type mode of tilt θ on the axis, is written in this case:

$$4a.k_0 n_1 \sin\theta + \Phi_2 + \Phi'_2 = 2\pi m$$

where Φ_2 and Φ'_2 are the phase shifts that the wave encounters at total reflections on higher and lower interfaces (see section 1.1.7). In the asymmetric guide case, these index dependent phase shifts are different, and the graphic resolution (see Figure 1.8) shows that when k_0 (then frequency) decreases, there may not be a solution for $m = 0$. This means that there is a non-zero cut-off frequency for the fundamental mode.

In fact, when the mode leans towards its cut-off, its β propagation constant leans towards $k_0 n_2$, and therefore becomes lower than $k_0 n'_2$ at a wavelength λ_c where it will be able to propagate in the material of index n'_2 (the substrate in the case of integrated optics). Geometrically, θ tends to become higher than θ'_2 , angle of limit refraction at substrate-guide interface, which causes a refraction in the material whose index is closest to the guide's index.

This phenomenon happens when the normalized V frequency decreases, i.e. when the wavelength increases or when the guide's thickness decreases.

In addition, internal reflection phase shifts do not have the same value for TE and TM modes, so the cut-off frequencies will not either. In an asymmetric guide, there is a range of wavelengths where mode TE_0 only, and not mode TM_0 , is guided, i.e. a polarized light.

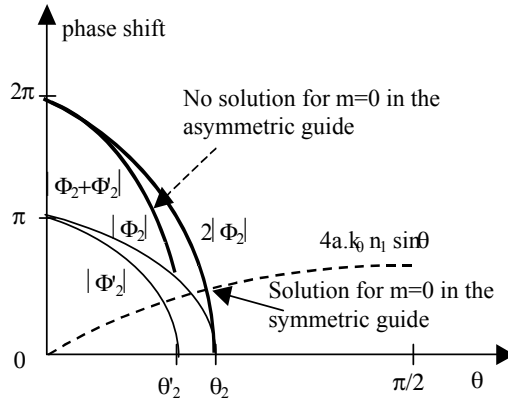


Figure 1.8. Search for a solution (curve intersection points) in both types of plane guides

1.2.4. Dispersion

Once the β constant is determined for each mode, we deduce:

– its phase velocity: $v_\phi(\omega) = \frac{\omega}{\beta}$ phase front propagation velocity; and its inverse called the phase delay (by unit of length):

$$\tau_\phi(\omega) = \frac{\beta}{\omega} \text{ (phase delay)}$$

– its group velocity: $v_g(\omega) = \frac{d\omega}{d\beta}$ pulse propagation velocity; and its inverse called the group delay (by unit of size):

$$\tau_g(\omega) = \frac{d\beta}{d\omega} \text{ (group delay)}$$

These values depend on both the mode order and angular frequency, which leads to a double dispersion:

– intermodal dispersion: caused by group delay difference between modes;

– intramodal dispersion, or chromatic dispersion: caused by group delay variation for each mode with its angular frequency, therefore with its wavelength. In practice, this effect is combined with the variations of refraction indices with the wavelength (called material dispersion).

We can note the limit values of these propagation velocities:

- if $\omega \rightarrow \omega_c$ (at mode cut-off, i.e. limit refraction), v_ϕ and v_g lean toward $v_2 = c/n_2$, propagation velocity in medium 2: since the mode spreads widely, it takes its propagation velocity; this corresponds to $\beta = k n_2$;
- if $\omega \rightarrow \infty$ (far from the cut-off), v_ϕ and v_g tend toward $v_1 = c/n_1$, propagation velocity in medium 1, where the mode is completely confined; this then corresponds to $\beta = k n_1$. These relations are exact if n does not depend on the wavelength.

The dispersion will be weaker as n_1 and n_2 are closer. Dispersion minimization is an essential point of optical fiber optimization.

1.3. Multimode optical fibers

1.3.1. Definition

When transverse dimensions of a guide are much larger than the wavelength, the equation in section 1.2.3 will have a solution even for high m , which means that a large number of modes can be guided.

We can then say that a mode corresponds to an authorized path, resulting from constructive interferences between multiple reflections on the dioptr between both materials.

A fiber-optic is a circular dielectric waveguide which is very probably multimode if the core, or in other words the central part where light propagates, has a diameter much larger than the wavelength. This diameter is approximately between 50 and 200 μm for silica fibers, and 0.5 and 1 mm for plastic fibers. We can then simply, but correctly, study propagation by geometric optics.

In Chapter 2, modes will be more rigorously defined by the resolution of the propagation equation deduced from Maxwell equations.

We will see that a mode is characterized by its path and by the distribution of the electromagnetic field around it. We must insist on the fact that in a multimode guide, the different modes are on the same wavelength.

1.3.2. Multimode step-index fiber

The simplest type of multimode fiber is a step-index fiber (see Figure 1.9), directly emerging from optical applications. In this structure, the core of refraction index n_1 is surrounded by a cladding of slightly lower index n_2 . These indices are

close to 1.5 for silica fibers. This cladding plays an active role in guiding and is also surrounded by a coating.

Within the Oz cylinder axis fiber-optic, the ray is guided if angle θ that it produces with Oz remains lower than θ_0 , the limit refraction angle deduced from the Snell-Descartes laws:

$$n_1 \cdot \cos \theta_0 = n_2$$

If $\theta > \theta_0$, the ray is refracted. Otherwise, it is guided by total reflection at the core cladding interface. This remains true if the fiber is not straight, as long as the bending is not too pronounced. This makes it possible to consider long haul transmission with low loss levels and without transmitted information leaking outside.

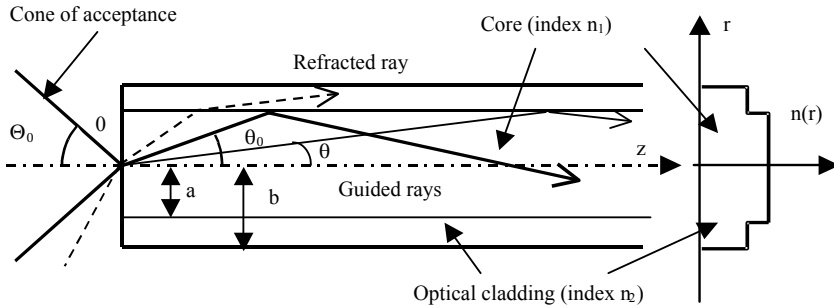


Figure 1.9. Step-index fiber

Because of this condition, the maximum angle of incidence at fiber input, i.e. the acceptance cone aperture, is given by the numerical aperture:

$$NA = \sin \Theta_0 = n_1 \sin \theta_0 = \sqrt{n_1^2 - n_2^2}$$

In return, it is the angle within which the light coming out of the fiber diverges.

Along with diameters, core at $2a$, and cladding at $2b$, the numerical aperture is the most important parameter of an optical fiber. A large numerical aperture makes it possible to couple a large quantity of light, even from a divergent source such as light-emitting diode (LED). On the other hand, it will lead to spreading of transmitted pulses over time, because there are large differences in the length, therefore in propagation time, of the different guided rays (intermodal dispersion effect).

These fiber optics are quite suitable for optical applications and for very short distance transmissions. There are a certain number of multimode fibers that are different in material (plastic, silica/silicone, or “all silica” – not widely used for step-index) and in their characteristics (see Chapter 2).

1.3.3. Multimode graded-index fiber

The graded-index fibers were designed specifically for telecommunications in order to minimize this intermodal dispersion effect without significantly reducing the numerical aperture or the coupled power. Their core index decreases according to a parabolic-like law from the axis to the core cladding interface (see Figure 1.10). In this way, the rays follow a sine type path, and those with the longest path go through lower index mediums, increasing their velocity and making it possible to approximately equalize propagation delays.

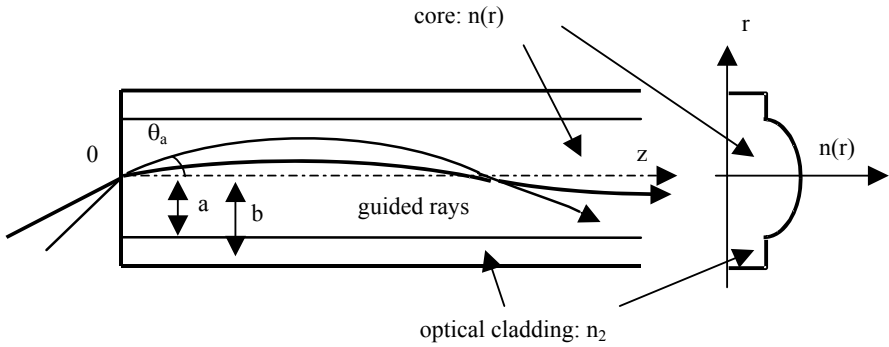


Figure 1.10. Graded-index fiber

The index profile law takes the form:

$$n(r) = n_1 \sqrt{1 - 2\Delta(r/a)^\alpha} \quad \text{with } \Delta \text{ relative index difference}$$

$$\Delta = \frac{n_1^2 - n_2^2}{2n_1^2} \approx \frac{n_1 - n_2}{n_1} \quad (\text{the approximation is true if } \Delta \text{ is small})$$

Exponent α is close to 2; its exact value is optimized to minimize intermodal dispersion and depends on the material and wavelength.

We again define the numerical aperture as with step-index fibers. However, n_1 is the core index only on the axis. Since the numerical aperture decreases the further away from the axis we move, with equal conditions approximately half as much power is coupled as in a step-index fiber.

The cladding does not occur in guiding itself, but plays an important spatial filtering role by eliminating the most tilted rays.

Several “all silica” graded-index (GI) fiber standards have been normalized for short distance telecommunications applications (50/125 fiber, now used for high bandwidth local area networks), local computer networks (62.5/125) and first generation video distribution (85/125, still not widely in use). Graded-index plastic fibers appear for the Gigabit Ethernet.

1.4. Propagation in multimode optical fibers

1.4.1. Ray paths

Figure 1.9 and 1.10 diagrams only represent meridional rays, remaining in a plane containing the optical fiber axis. In order to calculate all paths, we must switch to 3 dimensions. Due to the symmetry of revolution of the optical fiber, we use cylindrical coordinates (see Figure 1.11), by noting as:

- r, z, ψ coordinates from the path's current point, P;
- $\vec{u}_r, \vec{u}_z, \vec{u}_\psi$ local trihedral.

We must solve the ray equation:

$$\frac{d}{ds} \left(n \frac{d\vec{OP}}{ds} \right) = \text{grad } n, \text{ with } \frac{d\vec{OP}}{ds} \text{ unitary vector tangent to the path}$$

This vector has for components:

- over \vec{u}_r : $dr/ds = \sin\theta \cos\phi$;
- over \vec{u}_z : $dz/ds = \cos\theta$;
- over \vec{u}_ψ : $r \cdot d\psi/ds = \sin\theta \sin\phi$.

The resolution of this equation will result in the following wave vector:

$$\vec{k} = k_0 n(P) \frac{d\vec{OP}}{ds}$$

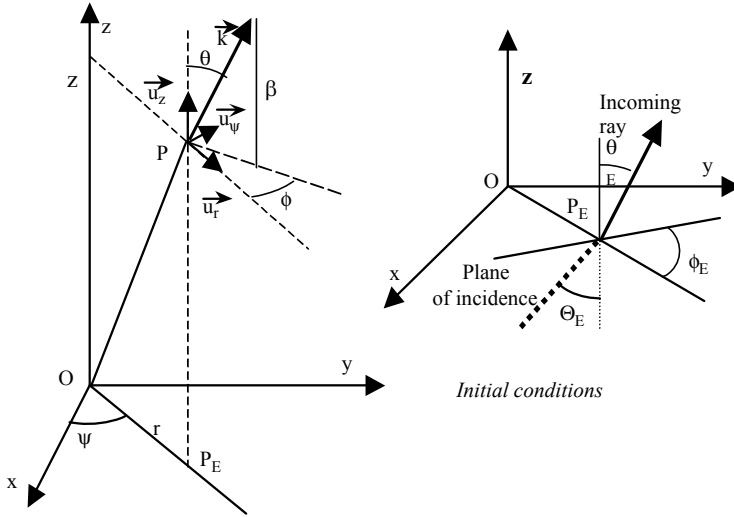


Figure 1.11. Calculation of ray paths in an optical fiber

1.4.2. Propagation equation resolution

Since index $n(P)$ only depends on r , distance from point P to axis Oz , the gradient of n is along the \vec{u}_r direction. We can therefore solve the equation along \vec{u}_z and \vec{u}_ψ , directions in which $\text{grad } n$ components are zero.

Along \vec{u}_z , which has a constant direction, we immediately have:

$$n(r) \cdot \frac{dz}{ds} = \text{constant} = \frac{\beta}{k_0}$$

where $\beta = k_0 n(r) \cos\theta$ is the longitudinal propagation constant.

Along \vec{u}_ψ which does not have a constant direction, the calculation is slightly longer (detailed in the appendix of this chapter) and leads to:

$$n \cdot r^2 \frac{d\psi}{ds} = \text{constant} = \frac{v}{k_0}$$

where $v = k_E n(r) r \sin\theta \sin\phi$ is a constant without dimension.

These two constants are deduced from initial conditions:

$$\beta = k_0 n(r_E) \cos \theta_E = k_0 \sqrt{n(r_E)^2 - \sin^2 \Theta_E} \quad \text{and} \quad v = k_0 n(r_E) r_E \sin \theta_E \sin \phi_E$$

where r_E , θ_E and ϕ_E correspond to the point of incidence and to the tilt of the incident ray at the fiber-optic entrance (see Figure 1.11) where Θ_E is defined outside of the fiber.

The wave vector can then be written as:

$$\vec{k} = f(r) \vec{u}_r + \beta \vec{u}_z + \frac{v}{r} \vec{u}_\psi$$

The radial component $f(r)$ can be deduced from constants and $n(r)$ index profile through module of \vec{k} which is given by:

$$k^2 = f(r)^2 + \beta^2 + \left(\frac{v}{r}\right)^2 = k_0^2 n(r)^2$$

1.4.3. Different ray types

Light rays will propagate where the wave vector is real, or where $f(r)^2$ is positive; otherwise we have an evanescent field. This condition must not be met at any point in the cladding in order for them to remain guided in the core. We must therefore study the sign of:

$$f(r)^2 = k_0^2 n(r)^2 - \beta^2 - \left(\frac{v}{r}\right)^2 \quad \text{versus } r$$

1.4.3.1. Meridional rays

Meridional rays remain in the plane containing the axis Oz , so ϕ and v are zero and these rays propagate where: $\beta < k_0 n(r)$.

They are guided in the core if: $\beta > k_0 n_2$, which corresponds to the initial condition:

$$\sin \Theta_E < \sqrt{n(r_E)^2 - n_2^2}$$

generalizing the definition of the numerical aperture at the point E.

1.4.3.2. Skew rays

v is not zero and we thus observe 3 cases (see Figure 1.12):

- the ray is *guided* if $f(r)^2 < 0$ in all the cladding, or as previously: $\beta > k_0 n_2$; this ray, which never cuts off the axis, is also called gallery mode;
- the ray is *refracted* if $f(r)^2 > 0$ in all the cladding, or:

$$\beta^2 < k_0^2 n_2^2 - \left(\frac{v}{a}\right)^2$$

- the ray is *leaking* in the intermediate case: $k_0^2 n_2^2 > \beta^2 > k_0^2 n_2^2 - (v/a)^2$.

In the case of leaking rays, $f(r)^2 < 0$ in the part of the cladding neighboring the core (we have an evanescent field), but becomes positive again further away, thus defining a zone in the cladding where a ray can propagate once more. This ray will gradually attract the energy propagating in the core and thus leak in cladding through the evanescent field, based on a phenomenon similar to the tunnel effect in quantum mechanics.

This type of ray therefore cannot guide energy in the core over a long distance, but can propagate over short distances before elimination, and thus disrupt transmission and measures.

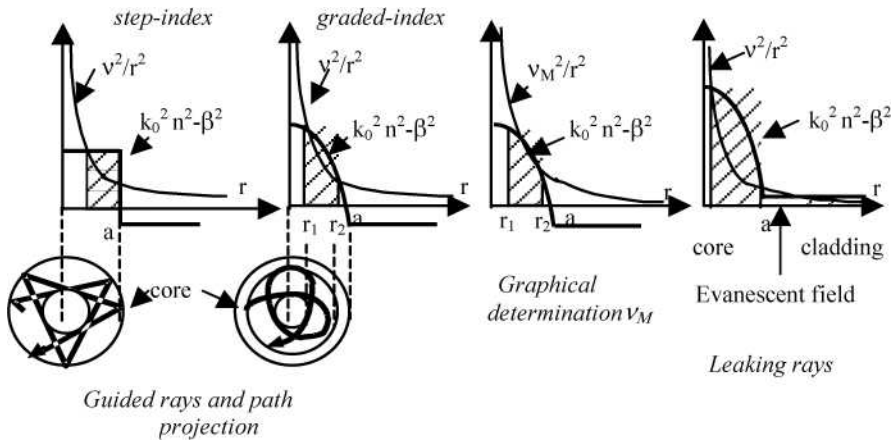


Figure 1.12. Different types of rays in a multimode fiber

1.4.4. Modes of propagation

Due to the wave vector expression, the electric field takes the following form:

$$E(r, \psi, z, t) = E_0 \exp j(\omega t - \vec{k} \cdot \vec{OP}) = E_0 \exp j(\omega t - r.f(r) - \beta z - v\psi)$$

This is a guided mode field if its distribution is stationary over a plane perpendicular to the fiber axis, which requires a phase matching:

– over \vec{u}_ψ : the phase shift equals $\int_0^{2\pi} \frac{v}{r} \cdot r \cdot d\psi = 2\pi v$; it must be an integer multiple

of 2π , then v , which is dimensionless, must be an integer, called azimuthal order. It is the number of field periods on a girth. v can be positive or negative, corresponding to both rotation directions of a skew ray around the fiber axis.

It has a maximum v_M value that can be graphically determined (see Figure 1.12), with the knowledge that it is not possible to have:

$$k_0^2 n(r)^2 - \beta^2 < \left(\frac{v}{r}\right)^2 \text{ in all the core}$$

In fact, there would no longer be a progressive field zone where the ray would propagate;

– over \vec{u}_r : path projection (see Figure 1.12) reveals two upturning points at distances r_1 and r_2 from the axis ($r_1 = 0$ for meridional rays, corresponding to $v = 0$). The envelope of these points defines on each side a cylindrical surface called caustic separating the progressive wave from the evanescent wave, characterized by $f(r) = 0$. It behaves like a dielectric diopter: we observe a $\Phi(r)$ phase shift. Total phase shift on a round trip between both caustics must be an integer multiple of 2π , defining the mode of radial order m (number of field periods on a radial path from r_1 to r_2).

If m is large, we can neglect phase shifts on caustics before the first term (propagation based phase shift) and write, by using the expression of $f(r)$:

$$\frac{1}{\pi} \int_{r_1}^{r_2} \sqrt{k_0^2 n(r)^2 - \beta^2 - \left(\frac{v}{r}\right)^2} \cdot dr = m$$

With a numerical calculation, this expression allows us to determine the β propagation constant of the v, m -order mode. Indeed, r_1 and r_2 values are deduced from $f(r) = 0$. The number of modes can be deduced by a rather long and

approximate calculation (we are still in geometric optics) of which we simply give the result:

– for a step-index fiber:

$$N \approx V^2/2 \text{ with } V = a k_0 \cdot \sqrt{n_1^2 - n_2^2} \text{ normalized frequency}$$

– for a parabolic graded-index fiber: $N \approx V^2/4$.

These results are only valid if V is large.

1.5. Dispersion in multimode optical fibers

1.5.1. Intermodal dispersion

Due to the dispersion of propagation delay between modes, called intermodal dispersion, a light pulse injected at the fiber-optic entrance will arrive in the form of a large number of shifted pulses. Since the modes are numerous and the propagation delay difference between two modes is much lower than the photodetector response time, it will deliver the pulse envelope, or a pulse response with a standard deviation $\Delta\tau_{im}$. For convenience of measurement purposes, the half-maximum width of the received pulse is generally considered.

It is very important to note that the envelope and mid-height pulse width do not only depend on differences in propagation delay between modes, but also on the light power distribution between them. This depends on light injection at entry as well as on geometric conditions of the continuation of the fiber (bending, constraints) modifying this distribution. We can however calculate the maximum received pulse width, which is the propagation delay difference between the slowest and fastest modes.

1.5.2. Pulse broadening calculation

1.5.2.1. In step-index fibers

In multimode fibers, we can approximately consider rays propagating in locally homogenous mediums. In this approximation, group delay locally equals:

$$\tau_g(s) = \frac{dk}{d\omega} = \frac{dk_0}{d\omega} \cdot \frac{dk}{dk_0} \text{ with } k = k_0 n \text{ and } k_0 = \frac{\omega}{c}$$

where:

$$\tau_g(s) = \frac{N(s)}{c} \text{ with } N = \frac{dk}{dk_0} = n + k_0 \frac{dk}{dk_0} = n - \lambda \frac{dn}{dk_0} \text{ group index}$$

s is the curvilinear abscissa along the ray. Propagation time over a fiber-optic L length is deduced by integration along this ray:

$$\tau = \int_{\text{ray}} \tau_g(s).ds = \frac{1}{c} \int_{\text{ray}} N(s).ds$$

For a step-index fiber, the index is constant throughout; we will have $N = n_1$ by assimilating refraction and group indices, which are close.

Global propagation delay of the meridional ray with a θ_a tilt on the axis then equals (see Figure 1.13):

$$\tau(\theta_a) = \frac{n_1 L}{c \cos \theta_a}$$

We can deduce the maximum propagation delay difference between the fastest mode, for which $\theta_a \approx 0$, and the slowest mode, for which $\theta_a \approx \theta_0$ with θ_0 angle of limit given by: $\cos \theta = n_2/n_1$ (the approximation comes from the discrete nature of modes which results in the fact that these limit values are not exactly reached).

This propagation delay difference equals:

$$\Delta\tau_{\text{im(max)}} = \frac{\tau(\theta_0) - \tau(0)}{L}$$

It is higher than half-maximum pulse broadening, and increases with the index difference between core and cladding. With formulas relating it to the numerical aperture and classical approximations on Δ , we find:

$$\Delta\tau_{\text{im(max)}} = \frac{n_1}{c} \Delta = \frac{ON^2}{2n_1 c}$$

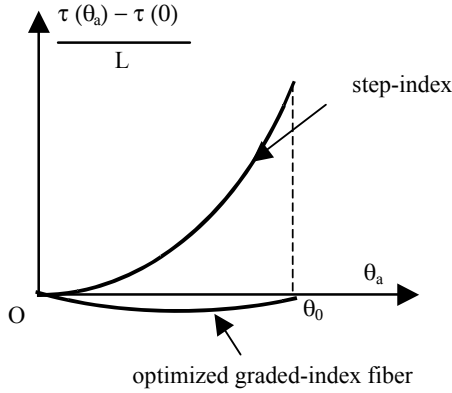


Figure 1.13. Propagation delay calculation of the different rays

1.5.2.2. In graded-index fibers

Now, the calculation is carried out in two steps: determination of the path and delay integration along it. With a graded-index based on the pseudo-parabolic law:

$$n(r) = n_1 \sqrt{1 - 2\Delta(r/a)^\alpha}$$

For meridional rays with θ_a tilt at the point where they cross the axis, we find:

$$\tau(\theta_a) = \frac{n_1}{c} \cdot \frac{L}{\cos\theta_a} \left(1 - \frac{2-P}{\alpha+2} \sin^2 \theta_a \right)$$

with P the profile dispersion parameter, which depends on the wavelength and material.

This expression is general because a step-index fiber corresponds to $\alpha = \infty$ and we find again the previous expression. Because of the corrective term, caused by the faster average velocity of rays that have a greater tilt, propagation delays are much closer to each other in a graded-index fiber than in a step-index fiber (see Figure 1.13). The intermodal dispersion is minimized for:

$$\alpha = \alpha_{\text{opt}} = 2 - 2P - 2\Delta$$

Since P and Δ are low, this value which is close to 2 depends on λ : the graded-index fiber can only be optimized for a single wavelength. In theory, it is possible to reach less than 100 ps/km for $\Delta = 1\%$, but in order to do this, the theoretical index profile must be very precisely respected. In fact, $\Delta\tau_{im}$ increases very rapidly as soon as the profile slightly moves away. In practice, it has an value in the range of 1 ns/km, for a less severe tolerance making it possible to produce an economical fiber. However, the most recent graded-index fibers, optimized for very high bandwidth local area networks, almost reach theoretical values.

1.5.3. Chromatic dispersion

As we have seen for plane wave guides, it adds to intermodal dispersion a chromatic dispersion effect $\Delta\tau_c$, caused by the variation of the group delay τ_g with the source's wavelength.

First, for a fiber length L , we can write:

$$\Delta\tau_c = D_c \cdot L \cdot \Delta\lambda \text{ with:}$$

– $\Delta\lambda$ spectral source width; pulse broadening is proportional to it. This value will therefore be high with light-emitting diodes, with very large linewidth;

– D_c chromatic dispersion coefficient, which depends on fiber and wavelength parameters. We can calculate this by:

$$D_c = \frac{d\tau_g}{d\lambda}$$

expressed in ps/nm/km, as $\Delta\lambda$ is in nm and $\Delta\tau_c$ in ps/km.

It is divided into: $D_c = D_M + D_G$ where D_M is the material dispersion, caused by variation of material index with the wavelength, and D_G is the guide dispersion. For multimode fibers, this last term is different for each mode, but it is negligible in practice. For single-mode fibers on the other hand, it plays an important role and we will discuss it in detail in Chapter 2. The material dispersion curve in silica (see Figure 1.14) cancels out at approximately 1.27 μm . The chromatic dispersion coefficient is negative under this wavelength, which means that light speed increases with the wavelength (ordinary dispersion), and it is the opposite above (extraordinary dispersion).

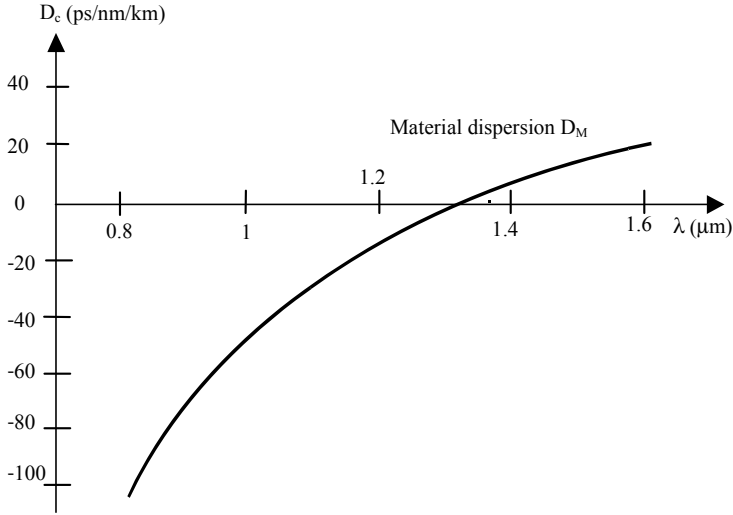


Figure 1.14. *Chromatic dispersion in a multimode fiber*

1.5.4. Time-domain response of multimode fibers

The global time-domain response is the result of the quadratic combination of two dispersion phenomena, acting as independent distributions:

$$\Delta\tau = \sqrt{\Delta\tau_c^2 + \Delta\tau_{im}^2} \text{ half-maximum width of the received pulse}$$

This pulse broadening is much lower for graded-index fibers than for step-index fibers (see Figure 1.15). Intermodal dispersion is generally predominant but not always: when a graded-index fiber is used with a $0.85 \mu\text{m}$ LED (cheapest configuration), the chromatic dispersion is then predominant and it is necessary to take this in consideration. In order to have an negligible chromatic dispersion effect in multimode fibers, we must either work at $1.3 \mu\text{m}$ or use laser diodes.

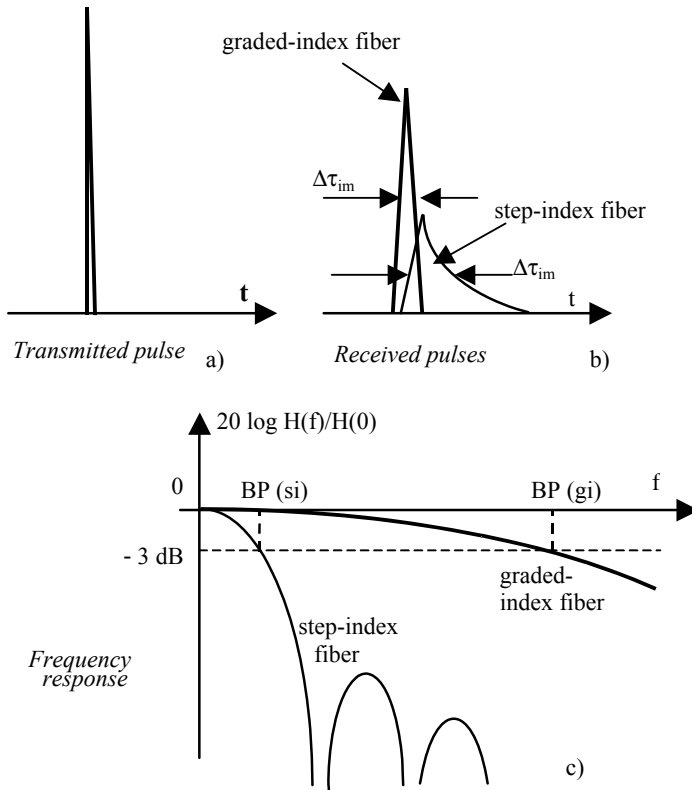


Figure 1.15. Time and frequency-domain responses in multimode fibers

1.5.5. Multimode fiber bandwidth

In telecommunications, the practice of using the bandwidth BW, deduced from the frequency-domain response, the Fourier transform of the pulsed response (see Figure 1.15) was maintained. This is the frequency at which the modulation amplitude of the received signal (and not its average power!), $H(f)$, is equal to $H(0)$ divided by $\sqrt{2}$ ($H(0)$ representing attenuation) because of intermodal dispersion. This measurement is done by using a laser source to avoid chromatic dispersion.

The relation between bandwidth and pulse broadening depends on the exact pulse form, and consequently on the energy distribution between modes. We generally accept the approximate relation:

$$BW \approx \frac{1}{2\Delta\tau_{im}}$$

This expression is valid in the absence of chromatic dispersion.

If the pulse broadening is proportional to the length of fiber L , the bandwidth is inversely proportional to it, and we can say that the resulting product of bandwidth \times length is constant. We will then use the term, expressed in MHz.km, corresponding to $\Delta\tau_{im}$ measured over 1 km; it is also called “kilometer bandwidth”.

Provided by the manufacturer in practice, this bandwidth is a essential characteristic of multimode fibers. Minimal values can be imposed by the applications (distribution, local area networks, etc.). Its range is:

- from 10 to 100 MHz.km for step-index fibers;
- from 100 to 1,000 MHz.km for graded-index fibers. Some recent fibers, optimized for the Gigabit Ethernet, reach 2 GHz.km (OM3 standard).

When chromatic dispersion is not negligible, the kilometer bandwidth becomes:

$$BW \approx \frac{1}{2\Delta\tau} \text{ with } \Delta\tau \text{ total pulse broadening given in section 1.5.5}$$

This bandwidth is, in this case, lower than the one given by the fiber manufacturer, which only involves intermodal dispersion. We have then calculated a global bandwidth depending on the fiber and spectral source width. We must not forget that (electrical) bandwidths of the source and receiver can also limit the transmission system bandwidth, and in particular with light-emitting diodes whose bandwidth does not exceed a few hundred MHz.

1.5.6. Mode coupling

We have considered that the pulse broadening caused by intermodal dispersion was exactly proportional to the length traveled. This is true that if energy coupled in a mode remains confined in this mode. However, most often, non-homogenities and distortions lead to energy coupling between modes, and consequences on propagation can be significant. In fact, modes have different propagation delays, but also slightly different attenuations: high order modes, close to the cut-off, have higher losses (they exchange energy with leaking modes, themselves leaking, in case of mechanical perturbations).

This mode coupling can be localized, for example when caused by a strong curve or by a misaligned connection (it is then called mode conversion because there is a discontinuity in the power transported by each mode).

In the case of statistically stationary perturbations along the fiber (material non-homogeneity effect, cable-induced constraint effect, etc.), we observe that a mode equilibrium distribution is established and characterized by:

- a near Gaussian power distribution transported by each mode, depending on its tilt θ_a on the axis (but it is not a Gaussian beam, because it does not have spatial coherence);
- a global attenuation supplement, as the different modes have a slightly different attenuation which increases with the mode order.

This equilibrium state happens after an equilibrium distance that is shorter as coupling is stronger. This distance can be reduced by creating strong constraints at the beginning of a fiber. This is done in measurements, using a wave scrambler, in order to measure its parameters at equilibrium, but attenuation increases.

When equilibrium is established, a larger bandwidth than the one expected by the relation bandwidth \times length = constant is observed. We then accept, instead of the L^{-1} law, an $L^{-\gamma}$ law where exponent γ is slightly lower than 1 but can only be known experimentally, and depends on conditions of usage (presence of connections and bending).

It is therefore difficult to predict with precision the link bandwidth over the multimode fiber, and the L^{-1} law gives a lower bandwidth limit that we are sure will be available. For a new installation, it is preferable to use a single-mode fiber when it is not sure that the multimode fiber will provide enough bandwidth. However, with the increase of throughputs in local networks, it may be necessary to use already installed multimode fibers at increasingly high throughputs, at the bandwidth limit. It is necessary to measure it experimentally and to plan a penalty in the loss budget (see Chapter 9). Moreover, bandwidth can be improved by using mode filtering at injection (although this results in a loss of power, which is perfectly acceptable at short distance).

The mode coupling phenomenon also prohibits multiplexing of different information on the different modes, which would be possible in theory (and has been realized under laboratory conditions at very short distances).

1.5.7. Modal noise

In the mode coupling theory, it is assumed that there is no coherence between modes, which is the case if the source is a low coherence LED. In the case of a high coherence source (laser diode), the coherence between modes is maintained along the fiber and we observe interference between them. Phase shift variation between modes is easily converted into intensity variation by spatial filtering, intentional or not (at a connection for example).

Used in some vibration sensors, this modal noise phenomenon is disturbing for transmissions, and the use of laser diodes is traditionally avoided with multimode fibers. However, an exception involves very short high bit-rate links on multimode fibers (particularly Gigabit Ethernet), where laser diodes are necessary for adequate speed, and which are limited by intermodal dispersion; in this case the level of received signal is high and thus noise is more easily tolerated.

1.6. Appendix: detail of calculation in section 1.4.2

The propagation equation resolution according to \vec{u}_ψ , which is not of constant direction, is done in the following manner. The transverse component (contained in plane \vec{u}_r, \vec{u}_ψ) of vector $n \cdot d\vec{OP}/ds$ equals:

$$n \cdot \frac{dr}{ds} \vec{u}_r + n \cdot r \frac{d\psi}{ds} \vec{u}_\psi$$

and its derivative equals:

$$\frac{d}{ds} \left(n \cdot \frac{dr}{ds} \right) \vec{u}_r + n \cdot \frac{dr}{ds} \frac{d\vec{u}_r}{ds} + \frac{d}{ds} \left(n \cdot r \frac{d\psi}{ds} \right) \vec{u}_\psi + n \cdot r \frac{d\psi}{ds} \cdot \frac{d\vec{u}_\psi}{ds}$$

thus:

$$\frac{d\vec{u}_r}{ds} = \frac{d\psi}{ds} \vec{u}_\psi \text{ and } \frac{d\vec{u}_\psi}{ds} = - \frac{d\psi}{ds} \vec{u}_r$$

The derivative component along \vec{u}_ψ , which is zero since n does not depend on ψ , equals:

$$\frac{d}{ds} \left(n \cdot r \frac{d\psi}{ds} \right) + n \cdot \frac{dr}{ds} \frac{d\psi}{ds}$$

By developing this term and by multiplying it by r , we obtain:

$$2n.r. \frac{dr}{ds} \frac{d\psi}{ds} + r^2 \frac{dn}{ds} \frac{d\psi}{ds} + n.r^2 \frac{d^2\psi}{ds^2} = \frac{d}{ds} \left(n.r^2 \frac{d\psi}{ds} \right) = 0$$

from where we deduce:

$$n.r^2 \frac{d\psi}{ds} = \text{constant} = \frac{v}{k_0}$$

where $v = kn(r) r.\sin \theta \sin \phi$ is a dimensionless constant.

Chapter 2

Single-Mode Optical Fibers

2.1. Fiber-optic field calculation

In order for a guide or an optical fiber to be single mode, its transverse dimensions must not be much larger than the wavelength. In these conditions, the geometrical optical approximation is no longer valid and calculations must use electromagnetism.

2.1.1. *Electromagnetic equations*

The exact calculation of electromagnetic fields in optical fibers requires the resolution of Maxwell equations in a dielectric material:

$$\text{rot } \vec{E} = -\mu_0 \frac{\partial \vec{H}}{\partial t} \text{ and } \text{rot } \vec{H} = \epsilon_0 n^2 \frac{\partial \vec{E}}{\partial t} \text{ (n refraction index, with } \epsilon = \epsilon_0 n^2)$$

from where the propagation equation or Helmholtz equation is deduced:

$$\Delta \vec{E} = \mu_0 \epsilon_0 n^2 \frac{\partial^2 \vec{E}}{\partial t^2} \text{ and } \Delta \vec{H} = \mu_0 \epsilon_0 n^2 \frac{\partial^2 \vec{H}}{\partial t^2}$$

or, for a sine wave of angular frequency ω :

$$\Delta \vec{E} = -\mu_0 \epsilon_0 n^2 \omega^2 \vec{E} \text{ and } \Delta \vec{H} = -\mu_0 \epsilon_0 n^2 \omega^2 \vec{H}$$

\vec{E} and \vec{H} being the complex fields.

Exact in a homogenous environment, this equation remains valid in a medium where index n slowly varies over a length equal to the wavelength. By introducing the wavenumber:

$$k_0 = 2\pi/\lambda = \omega \sqrt{\mu_0 \epsilon_0}, \text{ we rewrite } \Delta \vec{E} = -k_0^2 n^2 \vec{E} \text{ and } \Delta \vec{H} = -k_0^2 n^2 \vec{H}$$

Due to the limit conditions and especially the field continuity at core-cladding interface, there will be a finite number of solutions which will be the modes of propagation. As we have seen in section 1.4.4, they must have the form:

$$\vec{E}(r, \psi, z, t) = \vec{E}_1(r) \exp j(\omega t - \beta z - v\psi)$$

where v , the azimuthal sequence, is an integer.

Since the optical fiber is a circular dielectric wave guide, we solve the propagation equation by developing Laplacian Δ into cylindrical coordinates (r, ψ, z) . Since this equation is vectorial, we solve it for the longitudinal E_z component (it is the simplest, as \vec{u}_z is a constant direction), resulting in:

$$\frac{d^2 E_{1z}}{dr^2} + \frac{1}{r} \frac{dE_{1z}}{dr} + \left(k_0^2 n(r)^2 - \beta^2 - \frac{v^2}{r^2} \right) E_{1z} = 0$$

and an analogous form for H .

Transverse components will be deduced by Maxwell equations, which, for fields of the form required, result in:

$$E_r = -\frac{j}{\kappa^2} \left(\beta \frac{\partial E_z}{\partial r} + \frac{\omega \mu_0}{r} \frac{\partial H_z}{\partial \psi} \right) \quad H_r = -\frac{j}{\kappa^2} \left(\beta \frac{\partial H_z}{\partial r} - \frac{\omega \epsilon_0 n(r)^2}{r} \frac{\partial E_z}{\partial \psi} \right)$$

$$E_\psi = -\frac{j}{\kappa^2} \left(\frac{\beta}{r} \frac{\partial E_z}{\partial \psi} - \omega \mu_0 \frac{\partial H_z}{\partial r} \right) \quad H_\psi = -\frac{j}{\kappa^2} \left(\frac{\beta}{r} \frac{\partial H_z}{\partial \psi} + \omega \epsilon_0 n(r)^2 \frac{\partial E_z}{\partial r} \right)$$

with $\kappa^2 = k_0^2 n(r)^2 - \beta^2$ and $E_z = E_{1z} \exp(-v\psi)$.

2.1.2. Solution for step-index fiber optics

2.1.2.1. General form

When $n(r)$ is constant in each medium, the equation takes the classical Bessel function form, which has an analytical solution. We know that for guided modes, $k_0 n_2 < \beta < k_0 n_1$. Quantity $k_0^2 n^2 - \beta^2$ is therefore positive in the core and negative in the cladding, which determines two families of solutions:

– in the core: $E_{1z} = A.J_v \left(u \frac{r}{a} \right)$ and $H_{1z} = B.J_v \left(u \frac{r}{a} \right)$ with J_v Bessel function, $u^2 = a^2 (k_0^2 n_1^2 - \beta^2)$ and $r < a$;

– in the cladding: $E_{1z} = C.K_v \left(v \frac{r}{a} \right)$ and $H_{1z} = D.K_v \left(v \frac{r}{a} \right)$ with K_v modified Bessel function, also known as the Hankel function (it is the *evanescent field* of decreasing exponential shape), $v^2 = a^2 (\beta^2 - k_0^2 n_2^2)$ and $r > a$.

There are other mathematically possible solutions, but they are the only physically possible solutions, i.e. which transport a finite energy (they are bounded and lean towards 0 for $r \rightarrow \infty$).

2.1.2.2. Transverse components

Field components then have as complex amplitude all these terms that are multiplied by $\exp j(\omega t - \beta z)$:

– in the core: $E_z = A.J_v \left(u \frac{r}{a} \right) f(v\psi)$ and $H_z = B.J_v \left(u \frac{r}{a} \right) g(v\psi)$ with $f = \cos$ and $g = \sin$ for even modes, or $f = \sin$ and $g = -\cos$ for odd modes. This corresponds to both possible polarizations of a mode with a given wave vector. According to the previous equations, transverse components equal:

$$E_r = -j \frac{a^2}{u^2} \left(\beta \frac{u}{a} A.J'_v \left(\frac{ur}{a} \right) f(v\psi) + \frac{\omega \mu_0}{r} B.J_v \left(\frac{ur}{a} \right) v f(v\psi) \right)$$

$$E_\psi = -j \frac{a^2}{u^2} \left(\beta \frac{v}{r} A.J_v \left(\frac{ur}{a} \right) g(v\psi) - \omega \mu_0 \frac{u}{a} B.J'_v \left(\frac{ur}{a} \right) g(v\psi) \right)$$

$$H_r = -j \frac{a^2}{u^2} \left(\beta \frac{u}{a} B.J'_v \left(\frac{ur}{a} \right) g(v\psi) + \frac{\omega \epsilon_0 n_1^2}{r} A.J_v \left(\frac{ur}{a} \right) v g(v\psi) \right)$$

$$H_r = -j \frac{a^2}{u^2} \left(\beta \frac{v}{r} B J_v \left(\frac{ur}{a} \right) f(v\psi) + \omega \mu_0 n_1^2 \frac{u}{a} A J'_v \left(\frac{ur}{a} \right) f(v\psi) \right)$$

– in the cladding:

$$E_z = C K_v \left(v \frac{r}{a} \right) f(v\psi) \text{ and } H_z = D K_v \left(v \frac{r}{a} \right) g(v\psi)$$

$$E_r = j \frac{a^2}{v^2} \left(\beta \frac{v}{a} C K'_v \left(\frac{vr}{a} \right) f(v\psi) + \frac{\omega \mu_0}{r} D K_v \left(\frac{vr}{a} \right) g(v\psi) \right)$$

$$E_\psi = j \frac{a^2}{v^2} \left(-\beta \frac{v}{r} C K_v \left(\frac{vr}{a} \right) g(v\psi) - \omega \mu_0 \frac{v}{a} D K'_v \left(\frac{vr}{a} \right) f(v\psi) \right)$$

$$H_r = j \frac{a^2}{v^2} \left(\beta \frac{v}{a} D K'_v \left(\frac{vr}{a} \right) g(v\psi) + \frac{\omega \epsilon_0 n_2^2}{r} C K_v \left(\frac{vr}{a} \right) f(v\psi) \right)$$

$$H_\psi = j \frac{a^2}{v^2} \left(\beta \frac{v}{r} D K_v \left(\frac{vr}{a} \right) f(v\psi) - \omega \epsilon_0 n_2^2 \frac{v}{a} C K'_v \left(\frac{vr}{a} \right) g(v\psi) \right)$$

2.1.3. Mode calculation method

The above solutions depend on four integration constants noted as A, B, C, D. Determination of these parameters can be done with the help of continuity equations of tangent field components (in z and in ψ) at the core-cladding interface (where $r = a$). They provide a homogenous system with four linear equations in A, B, C, D, without a second member:

$$A J_v(u) - C K_v(v) = 0$$

$$B J_v(u) - D K_v(v) = 0$$

$$A \frac{\beta v}{u^2} J_v(u) - B \frac{k_0 Z_0}{u} J'_v(u) - C \frac{\beta v}{v^2} K_v(v) + D \frac{k_0 Z_0}{v} K'_v(v) = 0$$

$$A \frac{k_0 n_1^2}{u Z_0} J'_v(u) - B \frac{\beta v}{u^2} J_v(u) - C \frac{k_0 n_2^2}{v Z_0} K'_v(v) + D \frac{\beta v}{v^2} K_v(v) = 0$$

by using $\omega\mu_0 = k_0 Z_0$ and $\omega\epsilon_0 = k_0/Z_0$.

The solutions of this system (whose writing is identical for both polarizations) are usually zero, except if it is degenerated, i.e. if its determinant is zero. Physically, this means that only modes corresponding to certain discrete propagation constant values β (system eigenvalues) will propagate. The determinant notation (eigenvalues equation) is:

$$\left[\frac{J'_v(u)}{u.J_v(u)} + \frac{K'_v(v)}{v.K_v(v)} \right] \left[\frac{k_0^2 n_1^2 J'_v(u)}{u.J_v(u)} + \frac{k_0^2 n_2^2 K'_v(v)}{v.K_v(v)} \right] = \beta v \left[\frac{1}{u^2} + \frac{1}{v^2} \right]^2$$

For a given v , it is an equation with an unknown, which is β : in fact, previously defined u and v only depend on β and constant terms. We must therefore search for solutions of this equation between $k_0 n_2$ and $k_0 n_1$. These solutions depend on the azimuthal v order.

2.1.4. Nature of modes

2.1.4.1. Transverse modes

If $v = 0$, the second member is zero and the mode is a *transverse mode*, TE_{0m} or TM_{0m} (depending on its polarization). Geometrically it is a *meridional ray* (remaining in a plane containing the fiber axis). We then determine:

– **TE_{0m} mode:** m^{th} solution of $\left[\frac{J_1(u)}{u.J_0(u)} + \frac{K_1(v)}{v.K_0(v)} \right] = 0$ so A and C equal zero and

$E_{1z} = 0$. In this transverse electric mode, the electric field has an orthoradial distribution (see Figure 2.1);

– **TM_{0m} mode:** m^{th} solution of $\frac{n_1^2 J_1(u)}{u J_0(u)} + \frac{n_2^2 K_1(v)}{v K_0(v)} = 0$ then B and D equal zero

and $H_{1z} = 0$. In this transverse magnetic mode, the electric field has a radial distribution. In both cases, field lines have revolution symmetry, but that is not the case with intensity distribution.

These equations are established by using: $J'_0(u) = -J_1(u)$ and $K'_0(v) = -K_1(v)$.

2.1.4.2. Hybrid modes

If $v \neq 0$, we have a hybrid mode HE_{vm} or EH_{vm} (where none of the longitudinal components are zero). Geometrically, the propagation axis of these modes

helicoidally turns around that of the fiber. There is no exact solution, but an approximation is possible if the index difference is very small ($n_1^2 - n_2^2 \ll n_1^2$, hypothesis said to be *weakly guiding*): we can then do $k_0 n_2 \approx k_0 n_1 \approx \beta$ and the equation is simplified in:

$$\left[\frac{J'_v(u)}{u.J_v(u)} + \frac{K'_v(v)}{v.K_v(v)} \right] = \pm v \left[\frac{1}{u^2} + \frac{1}{v^2} \right]$$

By using the properties of Bessel functions, notably:

$$\left[\frac{J'_v(u)}{u.J_v(u)} \right] = \left[\frac{J_{v-1}(u)}{u.J_v(u)} \right] - \frac{v}{u^2} = - \left[\frac{J_{v+1}(u)}{u.J_v(u)} \right] + \frac{v}{u^2}$$

and:

$$\left[\frac{K'_v(v)}{v.K_v(v)} \right] = \left[\frac{K_{v-1}(v)}{v.K_v(v)} \right] - \frac{v}{v^2} = - \left[\frac{K_{v+1}(v)}{v.K_v(v)} \right] + \frac{v}{v^2}$$

we determine:

$$- \mathbf{EH}_{vm} \text{ mode: } m^{\text{th}} \text{ solution of } \left[\frac{J_{v+1}(u)}{u.J_v(u)} + \frac{K_{v+1}(v)}{v.K_v(v)} \right] = 0 \text{ (corresponds to } + \text{ sign);}$$

$$- \mathbf{HE}_{vm} \text{ mode: } m^{\text{th}} \text{ solution of } \left[\frac{J_{v-1}(u)}{u.J_v(u)} - \frac{K_{v-1}(v)}{v.K_v(v)} \right] = 0 \text{ (corresponds to } - \text{ sign).}$$

Because of the expressions of transverse components (respectively in $\pm \cos v\psi$ and $\sin v\psi$), we observe a property of \mathbf{HE}_{1m} modes: their transverse field practically keeps the same direction throughout the fiber section. These are quasi-linear polarization modes. This property is all the more true the smaller the index difference.

2.1.5. Cut-off frequency

In a dielectric guide, the cut-off corresponds to the limit refraction. The mode approaches a plane wave, which is transversally infinite. We then have:

$$- \beta \rightarrow k_0 n_2 \text{ hence } u \rightarrow V \text{ and } v \rightarrow 0; \text{ with } V, \text{ normalized frequency: } V = a.k_0 \sqrt{n_1^2 - n_2^2};$$

– $E_z \rightarrow 0$ hence $J_v(u) \rightarrow 0$ when $u \rightarrow V$.

These relations enable *cut-off frequency* calculation for each mode, i.e. the frequency above which it is no longer guided (it is then refracted in cladding). By using the following correspondences, for modified Bessel functions, when $v \rightarrow 0$:

$$K_0(v) \rightarrow -\text{Log } v; K_1(v) \rightarrow 1/v; K_v(v) \rightarrow \frac{2^{v-1}}{v^v} (v-1)!$$

we obtain the limits of the ratio involved in the equations which determine modes:

– for TE_{0m} and TM_{0m} modes: $\frac{K_1(v)}{v.K_0(v)} \rightarrow \infty$, it is necessary that $\frac{uJ_0(u)}{J_1(u)} \rightarrow 0$

when $u \rightarrow V$; cut-off of these modes then corresponds to m^{th} root of $J_0(V)$;

– for HE_{1m} modes: $\frac{K_0(v)}{v.K_1(v)} \rightarrow \infty$, it is necessary that $\frac{uJ_1(u)}{J_0(u)} \rightarrow 0$ when $u \rightarrow V$;

their cut-off then corresponds to m^{th} root of $J_1(V)$, $V = 0$ being the first;

– for EH_{vm} modes: $\frac{K_{v+1}(v)}{v.K_v(v)} \rightarrow \infty$, it is necessary that $\frac{uJ_v(u)}{J_{v+1}(u)} \rightarrow 0$ when $u \rightarrow V$;

their cut-off corresponds to non-zero root m of $J_v(V)$; as the ratio leans toward 1 when $u \rightarrow 0$, $V = 0$ is not a cut-off frequency;

– for HE_{vm} ($v > 1$) modes: $\frac{K_{v+1}(v)}{v.K_v(v)} \rightarrow \frac{1}{2(v-1)}$; it will be necessary that

$$\frac{J_{v-1}(u)}{u.J_v(u)} \rightarrow \frac{1}{2(v-1)}, \text{ but } 2(v-1) \frac{J_{v-1}(u)}{u.J_v(u)} = 1 + \frac{J_{v-2}(u)}{J_v(u)}: \text{ from which } \frac{J_{v-2}(u)}{J_v(u)} \rightarrow 0$$

when $u \rightarrow V$; cut-off of these modes corresponds to the m^{th} non-zero root m of $J_{v-2}(V)$; this time the ratio leans towards ∞ when $u \rightarrow 0$, $V = 0$ is not a cut-off frequency.

An essential property of circular dielectric wave guides is that the mode HE_{11} has a zero cut-off frequency: it is (in theory) guided regardless of wavelength.

The first non-zero cut-off frequency is the one of modes TE_{01} , TM_{01} and HE_{21} : it corresponds to $V = 2.405$, first root of $J_0(V)$. For $V < 2.405$, the fiber-optic is single mode.

2.1.6. Aspect of modes

The dispersion diagram (see Figure 2.1) gives the value of β/k_0 , or apparent index of each mode, versus the normalized frequency V . As we know, this value equals n_2 at each mode's cut-off, and leans toward n_1 when $V \rightarrow \infty$.

In this diagram, we see certain modes associate in groups of neighboring cut-off frequency and propagation constant $\beta(V)$. The resulting field of the superposition of these modes, which remain in phase together, is almost linear polarization. These groups are called *pseudo-modes* and are denoted $LP_{\ell m}$ (linear polarization) defined by:

- mode $LP_{0m} = \text{mode } HE_{1m}$ (in this way, fundamental mode HE_{11} is called LP_{01});
- mode $LP_{1m} = \text{modes } TE_{0m}, TM_{0m}, HE_{2m}$;
- mode $LP_{\ell m} = \text{modes } HE_{(\ell+1),m} \text{ and } EH_{(\ell-1),m} \text{ (for } \ell > 1 \text{)}.$

Physically, ℓ (azimuthal order) corresponds to the number of field periods over a circumference. Therefore, when this circumference has been traveled, there are 2ℓ maxima and 2ℓ zeros of mode intensity. Order m (radial order) corresponds to the number of intensity maxima over a radius, from the axis. LP_{0m} mode intensity has a symmetry of revolution, with a maximum on axis; other modes have zero intensity on the axis.

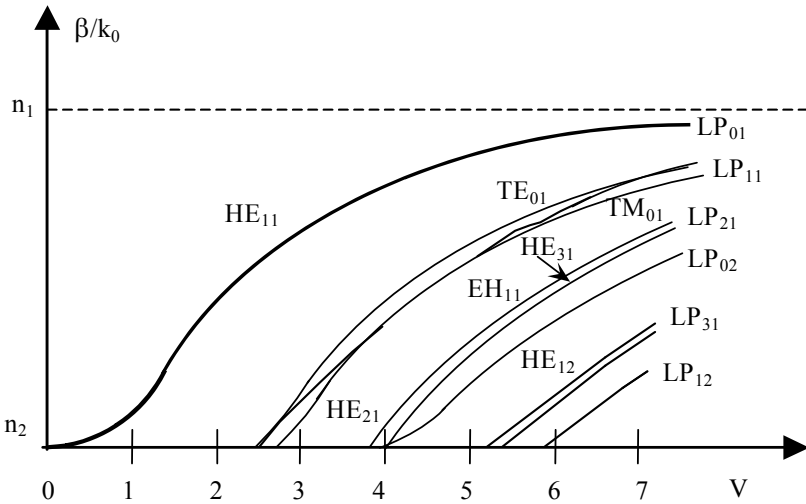


Figure 2.1. Dispersion diagram of step-index fiber

The transverse field of mode $LP_{\ell m}$ can be written from previous relations. In weakly guiding hypothesis and again in Cartesian coordinates, we obtain:

$$-E_x = E_0 J_\ell \left(u \frac{r}{a} \right) \cos(\ell \psi) \text{ and } E_y = 0 \text{ hence } H_x = 0 \text{ and } H_y = E_x \frac{n_1}{Z_0} \text{ in the core;}$$

$$-E_x = E_0 \frac{J_\ell(u)}{K_\ell(v)} K_\ell \left(v \frac{r}{a} \right) \cos(\ell \psi) \text{ and } E_y = 0 \text{ hence } H_x = 0 \text{ and } H_y = E_x \frac{n_2}{Z_0} \text{ in}$$

the cladding.

Longitudinal field components are more complex because they are the result of hybrid mode integration, except for modes LP_{0m} (we will be able to rebuild it with the expressions in section 2.1.2). They are of low amplitude compared to transverse components, especially for modes far from their cut-off. Polarization of mode (in x here) is determined by the polarization at the fiber entrance. Both orthogonal polarizations of mode LP_{01} , and all their linear combinations, propagate with the same constant β if the fiber is perfectly isotropic (see section 2.4 for the non-isotropic case where a birefringence appears). E_0 can be determined by light power P_0 injected at the fiber entrance:

$$P_0 = \iint_{xy} E(x,y) H^*(x,y) dx dy$$

over the fiber-optic section, including the cladding. It guides a significant part of the power, especially for modes close to cut-off. Figure 2.2 represents fields and light intensity for the first pseudo-modes.

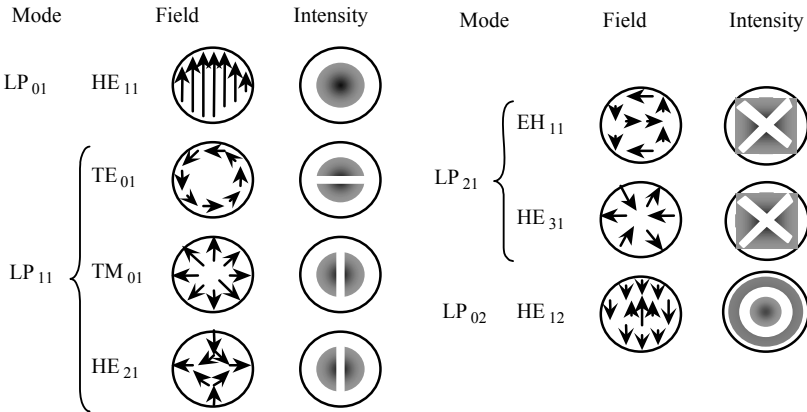


Figure 2.2. Step-index fiber modes

2.2. Single-mode fiber characteristics

2.2.1. Single-mode propagation condition

According to the previous calculations, in step-index optical fibers, this is written as:

$$V = \frac{2\pi a}{\lambda} \sqrt{n_1^2 - n_2^2} < 2.405$$

which is the first zero of $J_0(V)$ and corresponds to the cut-off of modes TE_{01} and TM_{01} , modes just above the fundamental mode.

This condition can be reached when the core diameter is small (less than 10 μm) and the index difference is low (less than 0.5%), justifying the weakly guiding hypothesis.

Consequently, the fiber is single-mode only beyond the corresponding wavelength, called *cut-off wavelength*, given by:

$$\lambda_c = \frac{2\pi a}{2.405} \sqrt{n_1^2 - n_2^2}$$

The main advantage of single-mode fibers (SMF) is their very large bandwidth allowing long distance transmissions, since there is no longer intermodal dispersion. They also have instrumentation applications because they maintain the coherence of the light, and its polarization for certain types of fibers.

Their main limitation comes from the small core diameter, requiring very high precision at the connections, as well as the use of laser sources; these two elements are more expensive than with multimode fibers (whereas the fiber itself is cheaper than good graded-index fibers).

The term “single-mode” means that for each wavelength (higher than λ_c) only one mode propagates, and does not mean that the fiber only guides one wavelength: on the contrary, single-mode fibers are very well suited for wavelength division multiplexing. In this case, the different wavelengths overlap without interfering, at least insofar as non-linear effects are insignificant.

2.2.2. Gaussian single-mode fiber model

According to previous results, mode LP_{01} field has as expression:

$E(r, \psi, z, t) = E(r) \exp j(\omega t - \beta z)$ with:

$$E_x = E_0 J_0\left(u \frac{r}{a}\right) \text{ in the core, } E_0 \frac{J_0(u)}{K_0(v)} K_0\left(v \frac{r}{a}\right) \text{ in cladding;}$$

$E_y = 0$ (if Ox is the polarization direction of the injected light);

E_z , longitudinal field, has a negligible amplitude compared to the transverse field (in low guidance approximation) but this amplitude, in $J_1(u.r/a)$, is not zero: mode LP_{01} is in fact not a transverse mode.

As we can see in Figure 2.3, the intensity profile of the transverse field, which has a revolution symmetry, is of Gaussian shape and it is written in an approximate manner:

$$E(r) = E_0 \exp\left(-\frac{r^2}{w_0^2}\right)$$

where $2w_0$ is called the *mode field diameter* or mode diameter. This approximation is particularly valid for V ranging between 1.8 and 2.4, i.e. by getting closer to the cut-off. It makes it possible to use Gaussian beam formalism applying to laser beams in particular. A good coupling between lasers and single-mode fibers can be achieved with the use of an appropriate lens.

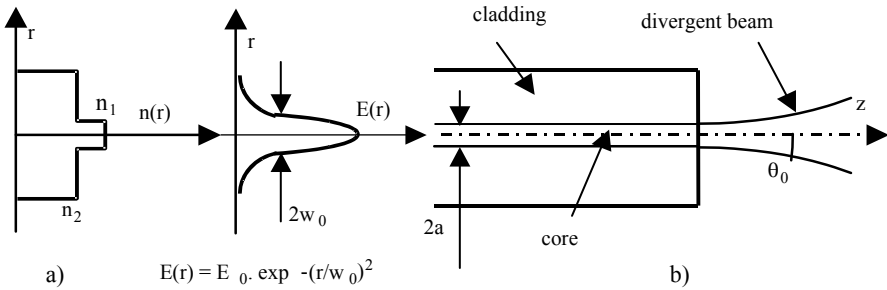


Figure 2.3. Single-mode optical fiber

This quasi-Gaussian field distribution, which greatly spreads in cladding, is directly linked to the diffraction phenomenon, which also occurs by a light divergence at fiber-optic output under the form of a Gaussian beam with an angle of aperture at $1/e$:

$$\theta_0 = \frac{\lambda}{\pi w_0} \text{ (see Figure 2.3)}$$

This divergence is not of the same nature as for a multimode fiber, because it is a spatially coherent wave, propagating in direction z from the light source or fiber output. At this point (near field), the wave is plane and has a Gaussian distribution. In far field, near field Fourier transform, the distribution is also Gaussian and the beam can be refocused with a lens.

2.2.3. Single-mode fiber parameters

As with multimode fibers, single-mode fibers can be defined by core-cladding diameters and by the relative index difference Δ . These primary parameters are characteristic of fiber manufacturing. For reasons of convenience of measurement (see Chapter 3) and use, they are more often characterized by their secondary parameters which are:

- the cut-off wavelength $\lambda_c = \frac{2\pi a}{2,405} \sqrt{n_1^2 - n_2^2} = \frac{2\pi a}{2,405} n_1 \sqrt{2\Delta}$

At a given wavelength, the fiber is single mode if product $a\sqrt{2\Delta}$ is lower than a constant proportional to λ . It is therefore harder to produce and use a single-mode fiber at $0.85 \mu\text{m}$ or in visible light than at 1.3 or $1.55 \mu\text{m}$; however, this type of fiber has applications in instrumentation;

- the mode field diameter resulting from the Gaussian approximation. We can establish its value by using the Marcuse numerical approximation:

$$w_0/a = 0.65 + 1.619 V^{-1.5} + 2.879 V^{-6}$$

Close to the cut-off, the mode field diameter is close to the core diameter, but it quickly increases when V decreases, i.e. when the wavelength increases. This mode spreading in cladding makes the propagation increasingly sensitive to the optical fiber deformations. Its use for $V < 1.6$ is not recommended.

A single-mode fiber can be characterized by its primary parameters, or by its secondary parameters. With core diameter and index difference, we have two degrees of freedom (contrary to the case of the metallic wave guide) which will be used for optimizing attenuation and dispersion.

2.3. Dispersion in single-mode fibers

2.3.1. Chromatic dispersion

Although much lower than in a multimode fiber, pulse broadening in a single-mode fiber is not zero, because chromatic dispersion remains, creating a broadening

$\Delta\tau_c$ after a unit length of fiber. We have seen in Chapter 1 that we can write at first order:

$$\Delta\tau_c = D_c \cdot \Delta\lambda$$

with:

- $\Delta\lambda$ spectral source width;
- D_c chromatic dispersion coefficient, which depends on fiber parameters and wavelength. We can calculate it by:

$$D_c = \frac{d\tau_g}{d\lambda} \text{ expressed in ps/nm/km and is deduced from } \tau_g(\lambda) \text{ calculation}$$

thus:

$$\tau_g = \frac{d\beta}{d\omega} = \frac{1}{c} \frac{d\beta}{dk_0} \text{ with } c \text{ light velocity in the vacuum.}$$

In order to use normalized results, we introduce:

$$B = \frac{\beta^2 - k_0^2 n_2^2}{k_0^2 (n_1^2 - n_2^2)} \text{ normalized propagation constant.}$$

This dimensionless term equals 0 at cut-off ($\beta = k_0 n_2$) and leans towards 1 for $V \rightarrow \infty$ ($\beta \rightarrow k_0 n_1$). With the weakly guiding approximation ($n_1^2 \gg n_1^2 - n_2^2$), we can then write:

$$\beta = k_0 [n_2 + B (n_1 - n_2)]$$

that we will derive with respect to k_0 :

$$\frac{d\beta}{dk_0} = N_2 + B (N_1 - N_2) + k_0 (n_1 - n_2) \frac{dB}{dk_0}$$

with:

$$N_i = n_i + k_0 \frac{dn_i}{dk_0} = n_i - \lambda \frac{d\lambda}{dk_0} \text{ group index of medium } i \text{ (} i = 1 \text{ or } 2\text{)}$$

By accepting that $N_1 - N_2 \approx n_1 - n_2$ we arrive at:

$$\tau_g = \frac{1}{c} [N_2 + (N_1 - N_2) \frac{d(VB)}{dV}]$$

This group delay varies from N_2/c , its value at cut-off (it is the inverse of group delay in the cladding), to N_1/c which is, at infinity, the inverse of group delay in the core.

We then obtain τ_g versus λ . By neglecting terms of the second order, we arrive at:

$$\frac{d\tau_g}{d\lambda} = M_2 + (M_1 - M_2) \frac{d(VB)}{dV} - \frac{N_1 - N_2}{c\lambda} \cdot \frac{N_2}{n_2} V \cdot \frac{d^2(VB)}{dV^2}$$

with:

$$M_i = -\frac{\lambda}{c} \cdot \frac{d^2 n_i}{d\lambda^2} \text{ material dispersion of medium } i \text{ (} i = 1 \text{ or } 2\text{)}.$$

The sum of the first two terms, close to M_1 and which we will note as D_M , is the material dispersion caused by the variation of its index with λ . It cancels out at the neighborhood of $1.3 \mu\text{m}$, which is the main advantage of this wavelength.

The last term, low and always negative, is the *waveguide dispersion*; it depends on guidance parameters, is zero for $V \rightarrow 0$ and ∞ (we lean toward a homogenous environment with two limits), and reaches a maximum when the mode is strongly shared between the core and the cladding.

2.3.2. Practical calculation

By using $n \approx N$ we can write a simplified formula of the chromatic dispersion coefficient:

$$-D_c = D_M - \frac{\Delta n}{c\lambda} \cdot V \cdot \frac{d^2(VB)}{dV^2} \text{ with } \Delta n = n_1 - n_2 \text{ (absolute index difference, not to}$$

be confused with the relative difference Δ);

$$-B, \frac{d(VB)}{dV} \text{ and } V \frac{d^2(VB)}{dV^2} \text{ without dimension, are determined according to } V$$

with a numerical calculus. For step-index structure, their curves are given in Figure 2.4. For this same structure and for $1.7 < V < 2.4$ we can use the approximation:

$$V \frac{d^2(VB)}{dV^2} = \frac{1.98}{V^2}$$

For other structures, these parameters must be recalculated, which is possible with numerical methods, and can result in quite different guide dispersion properties.

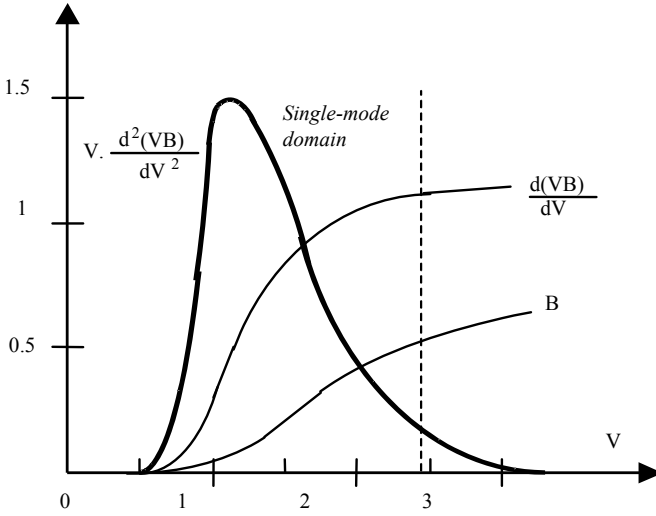


Figure 2.4. Normalized constants

2.3.3. Cancellation of chromatic dispersion

In silica, D_M cancels at $1.27 \mu\text{m}$. This term is negative underneath (dispersion said to be ordinary, that is observed in visible light) and positive above (dispersion said to be extra-ordinary). The guide dispersion is always negative: in fact, if the wavelength increases, the mode spreads wider in the cladding, decreasing its propagation time. We can, in theory, cancel chromatic dispersion for $\lambda > 1.27 \mu\text{m}$, if:

$$\frac{(n_1 - n_2)}{c\lambda} V \frac{d^2(VB)}{dV^2} = D_M$$

In the neighborhood of $1.3 \mu\text{m}$, we easily obtain this cancellation with standard fibers. By modifying the fiber structure we can also shift the zero dispersion wavelength at $1.55 \mu\text{m}$, where the minimum silica fiber attenuation is found

(*dispersion shifted* fiber, see section 2.3.5). However, in order to achieve that, it is necessary to:

- increase the index difference to V constant, which means the core diameter must be decreased; then intrinsic losses (by core index increase) and connection losses (by mode field diameter decrease) increase; or
- keep the index difference and decrease V , therefore a (in other words, decrease λ_c); a decrease of V results in the fact that the mode is not as well guided and leaks more easily.

From the attenuation point of view, these solutions are therefore not optimal and different profiles must be used, the simplest being the depressed inner cladding profile (see section 2.3.4). More complex index profiles (triangle, trapezium, trench, etc.) have also been developed for obtaining specific dispersion curves (lower and of lower slope). Propagation and dispersion calculations of these fibers are based on finite element numerical methods.

2.3.4. Depressed inner cladding fibers

The principle of these fibers is simply to increase the core-cladding index difference by decreasing the cladding index (see Figure 2.5), by incorporating fluorine. This makes it possible to avoid increasing the core index by increasing the quantity of germanium oxide, therefore attenuation. It is even possible to produce pure silica core fibers. However, for production reasons (see Chapter 3), it is necessary to preserve a pure silica external cladding. The index decreases in the inner cladding part, hence the name depressed inner cladding (DIC) profile.

In general, the thickness of this inner cladding is much larger than the penetration depth of the evanescent field. The external cladding plays a negligible role in the propagation, and we can, in parameter calculations (including dispersion), consider a parameter equivalent step-index fiber:

$$a_e \approx a \text{ and } \Delta n_e \approx \Delta n = \Delta n^+ + \Delta n^-$$

Δn^+ is the index difference between the core and pure silica; this term, proportional to the quantity of germanium oxide, directly occurs in intrinsic attenuation.

The depressed inner cladding fiber increases guide dispersion, and thus decreases global chromatic dispersion, without increasing attenuation. On the other hand, it presents a LP_{01} mode cut-off for a wavelength such that: $\beta = k_0 n_3$. In fact, when λ

increases, β/k_0 decreases and becomes lower than n_3 ; in addition, the mode diameter increases, which leads to a leakage of the mode in the outer cladding.

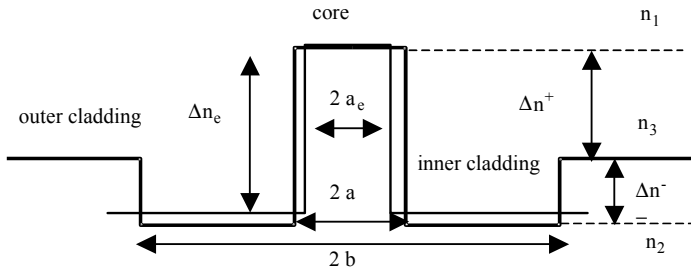


Figure 2.5. *Depressed inner cladding fiber*

Pure core silica depressed inner cladding fibers were designed to benefit from very low attenuation (the theoretical minimum being close to 0.15 dB/km) as well as low sensitivity to radiation (whereas germanium oxide darkens), which is useful for spatial applications or in nuclear physics for example. However, these fibers are very sensitive to curves.

2.3.5. Different types of single-mode fibers

The International Telecommunication Union (ITU-T) standardized several types of single-mode fibers for telecommunications (see Figure 2.6).

2.3.5.1. Standard fiber

Under the ITU G 652 standard, the standard fiber is the oldest, with a core diameter of 9 μm ; its dispersion cancels out at approximately 1.3 μm , which is its optimal use wavelength, mainly in very high bitrate local and metropolitan networks. However, it can also be used at 1.55 μm with monochromatic laser diodes ($\Delta\lambda \approx 0.1$ nm); in the absence of optical amplifier, the distance is limited by attenuation and this solution is satisfying, at least up to 2.5 Gbit/s bitrate.

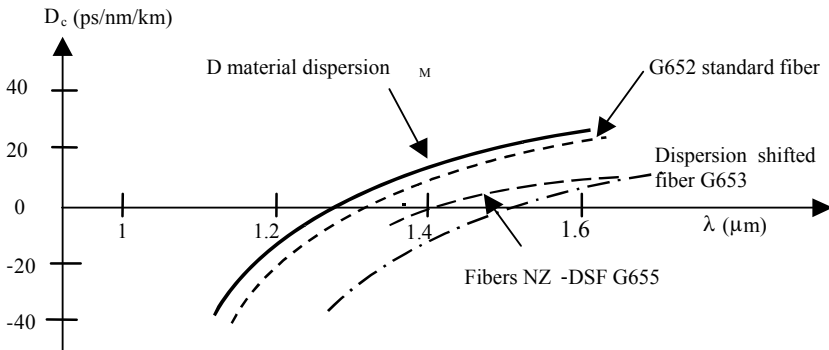


Figure 2.6. Chromatic dispersion of single-mode fibers

2.3.5.2. Dispersion shifted fiber

A G 653 standard *dispersion shifted fiber* or DSF has a 7 μm core diameter and an index profile that is often more complex, in triangle or trapezium. Its dispersion cancels out at approximately 1.55 μm , but its attenuation is slightly higher. It was mostly used for very long distance optical amplifier connections, where the critical parameter is dispersion and not attenuation, but it is not very compatible with WDM, because dispersion cannot be cancelled for all wavelengths, and zero dispersion leads to the accumulation of non-linear effects. It retreats to benefit the G 655 fiber.

2.3.5.3. Non-zero dispersion shifted fiber

The more recent (1995) G 655 standard NZ-DSF (non-zero dispersion shifted fiber) has a chromatic dispersion reduced to a low value, but non-zero (from 3 to 6 ps/km/nm in the 3rd window); it is in fact a family of fibers with parameters (and commercial names) that are different from one manufacturer to another. Thanks to a larger core diameter, it does not have as many losses as previously, and in addition is less sensitive to non-linear effects.

It is therefore well adapted to wavelength division multiplexing. The slope of its dispersion ($dD_c/d\lambda$) is lower than for the previous fibers (from 0.05 to 0.1 ps/km/nm²).

In 2004, the G 656 fiber was normalized, which is a variation presenting a higher dispersion over a larger bandwidth (2 to 14 ps/km/nm from 1,500 to 1,610 nm) adapted to coarse wavelength division multiplexing WDM (CWDM, see Chapter 5).

2.3.6. Chromatic dispersion compensation

A non-zero chromatic dispersion can be optically compensated with the help of a short fiber section of high negative dispersion (but generally of high attenuation) called DCF (*dispersion compensating fiber*). A chromatic dispersion compensating device (using a Bragg grating for example, see Chapter 4) can also be used to play this role, which is to delay the wavelengths arriving first.

This device is characterized by its slope, in ps/nm, which must be equal to $-D_c \cdot L$ in order to compensate the chromatic dispersion at the end of a fiber length L , independently from the source's spectral width $\Delta\lambda$. The development of these devices is delicate but their principle is simple; compensation is possible because as long as the propagation remains linear, the different wavelengths of a single signal do not interfere, contrary to the different multimode fibers or to both polarizations in a single-mode fiber.

In a wavelength division multiplexing system, dispersion compensation is generally applied in two steps: a rough compensation for the complete spectrum for each section, which is not very precise because it is difficult to have a fiber or a device with dispersion that is exactly symmetric to the link fiber in the whole spectrum, followed by a fine compensation, wavelength by wavelength, after the demultiplexer. This method is quite suitable for the NZ-DSF fiber but also allows the reuse of standard fibers at 1.55 μm .

2.4. Polarization effects in single-mode fibers

2.4.1. Birefringence of optical fibers

In theory, a single-mode optical fiber is isotropic, and the mode propagation constant β does not depend on light polarization. We then find, depending on injection conditions, classical polarization states in an isotropic medium (linear, circular or elliptical polarization).

In practice, single-mode fibers are not rigorously isotropic, because the core fiber is not perfectly circular (an elliptical core fiber is birefringent), and moreover a birefringence can exist, induced intentionally or not, by external causes which occur non-isotropically. In this case, propagation constants β_x and β_y according to x and y (main birefringence axes) are no longer equal, and a birefringence appears, characterized by:

$$-\Delta\beta = \beta_x - \beta_y \text{ (generally } \Delta\beta \ll \beta \approx \beta_x \approx \beta_y);$$

$$-B_R = \Delta\beta/\beta \text{ relative birefringence;}$$

$$- L_b = \frac{2\pi}{\Delta\beta} \approx \frac{\lambda}{n_1 B_R} \text{ beat length, at the end of which the fast axis wave has}$$

reached a phase advance of 2π over the other.

An initial polarization state other than a linear polarization along x or y (polarization eigenmodes) will therefore not be preserved. The resulting polarization will be a combination of the two eigenmodes but, because of the coupling, the light is depolarized along the fiber.

This is not intrinsically annoying in telecommunications, because receivers, and even erbium-doped fiber amplifiers, are not sensitive to the polarization. However, there appears between both inherent polarization modes a dispersion of the intermodal type, which, by unit of length equals:

$$\Delta\tau_p = \frac{1}{c} \cdot \frac{d(\Delta\beta)}{dk_0} \approx \frac{n_1 B_R}{c} \text{ in ps/km}$$

This dispersion term, called DGD (differential group delay), is weak but not necessarily negligible compared to the chromatic dispersion when it has been compensated.

2.4.2. Induced birefringence

The effects of induced birefringence are very interesting in sensors, because they can make the fiber sensitive to some parameters which do not modify the power transmitted and are therefore not (or not very) sensitive in telecommunications. There are mainly:

- mechanical constraints caused by the photo-elasticity phenomenon: a transversal (compression) force F , by unit of length, applied along the axis y , causes a linear birefringence proportional to F and of slow axis y ; a bending of radius R in plane yOz causes a linear birefringence proportional to $1/R^2$, the fast axis is aligned with y . In addition to the application to constraint sensors, the fiber bending is a simple way to control polarization in a laboratory;

- a fiber twist of N turns around its axis, resulting in circular birefringence from photo-elasticity, or in other words a rotation of the polarization axis, of an angle proportional to N . This property is used for developing fibers preserving the state of polarization while presenting a low linear birefringence;

- a longitudinal magnetic field of intensity H , resulting in a rotation of the polarization of angle $\theta = V_F \cdot H \cdot L$ over a length L . This is the Faraday effect, which is non-reciprocal: the direction of rotation depends on the light propagation direction.

V_F , the Verdet constant, is very low in silica (approximately $4 \cdot 10^{-6}$ rd/A). This effect is used to develop isolators (see Chapter 5), current sensors, and magneto-optical disk reading.

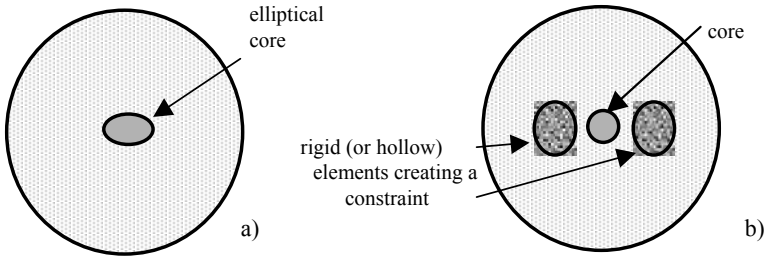


Figure 2.7. *Two types of single-mode fibers with constant polarization*

Mechanically induced birefringence (by permanent internal constraints) is also used to develop high birefringence fibers, called “polarization maintenance fibers”, which only guide one light polarization direction (see Figure 2.7). Expensive and of high attenuation, they are difficult to connect, because the correct orientation of both fibers must be achieved. They are used in some instrumental applications, or some interferometric sensors (gyroscope, constraint sensors) requiring polarized light.

2.4.3. Polarization dispersion

Polarization dispersion mainly occurs in optical amplification links, because of the very long lengths involved. In this case, because of the random character of the birefringence and the existence of coupling between both polarizations, pulse broadening $\Delta\tau_p$ caused by this effect increases proportionally to \sqrt{L} (L distance traveled):

$$\Delta\tau_p = \text{PMD} \cdot \sqrt{L} \text{ with PMD (polarization mode dispersion) in ps}/\sqrt{\text{km}}$$

If a single-mode fiber presents chromatic dispersion and polarization dispersion simultaneously, global pulse widening follows a quadratic combination law for these two phenomena, as with between the two dispersions of a multimode fiber:

$$\Delta\tau = \sqrt{\Delta\tau_c^2 + \Delta\tau_p^2} \text{ to calculate at the end of length } L$$

$\Delta\tau_p$ is generally much lower than $\Delta\tau_c$ at the end of the fiber, but it is not the case when a chromatic dispersion compensation device is used: polarization dispersion may become the factor limiting the link length. In fact, optical compensation of polarization dispersion is possible in theory, and partially achievable with retardation plates, but it cannot be perfect because of coupling between both polarizations. This phenomenon also prohibits the use of multiplexing of two signals over two orthogonal polarizations in practice, which has been demonstrated in lab conditions.

It is therefore necessary to use very low average birefringence fibers, with PMD much lower than $1 \text{ ps}/\sqrt{\text{km}}$ (classical standard fiber value); current G 655 fibers must not exceed $0.2 \text{ ps}/\sqrt{\text{km}}$, and the best submarine fibers reach $0.05 \text{ ps}/\sqrt{\text{km}}$. However, this is their manufacturing value, and cabling and laying must not deteriorate it (notably with bendings or other constraints).

2.5. Non-linear effects in optical fibers

2.5.1. Introduction

Glasses used in optical fibers, silica in particular, show extremely low non-linear effects in standard uses. However, these effects can be observed in single-mode fibers for relatively low power for two reasons:

- very low section of the fiber core, hence significant intensities (power densities);
- large interaction length, since the light propagates with few losses over very long distances.

Non-linear effects reveal power thresholds beyond which transmission is no longer adequate. These thresholds are higher than the normal power of sources, but may be reached in optically amplified and wavelength division multiplexed systems. On the other hand, they enable new applications: index change, frequency transpositions, interaction between two waves controlled by light, etc.

Non-linear optics is a discipline in its own right, opening new perspectives in processing, switching and optical storing of information. Hereafter, we will focus on the main non-linear effects in optical fibers.

2.5.2. Raman scattering

Raman scattering is a photon-phonon interaction, i.e. exchange of energy between optical wave and the vibrations of the material's molecular bonds.

When a *pump wave* goes through material, some photons transfer a part of their energy $h\nu_p$ to a phonon, a particle associated with the vibration of frequency $\delta\nu$ appearing in the matter. They are then scattered with lower energy, or in other words with a higher wavelength, and constitute a *Stokes wave* of frequency:

$$\nu_s = \nu_p - \delta\nu$$

Frequency shift: $\delta\nu = \nu_p - \nu_s$ depends only on the material, and not on the pump wavelength. Thus, the Stokes wave spectrum is represented independently from it, versus $\delta\nu/c$ expressed in cm^{-1} . In crystals, several rays may be observed in the spectrum of this wave, corresponding to the different vibration frequencies of interatomic bonds. In disorganized environments (glass, liquids) on the other hand, a relatively large continuous spectrum can be observed, where the peaks are characteristic of their composition (silica presents a peak characteristic at 490 cm^{-1}). It is a well-known method of analysis in chemistry.

Reciprocally, a few phonons will give their energy to photons, who in turn will scatter in the form of an *anti-Stokes wave* with a frequency:

$$\nu_a = \nu_p + \delta\nu \text{ therefore a lower wavelength}$$

The anti-Stokes wave spectrum is related to the Stokes wave spectrum and greatly depends on temperature T , which creates phonons by thermal agitation (see Figure 2.8). The ratio between Stokes and anti-Stokes rays equals:

$$\frac{\sigma_s(\delta\nu)}{\sigma_a(\delta\nu)} = \exp \frac{h \cdot \delta\nu}{kT}$$

This ratio only depends on temperature, making it possible to use Raman spectrometry to know the composition and temperature of the medium. When $T = 0 \text{ }^\circ\text{K}$, the anti-Stokes spectrum disappears (there is no thermal agitation any longer), and the Stokes spectrum is proportional to $\sigma_0(\delta\nu)$.

During propagation of the pump wave along an optical fiber, the Stokes wave, constantly provided with photons, is amplified according to an exponential law where the coefficient of gain is proportional to the pump wave power. When the gain becomes high, either because the pump wave is strong or because the interaction length is large, the Stokes wave empties the pump wave and creates new

rays. Then Stimulated Raman Scattering (SRS) occurs, which produces a quasi-continuous spectrum over a large range of wavelengths. This “multi-Stokes emission” is used in instrumentation to generate very short pulses (less than 100 ps) with a very large spectrum.

The Raman effect can also be used to obtain the *optical amplification* of an incident wave corresponding to one of the multi-Stokes emission wavelength. Its main advantage is that only the frequency shift between pump and Stokes waves (and not the frequencies themselves) is imposed by the amplifier medium: any wavelength can be amplified, as long as the wavelength of the pump wave is chosen accordingly. However, the quantum efficiency of such amplification is very bad in the silica and requires sources of high power (YAG laser at 1.06 μm); that is why amplification in rare earth doped fibers was preferred (see Chapter 8).

The advantage of the Raman amplification remains for future large number of wavelength systems, because it makes it possible to amplify wavelengths located outside of the erbium band and does not require special fibers: The line fiber itself becomes amplifying thanks to the pump wave.

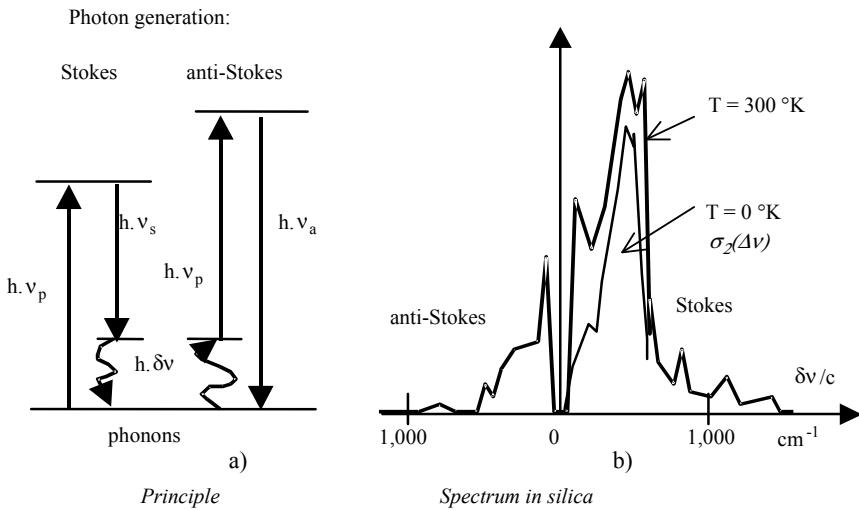


Figure 2.8. Raman scattering: a) principle; b) spectrum in silica

2.5.3. Brillouin scattering

Brillouin scattering follows a mechanism similar to Raman scattering, but the interaction occurs with acoustic phonons, i.e. material vibrations propagate at V_a

velocity of acoustic waves, a few thousand m/s. The resulting shift in frequency $\delta\nu_B$ is very low and is determined by a phase matching rule between optical and acoustic waves:

$$\delta\nu_B = \frac{2n}{\lambda_P} V_a$$

This wave is amplified with a Brillouin gain that is slightly higher than the Raman gain. From a certain threshold lower than for the Raman effect, it is the stimulated Brillouin scattering regime.

However, this effect can only be observed if the pump wave is very coherent (line width of less than 100 MHz) In practice, it is only disturbing for coherent transmissions (based on phase or light frequency modulation).

2.5.4. *Kerr effect*

In non-linear isotropic materials, the electric flux density equals:

$$D = \epsilon_0 n E + \chi_{(2)} E^2 + \chi_{(3)} E^3 + \dots$$

For reasons of molecular symmetry, there are no non-linearities of the second order in the silica, contrary to dielectric crystals. The dominant non-linear term is that of the third order which, in the presence of a wave of angular frequency ω , reveals:

- a term in $E^3 \cos 3\omega t$ (tripling of frequency);
- a term in $3E^3 \cos \omega t$ which is equivalent to an index increase:

$$\Delta(\epsilon_0 n^2) = \epsilon_0 2n \Delta n = 3E^2 \chi_{(3)} \text{ hence } \Delta n = n_{(2)} I \text{ with: } I = \frac{|E|^2}{2Z}$$

light intensity, which can be very high even if the total power is not very strong, because the core section of the optical fiber is very small;

- $Z = Z_0 n$ impedance of medium;
- $n_{(2)} = \frac{3Z_0}{n^2 \epsilon_0} \chi_{(3)}$ non-linear index.

This index increase (accompanied by an induced birefringence if the wave is polarized) is the optical Kerr effect, similar to the electric Kerr effect (induced by an external electric field, Δn being in ϵ^2). It is very low in the silica ($n_{(2)}$ value is $3.2 \cdot 10^{-20} \text{ m}^2/\text{W}$).

2.5.5. Consequences of the Kerr effect

The Kerr effect leads to several phenomena:

- *self-phase modulation* (SPM): the index variation causes a variation of the light phase which, at the end of length L , equals:

$$\Delta\phi = 2\pi n_{(2)} \frac{L}{\lambda} I$$

This effect can become sensitive if L is large, but also if the intensity is high, in particular over a long single-mode fiber length.

If this intensity is modulated, a modulation of the light frequency, thus the wavelength, appears. In the presence of positive chromatic dispersion, this is the basis of a temporal pulse compression which can lead to the propagation of *solitons* (see section 2.5.6);

- *cross-phase modulation* (XPM) by a non-linear mixing between the different carriers of a wavelength division multiplexed system; this effect limits the number of simultaneously usable carriers but has enabled wavelength conversion experimentation (transfer of a signal from one wavelength to another in fact);

- *four wave mixing* (FWM) by intermodulation between three wavelengths where propagation constants are related by a phase matching rule; it was used in parametric amplification experimentation, excessively difficult to set up;

- *self-focusing*: in a single-mode fiber, the index will increase proportionally to the local light intensity, which is not constant (it is approximately Gaussian). An index gradient will then be created which, if the intensity is high, will focus the wave that will be “self-guided” with a very small mode diameter (this phenomenon can even exist in a homogenous environment). A stationary solution may be reached, called the *spatial soliton* (the non-linear effect exactly compensates diffraction) by analogy with the temporal soliton where the non-linear effect exactly compensates dispersion. Self-focusing constitutes a limit to very strong power transmission in a single-mode optical fiber.

2.5.6. Soliton propagation

2.5.6.1. Description

A soliton is a short pulse, preserving its form and amplitude throughout its propagation. It is a singular solution to a non-linear equation, the result of the conjunction of both dispersion and non-linearity phenomena (the Kerr effect explained previously). The self phase modulation effect leads to a wavelength modulation when intensity I varies:

$$\Delta\lambda = \frac{1}{2\pi} \frac{\lambda^2}{c} \frac{d(\Delta\phi)}{dt} = \frac{\lambda\Delta z}{c} n_{(2)} \frac{dI}{dt} \text{ over a length } \Delta z$$

λ increases on an rising pulse edge and decreases on a falling pulse edge.

If the chromatic dispersion D_c is positive, the rising pulse edge corresponding to the highest wavelengths will slow down, whereas the falling edge will speed up for the opposite reason: we obtain a temporal pulse compression. If the chromatic dispersion is negative, the pulse widens. However, we obtain in this case a phenomenon similar with black solitons, an “engraved” pulse on a light background.

2.5.6.2. Soliton equation

In very precise conditions (form, pulse amplitude and duration), an equilibrium state between pulse compression and chromatic dispersion may be reached.

The pulse is a solution of the non-linear propagation equation in a lossless single-mode fiber. This equation is in the general form of Schrödinger equations:

$$\frac{\partial E}{\partial z} + \beta' \frac{\partial E}{\partial t} - \frac{j}{2} \beta'' \frac{\partial^2 E}{\partial t^2} - j \gamma |E|^2 \cdot E = 0$$

with:

$$-\beta' = \frac{d\beta}{d\omega} = \tau_g \text{ pulse group delay;}$$

$$-\beta'' = \frac{d^2\beta}{d\omega^2} = -\frac{\lambda^2 \cdot D_c}{c \cdot 2\pi} \text{ group velocity dispersion (GVD) factor. Solitons are}$$

observed if the GVD is negative, which actually corresponds to a positive chromatic dispersion;

$-\gamma = \frac{\pi n^{(2)}}{\lambda Z}$ coefficient related to the Kerr effect.

The pulse is a hyperbolic secant of duration T_0 and of peak amplitude E_0 :

$$E(z, t) = E_0 \operatorname{sech}(t/T_0) \exp(jz/2zc) \text{ (with } \operatorname{sech} x = 1/\cosh x \text{)}$$

with a form that is independent of z .

This solution, of the first order, is not the only one: there are solitons of the N order, with a form that periodically changes.

Pulse parameters are related by:

$$E_0^2 = \frac{|\beta''|}{\gamma T_0^2}$$

T_0 is typically in the order of magnitude of 10 to 20 ps. Peak power corresponding to E_0 is a few dozen mW.

The soliton is a solution of the equation if it remains an “isolated” pulse, i.e. if the time interval separating two solitons (representing two “1” bits in a transmission system) remains slightly higher than T_0 (approximately 5 times), otherwise there is coupling between the two consecutive solitons (see Figure 2.9). This typically limits the bitrate to 40 Gbit/s, in RZ format.

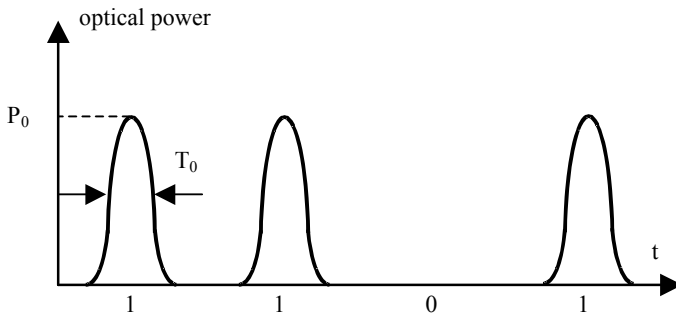


Figure 2.9. Digital signal transported by solitons

2.5.6.3. Soliton transmission systems

Soliton pulse propagation presumes that its form and power conserve themselves, then that it is amplified as propagation attenuates it. Thus, if the soliton propagation phenomenon has been known for a long time, it is thanks to optical

amplification that it becomes possible, by regularly re-amplifying them (all current 20 to 30 km/hr), to obtain their propagation on very long distances. In addition, different wavelength solitons can be multiplexed on a single optical fiber: since each one of them is a solution of the non-linear equation for its own wavelength, they will not suffer from pulse broadening.

Solitons can be transmitted at bitrates of a few dozen Gbit/s over thousands of kilometers, without pulse broadening, under the condition that they are often amplified. However, optical amplification accumulates noise which, by non-linear mixing, results in jitter in the frequency, or in the temporal position of solitons (Gordon-Haus jitter). This jitter, which evolves in z , is the main cause of error in soliton systems. Noise accumulation can be fought by using narrow optical filters that are slightly shifted from one amplifier to the other: solitons cross them by frequency sliding, thanks to the non-linear effect, whereas the noise corresponding to spontaneous transmission does not cross them. This frequency sliding filtering, which requires very precise settings, has made it possible to exceed 20,000 km without regeneration.

To reach even greater distances, it is necessary to develop *optical regeneration* of solitons, to eliminate noise and jitter: this can be done with the help of electro-absorption modulators which reshape pulses in a “temporal gate”. They require online clock recovery however. In 1996, CNET demonstrated a 20 Gbit/s transmission over a million kilometers with 140 km span between optical amplifier-repeaters. Propagation over *millions* of kilometers makes it possible to consider optical memory made up of solitons turning in optical loops for seconds, or even minutes, for the development of “all optical” routing and temporal switching.

Despite several laboratory research studies and the development of a few experimental links, the interest for solitons in the telecommunications field is set aside for now since less complex solutions for reaching throughput goals have emerged; however, even though they do not exactly use solitons, submarine links take non-linear effects into consideration in their modeling.

2.6. Microstructured (photonic) optical fibers

2.6.1. Introduction

For the last few years, great interest in the scientific and manufacturing field has grown for new structures called microstructured fibers and optical guides, in other words presenting a periodic structure on a length of the same order of magnitude as the wavelength, most often created from holes periodically placed in silica. This periodicity in wave propagation leads to phenomena similar to the propagation of

electrons in a periodic crystal, and especially the appearance of a “photonic bandgap” (PBG) phenomenon which prohibits propagation at certain wavelengths or in certain directions. These structured materials are called, by analogy, “photonic crystals” or even “photonic fibers”.

Table 2.1 presents analogies between these “photonic crystals” and semiconductor crystals. There are differences however, in particular the fact that photons do not interact with each other and, except for non-linear effects, cannot exchange energy.

Semiconductor crystal	Photonic crystal
Electrons	Photons
Schrödinger equation	Propagation equation (scalar)
Levels of energy	Propagation modes
Bandgap	“photonic bandgap”
Well of potential	Waveguide
Defects (dopant)	Periodicity break zone

Table 2.1. *Analogies of photonic crystals*

Depending on the number of directions in which we encounter structure periodicity, photonic crystals will be (see Figure 2.10):

- 1D for periodicity in one direction, which is performed by periodic stacking of thin layers perpendicular to this direction, for example interference filters and “Bragg mirrors” reflecting certain wavelengths for which elementary reflections on the different diopeters are in phase;
- 2D for periodicity in 2 directions, which takes the form of holes (or zones of different index) periodically placed and oriented in the 3rd direction; this is the case with fibers and “photonic” guides;
- 3D following a periodic structure said to be “wood pile” or Yablonivite, after the name of its inventor Yablonovich, which has mostly led to developments in millimetric waves, but has started to exist in optics despite realization difficulties, with the help of microtechnologies and is applied to certain laser cavities, thus making the “light caging” idea a reality.

The photonic crystal concept is not limited to optics: some developments exist in the field of microwaves, thus making the material microstructured, opaque at certain wavelengths. Finally, we should note that these structures exist in nature and explain

the color effects of butterfly wings, of certain bird feathers or of several precious stones.

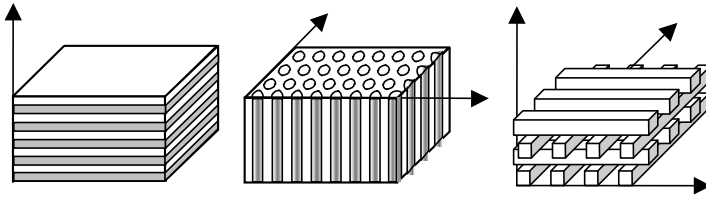


Figure 2.10. *Photonic bandgap material*

2.6.2. Photonic bandgap

The traditional diagram of energy bands in a semiconductor (electron energy according to its wavenumber in reciprocal space) has an equivalent for a photonic crystal of spatial period Λ .

In the diagram in Figure 2.11 illustrating a z -direction 1D structure (a Bragg mirror), we represent in abscissa the wavenumber, normalized $k\Lambda/2\pi$ over a period of the reciprocal network (from -0.5 to $+0.5$), and in ordinate the photon's normalized energy, $\omega\Lambda/2\pi c$ (which is proportional to v therefore to the energy of the photon). k is the wave vector component along z . Whereas in a homogenous environment, we would have lines of slope $1/n$, in the periodic structure, the resolution of the propagation equation along z shows a curve distortion (this is another representation of the dispersion diagram) and the existence of bandgaps, i.e. $\omega\Lambda/2\pi c$ values which are never solutions.

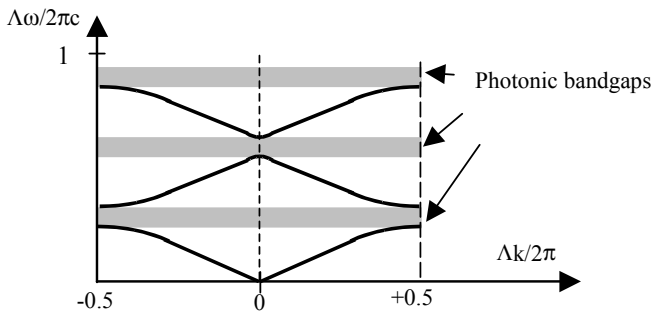


Figure 2.11. *Band diagram in a Bragg mirror*

In physical optics, it is the wavelengths for which we have constructive interferences between consecutive reflections, or $\lambda_p = 2n_a\Lambda/p$ (p integer). The light will be totally reflected and will not be able to propagate in the material in direction z .

Bands are centered on energy:

$$\frac{\omega\Lambda}{2\pi c} = \frac{p}{2n_a}$$

where n_a is the effective average index and their width increases with the index difference of alternate thin layers.

In more complex structures (2D or 3D), wave vector components must be calculated by numerical modeling based on reciprocal crystal axes. The calculation becomes even more complex if the crystal can no longer be considered as infinite (i.e. if the number of periods is no longer very large). This calculation reveals partial bandgaps, i.e. frequencies for which the light cannot propagate in certain directions or polarizations, and total bandgaps where the light cannot be propagated in the material at all.

2.6.3. Photonic waveguides

In order to create a waveguide in a photonic bandgap material, the “crystal” periodicity must be broken by filling (or by not creating) the holes on the guide axis (Figure 2.12). This is the equivalent of dopants in a semiconductor, introducing authorized levels in the bandgap. The light can then propagate along the guide but it is confined, since it cannot propagate in the photonic crystal surrounding the guide.

In planar integrated optics planar guides, the propagation axis is perpendicular to the holes (which are vertical and perpendicular to the horizontal substrate). The main advantage compared to traditional integrated optical guides (see Chapter 4) is the possibility of creating sharp angles in the guide, whereas in integrated optics the bend radius must be much larger to limit radiative losses. Several basic functions can be achieved with low congestion: Y junctions, coupled cavities, filters, etc. and are at the base of “photonic integrated circuits”. It is also a way to achieve optical interconnections in silicon integrated circuits.

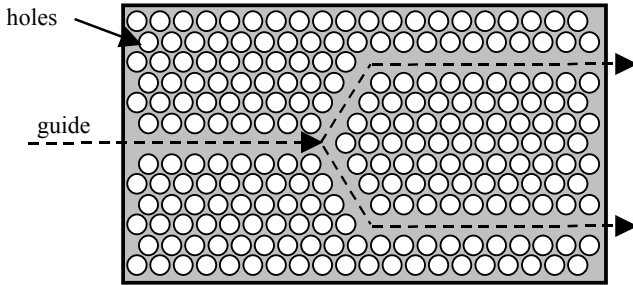


Figure 2.12. Photonic planar guide with Y junction

2.6.4. Photonic crystal fibers

Several types of photonic crystal fibers (PCF) can be created; in the first category the core is full and surrounded by micro-structured cladding. Now, in the photonic bandgap material, the holes are parallel to the light propagation axis (see Figure 2.13). Guiding can be interpreted as a consequence of the effective index in the cladding, which is the average between silica index and air index (weighted by the proportion of air in cladding, or “vacuum factor”) which is lower than the core index.

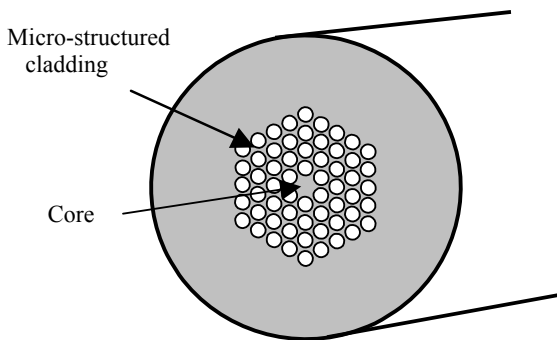


Figure 2.13. Fiber-optic in a “photonic crystal”

However, these fibers present important differences compared to classical step-index fibers:

- they are single mode at all wavelengths;

- their zero dispersion wavelength can be adjusted over a large range, including under the zero material dispersion wavelength;
- they can present a very large negative chromatic dispersion, with a negative slope, making their use possible as compensating dispersion fibers;
- they can support strong bendings without additional losses, which makes them attractive for internal cabling.

Depending on their structure, all sorts of unusual properties can be achieved:

- large mode diameter fibers, decreasing power density, therefore non-linear effects, making it possible to transport high power;
- or, on the contrary, very low mode diameter fibers, voluntarily increasing non-linear effects;
- anisotropic structure fibers, birefringent, preserving the polarization;
- concentric core and multiple core fibers;
- photo-sensitive fibers, amplifying doped fiber, etc.

However, they are more expensive and more difficult to connect than classical fibers, and despite significant technological progress, their attenuation remains high (not much better than 10 dB/km at best); they are therefore not suitable for long-distance transmission, but for several special applications such as the design of fiber components.

2.6.5. *Hollow fibers*

One of the most spectacular applications of photonic crystals is the development of hollow-core fibers, surrounded by a micro-structured cladding (see Figure 2.14). Light guiding can only be explained by the effect of a photonic bandgap in the cladding, where the effective index is higher.

Due to the absence of material in the core, there is no longer absorption, thus possibility of transmitting strong power or wavelengths where silica is not transparent, particularly CO₂ laser beams at 10.6 μm . There are no non-linear effects either, or Fresnel reflection at the ends. It is also possible to transport gases, fluid or even nano-objects in the hollow core.

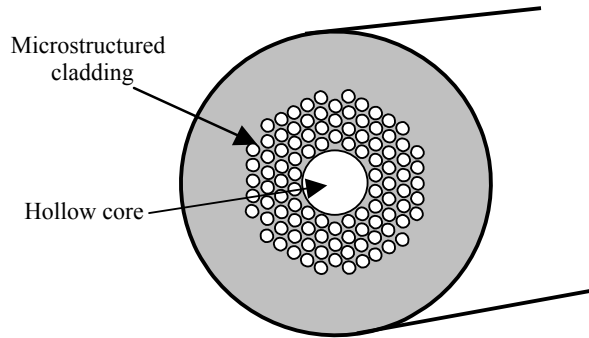


Figure 2.14. *Hollow core fibers*

This page intentionally left blank

Chapter 3

Fiber Optics Technology and Implementation

3.1. Optical fiber materials and attenuation

3.1.1. *Different types of optical fibers*

The most widely used optical fibers in transmission are “all silica” fibers, made with silica, and germanium oxide core “doping” which determines index value and profile. As indicated in Table 3.1, they turn into multimode fibers, especially graded-index, and single-mode fibers.

By erbium doping, they are also made into amplifying fibers. Plastic fibers, besides their lighting applications, progress for very short distance transmissions. There are other materials for much more specific applications.

3.1.2. *Intrinsic attenuation of silica fibers*

This comes from physical absorption and scattering phenomena in guidance material, and involves a lineic attenuation α , in dB/km, which means that the power transmitted to a distance L is given by:

$$P(L) = P_0 \cdot 10^{-\alpha L/10}$$

Material	Plastic	Silica/ silicone	All silica core: silica + germanium oxide			
Type	Multimode SI	Multimode SI	Graded-index multimode		Single-mode	
Core diameter/ cladding (μm)	980/1,000 (or more)	200/380 (or more)	50/125	62.5/125	Standard: 9/125	Dispersion- shifted: 7/125
Attenuation (dB/km)	200 (visible)	5 to 10 at 0.85 μm	3 at 0.85 μm; 1 at 1.3 μm	2.6 at 0.85 μm; 0.9 at 1.3 μm	0.5 at 1.3 μm; 0.2 at 1.55 μm	0.22 at 1.55 μm
Numerical aperture	0.5	0.4	0.20	0.27	*	*
Bandwidth (MHz.km)	20	20	500 (OM1) 2,000 (OM3)	300 (OM2)	*	*
Temperature of use	<80°C	<100°C	<150°C (depending on coating)			
Mechanical resistance	Flexible but malleable	Limited	Good if protected			
Radiation resistance	Average	Good	Bad (germanium darkens)			
Implement- ation	Very easy	Tricky	Easy		Not as easy and more expensive	
Cost of fiber	Low	High	Low		Low	
Cost of interfaces	Low	High	Relatively low		High	
Main applications	Lighting, visualization, local transmission (even high throughputs)	Light energy transport	Distribution, local high throughput networks	Local networks any throughput	Long distances, very high throughput LAN/MAN, FTTH access	Very long distance telecoms (DWDM + amplified)

* Parameters which only apply to multimode fibers

Table 3.1. Main types of optical fibers

P_0 is the power that is coupled at the fiber input. As we will see later, this term is difficult to correctly measure.

This attenuation α depends on material and wavelength λ . Generally, curve $\alpha(\lambda)$ reveals three phenomena (see Figure 3.1 for silica fibers):

- *Rayleigh scattering*, because of light interaction with material, which scatters it rather isotropically. It decreases rapidly when the wavelength increases, following a λ^{-4} law; this is why the sky appears blue in fine weather. In the germanium oxide doped silica, attenuation in dB/km equals:

$$\alpha_d = (0.75 + 66 \Delta n^+) \lambda^{-4}$$

with λ in μm , where Δn^+ is the absolute index difference between the germanium “doped” core and pure silica, hence the interest for a low level of germanium oxide or a depressed inner cladding structure. The Rayleigh scattering encourages the use of silica fibers in infrared. This phenomenon is used in a practical way in *backscattering* measures (see section 3.6.5);

- absorption by the material occurring in infrared, limiting the range of transparency to approximately 0.8 μm in plastic (which only transmits visible light), 1.7 μm in silica, but close to 5 μm for fluoride fibers can thus be used in infrared instrumentation;

- selective absorption peaks by different impurities, the most disturbing in silica because of OH bonds at 1.39 μm , since this peak is located close to the minimum attenuation. To avoid it, the silica must have very low water level, lower than 10^{-7} . Gradual elimination of this peak has been one of the major achievements in manufacturing, and attenuation is now very close to theoretical silica attenuation. This is far from being the case with fluoride fibers.

Single-mode fibers generally present a lower intrinsic attenuation because of a lower level of germanium oxide. We note an attenuation peak characteristic of the cut-off wavelength of higher order modes on their attenuation curve (in fact, it is a simple way to measure it).

Exceptional phenomena can lead to partially irreversible increases of the intrinsic attenuation. This is the case in particular:

- with gas penetration, in particular hydrogen, in the fiber material;
- with sensitivity to high energy radiations (nuclear and spatial fields) especially for fibers with a high level of germanium oxide.

These phenomena are used in gas or radiation sensors; in addition, reflectometry helps in localizing the exposed zone.

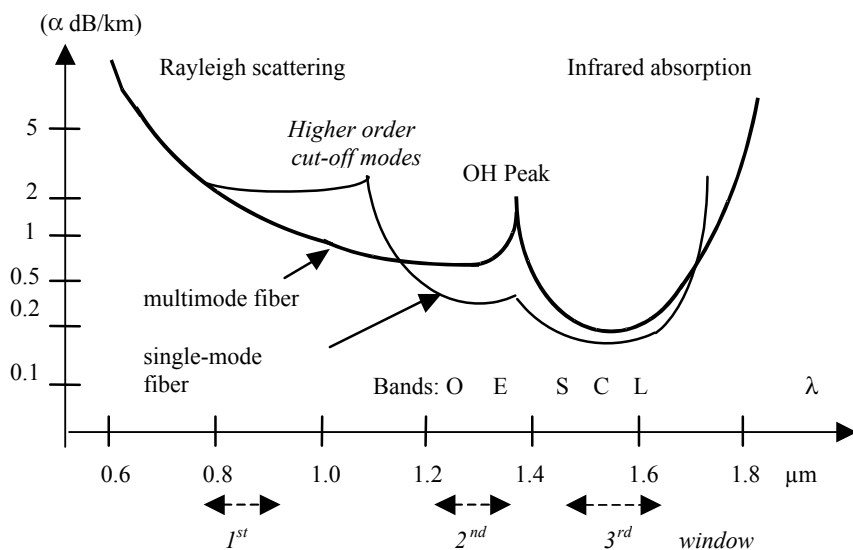


Figure 3.1. *Intrinsic attenuation of silica optical fibers*

3.1.3. Plastic fibers

Plastic fibers enable a large diameter as well as a large numerical aperture, while being flexible and light; their attenuation is high but regular in the visible spectrum (see Figure 3.2). The most widely used material is *polymethyl methacrylate* (PMMA); polystyrene is also used for a large numerical aperture, but it is not as transparent.

These fibers are widely used in short distance optical applications (lighting, visualization, display, etc.) in visible light. However, they are increasingly used for short distance data transmission (up to approximately 100 m), with visible LEDs (mainly red at 670 nm, but green can also be used and both colors can even be multiplexed), even at very high bitrates (100 Mbit/s). They are in fact very economical and easy to implement (in particular concerning connectors) for home automation, automobile, interconnections between computer equipment in a single location, benchmarks where they transport signals safe from electromagnetic parasites.

Graded-index plastic fibers are in development to transmit Gigabit Ethernet over 100 m with red VCSEL diodes (see Chapter 6). Their use is envisaged for subscriber connections up to 300 m.

The main limitations of plastic fibers involve environmental issues (temperature limited at approximately 80°C, bad resistance to humidity), and their lifetime is not completely known.

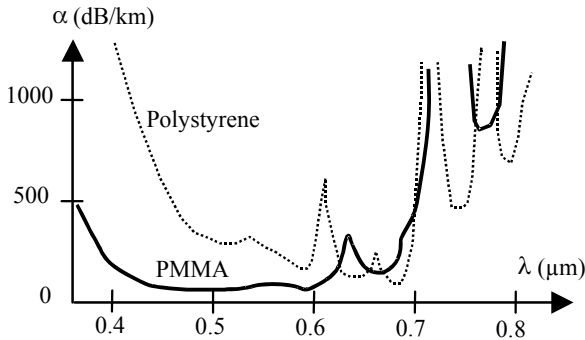


Figure 3.2. Plastic optical fiber attenuation

3.1.4. Other materials

Silica-silicone (pure silica core, silicone cladding) fibers, also called PCS (plastic cladded silica), can have a large numerical aperture, while maintaining low attenuation and low sensitivity to radiations. However, they are more rigid and more expensive than plastic fibers, and are harder to use because of their heterogenous structure. Their main application is light energy transport (laser beams, optical power feeding), around 1 μm .

In this family, hard clad silica (HCS), with a mechanical behavior that is closer to glass, are used in transmission or as sensors if high mechanical resistance is needed.

Fluoride fibers are actually glassy mixtures of different fluorides: ZrF_4 , BaF_2 , LaF_3 , AlF_3 , NaF , etc., a composition summarized in the acronym ZBLAN.

Their original advantage, a minimal attenuation lower than 0.01 dB/km, has remained completely theoretical because of major production and connection problems: not much better than 1 dB/km to 2.5 μm was ever reached and these fibers are very fragile.

Their main advantage is their transparency up to approximately 5 μm , and they are only used for some infrared instrumentation applications (see Chapter 11).

Other materials exist, which are transparent over short lengths in far ultraviolet or infrared and have much more specific uses (medical instrumentation for example).

Research has been carried out on chalcogenide fibers (made up of elements from the 6th column: S, Se, Te) or halides, which present some transparency at 10.6 μm ; but losses are high and these materials are difficult to use; for CO₂ laser beams, hollow fibers are now preferred (see Chapter 2).

3.1.5. *Transmission windows*

Due to optical fiber attenuation and dispersion, but also because of the characteristics of available optoelectronic components, *transmission windows*, are defined, which are wavelength bands with specific properties, within which wavelength division multiplexing can be practised.

In plastic fibers, the window at 0.67 μm (red) is used for very short distance links (less than 100 m), to take advantage of components with good efficiency; the main advantage compared with the twisted pair is electric and electro-magnetic security.

The fluoride fiber window, around 2.5 μm , is only used in infrared instrumentation.

In silica fibers, three windows are traditionally distinguished; in wavelength sequence, which is also historically the sequence in which these windows have been used (see Table 3.2):

- the first window, from 0.8 to 0.9 μm , is not an attenuation or dispersion minimum, but it is an optimum for the use of the most economical (and efficient) components: silicon for detectors, GaAs for transmitters; this window allows inexpensive short distance links or local area network over multimode fibers at low or medium bitrates. It has a new use for high bitrate short distance interconnections (Gbit/s and above), with VCSEL laser diodes over multimode fibers;

- the second window, sometimes called “O band”, at approximately 1.3 μm , is a relative minimum of attenuation (around 0.5 dB/km) and a minimum of chromatic dispersion; the components are more expensive than at 0.85 μm , but it is commonly used in middle-range transmission (a few dozen kilometers) over single-mode fibers, as well as at high bitrates in local network (Fast Ethernet, FDDI), generally over

multimode fibers; with 1 and 10 gigabit Ethernet, single-mode fibers emerge in the market of local and metropolitan networks and subscriber access;

- the third window, at approximately 1.55 μm , corresponds to the absolute minimum of attenuation (less than 0.2 dB/km) but requires more expensive components, because of the chromatic dispersion problem (monochromatic laser DFB diodes must be used, and eventually dispersion compensators). Used more recently, it is mostly used for long distance links over single-mode fibers (terrestrial or submarine) with ranges exceeding 100 km without amplifier, at bitrates of several Gbit/s. The optical amplification is used at this wavelength and large scale wavelength division multiplexing is practised. The 2nd and 3rd windows can also be multiplexed in both directions over the same fiber, which is performed in the new access network standard GPON.

Nowadays, the “C band” (1,530 – 1,570 nm) is used; it could be widened to L (1,570 – 1,620 nm) and S (1,460 – 1,530 nm) bands to increase capacities, which is what is planned with the new ITU G 656 standard for multiplexed terrestrial networks (see Figure 3.1). Even the “E band” (extended) between the 2nd and 3rd windows in fibers “without OH peak” could be used, but it is not now necessary.

Window	First	Second	Third
Wavelength	0.78 to 0.9 μm	1.3 μm	1.5 to 1.6 μm
Type of fiber used	Multimode	Multimode and single-mode	Single-mode
Attenuation	High (2 to 4 dB/km)	Low (0.4 to 1 dB/km)	Very low (0.2 dB/km)
Chromatic dispersion	High	Almost zero	Low, non-zero <i>very low in dispersion shifted fibers</i>
Transmitters: type	LED; laser diodes VCSEL (<i>very high throughputs</i>)	LED (<i>in multimodes</i>), standard laser diodes (<i>in single modes</i>)	DFB laser diodes (monochromatic)
Material	GaAlAs/GaAs	GaInAsP/InP	
Receivers: material	Silicon	GaInAsP/InP Ge, HgCdTe (very few used)	
Cost of components	Low	Medium	High
Applications	Short distance transmissions; local networks; gigabit over very short distance	Medium and long distance transmissions; high bitrate local and metropolitan networks	Very long distance and optically amplified transmissions
Multiplexing	Between both windows (for example: one per direction)		“Dense” (numerous channels in the same window)

Table 3.2. Transmission windows of silica fibers

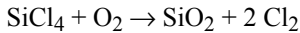
3.2. Manufacturing of optical fibers

3.2.1. Principles

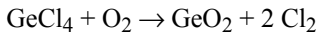
Since glass making methods, long ago used to manufacture glass fibers, do not offer adequate purity for telecommunications, optical fibers are manufactured by synthesis in two steps:

- realization of a preform, a cylinder approximately 1 m long with a diameter of a few centimeters, homothetic to the future fiber;
- drawing of this preform, to transform it into a fiber that is several dozen kilometers long.

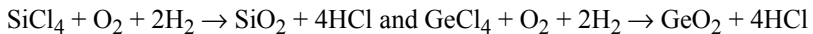
Plastic fiber preforms are manufactured by polymerization. Those for silica fibers are obtained by silica synthesis from chlorides, generally by oxidation reaction:



and, for core germanium oxide:



A chemical vapor-phase oxidation process is also used:



The oxide deposit is at first porous (amorphous state), it is then *vitrified* at high temperature. A little P_2O_5 phosphorus oxide is incorporated to decrease vitrification temperature, as well as fluorine, in the inner cladding, to compensate for the index increase created by the phosphorus oxide (or even to decrease the index in the depressed inner cladding fibers, see Chapter 2). There are several production processes.

3.2.2. Manufacturing of preforms by the MCVD process

The MCVD (modified chemical vapor deposition) process developed by Corning in the 1970s is the most widely used process outside of Japan. The internal deposit is carried out by concentric layers, obtained by oxidation within a rotating quartz tube (see Figure 3.3). Oxidation and vitrification are achieved in the heat of an external torch. The deposited layers correspond to the core and the inner part of optical cladding.

The index of each layer can be controlled by the level of germanium chloride in the gas mix (chlorides + oxygen) sent into the tube, and a very precise index profile can be obtained. Once a hundred or so layers have been deposited, the tube gradually closes on itself by softening at higher temperature (collapsing operation).

This process allows us to obtain fibers of very high quality, but a perfectly geometric tube is required at the start, and there is a limit in terms of speed of deposit and fiber length (the tube cannot be too thick). To increase it (up to several

hundred kilometers), different processes can be used to increase the quantity of cladding matter:

- jacketing, i.e. shrinking around the preform of a second tube;
- external lateral deposit of additional silica layers by CVD or by plasma.

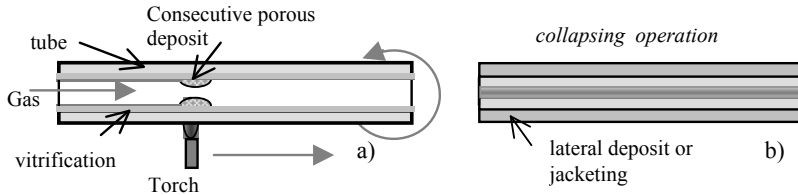


Figure 3.3. MCVD process for preform manufacturing

One variation is the PCVD (plasma chemical vapor deposition) process in which the torch is replaced by an internal plasma, induced by a microwave reactor. The deposit speed can thus be increased and thicker tubes can be used to produce longer fibers. This high performance process requires very large investments however, and is not widely used.

3.2.3. Preform manufacturing by external deposit

These processes do not use deposit tubes. The oldest, OVPO (outside vapor phase oxidation), deposits concentric layers around an alumina mandrel; it is necessary to dry the tube before vitrifying it (see Figure 3.4a). This process is mainly used for step-index fibers.

The VAD (vapor axial deposition) process, contrary to others, is not concentric but is done by preform axial growth, by hydrolysis or plasma (see Figure 3.4b). The porous deposit is immediately vitrified in drying gas. This process, mainly suited to step-index profiles, is extensively used in Japan, where very long fibers can be produced. It is often combined with lateral cladding deposit.

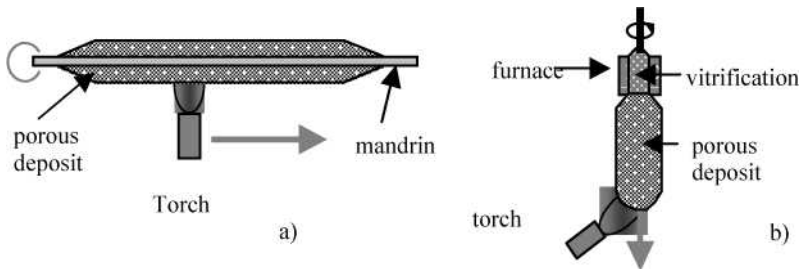


Figure 3.4. Preform production processes by external deposit:
 a) OVPO (outside vapor phase oxidation); b) VAD (vapor axial deposition)

3.2.4. Drawing

After its manufacturing, the preform is controlled: its index profile is measured by an optical process (laser beam refraction). Although “line drawing” experiments were carried out, it is preferable to keep the two distinct steps in order to enable this control.

For certain applications, preform can be the subject of particular processes: (machining, etc.). For example, plastic fibers assembled in bundles, for image transmission, are made from square or hexagonal section machined preforms. CNET also demonstrated the feasibility of multi-core fibers. More recently, photonic bandgap fibers (see section 2.6) are drawn from the assembly of a large number of hollow tubes.

Preform transformation into fiber is performed by drawing with no contact, by preform extremity fusion in an induction furnace, filled with inert gas (see Figure 3.5). The fused fiber goes down along the drawing tower, where its diameter is measured by a laser, which controls drawing speed to keep it constant. Drawing speeds are constantly increasing, now exceeding 10 m/s in production.

The fiber is immediately covered with a *primary coating*, which is generally a resin that is polymerized with ultraviolet. It has a triple role:

- it protects the glass against chemicals stresses;
- it cushions constraints and prevents the propagation of cracks, especially at bending;
- it absorbs cladding modes because of a slightly higher index.

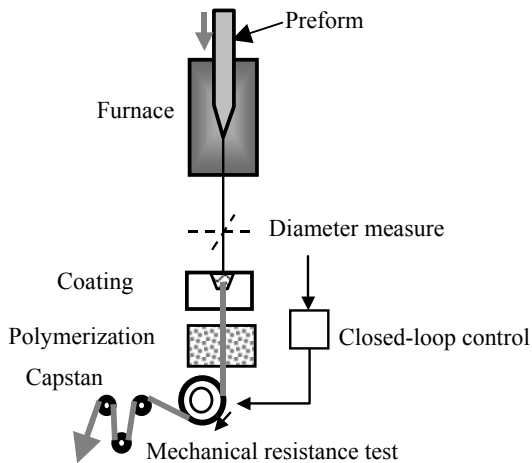


Figure 3.5. *Drawing*

Classical acrylate-epoxy type coatings, with a general diameter of 250 μm , do not modify transmission properties of the fiber, but have a limited temperature range (up to approximately 150°C). For higher temperatures, special (polyimide) coatings exist, inducing some constraints on the fiber, hence additional attenuation. Metallic coatings can be used for very specific cases (sealing).

Sometimes the fiber is coated with a more rigid secondary coating with an external diameter of 500 or even 900 μm . Most of the time, the fiber is provided and used with the simple primary coating (but never bare).

3.2.5. *Mechanical resistance*

Glass is very rigid material: the Young's modulus for silica (relative constraint/elongation ratio) is higher than 70 GPa. For a 125 μm diameter optical cladding fiber, this corresponds to approximately 1% traction stretch of 1 daN.

Their elongation is purely elastic, up to a break limit of 1.5 to 2% depending on manufacturing quality. Localized defects greatly decrease this limit. To eliminate them, at the end of drawing, the fiber goes through a test of mechanical resistance or screen-test, strong traction in a short amount of time, allowing us to verify that it has adequate mechanical resistance (see Figure 3.5).

On the other hand, plastic fibers are much less rigid, and are therefore more flexible even with larger diameters than 1 mm. They support elastic stretching of up to 6 or 7%, followed by a plastic distortion zone before their break. They thus keep a memory of mechanical stress (bending, constraints, etc.). Temperature and humidity greatly damage their characteristics.

3.3. Optical fiber cables and connections

3.3.1. *Principle of optical fiber cables*

The role of the cable is to protect the optical fiber against mechanical (shocks, abrasion, constraints, stretching, excessive bending), chemical and thermal stresses. The result is an increase in weight, size and sometimes even attenuation, which must be as limited as possible.

Cable structures are many and varied, depending on the number of fibers per cable (from 1 to more than 1,000), usage constraints, the presence of electrical conductors in the same cable to remotely feed equipment at end of line, or on the contrary the need for electrical insulation. “Exotic” structures exist such as thick and resistant cables used in crude oil exploration, and at the other end of the spectrum, there are thin “wires” connecting wire-guided engines, etc.

In telecommunications, cables have greatly evolved since the *grooved rod* structure, where optical fibers were placed in the helical grooves of a cylindrical rod, thanks to progress achieved in the mechanical resistance of optical fibers. In fact, cables are traditionally pulled into underground conduits, which implies adapted mechanical resistance. For access networks, cable blowing is increasingly practised.

However, three main categories can be distinguished, by the way the optical fiber is placed in the cable.

3.3.2. *Different cable types*

3.3.2.1. *Tight structure cables*

These cables generally only contain one fiber. Several layers of components are placed concentrically around the fiber (see Figure 3.6a). Size is reduced (near 1 mm diameter, sometimes even less) and connector performance is easier. On the other hand, the fiber is not isolated from constraints (compression or stretching).

With silica fibers, tight structure uses are limited to short distance “indoor cabling” (aeronautics, computer systems, in-building cabling, in particular when the fiber-optic cable is vertical). They are more systematic with plastic fibers.

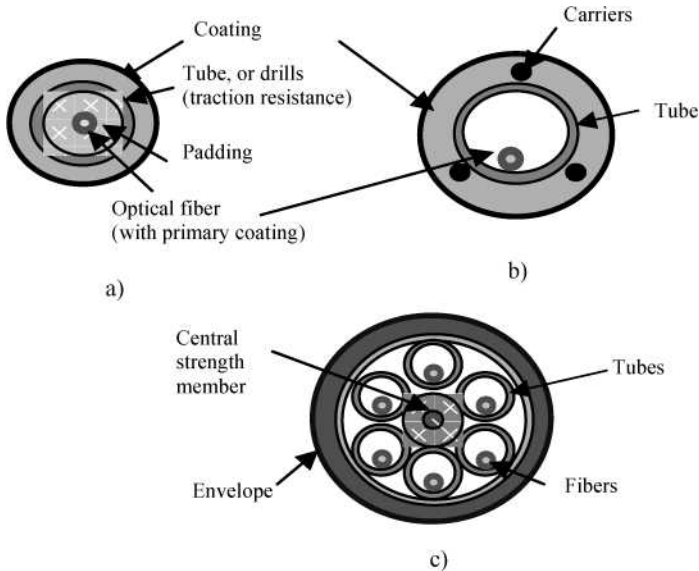


Figure 3.6. Structures of optical fiber cables:
*a) tight structure; b) loose tube structure;
 c) multi-tube loose structure*

3.3.2.2. Free structure cables

The classic example of this type of cable is the *loose tube*, where the fiber is free inside a small tube with a diameter of 1 to 2 mm (see Figure 3.6b). It is no longer subject to mechanical compressions transversally occurring on the tube; this tube must however be reinforced with steel or kevlar strength members protecting it from stretching or compression. In general, there is one fiber per tube, sometimes two or more (their coating can be colored to locate them).

Cables of this type are widely used in manufacturing and information technology, video links and local networks among other applications. They are also made into multi-fiber cables by combining tubes, similarly to electric cables, around a central strength member (see Figure 3.6c). Splitting and connection of the different fibers are then made easier. A bigger size is the drawback of this structure. However, this technique has improved and new “microtube” cables, each containing several

fibers, are emerging on the market and enable high capabilities with reduced size, making installation easier.

3.3.2.3. Compact structure cables

For long distance networks, or in distribution networks, cables with very large capacity (over 1,000 fibers!) with low size are used. Ribbon structure cables, which is an old technology (it was one of the first multi-fiber structures developed by Bell in the 1970s), currently dominate the large capacity cable market. Their principle is to stack polymer ribbons, each containing from 8 to 12 parallel fibers (see Figure 3.7). A stack of ribbons located in a small tube contains approximately 100 fibers and a large number of tubes can be combined.

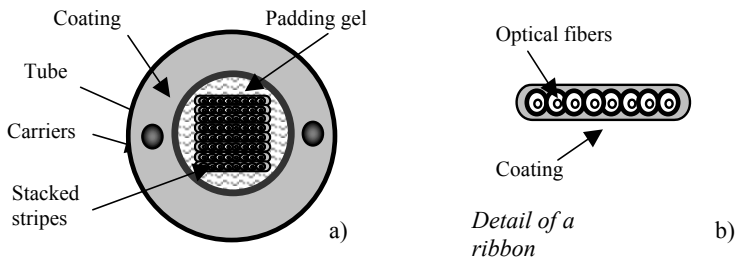


Figure 3.7. *Stripe cable*

Mass splicing techniques (simultaneous splicing of all the fibers of one stripe) have been developed for this type of cable.

3.3.2.4. Aerial cables

These are placed over high voltage lines, in particular in and around “overhead ground cables” (cables acting as a lightning conductor). They enable electric (or railway) network operators to build transmission or remote monitoring networks by using their existing infrastructures; the optical fiber is the only one capable of operating in these conditions. Their high transmission capacities are rented to telecom operators to be used as transport network. Lighter aerial cables can also be used for subscriber links.

3.3.2.5. Submarine cables

They build the infrastructure of a worldwide communications network with constantly growing range and capacity, even though this growth is highly cyclical. As well as large trans-oceanic links, short or average distance submarine links without repeater (between islands and shores, or in “festoons” between coastal

cities, which is more economical than by shore) constitute a growing market segment.

As with aerial cables, *submarine cables* have to go through considerable stress (several dozen tons during the laying of a submarine cable) in addition to the sea bottom pressure, and their possible repair is difficult and expensive. They must therefore have considerable mechanical resistance and because of this, they are made up of an optical core which is generally a tube containing fibers or ribbons, and placed inside a steel cable strand, protecting it and making it resistant to stress.

In long distance submarine cables, a layer of copper leads repeater remote power feeding current, of about one amp, the return is ensured by sea. The cable is electrically isolated by polyethylene, the voltage reaches dozens of kV at the extremities of a trans-oceanic link. The whole cable only has a diameter of a few cm (see Figure 3.8). Cables submerged at medium depth (up to 800 m) are protected against cut-off risks (anchors, fishing tools) by a layer of steel cables and are “embedded” (buried in the bottom sand) close to coasts.

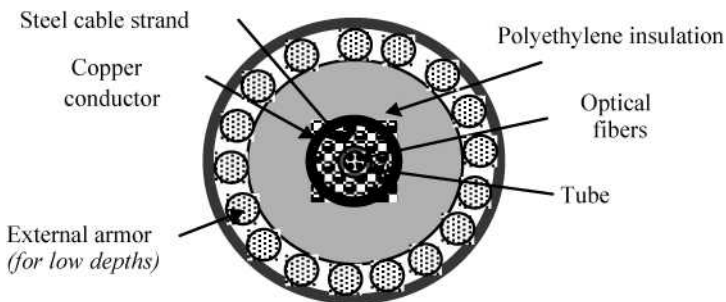


Figure 3.8. *Submarine fiber-optic cables*

3.3.3. Connection of optical fibers

In order to ensure long length cables, fibers are connected in a definitive way by a splice or fused-splice.

To build a network, components such as end interfaces, splitters, etc. can be connected by connectors if it must be able to be uninstalled, but permanent connections can also be made.

Despite realized progress, connections remain a tricky issue with optical fibers because of the disruptions they generate, the very high precision required and cost (in material and labor). That is why single-mode fiber systems are more expensive than multimode fiber systems, whereas the fibers themselves are relatively inexpensive.

End to end permanent connecting of two optical fibers can be carried out:

- by fused splice: mostly done by electric arc, more rarely with flame or laser; this technique provides better optical and mechanical results, but requires expensive material (automatic splicing machines exist, achieving optimal fiber alignment). Good splicing machines commonly reach losses lower than 0.05 dB per weld;

- by glued splice: fibers must already be in place in a common alignment support (groove, tube, etc.). This technique, more manual and requiring less investment, is the only one suitable for plastic or fluoride fibers. Mass splicing techniques have been developed for the collective connection of multi-fiber cables.

In both cases, transmission losses are very low because they are mainly limited to losses caused by misalignment; particularly reflection being zero. Size is very small (once a mechanical protection has been rebuilt, two spliced fibers have the same size as one fiber).

This operation is tricky, however: fibers must be perfectly bared and cleaved (in other words break the glass under tension from a tool-made fracture), and aligned with great precision. A slight angle in the cleaved section leads to loss by misalignment.

3.3.4. Optical connectors

3.3.4.1. Description

When connections must have the ability to be uninstalled (transmitting and receiving interfaces, network nodes), connectors must be used, which are more expensive and cause more perturbations than splices. In fact, beside attenuation that is generally higher (since the alignment is not as precise, and spacing losses are added), the connectors are liable to cause *retroreflections*, which are very disturbing if the light returns toward a laser diode or an optical amplifier.

Connection by connector is actually made up of a plug in each section of cable, permanently mounted by the provider or user, and an intermediate adaptor between two cables, or a fixed connector containing an optoelectronic component (called an “active base”). The main part of a connector is the ferrule, a device for very high

precision fiber alignment, which will be guided to the other ferrule (or to the component of the active fixed connector) by an alignment device. The fiber is glued, or crimped, in the ferrule. It is separated from the locking device ensuring some mechanical resistance. There are also connectors that can be taken off, mostly used in the laboratory or for measurements.

Criteria for choosing an optical connector are mainly:

- positioning precision and reproductibility, depending on the ferrule material (plastic, metal or ceramic);
- the existence (or absence) of a bayonet type device demanding location of connector orientation, improving connection reproductibility; this orientation is mandatory in the case of polarization-maintaining fibers or angled cleavage connectors;
- the ways that may be used to prevent retroreflections. This point is essential: light returns caused by the Fresnel reflection can be very disturbing (source disruption, crosstalk on duplex connections).

3.3.4.2. *Anti-reflection connectors*

Several techniques exist (see Figure 3.9):

- using index matching liquid: this traditional solution is not very practical to use (dust problems, etc.);
- applying slight pressure maintaining fibers in longitudinal contact: this solution is efficient if the ferrule is polished with a slightly convex form (PC type connectors, physical contact, which must be handled with care);
- angled cleavage of fibers (approximate angle of 8°), the solution now widely used with single-mode fibers (APC type connectors, angle physical contact): the reflected light deviates and is not retro-guided by the input fiber, even if there is no fiber connected. Mounting these connectors is trickier.

With these methods, a very high return loss: ($10 \log$ of the incident power/reflected power ratio) can be obtained: 50 to 70 dB.

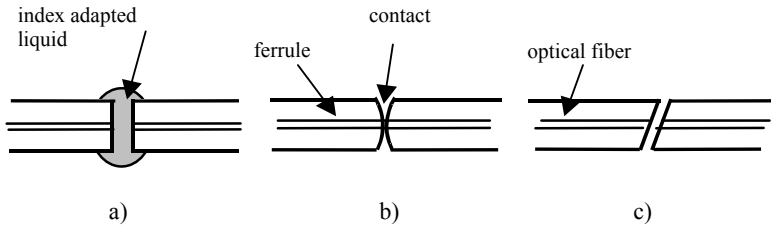


Figure 3.9. Low reflection optical connectors:
a) index matched; b) physical contact; c) angled cleavage

3.3.4.3. Different connector types

There is a large number of optical connectors on the market. A certain number of *de facto* standards have been imposed (see Table 3.3), the most popular of which are ST for local multimode fiber networks, FC/PC for single-mode links, SC for computer networks, which is easy to handle because of indexing, now succeeded by LC, with a smaller form factor. High precision but expensive and fragile connectors developed in early fiber-optic systems have disappeared from the market.

The emphasis is put on the cost and robustness of connectors. There are also connectors with two or more fibers, such as the FDDI network connector, or more recently MT/RJ and duplex LC, but their use remains limited. Finally, there are all sorts of connectors specific to particular environments (production or military applications) that are impervious, with widened beams, electrical/optical mixed, etc. and even optical rotating joints to connect rotating machines or radars.

Type	Optical characteristics	Type of fiber	Clamping	Application
SMA	Straight polishing	Multimode fibers	Screwing (without detection)	Local network power
ST	Straight polishing	Multi and single-mode fibers	Bayonet	Computer networks
FDDI		2-fiber multimode	Indexing	FDDI network
FC/PC, FC/APC	Convex polishing, angled cleavage	Single-mode	Screwing (with detection)	Long distance telecom; polarization-maintaining
FC/PC, FC/APC	Convex polishing, angled cleavage	Multi and single-mode	Indexing	Telecom; networks
EC	Membrane and bias polishing	Multi and single-mode	Indexing	Telecom; distribution; subscriber networks
LC	Small size exists in duplex	Multi and single-mode	Indexing	Local networks

Table 3.3. *Main fiber-optic connector types*

3.4. Extrinsic fiber-optic losses

These losses are leaks of light outside the guide caused by deformations or discontinuities. The amount of loss is directly related to the cabling and connection technologies used.

3.4.1. Losses by bending

When bending lowers by a few centimeters, high order modes are refracted in the cladding (see Figure 3.10) and lower order modes can leak (this is the case of the fundamental mode in single-mode fibers). Losses can also occur by microbending in the case of mechanical constraints in the fiber. In addition, mode conversion and birefringence effects appears, which are used in certain mechanical sensors.

The purpose of using an adequate cable structure is to avoid losses and protect the optical fiber(s) that it contains. Single-mode fibers are rather less sensitive to bending than multimode fibers (but their losses quickly increase with the mode

diameter, therefore with the wavelength); this sensitivity generally decreases when the core/cladding index difference increases hence the advantage for high numerical aperture fibers in cabling where a higher risk of strong bending exists (in buildings for example).

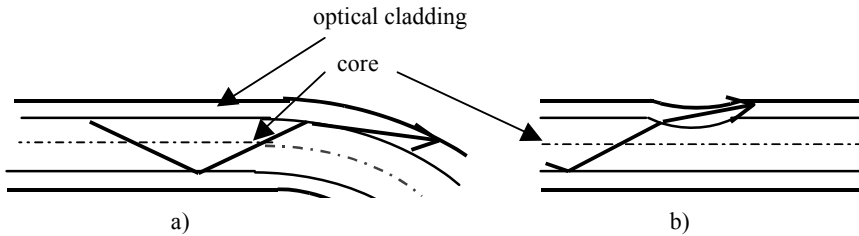


Figure 3.10. Losses by: a) bending; b) microbending

These phenomena have useful applications, however: they can be used to extract the light from a fiber (and also to inject it), in ways other than at its extremity.

This is for example used to locally measure (and minimize) a connection loss, or in traffic control, tools containing two receivers detecting the presence and direction of the light in the fiber.

One consequence is that in certain cases it is possible to detect the signal circulating in the fiber, but the attenuation caused by bending can then be immediately detected and located by reflectometry (see section 3.5.5).

3.4.2. Losses at connections

Connection between two fibers, whether by splicing or with connectors, must be done with care and precision to minimize losses.

3.4.2.1. Causes of losses

There are three types of losses at connections:

- loss by Fresnel reflection during consecutive light crossing of two air-glass interfaces. This loss is of 8% (or 0.35 dB) and reflected light may create disruptions. It can be avoided by splicing or by using adapted techniques in the case of connectors (see section 3.3.4);
- loss caused by difference between parameters (diameters and numerical apertures) of two fibers; this difference would come from manufacturing tolerance

on diameters, indices and core-cladding concentricity. The improvement in manufacturing processes tightens tolerances (they are now at $0.5\text{ }\mu\text{m}$ in single-mode fiber mode field diameter);

– loss caused by bad relative positioning of the two fibers (see Figure 3.11):

- transversal e_t off centering between fiber *cores*; may be due to core-cladding concentricity error;

- misalignment of angle D_α (in radians in charts and formulae); it is generally the consequence of a bad cleavage;

- longitudinal spacing D_e , in the types of connectors that do not put fibers into contact.

Losses caused by these last two causes depend on the presence of air ($n_0 = 1$) or index-matching liquid ($n_0 \approx 1.5$) between both fiber faces; this in fact changes light divergence at the fiber output.

3.4.2.2. Calculation in multimode fibers

In the case of a difference in diameter $2a$ or numerical aperture ON between both fibers, indexed 1 and 2 (the light goes from 1 to 2), there is a loss, in dB, of:

$$20 \log \frac{a_1}{a_2} \text{ if } a_1 > a_2; 20 \log \frac{ON_1}{ON_2} \text{ if } ON_1 > ON_2$$

In the opposite direction losses are generally lower; this non-reciprocity of these losses can be explained by that of modal distribution.

Losses caused by bad positioning can be approximately calculated by the geometric optic (ray launch method), and the results are given in decibels in the form of a chart (see Figure 3.11).

When they are low, losses due to each cause are added (in first order). However, these calculations suppose a uniform distribution of the optical power and are therefore not very precise and somewhat pessimistic.

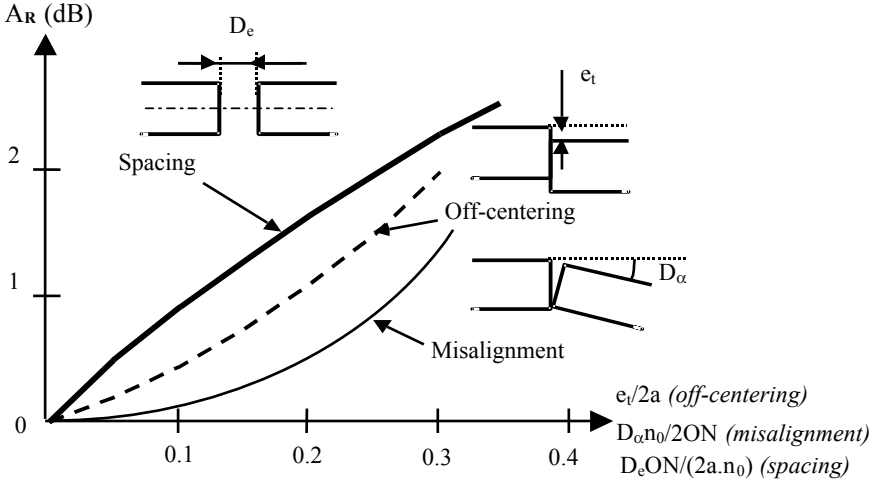


Figure 3.11. Losses at multimode fiber connections

3.4.2.3. Calculation in single-mode fibers

In this case, the transmission coefficient T of one fiber to another is more rigorously calculated by an overlap integral between E_1 and E_2 of both fibers:

$$T = \frac{\left| \iint_{x,y} E_1(x,y) E_2^*(x,y) dx dy \right|^2}{\iint_{x,y} |E_1(x,y)|^2 dx dy \iint_{x,y} |E_2(x,y)|^2 dx dy}$$

We deduce loss in dB: $A = -10 \log T$; this loss is reciprocal. In the Gaussian fields and low error hypothesis, this calculation gives losses in dB, which again add in first order between the different causes (see Table 3.4).

3.4.3. Fiber optics optimization

We can observe that the core diameter and index difference had contradictory effects on the different causes of optical fiber attenuation and dispersion. Table 3.5 shows these effects.

Cause	Loss in dB
Difference between mode $2w_0$ diameters	$20 \log \frac{w_{01}^2 + w_{02}^2}{2w_{01}w_{02}}$
Off-centering e_t	$4.34 \frac{e_t^2}{w_0^2}$
Misalignment D_α (radians)	$4.34 \frac{D_\alpha^2}{\theta_0^2}$ with $\theta_0 = \frac{\lambda}{\pi w_0 n_0}$
Spacing D_e	$10 \log (1 + Z)$ with $Z = \frac{D_e}{k_0 n_0 w_0^2}$

Table 3.4. Losses at single-mode fiber connections

If increased:	Losses				
	Intrinsic	To connections	By bending	By micro-bending	Dispersion
<i>For multimode fibers</i>					<i>Intermodal</i>
Core diameter	No change	Decrease	Increase	No change	No change
Numerical aperture	Increase	Decrease	Decrease	Decrease	Increases
<i>For single-mode fibers</i>					<i>Chromatic 1.55 μm</i>
Core diameter	No change	Increase	Increase	No change	Increases
Index difference	Increase	Slight increase	Decrease	Decrease	Decreases

Table 3.5. Optical fiber optimization criteria

A compromise needs to be reached, which will depend on conditions of use: bending, constraints, connection frequency and precision. For short links with a large number of connections such as networks or distribution, a multimode fiber with high diameter and numerical aperture is optimal (that is why fiber 85/125 was specified for video distribution, but 62.5/125 is the one that has taken over, especially for computer networks).

These fibers pick up a stronger signal from the transmitter. For longer or higher throughput point-point links, lower diameter and numerical aperture such as 50/125 are preferable.

In the case of long links over single-mode fibers, we can numerically determine parameters optimizing attenuation and dispersion according to conditions of use, by trying to make extrinsic losses insignificant.

That is why submarine links use optimized fibers with different values from terrestrial fibers.

3.5. Optical fiber measurements

3.5.1. *Classification*

Optical fiber measurements are divided into two categories:

- fiber parameter measurements: these are multimode fiber geometric parameters (optical cladding and core diameters, numerical aperture) optically measured; for single-mode fibers, since these parameters are not directly accessible because of diffraction, mode diameter and cut-off wavelength are measured. These measurements are mainly performed by the optical fiber manufacturer;

- transmission parameter measurements, which are of direct interest to the user. The user may actually have to redo these measurements, in particular after optical cable installation in the network, which can modify some initial fiber performances.

3.5.2. *Geometric measurements for multimode fibers*

This concerns core and cladding diameters, and numerical aperture. They can be deduced from simple geometric measurements on the light beam at the fiber output:

- the core diameter by the measurement of the near field;
- numerical aperture by the measurement of the far field (radiation pattern). In practice, the effective numerical aperture of the cone is measured:

- $ON_{\text{eff}} = \sin \theta_{\text{eff}}$ at 10% (or 5%) of the maximum. This is lower than the theoretical numerical aperture, because of the stronger attenuation of the higher order modes, which makes this curve smoother than the theoretical one.

These measurements must be done at mode equilibrium, after elimination of cladding modes. In order to do this, a mode scrambler is used (a device creating microbending in the fiber, hence strong mode coupling). The source must be a light-emitting diode, to avoid modal noise that a coherent source would create.

The numerical aperture can also be directly measured by injecting light beam in the optical fiber under a variable angle, until this beam is no longer guided in the fiber. This method, although closer to the theoretical definition, is only suitable for step index fibers, where selective mode excitation can be carried out by this method.

3.5.3. *Measurements of single-mode fibers parameters*

Due to diffraction, it is not possible to directly measure the core diameter or index difference. The single-mode fiber is characterized by its secondary parameters (see Chapter 2): the cut-off wavelength and the mode field diameter. These values are important in predicting single-mode fiber attenuation and dispersion.

Different methods have been developed, the main one being the variable aperture lens method, which is an optical method consisting of measuring the coupling efficiency of a Gaussian beam whose aperture is varied.

They require complex equipment and are only carried out by the fiber manufacturer. Determination of $2w_0$ by the far field is more simple but less precise.

A good estimation of the *cut-off wavelength* can be made from the spectral attenuation curve. In fact, just above λ_c , the mode LP_{11} is guided but with much loss, resulting in abruptly dropping additional attenuation when λ reaches λ_c , because the mode LP_{11} is no longer guided (see Chapter 2).

3.5.4. *Spectral attenuation measurement*

This involves all fibers. The goal is to measure curve $\alpha(\lambda)$ (see Figure 3.1). In order to do this, for each wavelength λ , is calculated:

$$\alpha(\lambda) = \frac{10 \log[P(L_1)/P(L_2)]}{L_1 - L_2} \text{ where } L_1 \text{ is the initial fiber length}$$

The power P is measured at the end of this length. To determine intrinsic attenuation of the optical fiber, the injected power must be known. In order to do this, the fiber is cut at the end of a short L_2 length, at the end of which the mode equilibrium must be established with the help of a mode scrambler, the power is measured once again. The global attenuation is deduced, which is then reduced to the unit of length.

This method, called *cut-back*, is illustrated in Figure 3.12. We can observe that it is a destructive method which is only practised once, during fiber manufacturing. Its quality can be controlled with good precision, but only gives average fiber attenuation and cannot be practised once the fiber is installed in the network. That is why the most widely used method is reflectometry.

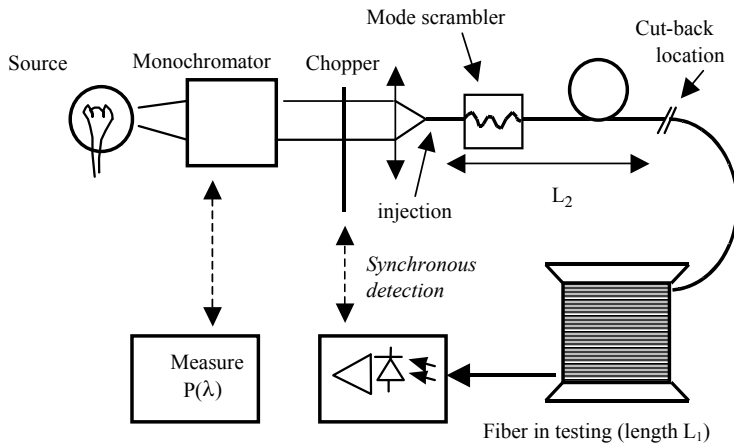


Figure 3.12. Spectral attenuation measure of optical fibers

3.5.5. Reflectometry measurement

3.5.5.1. Principle

Optical time domain reflectometry (OTDR) is a method of fiber optic characterization from a single extremity, which not only measures reflections, but also attenuation, based on backscattered light (it is also called backscattering measurement). Even though this technique uses relatively expensive equipment, it is much used by fiber manufacturers, installers and network operators because it makes it possible to measure and monitor installed links.

It operates as illustrated in Figure 3.13. At moment t_0 , a brief pulse of duration $\delta\tau$ is sent into the fiber by a laser diode.

With the help of a splitter, a large band and highly sensitive receiver observes the light that the fiber sends by reflection and Rayleigh scattering. The signal received at moment $t_0 + t$ comes from the point located at distance:

$$z = t \cdot v_g / 2 \text{ with } v_g = c/n_1 \text{ group velocity in the optical fiber}$$

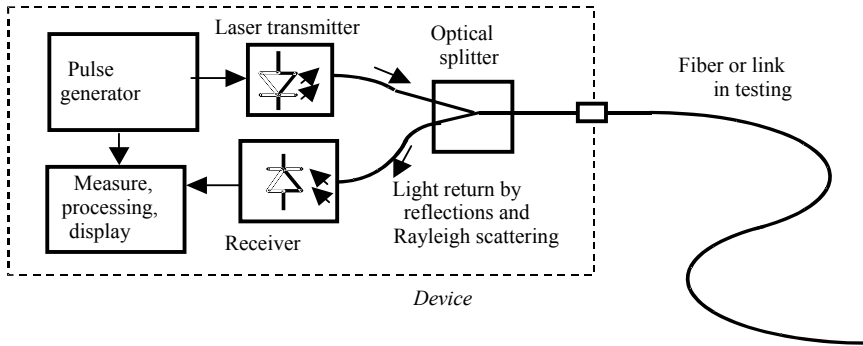


Figure 3.13. *Reflectometry*

The t/z ratio is very close to 10 ns/m. Due to this, the measure can be time-resolved. In the first approximation, spatial resolution will be:

$$\delta z = \delta\tau \cdot v_g / 2$$

the minimum distance between two points which can be distinguished on the curve, without having to use complex signal processing. High resolution (better than 1 m) requires short pulses (less than 10 ns).

3.5.5.2. Power received

Signal power received at moment $t_0 + t$ equals (in logarithmic units):

$$P_r \text{ (dBm)} = P_e \text{ (dBm)} - A \text{ (dB)} + S \text{ (dB)} - 2 \int_0^z \alpha(x) dx$$

with:

– P_e power transmitted in dBm;

- A attenuation in splitter and connector dB, forward and back;
- S, which is highly negative, is the part of power sent back to the fiber input:
 - either by reflection, S is then the reflection factor:

$$S \text{ (dB)} = 20 \log \frac{|n_1 - n|}{n_1 + n}$$

in case of index discontinuity (example: crack perpendicular to the fiber axis);

- or by Rayleigh scattering, and S is given by:
 - $S \text{ (dB)} = 10 \log (\alpha_D v_g / 2 \cdot \delta\tau \cdot \kappa)$ with: $\delta\tau$ pulse time;
 - α_D Rayleigh scattering coefficient = $2.2 \cdot 10^{-4} \cdot \lambda^{-4} \text{ m}^{-1}$ (with λ in μm);
 - κ back coupling factor (part of scattered power returning to the entry):

$$\kappa = \frac{3}{8} \left(\frac{ON}{n_1} \right)^2 \text{ for a step-index fiber (with usual notations)}$$

$$\kappa = \frac{1}{4} \left(\frac{ON}{n_1} \right)^2 \text{ for a parabolic graded-index fiber}$$

$$\kappa = \left(\frac{\lambda}{2\pi \cdot w_0 n_1} \right)^2 \text{ for a single-mode fiber (very low in this case)}$$

The last term comes from signal attenuation on the return trip path. In the absence of reflection, S is constant and, with a simple derivation, we obtain the attenuation profile along the fiber:

$$\alpha(z) = - \frac{1}{2} \cdot \frac{dP_r}{dz}(z)$$

Commercial equipment and operating systems directly give the attenuation value; there is no need to divide the levels by 2.

3.5.5.3. Reflectometry curve interpretation

Reading the curve (see Figure 3.14) helps in measuring fiber attenuation as well as locating its variations, due for example to defects, bending or constraints. Reflection peaks localize cracks; the end of fiber reflection measures its length

precisely. In particular, connectors can be characterized in transmission and reflection once the connection is established. This instrumentation also makes it possible to remotely measure attenuation or reflection caused by sensors placed along the fiber.

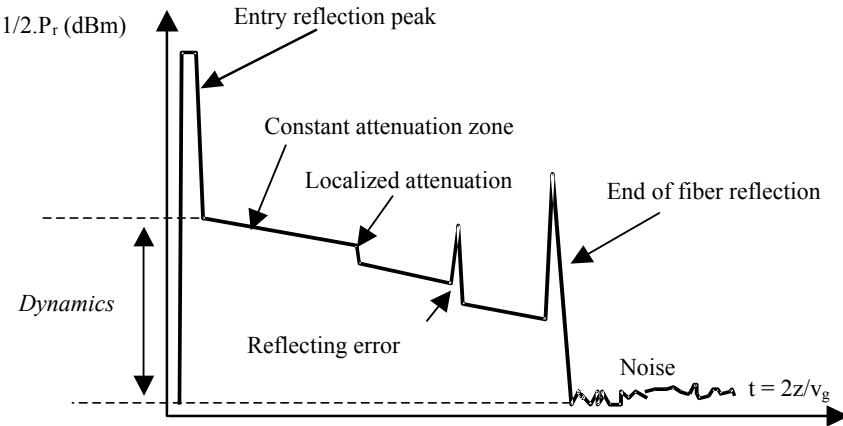


Figure 3.14. *Reflectometry curve*

Entry reflection peak is quite a hindrance because it saturates the receiver for a time corresponding to several dozen meters of fiber, creating a blind zone at the start of the link. To avoid this, notably in local networks, it is necessary to insert a fiber pigtail between the equipment and the beginning of the fiber to be characterized.

A localized attenuation (splicing, bending, etc.) is directly measured by the height of the step separating the two fiber sections, when they have the same S factor. If that is not the case, the measures taken in both directions must be averaged.

In certain cases, “ghost” peaks can emerge at twice the distance of the distance to the connector; this is a part of the pulse that has traveled two times consecutively in the fiber. They are recognizable by their location, and by the absence of attenuation, contrary to a connector.

3.5.5.4. Dynamics

An important parameter of a reflectometer is its dynamics, the difference in dB between the power scattered by the fiber input and the minimum power P_{\min} , required at receiver for a given signal-to-noise ratio:

$$D = P_e - P_{\min} - A + S \text{ (in dB)}$$

In this theoretical definition (bidirectional dynamics), D allows us to characterize a total fiber attenuation of $D/2$. In order to simplify the interpretation of measures, in practice the *unidirectional dynamics is used*, equal to $D/2$ then to the maximum fiber attenuation. There are two official definitions:

- the RMS dynamics (unidirectional) where P_{rmin} is the rms (root mean square) noise level;
- the CEI dynamics (unidirectional) where P_{rmin} is the level containing 98% of the noise.

The dynamics can be increased by increasing the pulse duration, or S , but the resolution decreases. In order to optimize the measurement, reflectometers can generally transmit different pulse lengths, from a few ns to a few hundred ns, with automatic or manual selection of the appropriate duration.

In addition, the equipment generally practices an average between N measures, which improves the signal-to-noise ratio by $5 \log N$ (but increases acquisition time). More complex processes exist, for example by deconvolution, enabling us to improve the resolution without reducing the dynamics.

Current reflectometers require us to disconnect the link in order to measure it. New equipment has emerged that uses a specific wavelength to perform the measurement simultaneously with the traffic using other wavelengths. Located above WDM bands (1,625 nm wavelength is reserved for this purpose), this wavelength also has the advantage of being more sensitive to bending and thus better detecting constraints in the cable.

3.5.6. Bandwidth measurement

This is the multimode fiber bandwidth. It is most often measured with the help of the time-domain response $h(t)$, from where the pulse broadening $\Delta\tau_{\text{im}}$ caused by intermodal dispersion is deduced (see Chapter 1). A laser diode is used to deliver very short input pulses $e(t)$ and to avoid creating chromatic dispersion.

The time-domain response is determined by a deconvolution: in fact, the pulse measured at the fiber output, $s(t)$, is given by the convolution product:

$$s(t) = \int_{-\infty}^{+\infty} e(t-\tau)h(\tau)d\tau$$

Deconvolution calculation also provides the *transfer function* $H(f)$, the Fourier transform of $h(t)$. This transfer function represents the light modulation by an electric sine signal with a frequency f , which experiences attenuation that is larger the higher the pulse widening. This response is normalized with respect to $H(0)$, measured to a modulation frequency that is zero or very low, making it possible to take into account the attenuation of the optical power by the fiber.

The optical fiber *bandwidth* can deduced from the diagram:

$$20\log\frac{H(f)}{H(0)} \quad (\text{see Figure 1.15})$$

It can also be measured by a traditional frequency analysis: a network analyzer measures $H(f)$, by using a short link between transmitter and receiver as reference, in order to take into consideration inherent interface response.

It is necessary to carry out these two measures at mode equilibrium, by using a mode scrambler.

3.5.7. Chromatic dispersion measurement

This is performed for single-mode fibers, but we must not forget that it also exists for multimode fibers, especially at 0.85 μm . In their case, the chromatic dispersion factor is very close to material dispersion given by diagrams.

The principle is to measure $D_c = d\tau_g/d\lambda$ where τ_g is the light group delay by unit of length in the fiber, and which depends on the wavelength. This measure is difficult, because very short pulses (a few hundred ps) have to be generated over a large range of wavelengths. The main method consists of measuring $\tau_g(\lambda)$ point by point, by using several laser diodes of shifted wavelengths, working in pulses and the result is:

$$\frac{d\tau_g}{d\lambda} = \frac{\tau_g(\lambda_{i+1}) - \tau_g(\lambda_i)}{\lambda_{i+1} - \lambda_i}$$

where λ_{i+1} and λ_i are two neighboring wavelengths.

$\tau_g(\lambda)$ is the group delay, i.e. $\tau(\lambda)/L$, where L is the fiber length, and $\tau(\lambda)$ the global propagation time. The use of tunable wavelength laser diodes provides this curve in a continuous way instead of point by point.

There are other indirect but very precise methods using phase shift of a sine signal of frequency f modulating the light of wavelength λ .

Chromatic dispersion measurements are also applied to dispersion compensation devices (described in Chapter 5) such as Bragg gratings equalizers, the goal being then to measure their slope $d\tau/d\lambda$ in ps/nm.

3.5.8. Polarization measurements

With the increase of bitrates in very long links, these are increasingly important. They involve single-mode optical fibers, because of the polarization mode dispersion (PMD), as well as passive optical components where attenuation and even propagation time may depend on light polarization (respectively characterized by PDL (polarization dependent loss) and DGD (differential group delay) measured in ps per component). Very high precision benchmarks analyze attenuation and group propagation time according to light polarization.

To measure polarization mode dispersion (PMD) in $\text{ps}/\sqrt{\text{km}}$, pulse $\Delta\tau_p$ widening has to be measured according to fiber length, in maximum coupling conditions between polarization modes, while being freed from chromatic dispersion with the help of compensating devices. Remember that measured PMD in the fiber may not be found again in practice because of cable effects (bending, constraints, etc.).

This page intentionally left blank

Chapter 4

Integrated Optics

4.1. Principles

4.1.1. *Introduction: classification of components*

Different components are used in the implementation of fiber optics links and networks, which can be classified according to their function and technology (see Table 4.1).

The following chapters will describe passive and active optical components, with optical and most often reciprocal access (with the exception of isolators and amplifiers), and optical electrical interfaces: transmitters and receivers.

4.1.2. *Technologies used*

Fiber-optic assembly based technologies, used for the development of passive functions such as couplers (see Chapter 5), are advantageous because of their very low level of losses, in particular at fiber connections, but have a bad reproducibility.

Type of Technology	Passive optics	Non-reciprocal optics	Active optics	Optoelectronics
Glass (optical fibers or glass substrates)	Couplers, attenuators, wavelength multiplexers	Erbium doped fiber amplifiers (fiber based or integrated)	Mechanical switches (slow)	
Dielectric crystals (LiNbO ₃ type)	Same functions	Isolators	Time-division multiplexers, modulators, switches	
Semi-conductors (GaAs, InP, Si)	Same functions	Semiconductor optical amplifiers	Same functions	Transmitters (LED, DL), receivers, electronic components

Table 4.1. *Fiber optics system components*

Integrated optics technologies offer much better reproducibility of the components, which are created by masking techniques on dielectric or semiconductor substrates, and a much larger variety of functions, notably with the possibility of integrating different functions, including light emission and reception. Losses are higher, however, especially at the connections (see section 4.1.5). The three families of material used are:

- glass, of very low loss level, with index close to 1.5; they only enable passive functions, except if they are doped for making amplifiers;
- dielectric crystals, notably lithium niobate LiNbO₃, with index close to 2.2, where the electrooptic effect creates active functions with very high operating frequencies;
- semiconductors, particularly III-V, with a high index (3.5), with higher losses, but where, in addition to the previous functions, optoelectronic (transmission, reception, amplification) and electronic, logical or analog functions can be developed. A few integrated optics applications in silicon exist: guides, filters, interferometers, sensors.

Finally, photonic crystal type technologies (see Chapter 2), generally on silica, are beginning to be used to create much more compact guides.

4.1.3. Integrated optics planar guides

Due to their manufacturing technology, they are generally asymmetric rectangular section guides: the planar guide is a thin layer of index n_1 and is inserted between a substrate of slightly lower index n_2 , and a coating of index n_3 that is lower than n_2 (see Figure 4.1).

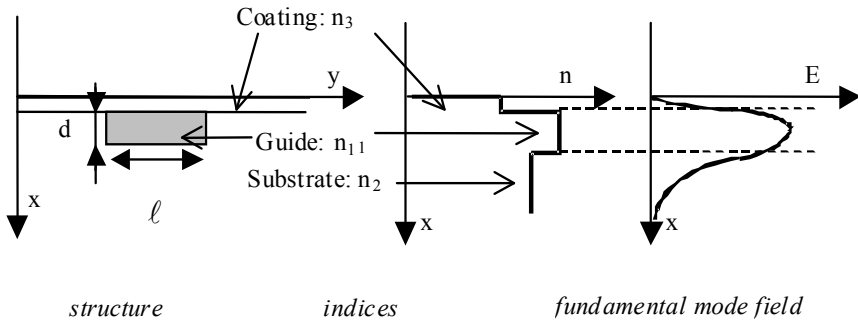


Figure 4.1. Dielectric planar guide in integrated optics

As we have seen in Chapter 1, the asymmetric dielectric planar guide model exhibits a non-zero cut-off frequency for the fundamental mode, by mode refraction in the substrate.

Moreover, this cut-off wavelength depends on polarization, and it is possible to have a guide which only guides mode TE_0 but not mode TM_0 , i.e. which polarizes light. Another consequence is that the fundamental mode field has an asymmetric transverse distribution, extending more in the substrate than in coating (see Figure 4.1).

4.1.4. Lateral guiding

In most devices, the guide is laterally limited to a width ℓ by one of the following production processes (see Figure 4.2):

a) relief stripe, not much used;

b) stripe obtained by diffusion from the substrate surface, or by ionic exchange, which is a technology that is widely used with glass; in silicon, oxidation from the surface helps to create the silica guide;

c) induced guide by a deposited dielectric stripe (which increases the effective β/k_0 index in this stripe) or by an electrode (operating by electrooptic effect, in active material);

d) buried stripe in the substrate, by epitaxy, technology mainly used with semiconductors (for diode lasers in particular). In principle, it corresponds to the symmetric guide case.

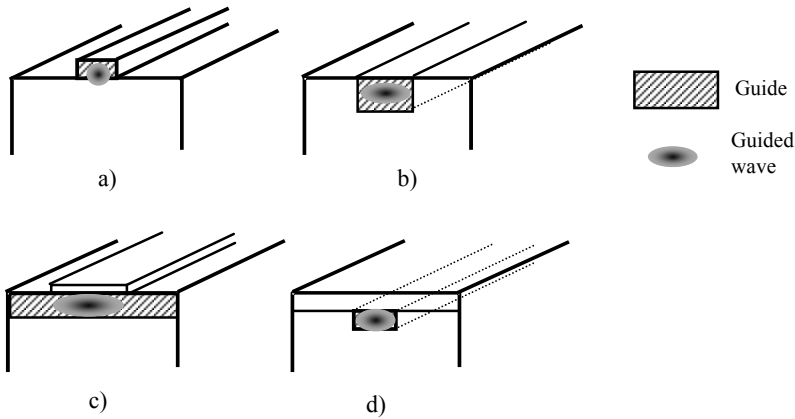


Figure 4.2. *Creation of integrated optics guides with: a) in relief; b) scattered; c) induced; d) buried guide*

Lateral guiding is then ensured by total reflections to the guide's limits, or, for induced guides, by the graded index created in the guiding layer. In this rectangular guide, HE_{mp} modes (or EH_{mp} depending on their polarization) will be observed with:

$$m = \text{transversal order, } p = \text{lateral order}$$

equal to the number of nodes of the field in each direction.

As with fiber optics, numerical resolution of propagation equations makes it possible to trace dispersion diagrams: B , normalized propagation constant of each mode, versus the normalized frequency V and the width to height ratio (ℓ/d) of the guide.

Lateral field distribution follows a sine law in the guide, and decreasing exponential outside (evanescent field zone). Lateral field distribution of the

fundamental mode is Gaussian-like (see Figure 4.4). In most applications, integrated optic guides are used in *single mode*.

4.1.5. Losses in guides

Losses in integrated optics components can be divided into three categories:

- *absorption losses* in guides, by the following phenomena:

- absorption by impurities, very low because of technological progress;
- absorption specific to semiconductors: interband (photons are absorbed by carriers located in the bandgap) and intraband (photons increase the energy of conduction band carriers) absorption.

Absorption is the major cause of loss in semiconductors, satisfactory values of approximately 0.1 dB/cm are now reached;

- *scattering losses*, mainly due to non-homogenities of guide volume and surface; this is the main cause of loss, although quite low, in dielectrics;

- *radiative losses* out of the guide, at angles and bendings which are necessary for the implementation of complex forms in components. They can be limited by giving a relatively strong value to the substrate guide index difference, with a resulting large mode mismatching with optical fibers. These losses are generally difficult to calculate and numerical methods must be used, such as BPM (beam propagation method) software. In the future, photonic crystal structures with their very strong bending and large angles will be able to avoid these losses;

- *losses to the access* of the guide which often constitute the major part of losses involved in the use of integrated optics components. They come in part from the large index difference, and from mode mismatching between guides and optical fibers, or sources, to which guides are connected. Butt-joint coupling between a guide and another guide, a laser diode or an optical fiber, requires very precise alignment of the different elements and generally a lens, external or integrated in guides. Some devices integrate a mode matching guide section, for example of variable width; a diffraction grating can also be used (see section 4.3.3) to limit these losses.

4.2. Mode coupling and its applications

Coupling between the modes of one guide or between neighboring guides has several applications. The general formalism is that of mode coupling.

4.2.1. Formalization

When two guided waves A and B, with fields as expression:

$$E_A = A(z) \exp j(\omega_A t - \beta_A z) \text{ and } E_B = B(z) \exp j(\omega_B t - \beta_B z)$$

exchange energy, their complex amplitudes $A(z)$ and $B(z)$ vary:

$$\frac{dA}{dz} = \kappa_{AB} \cdot B \exp(-j\delta z) \text{ and } \frac{dB}{dz} = \kappa_{BA} \cdot A \exp(-j\delta z) \text{ with } \delta = \frac{|\beta_A| - |\beta_B|}{2}$$

Term δ , the phase mismatch parameter, shows that coupling can only be complete between matched guides ($\delta = 0$), but it can be partial between mismatched guides, as with resonators.

Terms κ_{AB} and κ_{BA} are *coupling coefficients* by unit of length. Their expression depends on the physical phenomenon which caused coupling. In linear mediums, this can only happen between waves of the same frequency (that is if $\omega_A = \omega_B$). If the phenomenon is reciprocal, we have $\kappa_{AB} = \kappa_{BA}$.

4.2.2. Coupling within a single guide

Within a single guide, we can observe:

- coupling between two modes of a single multimode guide. Zero in theory, because of mode orthogonality, it emerges in the event of guide perturbations (constraints, non-homogenities), constituting mode coupling which plays an important role in multimode fiber propagation;

- coupling between both directions in the same guide, even single-mode. It can for example, be caused by Rayleigh backscattering. In integrated optics, it can be deliberately caused by a diffraction grating of spatial period π/β , causing a very wavelength-selective distributed reflection.

A strong mode coupling in both directions can also be created by modifying the core diameter (tapered fiber technique for filters and splitters).

By noting as L the length of the coupling zone, and by assuming energy conservation:

$$\frac{d}{dz} (|A|^2 - |B|^2) = 0 \text{ hence } A \cdot \frac{dA^*}{dz} + A^* \cdot \frac{dA}{dz} = B \cdot \frac{dB^*}{dz} + B^* \cdot \frac{dB}{dz}$$

where * indicates conjugated complex. We then obtain:

$$AB^*.\kappa_{AB}^* + A^*B.\kappa_{AB} = BA^*.\kappa_{BA}^* + B^*A.\kappa_{BA}$$

which demands $\kappa_{AB} = \kappa_{BA}^* = \kappa$. This coupling coefficient must be real since $\kappa_{AB} = \kappa_{BA}$.

The equation becomes:

$$\frac{d^2A}{dz^2} = \kappa^2.A$$

hence the solution (see Figure 4.3):

$$A(z) = A_0 \text{ch } \kappa (L - z)/\text{ch } \kappa L \text{ and } B(z) = A_0 \text{sh } \kappa(L - z)/\text{ch } \kappa L$$

for $A(0) = A_0$ and $B(0) = 0$.

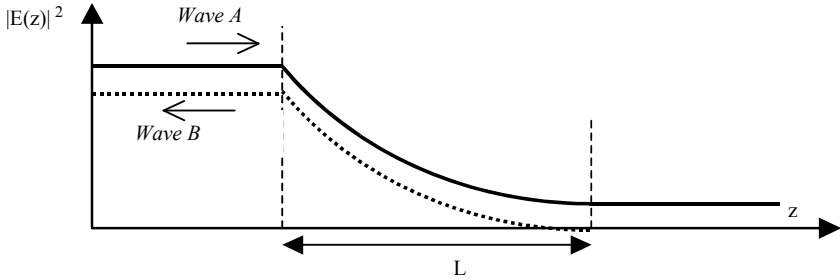


Figure 4.3. Coupling between both directions caused by a distributed reflector

The reflection coefficient equals:

$$R = \left| \frac{B(0)}{A(0)} \right|^2 = \text{th}^2 \kappa L$$

It can be close to 1 if $\kappa L \gg 1$.

4.2.3. Coupling between matched guides

When, in a single substrate, two parallel neighbor guides are created close to one another, they can be coupled with the help of evanescent fields (see Figure 4.4). The coupling coefficient, calculated by the overlap integral, equals:

$$\kappa = \frac{2\alpha^2 \gamma e^{-\gamma D}}{\beta \ell (\alpha^2 + \gamma^2)}$$

with:

- ℓ guide width;
- D distance between guides;
- $\beta = \beta_A = \beta_B$ propagation constants in both guides, presumed identical;
- α and γ transverse propagation constants in the guide and substrate.

As the propagation directions are now the same, energy conservation gives:

$$\frac{d}{dz} (|A|^2 + |B|^2) = 0$$

which, by a similar calculation to the previous one, leads to:

$$\kappa_{AB} = -\kappa_{BA}^* = j\kappa$$

which must be purely imaginary. The equation becomes:

$$\frac{d^2 A}{dz^2} = -\kappa^2 A$$

hence the solution (see Figure 4.4):

$$A(z) = A_0 \cos \kappa z \text{ and } B(z) = -j A_0 \sin \kappa z, \text{ again for } A(0) = A_0 \text{ and } B(0) = 0$$

The term in $-j$ indicates that the coupled field B is in late phase quadrature in relation to field A .

The solution shows that total and periodic energy exchange occurs between matched guides: in fact, energy has completely passed from guide A to guide B at the end of a *conversion length*:

$$L_c = \frac{\pi}{2\kappa}$$

Since this phenomenon depends on the wavelength, it is possible to create devices (integrated guide or edge-fused single-mode fibers, devices in which both cores are very close within a certain length) which will be in parallel state for λ_1 and in cross state for λ_2 , i.e. two-way *wavelength division multiplexers*. They are more selective than filter multiplexers. They can be used as interleavers (see Chapter 5). In fact, α , β and γ (wave vector components) are approximately in $1/\lambda$. The dominant term in κ is in $e^{-D/\lambda}$ (D is the distance between cores) which increases with λ . L/L_c , the ratio proportional to κ , will also increase with λ . Each time it goes through an odd integer, there is total coupling, these are values $\lambda_1, \lambda_3, \lambda_5$, etc. exiting by the second fiber. Each time it goes through an even integer value, coupling is zero, they are values $\lambda_2, \lambda_4, \lambda_6$, etc. exiting by the first fiber and which are interleaved with the first comb. The values are all the more tightened the larger p , and thus the ratio L/L_c , is.

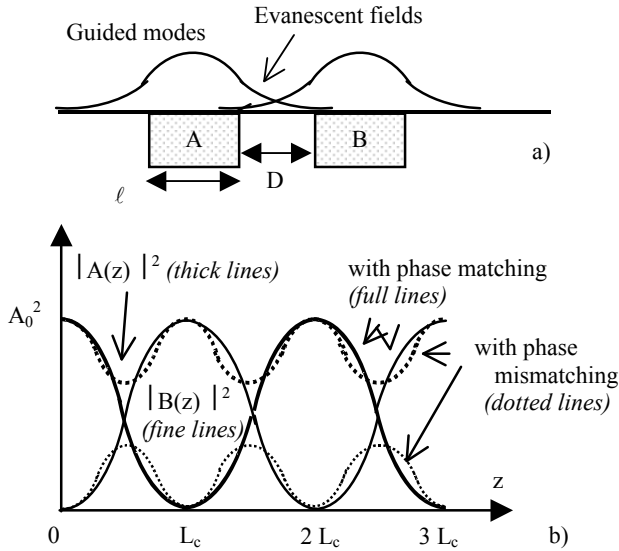


Figure 4.4. Coupling between neighbor guides

4.2.4. Coupling between mismatched guides

If there is mismatch, intentional or not, between guides ($\delta \neq 0$), the exchange is only partial and calculation leads to:

$$A(z) = A_0 \left[\cos z \sqrt{\kappa^2 + \delta^2} + \frac{j\kappa}{\sqrt{\kappa^2 + \delta^2}} \sin z \sqrt{\kappa^2 + \delta^2} \right]$$

$$B(z) = A_0 \frac{j\kappa}{\sqrt{\kappa^2 + \delta^2}} \sin z \sqrt{\kappa^2 + \delta^2}$$

or a maximum power transfer of: $\frac{\kappa^2}{\kappa^2 + \delta^2}$.

The larger the mismatch parameter δ , the lower the exchange and shorter the period (see Figure 4.4).

It is then possible to adjust parameters in order for the energy to be back in the input guide at the end of length L_c . We are then in a parallel state.

This phenomenon is most interesting when it is possible to create switching between the cross state and parallel state, using the electrooptic effect for example (see Chapter 5).

4.3. Diffraction gratings

4.3.1. Principle

Widely used in optics, diffraction gratings take the form of periodic geometric patterns, whose spatial period Λ has the same order of magnitude as the wavelength λ , causing large diffraction. This pattern can take the form:

- of the pattern of a reflecting surface (engraved gratings, Figure 4.5a) which can have a triangular profile (widely used blazed grating), square, sine, etc.;
- of the periodically variable index of a transparent layer (holographic gratings, see Figure 4.5b, used for optical spatial switching prototypes).

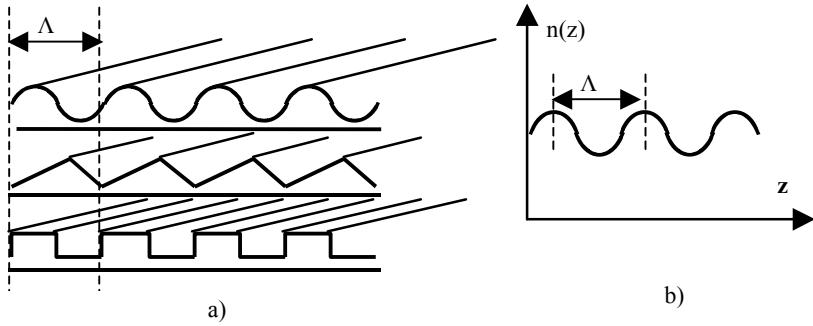


Figure 4.5. Diffraction gratings: a) engraved gratings; b) holographic gratings

4.3.2. Operation

Diffraction gratings operate on *interferences* between waves diffracted by each grating element (see Figure 4.6).

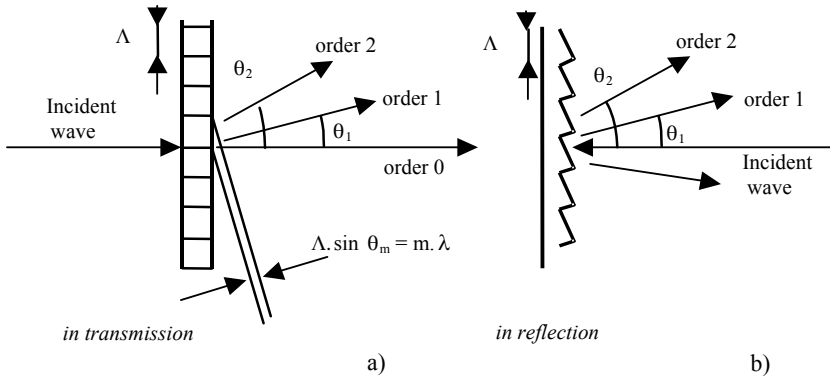


Figure 4.6. Diffraction gratings operation

An incident wave on a grating with an infinite (or very large) number of periods will be diffracted, and we can observe a discrete distribution of directions, or orders, corresponding to constructive interferences between diffracted waves, for angles θ_m verifying:

$$\sin \theta_m = m \frac{\lambda}{\Lambda}$$

In fact, since the near field is periodic, the far field, which is its Fourier transform, is discretized.

The main quality parameters for these gratings are:

- their spectral resolution or finesse: this increases with the number M of grating periods. For a perfectly periodic grating, maximum resolution equals $\Delta\lambda/\lambda = 1/M$;
- their performance in the chosen order (generally 1st order); for example, for a blazed grating with a tilt of ϕ , it is maximal to sequence m around the wavelength:

$$\lambda_m = \frac{2\Lambda \sin \phi}{m}$$

- the parasite scattered light rate, related to surface quality.

The main application of these gratings, which are used in monochromators, and optical spectrum analyzers, is to spectrally decompose the incident light, since the direction of diffracted light is related to its wavelength. This is the principle of some wavelength multiplexers (see Chapter 5).

4.3.3. Application to light coupling in a guide

As we have seen, guide access losses are high because of mode mismatching. An interesting laboratory process (for example, for measures) is to use coupling through a prism (see Figure 4.7). It simply uses refraction of light in the prism to inject and extract light from the guide without going through its extremities.

An incident beam normal to the prism surface, which has a tilt of θ_i , is completely coupled in the guide if:

$$k_0 \cdot n_p \cdot \sin \theta_i = \beta, \text{ mode propagation constant in the guide}$$

This relation shows that the index of prism n_p must be quite high. It must be coated with an antireflection layer.

If the guide is coated, the coupling is carried out by evanescent fields and it therefore becomes weaker the thicker the coating. The length L of the coupling zone must then be increased.

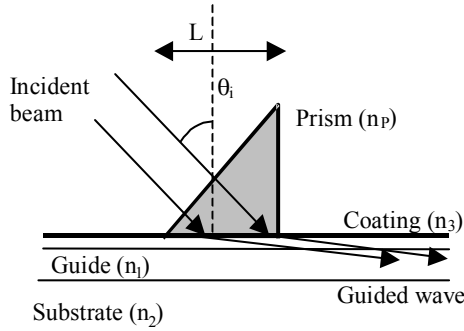


Figure 4.7. Light coupling in a guide through a prism

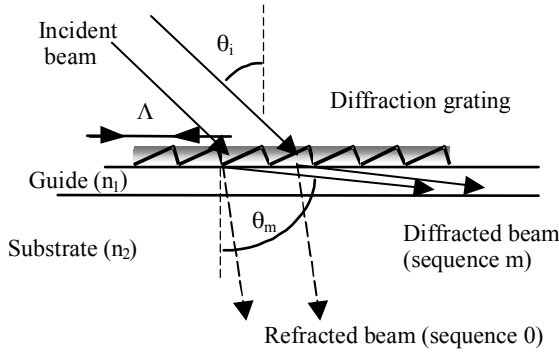


Figure 4.8. Light coupling in a guide through a diffraction grating

Coupling using a *diffraction grating* (see Figure 4.8), even though it experiences more losses, has the advantage of being integrated and very selective in wavelength. Order m , diffracted in direction θ_m , given by:

$$n_1 \sin \theta_m = \sin \theta_i + m \frac{\lambda}{\Lambda}$$

is totally coupled to the guide if:

$$k_0 \cdot n_1 \cdot \sin \theta_m = \beta, \text{ hence } k_0 \cdot \sin \theta_i + m \frac{2\pi}{\Lambda} = \beta$$

This process makes it possible to separate different multiplexed wavelengths in the same guide.

4.3.4. Bragg grating principle

This is a specific diffraction case through a *thick* grating, much thicker than λ^2/Λ (see Figure 4.9). Most of the light is diffracted in the first order, and the configuration is symmetric; input and output angles are equal to θ_B given by:

$$\sin \theta_B = \frac{\lambda}{2\Lambda} \quad (\text{Bragg angle})$$

This configuration is used in acousto-optic modulators for its high efficiency, since the diffraction grating is created here by acoustic wavefronts propagating in a crystal and periodically modulating its index (photo-elastic effect).

In this way light direction is modulated (as well as its frequency by the Doppler effect). This process is used in some integrated optical switches, their switching times have the order of magnitude of a μs .

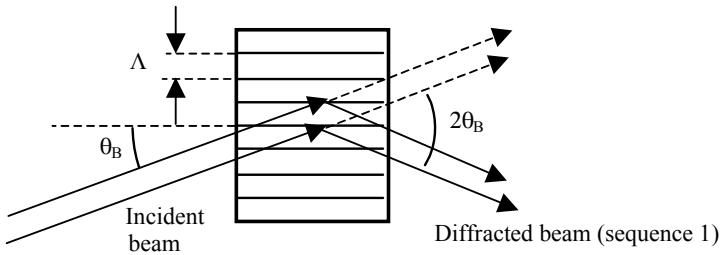


Figure 4.9. Massive Bragg grating

4.3.5. Bragg gratings in integrated optics

In this case, the Bragg grating is integrated longitudinally in a guide (see Figure 4.10). Therefore $\theta_B = \pi/2$ and we have:

$$\Lambda = \frac{\lambda}{2n_a} \quad \text{with } n_a = \frac{\beta}{k_0} \text{ apparent index in the guide, or } \Lambda = \pi/\beta$$

meaning that consecutive reflections of the grating patterns are in phase.

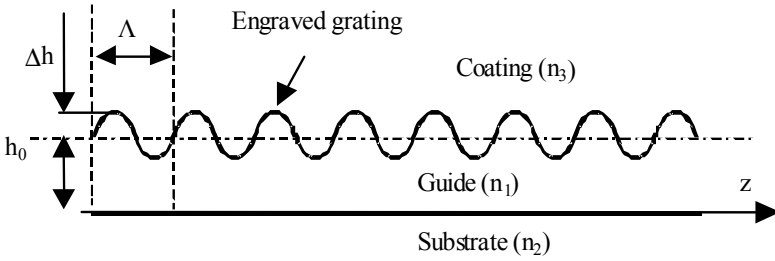


Figure 4.10. *Bragg grating in integrated optics*

This distributed reflection will cause strong coupling with a reflected wave that propagates in the opposite direction. The coupling coefficient (used in section 4.2.2) is given by:

$$\kappa = \frac{\pi}{\lambda} \frac{\Delta h}{h_{\text{eff}}} \frac{n_f^2 - n_a^2}{n_a}$$

with: Δh = grating amplitude.

$h_{\text{eff}} = h_0 + 1/\gamma_2 + 1/\gamma_3$ is the “reflected density” of the guide, a term taking into account apparent widening of the guide by the Goos-Hanchen effect: h_0 , the actual thickness, is increased with penetration depths in the substrate and coating (see Chapter 1).

The main advantage of this structure is its high selectivity in wavelength (all the more so the longer the network). It is used to make integrated filters in guides, distributed feedback monochromatic lasers (see Chapter 6):

- DFB (distributed feed-back), with integrated grating in the active zone;
- DBR (distributed Bragg reflector) with integrated grating in the active outside zone axis;
- selective wavelength splitters.

They are also used to make wavelength-tunable filters or laser diodes over a dozen nm, using the electrooptic effect to vary the apparent index, and therefore the reflected wavelength, caused by an electric field (in crystals) or a current (in semiconductors). In passive material, this effect can be obtained from temperature or even from stretching.

4.3.6. Photo-inscribed Bragg gratings in optical fibers

4.3.6.1. Principle

In optical fibers, a *Bragg grating* can be created by photo-inscription in the fiber core matter. It uses the photo-refractivity phenomenon (permanent modification of the core refraction index caused by ultraviolet illumination; core fibers co-doped with germanium and boron are well suited for this). This technique, derived from holography, enables the creation of integrated filters in optical fibers (see Figure 4.11). The step, and thus the reflected wavelength, can be controlled with precision by illuminating the fiber with interference fringes.

One of the applications of photo-inscribed Bragg gratings is the stretching sensor: by increasing the grating step, fiber stretching will involve a variation of the reflected wavelength, which can be measured remotely. Reciprocally, a stretching constraint of the fiber creates a filter that can be tuned over a rather narrow range.

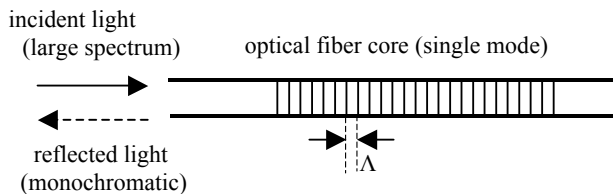


Figure 4.11. Photo-inscribed Bragg grating in a fiber

4.3.6.2. Bragg grating filters

Photo-inscribed Bragg gratings are stop-band filters used to eliminate residues from the pump wave in optical amplifiers, to strengthen selectivity in wavelength demultiplexers, or in the laser diode pigtail, in order to better control their wavelength and to decrease their spectral width. They can also be used to reflect a reference wavelength in some sensors or networks.

Designing a photo-inscribed Bragg grating filter is carried out by knowing that its spectral response is the Fourier transform of the index modulation envelope. The bandwidth and the selectivity of the filter can be controlled. A photo-inscribed Bragg grating on a finite length with constant modulation amplitude will have a cardinal sinus spectral response, presenting secondary lobes, which is usually disrupting. To avoid this effect, the grating must be “apodized” by giving a specific form to the modulation amplitude, for example Gaussian (see Figure 4.12), but the spatial period must still be constant.

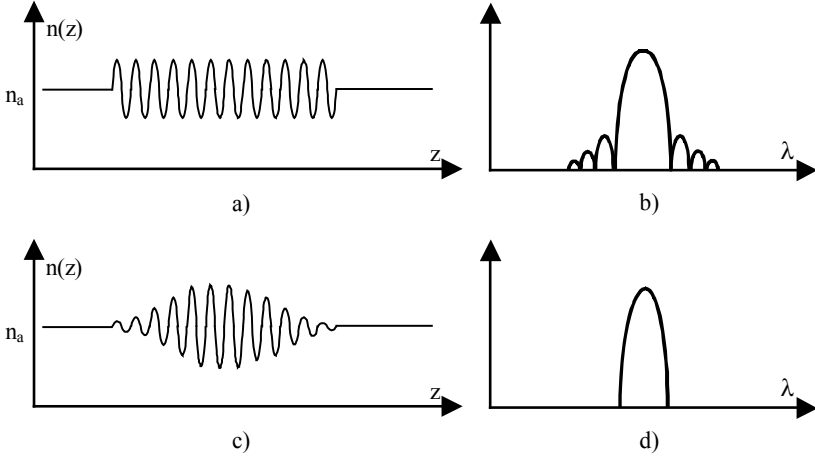


Figure 4.12. *Apodization of a photo-inscribed Bragg grating: a) grating with an amplitude of constant modulation; b) spectral response; c) apodized grating; d) spectral response*

4.3.6.3. Chirped Bragg gratings

Chirped gratings are a specific case; they are gratings with a spatial period varying regularly along the zone inscribed in the fiber. This device reflects a wide range of wavelengths, with a time shift that is linearly related to the reflected wavelength. They are used in chromatic dispersion compensation devices (see Figure 4.13): short wavelengths, which arrived first in the case of positive dispersion ($d\tau/d\lambda > 0$) will travel a longer path in the Bragg grating before reflecting, and will be more delayed than the larger wavelengths. If the grating period has a linear variation of $\Delta\Lambda$ on a length L , this device's dispersion coefficient in ps/nm is given by:

$$D = \frac{L}{c \cdot \Delta\Lambda}$$

In this case, a linear dispersion (constant slope) can be compensated on a wavelength range $\Delta\lambda = 2 n_a \cdot \Delta\Lambda$. However, it is possible to photo-inscribe a Bragg grating with a non-linear law $\Lambda(z)$ to compensate for another dispersion law (as long as it is monotone). It is nevertheless difficult to create such devices to compensate for strong dispersion over a large range.

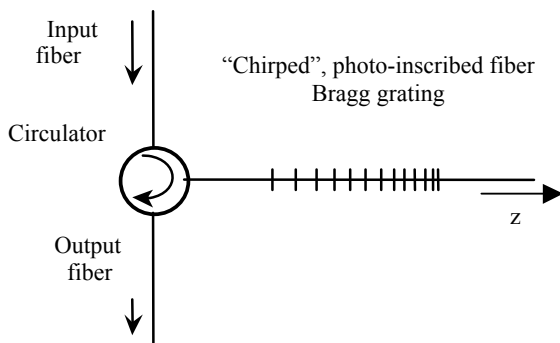


Figure 4.13. *Chromatic dispersion compensator*

Chapter 5

Optical Components

5.1. Passive non-selective optical components

5.1.1. Definitions

We call “optical components” the components with access where the signal remains optical, without modifying its nature (see Table 4.1). The component is said to be passive if its operation is constant in time, and does not require control signal (electric or optical).

The optical signal is generally attenuated and it is important to distinguish between:

- component’s *insertion loss* between input E_i and output S_j equaling, in dB:

$$T_{ij} = 10 \log \frac{P_{Ei}}{P_{Sj}}$$

where P_{Ei} is the power at input E_i and P_{Sj} is the power output at S_j ;

- excess loss, caused by component imperfection as defined by:

$$p_e = 10 \log \frac{P_{Ei}}{\sum P_{Sj}} \text{ (in dB)}$$

part of the input power that is not found at any output.

For example, in the case of optical power sharing on multiple paths, for a splitter with n symmetric branches, we have:

$$T_{ij} = 10 \log n + p_e$$

Excess loss is deduced from the comparison between theoretical and measured loss.

In principle, insertion loss is the same in both directions, except for specific components such as isolators. In multimode fiber devices however, slightly different attenuations can be measured in both directions if the modal distribution is not the same in both measures.

A good optical component must be characterized by:

- low excess loss (in dB, it increases with the number of branches);
- low reflection at each access (return loss: $10 \log T_{ii} > 20$ dB);
- strong isolation between access at the same side (low crosstalk);
- in certain cases, low perturbation of the modal distribution or the polarization.

These definitions are also valid for wavelength selective components (whose parameters depend on λ) and for active optical components (they vary over time by a command).

5.1.2. Optical couplers

These realize sharing or grouping of optical signals, which are constant over time. In the first mode or splitter, the same signal is simultaneously addressed over several output paths. In the coupler mode (but the same component), different signals are grouped and it is necessary to distinguish them by their wavelength, their coding or an access control protocol, otherwise they get mixed up... The main categories are (Figure 5.1):

- *X couplers* (2 inputs, 2 outputs), realized by assembling polished optical fibers, or by edge fusion/stretching; symmetric (50/50) or asymmetric (90/10, 95/5, etc.) couplers can be produced;
- *Y couplers* (1 input, 2 outputs or the other way around), made from half coupler X and a fiber; because reciprocity, loss is the same in both directions, loss is at least 3 dB by using a Y coupler (symmetric) to group 2 signals;
- *star couplers* or distributors (n inputs, n outputs), which can be produced by twisting and fusion of an n fiber bundle. They commonly have between 7 and 10 fibers.

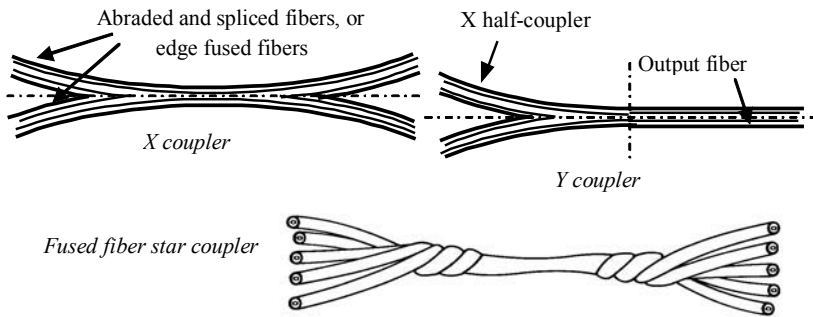


Figure 5.1. *Fiber-based optical couplers*

These technologies present low connection losses and are not very reproducible. Passive integrated optics in glass or silicon substrate are much more reproducible but access losses are more prevalent.

Figure 5.2 shows a Y coupler with this technology, a brick allowing much more complex structures (it is generally not interesting by itself, but is interesting when combined with filters, multiplexers or active elements). Star couplers to 32 channels are also produced for passive optical networks (PON, Chapter 10) in planar technology which is less expensive than fiber technology.

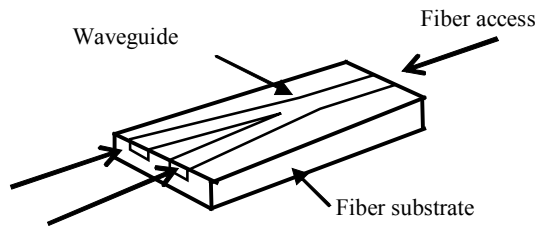


Figure 5.2. *Y couplers realized in integrated optics*

With the exception of certain single-mode couplers which use coupling selectivity between guides to serve as demultiplexers (section 5.2.2), these components are not wavelength selective. On the other hand, because of anisotropy created in guides by the geometry of couplers, birefringence effects can appear. The coupler must be calculated and realized with much precision if the coupler has to be independent from input polarization or on the contrary, selective in polarization (there are separating polarization couplers created with birefringent fibers).

5.1.3. Isolators and circulators

Even though they use an active effect, the *Faraday effect* (also used as the current sensor), these are passive components in the sense that they do not require feeding current or commands.

The Faraday effect (see Chapter 2) is caused by a longitudinal magnetic field \vec{H} , turning light polarization by the following angle:

$$\phi = 2 V_F \cdot L \cdot H$$

where L is the interaction length and V_F is the Verdet constant, characteristic of the material.

In the isolator application (Figure 5.3), the magnetic field is provided by a permanent magnet, which turns polarization by 45° in a magneto-optical crystal (with high Verdet constant). This crystal is placed between two 45° polarizers. Due to this, the light which propagates in the “transmitted” direction experiences a 45° polarization turn in the right direction, and crosses the output polarizer. On the other hand, the light propagating in the reverse direction experiences a polarization turn in the wrong direction and is cut off by the output polarizer.

Good isolators have more than 40 dB isolation rates, but present a maximum efficiency wavelength. Isolators are sometimes used following a laser diode to avoid a return of reflected light in the optical fiber, as well as in erbium-doped fiber amplifiers. For this last application, polarizers are replaced by birefringent crystals, enabling them to work independently from the incident polarization.

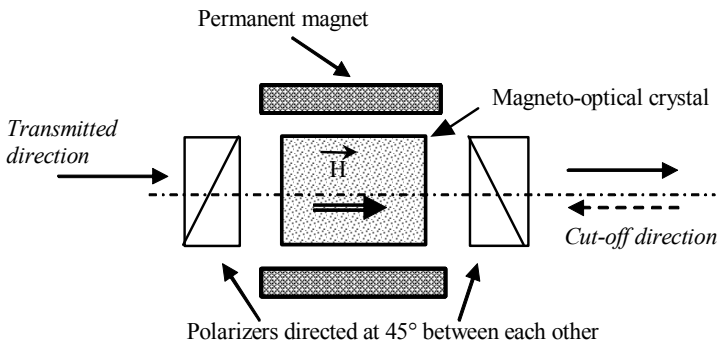


Figure 5.3. Optical isolators

3-port *circulators* with similar functions as circulators in microwave frequency, based on the Faraday effect, are emerging on the market. Associated with Bragg photo-inscribed gratings, they have their use in several filtering and wavelength division multiplexing devices (see the add-drop multiplexer example in Figure 5.7).

5.1.4. Optical attenuators

Fixed or variable attenuators are traditionally used for measures. They simulate the attenuation of a long fiber and make it possible to determine the transmission systems margin. Since they do not present propagation time dispersion, they also allow us to evaluate the penalty caused by dispersion in actual systems. They are also beginning to be used in high throughput (Gbit/s and more) local area networks because the use of laser diodes, which is necessary to reach these throughputs, leads to a too high level of received signals and saturates the receiver.

Attenuators can be realized in several ways:

- with neutral optical filters with a density that can be either uniform, or variable step by step or continuously (with mechanical command);
- or by using losses caused by mismatching between two optical guides or fibers opposite each other, ensuring a more compact installation.

In reconfigurable ADMs (section 5.4.4) and in optical amplifiers (Chapter 8), variable optical attenuators (VOA) are also used to dynamically flatten the gain between the different amplified wavelengths. Gain flattening devices based on photo-inscribed Bragg gratings have also been developed.

5.2. Wavelength division multiplexers

5.2.1. Different types of wavelength division multiplexing

Wavelength division multiplexing or WDM has become increasingly important in increasing network capacity and flexibility. It uses wavelength division multiplexers, *selective and reciprocal* components (they can serve as multiplexers as well as demultiplexers). Contrary to couplers seen above where the same signal is distributed between the different outputs, multiplexers offer one common access and n selective accesses. Signals carried by different wavelengths and arriving by the common access are sent toward different outputs. Conversely, signals with different wavelengths arriving from their own access are multiplexed, theoretically without loss, toward the common output. It is also possible that some wavelengths propagate in one direction and others in the reverse direction.

There are three types of wavelength division multiplexing:

- two way multiplexing (two relatively spaced out wavelengths, or two windows) described in section 5.2.2;
- dense WDM (DWDM) between a large number of very close wavelengths (gap of less than 1 nm) in the same window, described in section 5.2.3;
- more recent to the market, coarse wavelength division multiplexing technologies (CWDM) multiplex within the same window 4 to 8 wavelengths spaced between 10 and 20 nm, mainly based on filter technologies; these are cheaper components than the DWDM multiplexers, which can respond to metropolitan network requirements.

5.2.2. Filter multiplexers

Two way couplers are generally realized by *dichroic filter* technology (filters made by the stacking of thin layers, transparent for certain wavelengths and reflecting for others), which separates two rather large and spaced windows: for example, 0.85 and 1.3 μm , or more recently, 1.3 and 1.5 μm for PON access networks.

These components can be realized by fiber assembly as well as by integrated optics (Figure 5.4) and are characterized by a low level of insertion loss (typically 0.5 to 1 dB) and high isolation between channels (at least 20 to 40 dB). They enable the sharing of a fiber that is already installed with a new user, or the creation of a bidirectional link in a single fiber, with a wavelength per direction. Because of the price of multiplexers, this is only economical from a certain fiber length (access networks), or if installation constraints demand a single fiber.

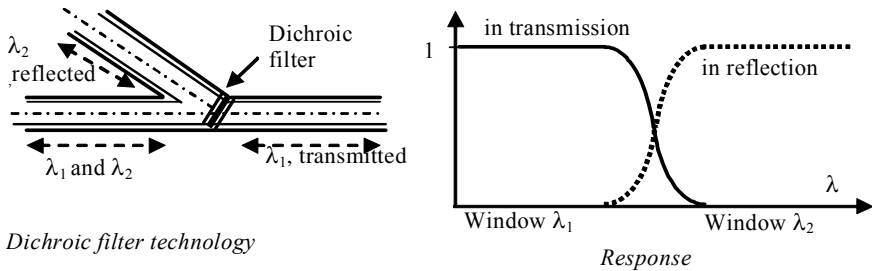


Figure 5.4. Dichroic filter wavelength division multiplexers

5.2.3. Coupler-type multiplexers

These multiplexers use the selective coupling between two single-mode guides (see section 4.2.3) which are also two channel couplers, but they selectively separate two close wavelengths (for example, the signal and pump in optical amplifiers).

They can be used as interleavers where their principle, explained in section 4.2.3, is based on the law of coupling between two single-mode guides in a coupler, which varies periodically with the wavelength.

There remain two channel couplers, but a channel contains all even wavelengths, the other one has all the odd wavelengths (Figure 5.5). Their application is to multiplex, in an interlaced way, two wavelength meshes coming from different subnetworks in access nodes to the core networks.

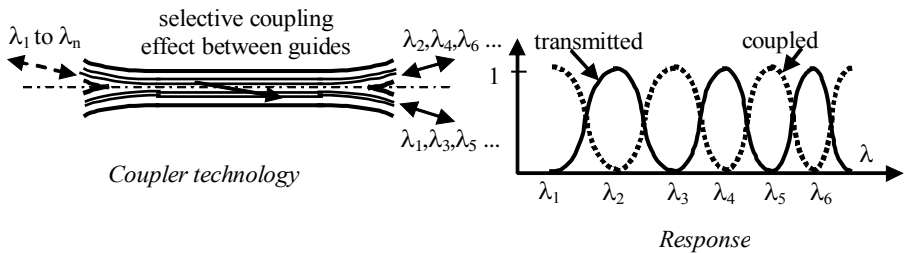


Figure 5.5. Interleaver

5.2.4. Dense wavelength division multiplexing

DWDM (Dense Wavelength Division Multiplexing) reaches gigantic capacities (higher than 10 Tbit/s) in networks and long distance links, and its market mainly involves single-mode fibers and the 1.55 μm window. It is very selective since the frequency spacing between channels, standardized by ITU (International Telecommunications Union), is 100 GHz (or approximately 0.8 nm to 1.55 μm); this “grid” defines channels from 192.1 to 196.1 THz, in other words from 1,561 to 1,529 nm. Grids where channels are two, or even four times as tight (or a gap of 50 or 25 GHz, this multiplexing is then said to be “ultra-dense”) can be used, or on the contrary settle for a gap of 200 or 400 GHz. These multiplexers use technologies based on diffraction gratings and Bragg gratings, in fibers or integrated optics, or also on interference between integrated guide arrays.

Although still expensive (and involving the use of high purity and spectral stability laser diodes), these wavelength division multiplexers are passive

components of a technology that is more mature and reliable than time-division optical multiplexers. They allow us to gradually increase the capacity of existing links and to adapt to traffic increase with flexibility. They are also very useful in developing multi-terminal networks, particularly when the terminals are not grouped geographically. The economic advantage of dense wavelength division multiplexing is largely due to the development of optical amplifiers, which can simultaneously amplify all the wavelengths in the same window (1,530 to 1,565 μm), whereas before, a repeater-regenerator was required for each wavelength.

Classical multiplexers (Figure 5.6), where all wavelengths are (de)multiplexed at the same point, are traditionally realized with diffraction gratings (see section 4.3), resulting in a “bulky” component. These multiplexers present high separating power, a few dozen nm (possibly reinforced by Bragg gratings) and offer a large number of channels (several dozen, even over 100 channels for massive 3D structures), high diaphonic isolation (20 to 30 dB between adjacent channels) and typical losses from 1 to a few dB. Their cost is high, however, all the more so because they generally require thermal regulation.

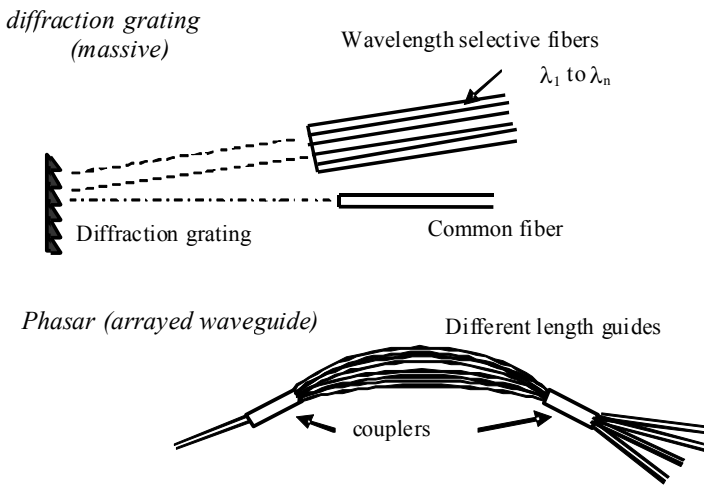


Figure 5.6. Dense wavelength division multiplexers

“Phasars” or AWG (arrayed waveguides) have emerged recently, benefiting from the advantages and low cost of passive integrated optics. They are based on interferences between integrated guides of different lengths creating a phase shift between each other depending on the wavelength: between two guides with lengths different from Δl , this equals:

$$\Delta\phi = (2\pi/\lambda)n \cdot \Delta l \quad (n \text{ is the guide index})$$

Following a principle similar to phased array antennae (in microwave frequencies), the output light transmission direction depends on the wavelength, which achieves demultiplexing.

5.2.5. Add-drop multiplexing

In *optical add-drop multiplexers* (OADM), a signal at wavelength λ_i is dropped from the group and is replaced by *another* signal at the *same* wavelength λ_i . They are generally realized with photo-inscribed Bragg gratings and circulators (Figure 5.7). These components are in strong development in multi-terminal networks, because each terminal can then operate on its own wavelength and add/drop its signals without having to demultiplex the complete spectrum.

By associating wavelength-tunable sources (or more rarely receivers), or sometimes by tuning optical ADM with acoustic waves, optical routing is beginning to be realized. Thus, functions developed so far by electronic layers (ADM was introduced in electric form by the synchronous SDH hierarchy) are now in the *optical layer* (see Chapter 10).

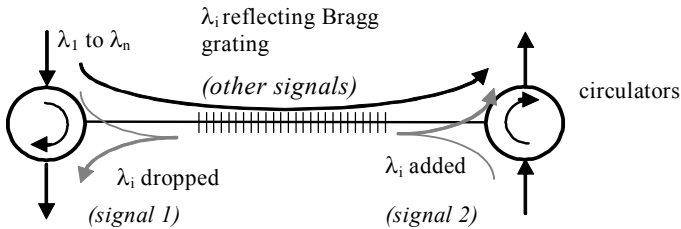


Figure 5.7. Optical add-drop multiplexer (OADM)

5.3. Active optical components

5.3.1. Principles

By active optical components, we mean the components in which the signal will remain optical at access but be submitted to processes (modulation, switching, etc.) driven by an external signal. This signal is most often electric, with the use of the electro-optic effect, allowing us to reach very high frequencies (several dozen GHz). However, the command can also be:

- mechanical, in certain switches, they are slow and of a large size, but reliable and without consumption outside of switching; they are used in securing networks or routing devices. MEMS (see section 5.4.2) enable the development of high capacity and rather high speed spatial switching matrices (response time is in ms);

- acoustic, in the case of acousto-optic modulators, application of bulk diffraction gratings or in guides (see section 4.3.4); they are slower but less expensive than electro-optic modulators. Acousto-optic switches also exist with a response time in μs ;

- thermal, in certain switches using material differential dilatations; we also use the effect of temperature on glass indices;

- optical, by using optical non-linear effects, mainly for the development of bistable components, but these devices are still in the research stage.

In integrated optical circuits, semiconductor or erbium-doped optical amplifiers are emerging, allowing the compensation of passive integrated optical component losses. They also provide optical gate-based switching architectures.

5.3.2. *Electro-optic effect*

This is the modification of permittivity ϵ , thus of the index of the material, resulting from an external electric field \vec{E} . This effect is important in certain asymmetric crystals such as lithium niobate (LiNbO_3). In the most general case, the material is not isotropic and permittivity is a tensor $\vec{\epsilon}$ given by relation:

$$\vec{D} = \vec{\epsilon} \vec{E}, \text{ or the inverse relation: } \vec{E} = \vec{a} \vec{D}$$

where \vec{a} is the inverse of the permittivity tensor.

An external electric \vec{E} field modifies this tensor. In crystals, the predominant component of its variation is linear and is called the *Pockels effect*. It leads to a variation of the :

$$\Delta n = n^3 \cdot r' \frac{E}{2} \text{ at the first order}$$

r' being the effective electro-optic coefficient; its exact value depends on relative directions of \vec{E} and \vec{E} (light polarization) in relation to the crystal.

Over a propagation length L , the light phase then varies by:

$$\Delta\phi = 2\pi L \frac{\Delta n}{\lambda}$$

If field \vec{e} is longitudinally applied, the voltage producing a phase shift of π is taken out from $V = e.L$ and equals:

$$V_{\lambda/2} = \frac{\lambda}{n^3.r'}$$

This voltage is called *half wave* and is characteristic of the material. It is approximately 2V in lithium niobate. This low value is one of the advantages of integrated optics.

There is also a quadratic term in e^2 , called the *Kerr effect*, much weaker than the Pockels effect in crystals, but the only one existing in fibers. It creates a slight birefringence in optical fibers submitted to an external electric field.

5.3.3. Directional electro-optic coupler

This is the most classical electro-optic component. The electro-optic effect enables the modification of coupling factors between two parallel integrated guides (Figure 5.8a). A control voltage of a few volts, applied between two electrodes placed on the guides, creates a field \vec{e} in each of them, hence an index Δn variation, in opposite directions. A mismatching of propagation constants then appears between both guides and it equals:

$$\Delta\beta = 2k_0.\Delta n = k_0 n^3.r'.e$$

This enables switching between the cross state and parallel state (see section 4.2.4). Length L must be an odd multiple of conversion length L_c , in order to obtain the cross state in the absence of control voltage; meanwhile voltage applied to a precise value switches to the parallel state. Since it is not easy to achieve that with precision, a four electrode configuration is used (Figure 5.8b). In this one, it is possible to obtain both states (cross and parallel) for any L value between L_c and $3L_c$, by adjusting control voltage values to $V_{//}$ (parallel state) and V_x (cross state).

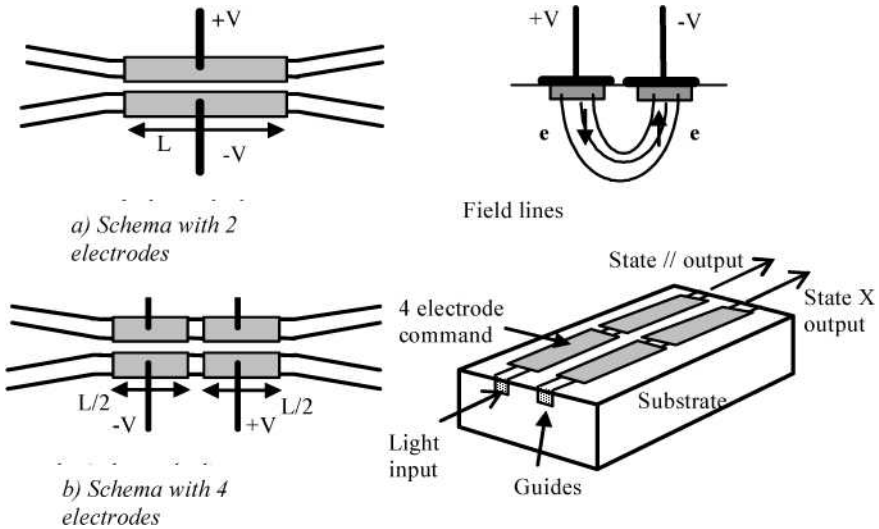


Figure 5.8. *Electro-optic coupler principle*

This component has several applications:

- extremely fast switch (less than 100 ps of switching time);
- on-off external modulator, by coupling one of the guides toward output (40 GHz was reached but the Mach-Zehnder modulator is more efficient);
- time-division multiplexer (two inputs alternatively switched toward the same output); optical time-division multiplexing (OTDM) experiments have thus reached 160 Gbit/s but this remains very complex;
- switching matrices, by integrating several basic elements in the same substrate.

Although lithium niobate offers the best components, the active integrated optics also uses semiconductors, in particular indium phosphide (InP). These actually make it possible to integrate both active and passive optical functions in the same substrate, as well as light receivers and transmitters, and logical or analog electronic functions.

This technology is called integrated optoelectronics.

5.3.4. Electro-optic modulator

The electro-optic effect is also used to realize phase modulators, most often integrated in semiconductors, with laser diodes, which modulate the transmission in an “external” way. It is also used in wavelength tunable diodes (Chapter 6).

Interferometers mainly exist in integrated optics. The most classical set up is the Mach-Zehnder interferometer (Figure 5.9) in which both electrodes, placed on both arms, command a phase shift ϕ which is translated into a light output intensity modulation by $\cos^2\phi$. It is mainly used in on-off external modulation devices, controlled by a voltage V_0 giving $\phi = \pi/2$, used at 10 and at 40 Gbit/s (below, internal laser modulation is possible and much more economical).

It is a very efficient component but delicate to realize, because impedance matching over a wide band, phase matching between microwave and optical signals (that is why electrode co-planar disposition is also used) and electric signal amplification, whose peak to peak voltage is approximately 5V, must all be ensured.

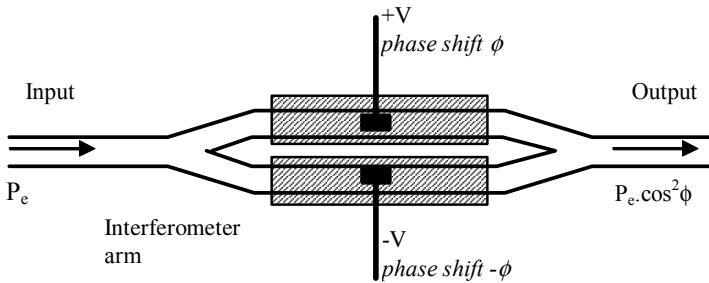


Figure 5.9. *Integrated optics Mach-Zehnder interferometer*

An analog modulation of signal intensity can also be achieved, to generate solitons, or to modulate light by a microwave sub-carrier. In this case, a bias voltage must be applied to electrodes in order to set the rest point to $\Phi = \pi/4$ and to work in the rather linear zone of the $\cos^2\phi$ law.

A more recent use of these modulators is duobinary or bipolar modulation, in which 0 is coded by 0 and 1 is alternately coded by +1 and -1, which means phase reversal in optics. In the Mach-Zehnder interferometer modulator, if a voltage $2V_0$ double of the one providing a zero power is applied, then $\Phi = \pi$, $\cos \phi = -1$ which results in maximum power (demodulation does not change) but a reverse phase on

light. This process is more resistant to chromatic dispersion (see section 9.1.4). The same component but with a different control signal, can achieve binary phase-shift modulation with 2 states (0 and π) and differential phase shift keying (DPSK) that are easier to demodulate (section 9.1.5).

5.3.5. Electro-absorption modulator

This amplitude modulator (EAM) uses a different principle which is the variation of the photon absorption in a semiconductor, caused by the application of an electric field. In fact, semiconductors present a very fast variation of their absorption coefficient with wavelength at the neighborhood of their cut-off wavelength, i.e. for photons with energy close to their bandgap (see section 6.1.3).

These high slope characteristics can be shifted by the application of a perpendicular electric field (Figure 5.10). The absorption coefficient then varies into large proportions for a wavelength close to the cut-off (1.55 μm for GaInAsP). This is at the base of amplitude modulator use.

Electro-absorption involves a complex *absorption by exciton* phenomenon, i.e. the creation of an electron hole pair where the electron is in orbit around the hole. This absorption is very selective and is observed by a peak in the absorption curve. It is usually observed at very low temperature, but can be obtained at ambient temperature in quantum well devices. The realized devices use multiple quantum well structures. In these structures, applying an electric field perpendicular to layers shifts the resonance peak of the excitonic absorption, while remaining very selective, because of quantization imposed by the structure. On the other hand, a parallel electric field widens this peak using the Stark effect, as in bulk materials.

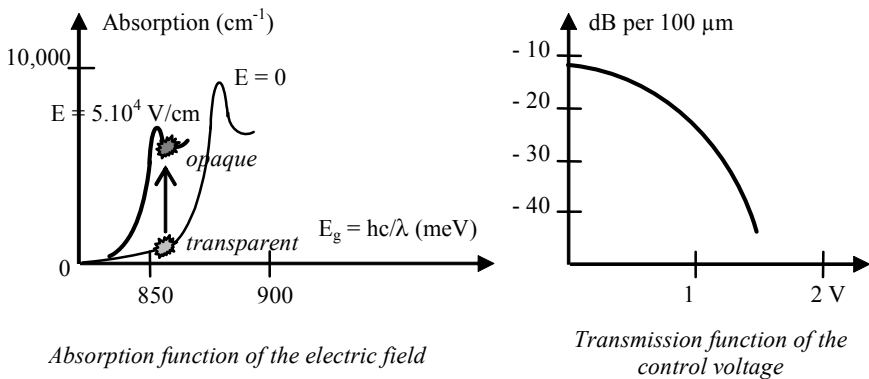


Figure 5.10. Principle of electro-absorption modulation

This enables the control of the modulator with low voltages (about one volt) and to obtain very high modulation frequencies: from 20 to 40 GHz depending on control voltages, much more than with internal laser diode modulation. These modulators are therefore used to reach very high bitrates (10 to 40 Gbit/s) in digital transmission, with modulation depths of 10 to 20 dB. However, they can be used in analog modulation, to generate solitons or for microwave optical fiber transport, by transposing modulation carrier from radio frequency to optical frequency. They are slightly less efficient and more limited in wavelength than Mach-Zehnder modulators, but they are easier to integrate with laser diodes.

These components present high attenuation however (approximately 10 dB for 100 μm , a typical length for this component, compared to 4 to 5 dB for Mach-Zehnder), even in the “on” state; because of this, the integration of the modulator with an optical semiconductor amplifier has been developed. Their response depends on the source wavelength, which is quite suitable for use when they are integrated with the transmitter. A parasite phase modulation also exists, causing a *chirp* effect. As a last point, the electro-absorption phenomenon presents a certain sensitivity to light polarization, sensitivity which can be compensated by the modulator structure.

Electro-absorption modulators have also been used in optical regeneration experiments which remain difficult to implement.

5.4. Fiber-optic switches

5.4.1. Functions

Optical switches were developed as early as the first fiber-optic systems. We must distinguish between, however:

- switches from one to two (or a small number) channels, often found in security (switching toward a stand-by emergency component) or measurement devices; these do not need to be very quick and generally use mechanical devices;
- switching matrices in the sense of a switching function in networks, which can be spatial or temporal, and from which a large capacity is expected ($n \times n$ with n in the hundreds, or even more) and a more or less high speed. The interest in these devices, which for a very long time have not passed the laboratory stage, returned in 2000. In fact, current network switches called OEO (optical-electric-optical) perform electronic switching, that requires a double conversion and is limited in speed.

However these studies have still not resulted in massive use in networks, because of cost and lack of device maturity, as well as their impact on network protocols and architecture, because they only ensure circuit switching. They are actually used as cross-connects, to provide network reconfiguration according to traffic, more than to

switch channels in real time. Complementary devices, such as reconfigurable OADMs (section 5.4.4) or wavelength conversion, are necessary to arrive at a real all-optical network (Chapter 10).

5.4.2. *Switching technologies*

The technologies used can be (Table 5.1):

- mechanical (mirror and switch based); they are slow (response time in dozens of ms) and their consumption is low, but they are of large size and have limited capacity. There are thermal controlled mechanical switches, mainly on silicon. They are mostly used in security (switching toward a fiber or a security component), possibly for routing;

- micro electro-mechanical structures (MEMS; faster (response time in ms), allowing packet switching, they have higher capacity because of their integration, especially in 3D structures (section 5.4.3) and can be used as cross-connects; there are also 1 to 2 switches realized in silicon microtechnology (micro-movement of an integrated optics guide), very quick but of uncertain reliability;

- in integrated optics, based on electro-optic couplers (section 5.3.3); their speed is much higher (100 ps), and their higher consumption directs them to time-division switching, and are currently in the experimental phase. Despite their monolithic integration, they are not well suited for high capacity matrices because losses increase quickly with the number of basic 2 x 2 switches;

- 3D free beams: their main advantage for very wideband spatial switching comes from their three-dimensional structure authorizing large capacity matrices (100 x 100 or more) with low loss levels (Figure 5.11).

Technology	Switching time	Congestion	Consumption	Capacity	Applications
Mechanical	50 to 100 ms	very high	low	low	network security
Micro electro-mechanical (MEMS)	a few ms	low	medium	high	cross-connects
Integrated optics	< 1 ns	very high	high	relatively low	temporal switching
3D	10 to 100 ms	medium	low	very high	cross-connects

Table 5.1. *Optical switching technologies*

In the 1980s holographic prototypes (based on holographic diffraction gratings) were developed. They were awkward and very slow because of hologram rewriting time.

More compact and faster prototypes based on liquid crystals were recently presented, but despite the interest for 3D devices, they are not really operational.

Other prototypes, such as acousto-optic, microbubble, optical gate based on semiconductor optical amplifiers, etc. were developed, but none stands out.

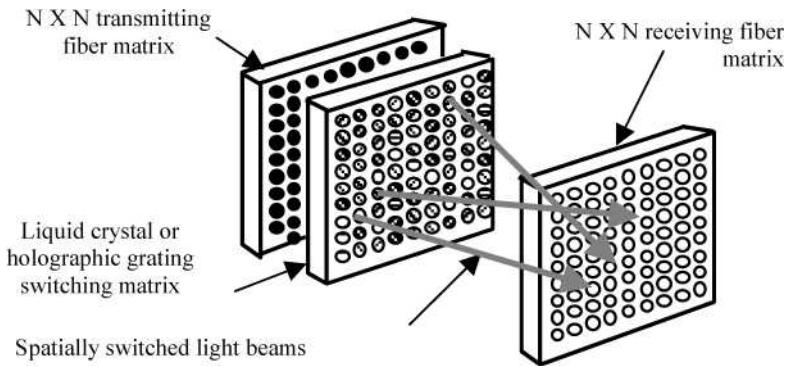


Figure 5.11. *Free beam optical switching matrix*

5.4.3. Example of micro electro-mechanical switching matrices

The development of large capacity matrices using micromirrors can be carried out from two architectures. In 2D devices, derived from the traditional electric switch Crossbar, an N input and N output switching matrix can be realized with N^2 basic mirrors (Figure 5.12). They only have two possible positions, on and off, hence quick switching (a few ms).

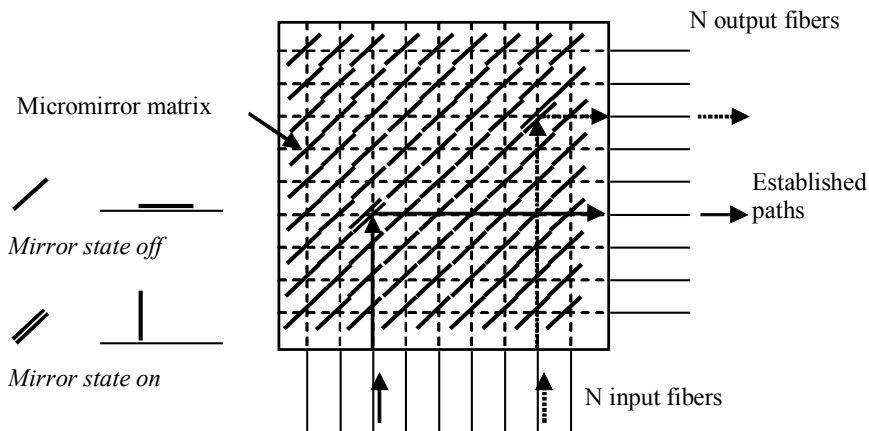


Figure 5.12. Principle of a micromirror 2D switching matrix

On the other hand, in the 3D concept, only $2N$ mobile micromirrors are used: N facing input fibers and N facing output fibers (Figure 5.13), but since they have N possible positions, their direction must be precise and switching is not as quick.

In 2001 Lucent developed a 256 channel prototype, but the conjuncture has not enabled its massive deployment in networks. However, all optical cross-connects based on MEMS microtechnologies progress in network cores (see Chapter 10).

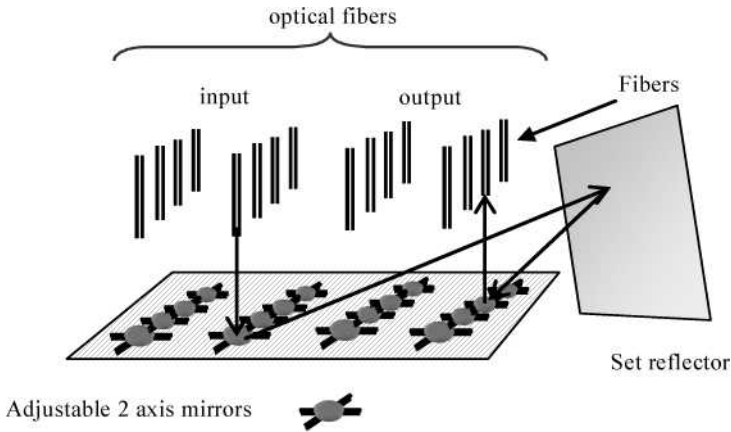


Figure 5.13. Principle of a micromirror 3D switching matrix

5.4.4. *Reconfigurable optical add-drop multiplexers (ROADM)*

OADM (section 5.2.5) can be made to be reconfigurable by combining wavelength division multiplexing and optical switching functions. Equipment thus defined becomes reconfigurable optical add-drop multiplexers or ROADM and is expected to play a very important role in the future of all optical networks (Chapter 10).

In fact, as with passive OADM, they enable the drop of a signal at one (or several) wavelength(s) and its replacement by another signal at the same wavelength(s) without needing to reconvert the signal into electric or to process it, in an all optical node. However, reconfigurable OADM allow the fast change of dropped wavelength(s), making it possible for the network to adapt in real time to traffic and to evolve to all optical routing. Moreover, dropped/added wavelengths at node level can be of any number and distributed in any way.

On the other hand, whereas OADM are passive, reliable and do not require feeding or control signals, ROADMs require a control by electric signals from the network control plane, which uses signaling channels distinct from data channels, at a specific wavelength in the case of new optical transport networks (OTN, Chapter 10).

Different technologies can be integrated into this equipment (Figure 5.14); essential functions are:

- a wavelength demultiplexer in input, and reciprocally a wavelength division multiplexer at output; these two components are identical (but signals are in opposite directions) and can very well be realized in planar integrated optics (AWG, section 5.2.4);
- a switching matrix with 4 access groups: input channels, output channels, drop channels and add channels. In each group, a channel corresponds to a fixed wavelength. Basic switches are 2 x 2 type and have two positions: parallel (input then goes to output), and crossed (input is dropped; the added channel goes to output). Current ROADMs use basic switches based on MEMS or silicon-integrated optics with thermal command (for network reconfiguration, switching does not need to be fast); other technologies, based on wavelength blockers, or wavelength selective switches (based on diffraction gratings for example) have led to prototypes;
- an automatic level equalization device, based on variable optical attenuators (VOA, section 5.1.4) and level monitoring at each wavelength;
- and finally switch control electronics and VOAs (but data remains in all-optical form).

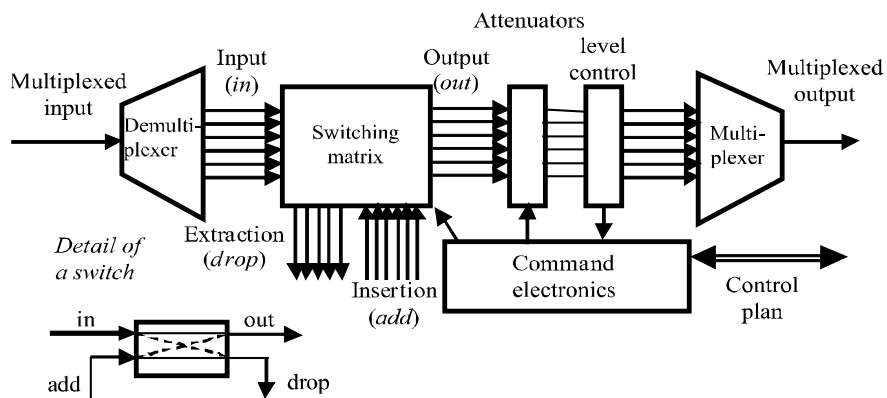


Figure 5.14. *Reconfigurable optical add-drop multiplexer (ROADM)*

Chapter 6

Optoelectronic Transmitters

6.1. Principles of optoelectronic components

The role of these components is to convert electric signal into an optical signal, and reciprocally, with the help of semiconductor emitting (Chapter 6) and receiving (Chapter 7) diodes. These easy to use components can indeed be modulated at high frequencies with low voltages.

6.1.1. *Electroluminescence principle*

In direct semiconductors, the recombination of an electron-hole pair is radiative, i.e. its energy, close to bandgap E_g , is transferred to a photon with the same energy $h\nu^1$. This is electroluminescence. In fact, in these semiconductors, the minimum energy of the conduction band is reached for the same value of k (electron wave function) as the maximum energy of the valence band (Figure 6.1) and recombination is carried out without modifying movement quantity. A diode structure allows us to create a large number of recombinations of minority carriers injected throughout the junction, and therefore the emission of a large number of photons.

On the other hand, in indirect semiconductors, these extrema do not match and recombination is carried out using a phonon possessing a low energy E_ϕ for the conservation of movement quantity. During a recombination, the electron-hole

1. h is the Planck constant = $6.62 \cdot 10^{-34}$ J/Hz.

pair energy is transferred in mechanical form and ends up as heat. The radiative recombination probability is not zero, but it is extremely low.

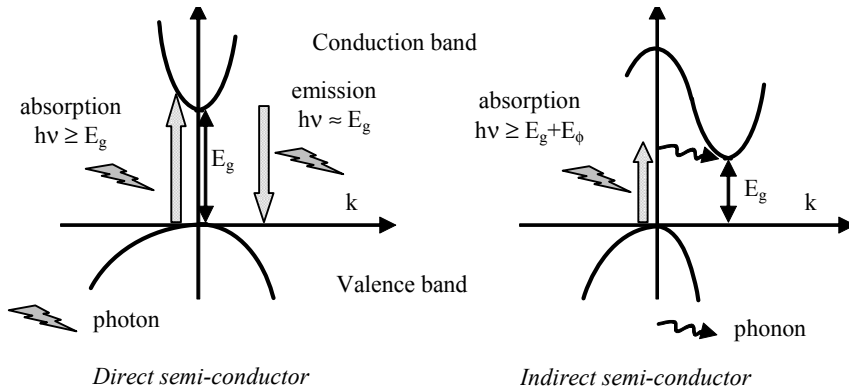


Figure 6.1. Direct and indirect semiconductors

Therefore, it is an emission of a relatively monochromatic light. However, the emitted photons are independent of each other; this emission is *incoherent*.

In addition, since energy distribution is almost continuous within each band, the spontaneous emission spectrum presents a width $\Delta\lambda$ around a central wavelength that is slightly lower than λ_g , and a relatively Gaussian general form (see the spectrum of an LED in Figure 6.7):

$$\lambda_g = h.c/E_g = 1.24/E_g \text{ when } \lambda_g \text{ is in } \mu\text{m} \text{ and } E_g \text{ in eV}$$

Reciprocally, a photon absorbed by a semiconductor can create an electron-hole pair, as long as $h\nu$ is higher than E_g . In an indirect semiconductor, this absorption also possibly involves a phonon, for which $h\nu \geq E_g + E_\phi$ must occur. *Photodetection* has many applications (photovoltaic cells, image sensors, photoresistors, etc.) and is responsible for the fact that material reabsorbs its own emission.

Due to this reabsorption and the confinement of a certain number of photons within the material because of its high refraction index, are defined:

– internal quantum efficiency:

$$\frac{\text{number of photons created}}{\text{number of recombinations}}$$

– external quantum efficiency:

$$\frac{\text{number of photons transmitted outside}}{\text{number of recombinations}}$$

6.1.2. Electroluminescent material

Silicon and germanium are indirect semiconductors and cannot emit light. Silicon-integrated transmitters have recently been realized, but the active element (rare-earth-doped or thin layers of direct semiconductors) is not silicon.

In addition, organic electroluminescent material is now used for displays, but cannot be quickly modulated for transmissions.

The used emitting materials are mainly III-V semiconductors (made up of elements from the 3rd and 5th periodic table columns), or their alloys, where many are direct:

- nitrogen-doped GaP emitting green ($\lambda = 565$ nm, leaning toward yellow);
- GaAs_xP_{1-x} emitting from yellow to red, according to x value;
- GaAlP emitting red, with high efficiency;
- GaAs emitting in the first infrared window ($\lambda = 900$ nm);
- Ga_{1-x}Al_xAs emitting between 700 and 900 nm in (decreasing) function of x;
- Ga_{1-x}In_xAs_yP_{1-y} emitting in the second or third window: $\lambda = 1,200$ to 1,600 nm in (increasing) function of x and y;
- Ga_{1-x}In_xAs_ySb_{1-y} emitting around $\lambda = 2.5$ μm .

These materials are also used in detection, as well as silicon and germanium (indirect semiconductors can detect light).

The diagram in Figure 6.2 presents the main compositions used.

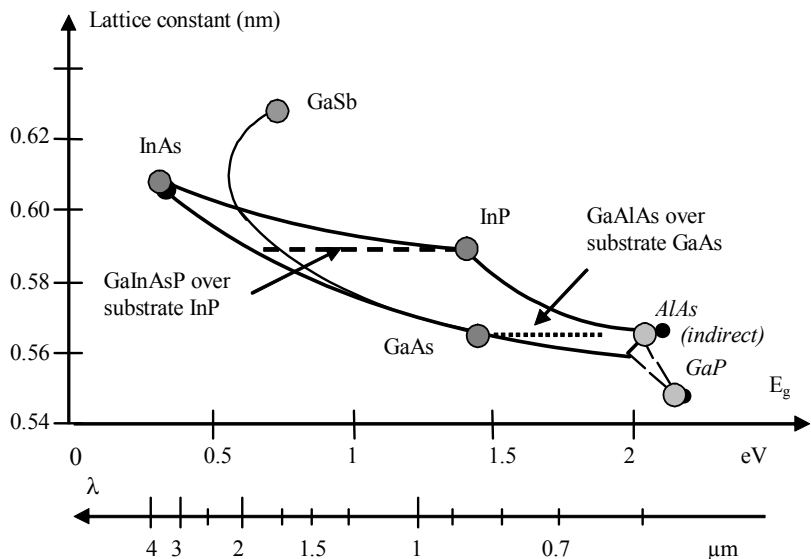


Figure 6.2. Electroluminescent III-V semiconductor material

Blue emission has been the subject of active research, mainly for displays and recording on optical disks (blue-ray and HD-DVD standards). It was first obtained with correct efficiency in II-VI materials such as ZnCdSe (blue) and ZnTe (green-blue). More recently, blue diodes (LED and lasers at 405 nm) based on InGaN or AlInN quantum wells over GaN were developed, enabling lighting and visualization in blue light applications and in the medical field in near-ultraviolet (275 to 340 nm).

A consequence has been the development of the white LED (the light is re-emitted by phosphorescent material that is excited in blue-violet) which is taking over the lighting and visualization market (LCD display backlighting), since its energy efficiency exceeds 120 lumen/W or ten times more than incandescence with a much longer lifetime.

In the case of alloys, the composition is on one hand determined by the desired emission wavelength, and in the other hand by the lattice constant. In the case of heterostructures, there must be lattice matching between the different layers and substrate (which is, depending on the case, GaAs or InP), if not, there is the risk of crystal dislocation. However, lattice mismatched layers can be inserted, under constraint, as long as they are very fine (quantum well structures, see section 6.1.5).

6.1.3. Photodetection principle

In order for the absorption of a photon by a semiconductor to lead to an electron-hole pair, photon energy must be higher than E_g , hence the condition:

$$h\nu > E_g \text{ therefore } \lambda < \lambda_{\text{lim}} = hc / E_g \text{ limit detection wavelength}$$

In the case of indirect semiconductors, this value shifts downward because the energy of phonon E_ϕ must be added to E_g , which is necessary to assist the absorption of a photon by an atom. This is actually done with a low probability, characterized by the *absorption coefficient* α in cm^{-1} , which determines the number of photons transmitted at a depth x :

$$\Phi(x) = \Phi(0) \cdot e^{-\alpha x}$$

hence the definition of the absorption depth: $1/\alpha$.

α depends on the material and decreases when the wavelength increases, up to 0 at limit wavelength (Figure 6.3). For adequate efficiency, absorption depth must be low (to absorb the maximum number of photons) but not too low (otherwise they are all absorbed at the surface, before reaching the active layer). There is an optimum efficiency wavelength (close to $0.8 \mu\text{m}$ for silicon).

As with emission, two types of photodetection efficiencies are defined:

– *internal quantum efficiency*:

$$\frac{\text{number of pairs created}}{\text{number of photons absorbed}}$$

generally quite high, but limited by electron-hole pair recombinations, especially near the surface; in addition, not all photons reach the active zone because of surface reflections. Then the following is defined:

– *the external quantum efficiency*:

$$\frac{\text{number of pairs created}}{\text{number of incident photons}}$$

typically equal to 50 to 80%.

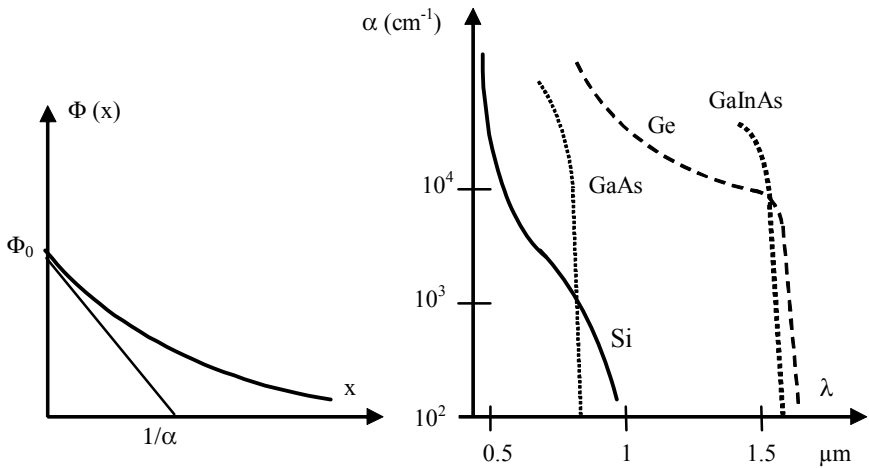


Figure 6.3. Absorption coefficient

The absorption coefficient decreases very quickly near the cut-off wavelength, especially in III-V semiconductors. The absorption edge is dependent on temperature, which modifies the bandgap; this is used in optical temperature sensors. It is also shifted by the application of an electric field, which is at the basis of electro-absorption modulators (section 5.3.5).

In telecommunications, photodetection is mainly used in photovoltaic mode: charges created lead to a current in a diode structure, biased or not. The photoconductor mode also exists, the increase of free carriers increases conductivity of lighted semiconductor material. Simpler but slower, this mode is used to detect the brightness level for example.

6.1.4. Heterojunction use

In order to obtain a good efficiency, heterojunction structures are used in components intended for optical telecommunications (fiber based on direct infrared link): the active layer, which is very thin (less than a micron), is surrounded by confinement layers (Figure 6.4) characterized by:

- a higher gap, which confines the recombinations (or emission) and absorption in the active layer. Most often, a double heterojunction (DH) is realized to ensure confinement of both types of carriers;

- transparency to emitted photons, which will not be reabsorbed; this improves the external efficiency in emission as well as in detection (no absorption out of the active layer);
- a lower refractive index, hence confinement and light guidance possibility, as in integrated optics, mainly used in edge-emitting diodes and laser diodes. We have seen that this property is used to develop semiconductor integrated optics devices.

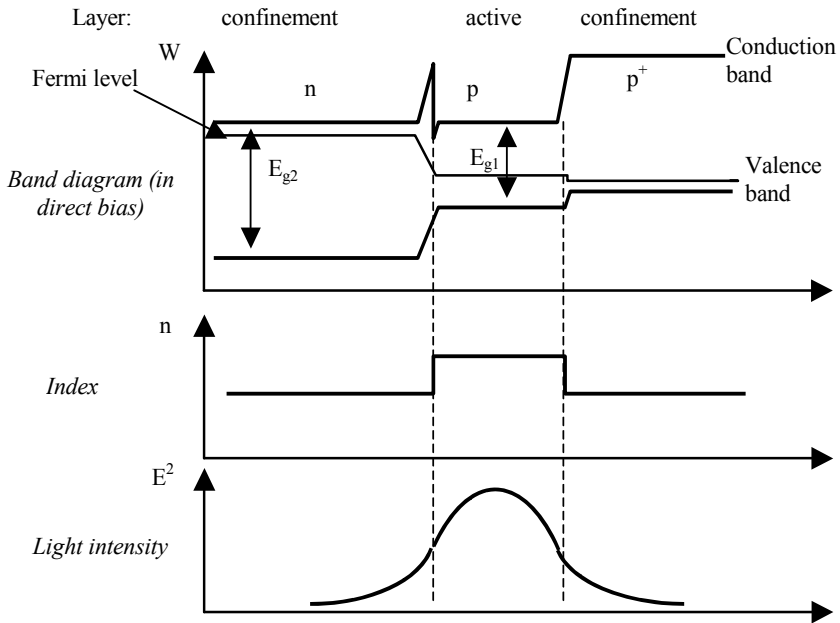


Figure 6.4. Double heterojunction

The growth of these layers is realized by *epitaxy*, most commonly in the vapor phase (MOCVD process for metal-organic chemical vapor deposition). To realize very thin layers (less than 100 nm), molecular beam epitaxy (MBE) is used.

6.1.5. Quantum well structures

Mainly used for laser diodes, quantum well structures consist of separating optical confinement (light guiding in a layer that cannot be much thinner than the wavelength) from electric confinement in the thickness of the active layer. It is reduced to a very thin layer, in the range of a dozen nanometers (Figure 6.5) or,

more often, several stacked layers (this is called a multiple quantum well structure or MQW). These layers are deposited by molecular beam epitaxy.

The advantages of this structure are:

- strong reduction of the threshold current density (less than 100 A/cm^2) therefore threshold current (less than 10 mA) and heating; the quantum efficiency is also higher, enabling the development of power laser diodes;
- the possibility of adjusting the emission wavelength with precision by modifying the active zone depth: in fact, energy levels, and therefore radiative transitions, are quantified (hence the structure name) to a value depending on thickness; a single-mode spectrum can easily be obtained;
- at last, the active layer can be made from material with a lattice that does not match the substrate. The crystal is then submitted to mechanical constraints (this structure is called constrained quantum wells) which is only possible without dislocations if the layer is very thin. It gives an additional degree of freedom in the choice of material, therefore wavelength, in relation to the diagram in Figure 6.2, since it is possible to use slightly higher lattice constant material and compress it.

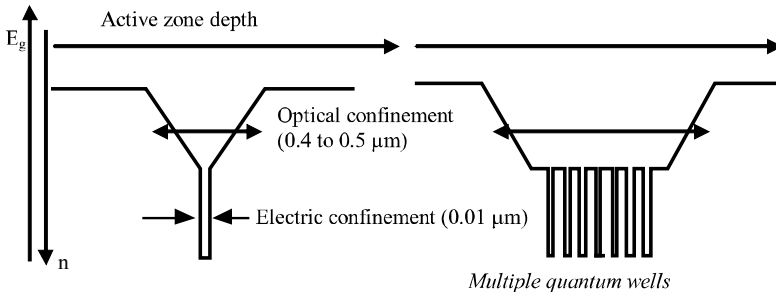


Figure 6.5. *Quantum well structures*

In this way, constrained InAlAs over InP material or constrained GaInAs over GaAs material allows us to make pump laser diodes at $0.98 \mu\text{m}$ for optical amplification. Blue diodes also use multiple quantum wells, with constrained InGaN layers over GaN.

6.1.6. *Optical amplification principles*

Optical amplification is based on the *stimulated emission* phenomenon in which the generation of a photon by transition between two levels is triggered by the

arrival of an incident photon in the emitting excited material. Since the new photon has the same frequency, direction, phase and polarization as the incident photon, light will be amplified during its propagation in the medium, according to the law:

$$P(z) = P_0 \cdot \exp(gz)$$

where g is the gain factor in cm^{-1} .

The necessary condition for stimulated emission is the population inversion between the two neighboring levels between which a radiative recombination occurs. In this way, in direct semiconductors, the conduction band must be more populated than the valence band. This condition is not possible at thermodynamic equilibrium, and can only be obtained by pumping, the outside supply of a large quantity of energy (electric, optical or other) for taking carriers to a higher energy state.

The light that will be amplified can come from:

- spontaneous emission of the material: a powerful *source* is then realized; if this source is associated with a selective device (resonant type cavity) which selects a wavelength among amplified wavelengths, it is a laser (*Light Amplification by Stimulated Emission of Radiation*), which is a coherent light source;
- or external light, as long as its wavelength corresponds to energy transitions of the material: an amplifier can then be realized.

For optical telecommunications applications, which interest us here, the materials enabling optical amplification are III-V semiconductors and erbium-doped fibers.

In semiconductors, population inversion can easily be obtained by a very strong direct injection of carriers in a biased PN junction. Carrier density must exceed a threshold (in the range of 10^{18} cm^{-3} in GaAs) corresponding to a threshold density $J_0 \cdot d$ where d is the recombination zone depth, and J_0 is a threshold with an approximate value of:

$$J_0 = 4.5 \cdot 10^3 \text{ A/cm}^2/\mu\text{m in GaAs}$$

The use of heterojunctions provides optical amplification in a very thin active zone, with low current (a few dozen mA). Semiconductor laser structures or *laser diodes* (section 6.3). Semiconductor optical amplifiers (SCOA) can also be realized, less often used for transmissions because they are not as powerful as EDFAs, but which are interesting for integrated optics or signal processing applications.

Erbium-doped fiber amplification, the subject of Chapter 8, enables the realization of lasers, and mainly erbium-doped fiber amplifiers (EDFA) which have become dominant in fiber transmission systems over the last few years. This type of amplification presents several advantages compared to semiconductor amplifiers:

- low noise, caused by amplified spontaneous emission (ASE);
- very low fiber-optic connection losses;
- very low sensitivity to light polarization;
- high saturation power (over 30 dBm).

Both types of amplifiers have a relatively large gain band (several dozen nm), allowing the simultaneous amplification of numerous multiplexed wavelengths.

Beyond the stimulated emission principle, optical amplification is possible with the help of non-linear effects (Raman or parametric amplification, see Chapter 2); this is actually interaction between two waves with the help of non-linear material, which has not much passed the experimental stage.

6.2. Light-emitting diodes (LED)

6.2.1. Structure

A light-emitting diode (LED) is the simplest emitting component, directly performing emission of photons by carrier recombination in a directly polarized heterojunction (Figure 6.6). The material used is chosen according to the emission wavelength (section 6.1.2).

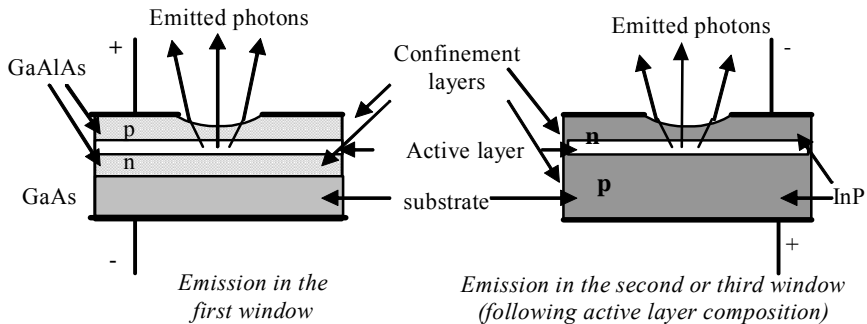


Figure 6.6. Light-emitting diodes

6.2.2. Main light-emitting diode characteristics

The main characteristics are (Figure 6.7):

- a spectrum typical of spontaneous emission, continuous and quite large (hence high sensitivity to chromatic dispersion);
- a linear power-current characteristic, with a slope of approximately 10 mW/A, up to a few milliwatts, value limited by diode heating;
- a typical diode current voltage characteristic, with threshold voltage in the range of 1.5 V (and depending on material). A LED must be biased (in telecommunications as in visualization) in current, and not in voltage;
- a Lambert law emission diagram, i.e. the intensity of radiation in a θ direction equals: $P(\theta) = P_0 \cdot \cos \theta$ (P_0 intensity of radiation in the axis). This is interesting for direct infrared links, but it is not very suitable for coupling in fiber optics; LEDs are either used with multimode fibers with strong numerical aperture NA (split power increasing as NA^2), or with lenses to improve coupling in fibers with lower numerical aperture;
- high response time (in the range of a dozen ns) limiting bandwidth of signals transmitted by LEDs at about 100 MHz. Some optimized structures now exceed this value. The best LEDs currently offer bitrates of 100 Mbit/s (for FDDI, Fast Ethernet) and 155 Mbit/s (first SDH level); laboratory LEDs have reached 250 Mbit/s, but the Gbit/s level is out of reach.

This component of limited performance is very useful however because it is inexpensive, has a very low-noise and is very reliable.

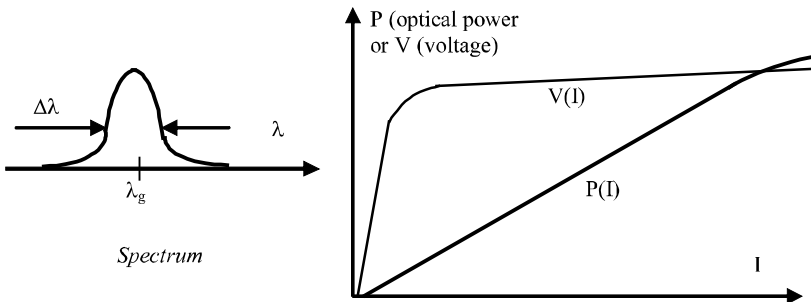


Figure 6.7. Characteristics of a light-emitting diode

6.2.3. Light-emitting diode transmitters

Their structure is simple, since modulating the current in the diode is sufficient for the optical power to reproduce electric current with enough linearity. In analog transmitters (Figure 6.8a), this current is generally amplified by a transistor for sufficient amplitude (typically a few dozen mA). In logical transmitters (Figure 6.8b), the diode operates in on-off mode since the current is switched by a switching transistor (open-collector output of a driver for example).

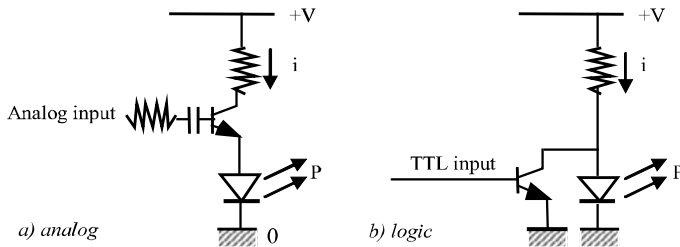


Figure 6.8. Light-emitting diode transmitter

6.2.4. Other types of light-emitting diodes

Edge-emitting LEDs exist, where light is guided in the active layer, since it has a refraction index that is higher than confinement layers. Light then exits by both guide extremities (as in the laser diode in Figure 6.9). Their speed, performance and cost are higher than classical LEDs (called surface-emitting LEDs).

There are also superluminescent diodes (SLD) similar to lasers, with edge emission and amplification, but without resonance; the light is then non-coherent (with a continuous and Gaussian spectrum). They have some measurement applications (interferometry in non-coherent light, gyroscopy) and medical applications, because of high beam concentration with a spatial but non-temporal coherence.

6.3. Laser diodes

6.3.1. Principle

Their structure is more complex. Except in the case of VCSELs, they are edge emission components where the light is confined in the active layer. In addition, laser diodes must carry out the two functions of the *optical oscillator* that is a laser: amplification and resonance.

Light amplification is obtained by stimulated emission (section 6.1.6). Population inversion is obtained by injection of a very strong current density in the junction (in the order of a kA/cm^2). Amplification therefore occurs when the current exceeds a *threshold* value noted as I_{th} which is from mA to several dozen mA according to the component structure; at that time, carriers which are usually in the minority after going through the junction then become a majority corresponding to population inversion.

The amplified light comes from spontaneous laser emission, non-zero when below the threshold, it can also be an external incident light (used in semiconductor optical amplifiers, Chapter 8).

In the stimulated emission regime, light power increases during its propagation along Oz following the law:

$$P(z) = P_0 \cdot e^{gz}$$

with g = gain coefficient, generally expressed in cm^{-1} .

This coefficient depends on the wavelength and is only positive within a “gain band” which is narrower than the spontaneous emission band, where amplified photon frequency ν follows the relation:

$$E_g < h\nu < F_2 - F_1$$

where F_2 and F_1 are Fermi pseudo-levels of electrons and holes. In order for the inequality to be possible, they need to be respectively *in* the conduction band and valence band, corresponding to population inversion. The amplified light is therefore not monochromatic: a selective optical device is necessary for obtaining a unique wavelength.

Gain also increases with current density J following the law:

$$g = \beta (\eta_i J/d - J_0)$$

with:

- β gain coefficient ($5 \cdot 10^{-2} \text{ cm} \cdot \mu\text{m/A}$ for GaAs);
- η_i quantum efficiency of spontaneous emission;
- d active zone depth;
- J_0 threshold density ($4.5 \cdot 10^3 \text{ A/cm}^2/\mu\text{m}$ for GaAs).

It is therefore necessary to have a very thin (approximately 0.1 μm) and narrow (a few μm) recombination zone to operate with a low threshold current, which is possible thanks to double heterojunction structures.

In addition, losses in the guide (in $e^{-\alpha z}$) and light emission by the sides must be compensated, therefore:

$$e^{2gL} \cdot e^{-2\alpha L} \cdot R^2 = 1 \text{ or } g = \alpha - \frac{\text{Ln } R}{L}$$

with R as reflection coefficient at edges, as $R < 1$, $\text{Ln } R < 0$ and g must be slightly higher than α .

Resonance is obtained by the cavity structure, for the selection of amplified frequency(ies).

6.3.2. Fabry-Pérot structure laser diodes

This is the classical structure (Figure 6.9), using a Fabry-Pérot (solid) “cavity” made up of the guide and partial reflection ($R =$ approximately 30%, because of the strong difference between the semiconductor index with air) at the cleaved edges at extremities. Resonance occurs when guide length L is an integer of the half wavelength (or $\lambda/2n$ in the material of index n), which selects longitudinal modes of wavelengths:

$$\lambda_p = \frac{2Ln}{p}$$

with integer p, hence spacing between lines:

$$\delta\lambda = \frac{\lambda^2}{2LN}$$

with $N = n - \lambda \frac{dn}{d\lambda}$ group index, very close to n.

In general, since p is large, several wavelengths able to be amplified (because they are contained in the gain curve) verify this relation. The laser spectrum then contains several lines (Figure 6.9b); this spectrum is said to be longitudinally multimode. Although lower than for an LED, the spectral width is significant, which is acceptable at 1.3 μm but not at 1.55 μm , because of chromatic dispersion. In

addition, a mode partition noise can be observed by energy fluctuation between modes.

This spectrum also depends on current and temperature, acting on the spectrum envelope (by shifting the gain curve toward large wavelengths) and on the wavelength for each mode simultaneously, using the index dependence on these two parameters.

Temperature increases λ whereas current decreases it. In Fabry-Pérot structures, this shift is discontinuous, by mode hops, with a slope of approximately 0.5 nm° .

This is the oldest laser diode structure, which is economical but has a mediocre performance: strong threshold current, noise, astigmatic radiation. These components remain used at $1.3 \mu\text{m}$, notably in the FTTH / GPON network in the upstream direction (Chapter 10), while waiting for VCSEL availability at $1.3 \mu\text{m}$.

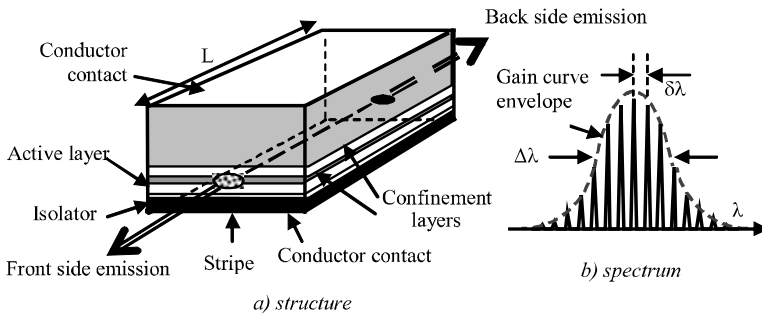


Figure 6.9. *Fabry-Pérot laser diode*

6.3.3. DFB laser diodes

In order to obtain a single-mode spectrum, a “distributed feedback” (DFB) structure can be used, by integrating a Bragg grating (see Chapter 4) of period Λ along the guide (Figure 6.10). This periodic perturbation will lead to a distributed reflection of the wavelength verifying: $\lambda_B = 2\Lambda.n$.

The spectrum is normally longitudinally single-mode (Figure 6.10b). To ensure phase matching at λ_B between both propagation directions, a phase shift section of length $\lambda_B/4$ is inserted in the middle of the guide, otherwise two symmetric modes around λ_B appear. In order to avoid Fabry-Pérot cavity spectrum residues, the edges must have anti-reflection treatments. The cost of this component is rather higher than for Fabry-Pérot type laser diodes.

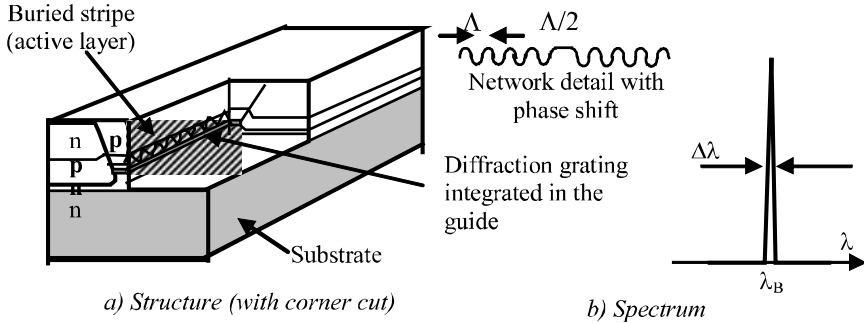


Figure 6.10. DFB laser diodes

On the other hand, the single spectrum line widens (chirp effect), when the laser is modulated because of the electro-optic effect (variation of the current index, which will vary the optical frequency by typically several hundreds of MHz per mA). In order to avoid this spectral widening, the laser must be operated at constant current and use external modulation of the light, in amplitude or in phase, with integrated optics or an electro-absorption modulator (see Chapter 4).

Due to this index variation, the spectrum depends on the average current as well as temperature (now continuously, with a lower slope than for FP lasers, in the range of 0.1 nm/°C). Systems that must function at very precise wavelength (particularly for dense wavelength division multiplexing) require precise control of the current and temperature. It is then possible to modulate optical frequency of the laser by modulating its current. It is also possible to modify the temperature to obtain wavelength matching to a precise value (but in a narrow range).

6.3.4. Lateral guiding in laser diodes

Laser diode structures can also be distinguished by the way *lateral guiding* of the light is performed in the active layer:

- active or “gain-guided”, i.e. that current flow, or the zone where light will be created and amplified, is laterally confined by a conductor “stripe” (Figure 6.11a). Only used with Fabry-Pérot diodes, it is the oldest laser diode structure, economical but with mediocre performance: high threshold current, noise, astigmatic radiation;

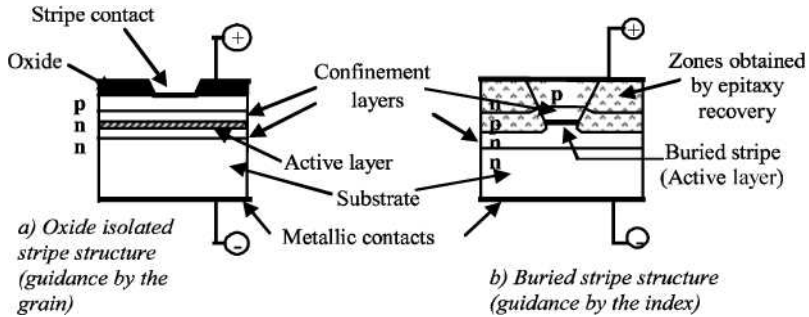


Figure 6.11. Lateral guidance structures of laser diodes

– passive or “index-guided”, by realizing in the component an integrated guide (“buried stripe”) laterally limited by lower index material (Figure 6.11b); the electric confinement is ensured by higher potential barriers of lateral heterojunctions. The emitting zone is much narrower than previously hence low threshold current and relatively symmetric Gaussian radiation, well adapted to single-mode fibers. This principle is used for DFB structures, as well as for most of the Fabry-Pérot lasers at 1.3 μm .

6.3.5. Wavelength-tunable laser diodes

For a long time now, heterodyne detection experiments, as well as instrumentation and measure applications, have required the development of wavelength-tunable laser diodes. Subsequently, the development of optical networks using dense wavelength division multiplexing (DWDM) between many optical carriers required the development of tunable laser diodes that are completely integrated and fast tunable.

External tuning cavities (diffraction gratings for example) were used for a long time for varying the laser diode wavelength over a more or less large range, as well as by controlling temperature. These methods are precise but complicated and are mostly used in the laboratory. However, MEMS technologies, such as micro-structured silicon resonant cavities, tuned by control voltage, could lead to new, more compact external cavity structures.

The most widely currently used structure is the DBR (Distributed Bragg Reflector) laser diode including three sections aligned in a monolithic structure (Figure 6.12):

- the “gain section” which is the actual laser diode, current I_1 controlling the emitted power; it includes the active layer, close to the guiding layer which is larger;
- the “Bragg section” which, under the guiding layer, includes a Bragg grating, which selects the reflected wavelength (hence the structure name). This wavelength is controlled by current I_2 , by the electro-optic effect which changes the index, with a slope of approximately -0.1nm/mA . This effect also exists in DFB lasers, but it is caused by control current, whereas in the DBR structure, intensity and wavelength can be separately controlled, and tuning is achieved over a larger range;
- between the two, the “phase section”, where current I_3 performs the phase matching between the light reflected by the grating and the one reflected by the other cleaved edge by varying the guide index; it also ensures decoupling between the two other sections.

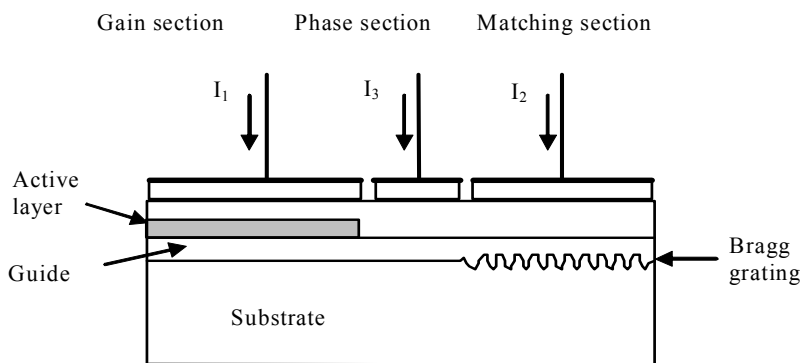


Figure 6.12. *Wavelength matching DBR laser diode*

High tunability is then reached, almost continuous in a range reaching over a dozen nm, without the wavelength being affected by laser modulation. To cover a larger range, several shifted DBR diodes can be used. In wavelength division multiplexing networks, these diodes allow the precise adjustment of the wavelength of each channel, and can even vary for wavelength routing, a technique in development (Chapter 10). They simplify network maintenance because having a different diode in reserve for each wavelength is no longer necessary.

The response time of these components is very quick and is in the range of dozens of ns for electronic control, and in μs for thermal control.

6.3.6. Vertical cavity surface emitting lasers (VCSEL)

Vertical cavity surface-emitting lasers (VCSEL) are more recent components with a structure that is different from the other laser diodes. The “cavity” is vertical, perpendicular to the substrate, the light is vertically emitted by the component surface. This property makes them economical components to produce and test in large quantity on a single wafer, as well as to integrate in communication or signal processing monolithic devices.

Due to this structure (Figure 6.13), the “cavity” is very short, making the longitudinal single-mode operation easier, but requiring us to respect the gain equation (see section 6.3.1):

- a large gain in the cavity, which is obtained with an injected current of a few mA thanks to its very small transversal dimension; the active zone, generally made up of a few quantum wells, is only a few dozen nm thick;
- high reflectivity mirrors (typically 99%), which are obtained by thin layer stacking, acting as distributed Bragg mirrors, matched to the transmission wavelength, increasing spectral selectivity (but the Fabry-Pérot cavity made up of these mirrors is the one selecting the mode). Tunable VCSEL diode prototypes, where mirrors are carried by mobile microstructures (MEMS), have been developed.

Layer thickness must be very precise but epitaxy production methods are well controlled and a large number of identical lasers are simultaneously produced in the same wafer. The largest size and the lowest divergence of the transmitted beam in fact authorize a cheaper connection than for edge-emitting diodes.

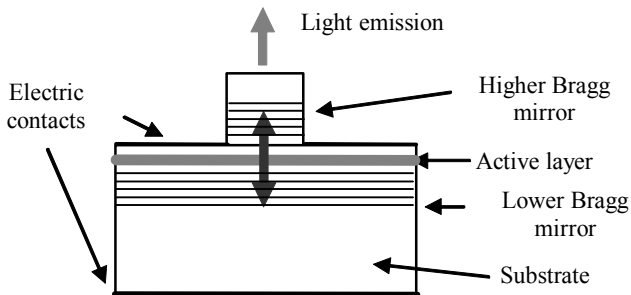


Figure 6.13. VCSEL laser diode

For reasons related to material properties, the first VCSEL (in GaAlAs/GaAs) were developed at 0.85 μm with very good commercial performance. Due to their

low cost and ease of integration, they have quickly found several applications in the fields of optical reading and recording, laser printing, high bitrate optical interconnections internal to computer equipment, and very high bitrate local networks (several Gbit/s), even over multimode fibers. VCSEL diodes which can be directly modulated at 10 Gbit/s have appeared.

Red VCSELs have also emerged recently for plastic fibers, and orange for DVD reading and writing. InP components for 1.3 and 1.55 μm are in development, but despite regular laboratory announcements, they are still not really available.

6.4. Optical transmitter interface

6.4.1. *Description*

The optical transmitter interface includes, in addition to the emitting component (LED or LD), the circuits necessary for its feeding, its modulation, its protection and possibly its cooling function, and finally an optical coupling device (lens or pigtail connection). The cost of the interface is therefore significantly higher than the cost of the component especially because of the last point which requires very high precision.

A certain number of electronic and optoelectronic devices (photodiodes, amplifiers) are part of the interface, and their monolithic integration is the subject of several research studies, even though it is still not economically appealing. The integration of optical devices (filters, isolators, modulators, switches, amplifiers, etc.) at transmitter output is in development.

6.4.2. *Laser diode characteristic*

The use of laser diodes is much more complicated than the use of LEDs because of the optical power versus current characteristics (Figure 6.14) which is not regular. It presents a threshold current I_{th} below which only very low spontaneous emission occurs; above the threshold, stimulated emission occurs with a strong slope of the characteristics :

$$\frac{dP}{dI} = 100 \text{ to } 200 \text{ mW/A}$$

corresponding to differential external quantum efficiency:

$$\eta_D = \frac{2q}{h\nu} \cdot \frac{dP}{dI}$$

from 25 to 50% (factor 2 is caused by emission from both edges).

The linearity of this slope is better or worse depending on the laser diode structure; it is high in quantum well structures, making it possible to use them for analog transmissions of frequency-multiplexed video signals.

The threshold current also depends on the laser structure, and increases irreversibly with age. It greatly depends on temperature T according to the law:

$$I_{th}(T_2) = I_{th}(T_1) \cdot \exp \frac{T_2 - T_1}{T_0}$$

with T_0 as temperature coefficient, which is near 50°C for GaAlAs and 70°C for GaInAsP.

Due to these characteristics and the increase of threshold current with temperature and with laser age, it is necessary to control its bias current to let it operate at constant average optical power.

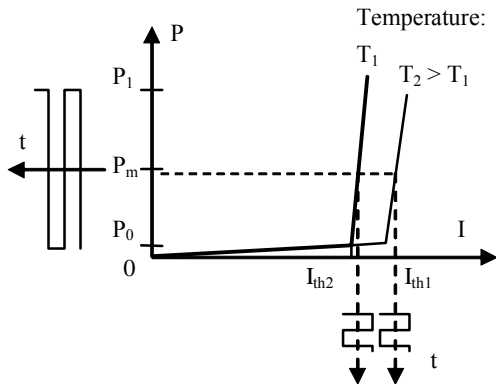


Figure 6.14. Power versus-current characteristic of laser diodes

6.4.3. Laser diode modulation

Internal modulation of the laser diode, the most usual process, is obtained by modulating laser current. The modulating signal is superposed on this polarization current; its frequency can reach several GHz (Figure 6.15) and even more than 10 GHz for some VCSELs. The matching of laser impedance must be achieved in this very large band, involving microwave frequency technologies. The presence of

this control prevents the transmission of continuous components. Modulation of the current also leads to wavelength modulation (chirp effect) because of the index variation that it causes. It is the second limitation to modulation frequency when there is chromatic dispersion in the fiber.

The modulating signal can be analog if linearity is adequate, but it is most often binary. In this case, the low level is set near the threshold and corresponds to low (but not completely zero) optical power. In fact, in pulsed operation (with low level and zero current), the response time is longer.

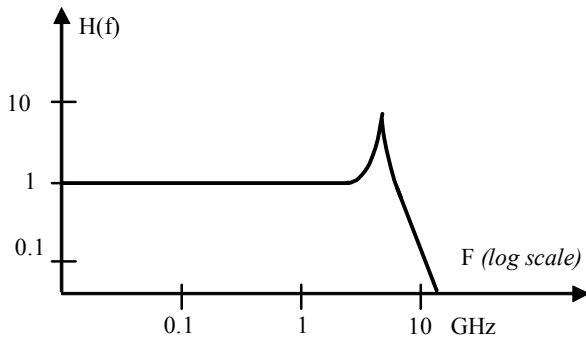


Figure 6.15. *Frequency response of laser diodes*

For very high modulation frequencies (from 5 to 10 GHz), an amplitude *external* modulation must be used, using an integrated optical modulator which follows the laser (see Chapter 5).

Generally an electro-optic interferometer Mach-Zehnder modulator (MZM) or the less costly electro-absorption modulator (EAM) integrated into the laser achieves an on-off or analog modulation of the intensity it transmits.

6.4.4. Transmitter noise

At emission, a shot type noise exists and is caused by the random character of photon-electron interactions, even at constant current. It is characterized by the relative intensity noise (RIN) defined by:

$$\text{RIN} = \frac{\langle \Delta P^2 \rangle}{P^2}$$

with $\langle \Delta P \rangle$ as the average fluctuation of optical power P , measured in a band of 1 Hz. RIN is expressed in Hz^{-1} corresponding in detection to an electrical signal to noise ratio (proportional to the square of the optical power ratio, due to quadratic detection) inversely proportional to $\text{RIN} \cdot \Delta F$.

Negligible with LED, the RIN equals approximately 10^{-14} Hz^{-1} (or $-140 \text{ dB} \cdot \text{Hz}^{-1}$) for laser diodes, the best values reaching $-155 \text{ dB} \cdot \text{Hz}^{-1}$. It increases at very high (laser resonance) and very low (noise in $1/f$) frequencies, as well as near the threshold current. The resulting signal to noise ratio is largely sufficient in digital transmissions, but can be limiting for high quality analog transmissions.

6.4.5. Laser diode emission module

6.4.5.1. Control

For correct use in telecommunications, the laser diode requires a power control. The control loop (Figure 6.16) uses a photodiode measuring power at the back side of the laser, compares it to a reference value and controls the laser current. With the coupling device, it is contained in a hermetic package called the *optical head*. Its cost is quite high because of the very high precision required for the alignment of these elements.

6.4.5.2. Mounting in the optical head

The emission diagram of laser diodes, because of the guide's small size and the resulting diffraction, is highly divergent. A lens will therefore be necessary to adapt it to the mode guided by the single-mode fiber. That is why laser diodes are generally used with a pigtail positioned with great precision facing the laser emission zone. Its extremity must be prepared in the form of a lens, to improve coupling. This lens can be engraved by chemical etching, but the simplest method remains to stretch the extremity of the fiber into a cone, and to give it a hemispheric form by fusion (Figure 6.17).

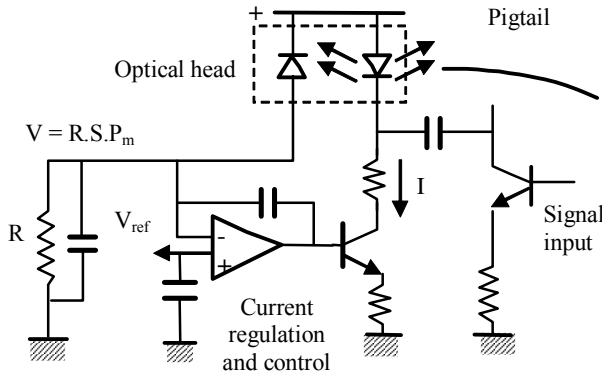


Figure 6.16. *Laser diode emission module*

The advantage is the reduction of reflections toward the laser, which is very sensitive to it: in fact, light re-injection in the cavity increases noise and threshold current. Due to their larger emitting zone, VCSELs have less divergence and are simpler to couple in optical fibers, even multimode.

The optical head can also contain a thermistor and a Peltier cooler allowing a thermal control. Its usage can be avoided for lasers with low threshold current, which do not disperse much heat. However, temperature control is required to precisely control the emitted wavelength. In some applications an optical isolator is also used, which prevents the possible return of light coming from the optical fiber towards the laser.

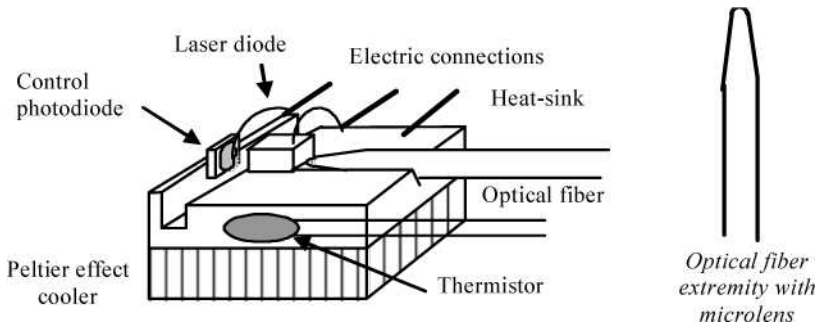


Figure 6.17. *Optical head*

6.5. Comparison between optoelectronic emitters

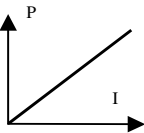
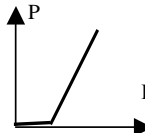
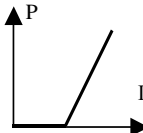
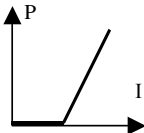
Component	LED	LD (laser diode)		
		VCSEL (vertical cavity)	Fabry-Pérot	DFB
Optical power	< 1 mW	a few mW	a few mW	a few mW
Coupling in an optical fiber	a few % (multimode fiber)	> 50% (multimode fiber)	> 50% (single-mode fiber)	> 50% (single-mode fiber)
Emission diagram	by the surface, very divergent	by the surface, not divergent	by the edge, quite divergent	by the edge, quite divergent
Spectrum and spectral width	large, continuous 20 to 50 nm	a fine line < 0.5 nm	several lines 5 to 10 nm	a fine line < 0.1 nm
Characteristic P (I)				
Threshold current		5 to 10 mA	10 to 30 mA	10 to 30 mA
Max. modulation frequency	100 to 200 MHz	10 GHz	several GHz	several GHz
Noise	very low	very low	low	low
Main wavelengths	0.67 μm 0.8 to 0.9 μm 1.3 μm	0.78 to 0.9 μm	1.3 μm	1.3 μm 1.5 to 1.6 μm
Cost	low	relatively low	average	high
Applications	short distance and analog transmissions (in multimode fibers)	sensors, optical reading, high throughput short distance transmission (in multimode and single-mode fibers)	high throughput medium distance transmission (in single-mode fibers)	very high throughput long distance and wavelength multiplexing transmission (in single-mode fibers)

Table 6.1. Comparison between optoelectronic emitters

Table 6.1 compares performance ranges from the different types of transmitters that we have just studied. In each family, there is a large number of technological variations, corresponding to characteristics (and cost) varying around these typical values. They are the components commonly used in telecommunications. There are other types of emitting diodes, for visualization, instrumentation, high power or ultra-short pulses, that we will not discuss here.

Chapter 7

Optoelectronic Receivers

7.1. Photodetectors

Semiconductor photodiodes, although they are not the most sensitive photodetectors, have the advantage of being very quick and easy to use in a transmission system. There are two main types of photodiodes.

7.1.1. *PIN photodiode*

This uses *photodetection* (conversion of a photon into a hole-electron pair) in a semiconductor. As we have seen in Chapter 6, only photons with energy $h\nu$ higher than E_g can be detected.

In order to obtain a good performance, a PIN diode reverse-biased structure, is used (Figure 7.1): photons are absorbed in the intrinsic (i) zone which, because of bias, does not have mobile carriers (depleted zone); electrons and holes thus created have a low probability of recombining. They are separated by the electric field \vec{E} which is in the intrinsic zone and directs them toward zones n and p where they are a majority.

The zone receiving the light must be thin and protected by an anti-reflection coating which increases external efficiency and protects material.

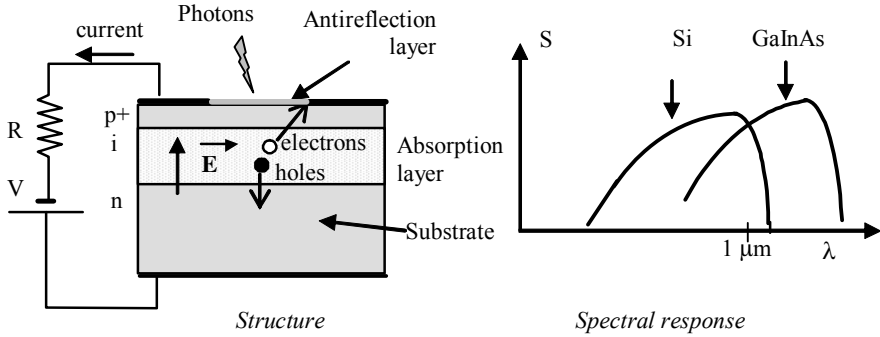


Figure 7.1. PIN photodiode

7.1.2. Photodiode characteristics

A reverse current is established in the photodiode junction, with expression:

$$i = i_s + i_D$$

with: $i_s = S \cdot P$ *photocurrent* proportional to optical power P .

S , in A/W, is the *responsivity* of the photodiode:

$$S = \frac{\eta q}{h\nu}$$

with:

- η = quantum efficiency;
- q = electron charge = $1.6 \cdot 10^{-19}$ C.

Responsivity S increases with wavelength, up to a value where it is maximal, then abruptly drops near the limit wavelength, given by:

$$\lambda_c = \frac{hc}{E_g}$$

Beyond this the material is transparent.

i_D is the *dark current* circulating in the junction in the absence of illumination. It comes from leaking and thermal generation currents; it increases with temperature and bias voltage.

When it is zero, $i_D = 0$; the photodiode behaves as a current generator (still reverse), taking its energy from light received and presenting a direct voltage when it flows in a load R , corresponding to the potential barrier. This is the photovoltaic operation of the detector (Figure 7.2) used in solar cells or in optical power measurement devices; however, response time is too large for transmission use. It is the mounting used in optical measure devices which, because of this are very sensitive and quite slow (they measure average power).

On the other hand, when a photodiode is reverse-biased (a few volts are sufficient), its response time is very short (less than a nanosecond for a classical surface-illuminated photodiode; it decreases by increasing bias voltage). It behaves as a current source parallel with junction capacitance. A direct-biased photodiode has the classical characteristic of a diode, which is of no interest here.

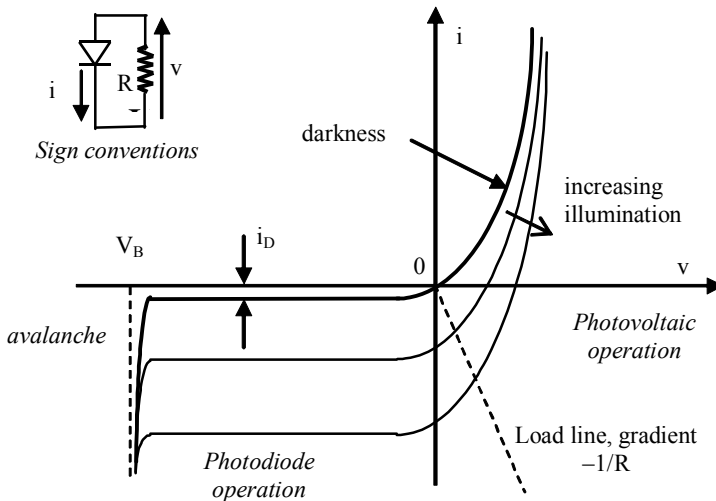


Figure 7.2. Characteristic of a photodiode

7.1.3. Avalanche photodiode

The photocurrent must be amplified because the signal received is often very low. Since the preamplifier noise can be predominant, it may be interesting to use an internal gain component called an avalanche photodiode (APD).

Its principle is chain ionization by carrier impact caused by a very intense electric field. The avalanche effect, if it is not controlled, leads to junction

breakdown for a reverse voltage V_B (see Figure 7.2). Each primary carrier will produce m secondary carriers.

This electric field is obtained with high reverse bias voltage, in a pn abrupt junction, generally separated from the absorption zone, which is thick and slightly doped; this is the $p\pi pn$ structure principle (Figure 7.3), mostly used in silicon APD (π corresponds to p^+). High multiplication coefficients M are then obtained: M is the average number of secondary carriers created (i.e. the average value of m).

The photocurrent then becomes:

$$i'_s = M.S.P$$

The dark current is multiplied by a factor that is slightly lower than M . It increases with bias voltage and temperature simultaneously.

Thanks to high zone π resistivity, the gain can be controlled. For reasons due to material, germanium APDs generally adopt a simple pn structure; the gain is lower but obtained under lower voltage. In this case, a law of the following type is used:

$$M = \frac{1}{1-(V/V_B)^{m'}}$$

in which m' has a typical value from 3 to 6.

Also defined are the ionization coefficients of electrons, α_n , and holes, α_p , which are the probability of each carrier creating a second carrier by ionization, which equals αdx in a material depth dx . Carriers with the highest ionization factor must be injected (this is the case with electrons in silicon).

The use of avalanche photodiodes is decreasing due to the development of erbium-doped fiber optical preamplifiers.

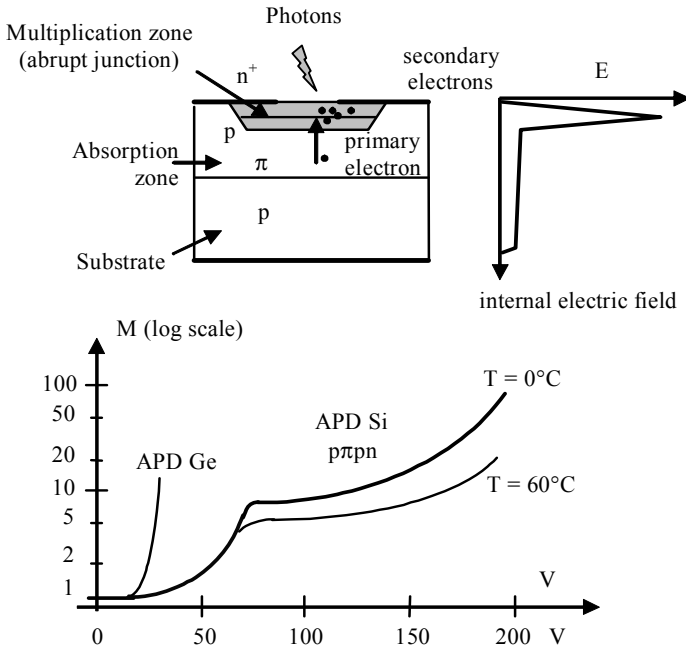


Figure 7.3. *Avalanche photodiode and gain-voltage curve*

7.1.4. Materials used in photodetection

Contrary to emission, the semiconductor used does not have to be direct. Silicon which is an indirect semiconductor widely used for image sensors and solar cells, is used up to the limit of its responsivity (approximately $1\ \mu\text{m}$). Its performances are very good and cost is low, hence the interest of the “first transmission window”. However, silicon APDs require large bias voltages and are now used mainly for instrumentation applications (reflectometry, spectroscopy, image intensifiers, etc.).

Beyond $1\ \mu\text{m}$, other material must be used. Germanium is a traditional material that is mediocre in performance. It has progressively been replaced by III-V semiconductors (GaInAs over InP), with much better performance because they can be developed as heterojunction structures (Figure 7.4). Illumination through the substrate, in particular, increases performance and decreases leakage currents because it is transparent to the detected wavelength.

Edge illumination in high speed photodiodes uses the active layer as a guide (of great depth for photons but low transit time for carriers) and also requires a heterojunction. Combined with a matched propagation line structure, these

components have a bandwidth that is larger than 40 GHz, but their connection with fiber optics is as tricky as for edge transmission laser diodes.

In addition, III-V material enables the integration of detectors, transmitters, integrated optical devices (couplers and optical switches) and electronic components in the same substrate. In this way a complete transmission module, with monitoring photodiode, control circuit and even optical multiplexer can be monolithically integrated.

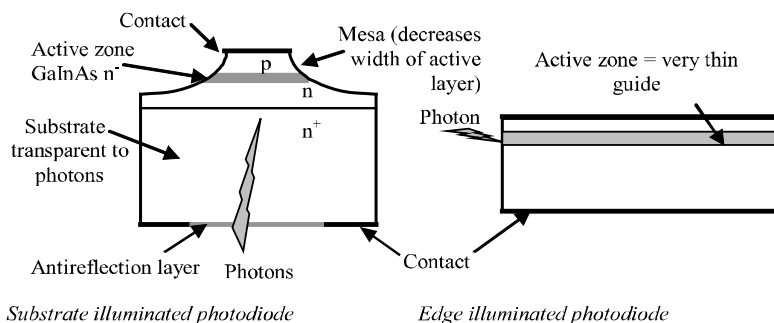


Figure 7.4. *GaInAs photodiodes*

Table 7.1 illustrates the main characteristics of the different material. HgCdTe, a II-VI compound, is mainly used in infrared instrumentation and very little in telecommunications.

Germanium has seen a renewed interest in the form of SiGe alloy, for the development of high speed components which can be integrated with silicon circuits. However, SiGe compositions compatible with a silicon substrate have a low germanium content, in order for there not to be too much lattice mismatched (they are constrained layers), and can mostly be used in the first window up to 0.98 μm . Research projects concerning germanium photodiodes bonding on SoI (*Silicon on Insulator*) substrate are also being carried out.

Window	Second and third			
Material	Si	Ge	GaInAs	HgCdTe
λ_{lim} (μ m)	1.0	1.6	1.7	1.7 to 2.2
S_{max} (A/W)	0.6	0.7	0.8	0.9
i_D (nA)	1 to 5	500	1 to 5	10
Avalanche: V_B (V)	100 to 200	25	100 to 160	100
max gain	100	10	20	30
exponent x	0.5	1	0.7	0.5

Table 7.1. Photodiode characteristics according to their material

7.1.5. Phototransistor

This is a transistor with an illuminated base (Figure 7.5). The depleted zone of the reverse-biased base collector junction acts as a photodiode. If the base-emitter junction is biased, the photocurrent re-injected in the base is amplified by the transistor’s gain β , with a typical value ranging from 30 to 100. It is therefore an internal gain component, simpler and more reliable than an avalanche photodiode, because it does not require high voltage.

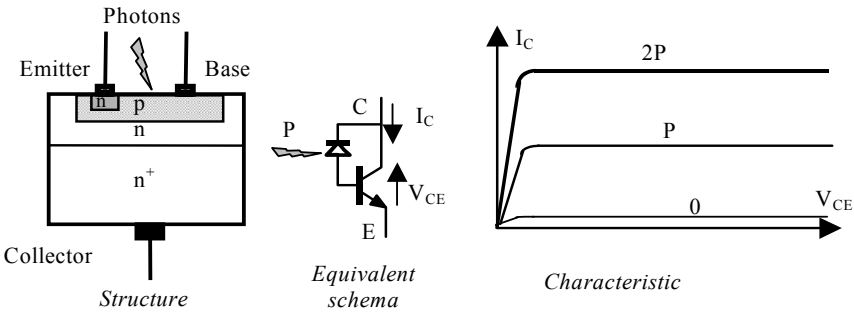


Figure 7.5. Phototransistor

The silicon phototransistor is not very efficient, however, because the base must be relatively thick because of the penetration depth. In these conditions, transistor gain and transition frequency are quite low. This component is interesting because of its low cost and is mainly used in automations or infrared remote control receiving, most often in logical mode (the reception of a certain level of light puts the transistor on, otherwise it is blocked).

Heterojunction phototransistors (HPT) GaAlAs on GaAs, GaInAs on InP or more recently SiGe on Si are much more efficient. Developed from heterojunction bipolar transistor (HBT) structures, they present transition frequencies of several dozens of GHz and gains exceeding a hundred. Their efficiency is better because only the base is made out of the lowest gap material, it absorbs the majority of photons and there is current gain (whereas photons absorbed in the collector produce a photocurrent that is not multiplied). They may be interesting for their integration capacity in amplifiers or oscillators, but are still not widely used.

7.2. Optical receiving interface

7.2.1. Structure

The set made up of photodiode, its polarization circuit and the preamplifier is often integrated in a single package, connected to the cable by a pigtail fiber, or mounted with an optical connector. The hybrid technology is much used for high frequencies. If the signal does not contain continuous components, the photodiode can be linked to the preamplifier by a decoupling capacity, which eliminates the dark current i_D (but not the associated quantum noise).

The optical receiving interface is an *analog* subset, providing a signal voltage proportional to the optical power received. It is used in all link types. It is often followed by several amplification stages. However, this interface is the circuit that will provide most of the noise on the link and its design must be carried out with particular care.

There are two preamplifier structures (Figure 7.6):

- high input impedance amplifiers (without feedback), using an operational amplifier (at low frequency) or a field effect transistor. By giving high value to R_P , the receiver is very sensitive (the v/P ratio, generally provided in $mV/\mu W$, is very high) and very low noise. However, the time constant $\tau = RC$ is very high, hence a low-pass filtering effect (or the signal integration beyond the cut-off frequency). The amplifier must have high dynamics and be followed by an equalizer, difficult to adjust because τ is not very reproducible, and which increases high frequency noise;
- transimpedance amplifiers with a parallel R_C feedback resistor. If the (discrete or integrated) amplifying chain gain is large, then $v_s \approx -R_C i_s$. Ratio v/P is not as high as in the previous structure, but it is flat and reproduced over a large bandwidth. The time constant is divided by the feedback ratio. On the other hand, feedback resistance provides additional noise.

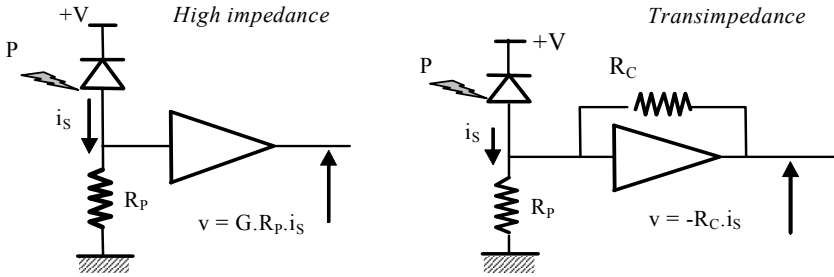


Figure 7.6. Preamplifier structures

7.2.2. Photodiode noise

7.2.2.1. In PIN photodiodes

Because of the random distribution of photon arrival instants or generation of electron-hole pairs, a shot noise appears in the junction, which is also called quantum noise. This is a Gaussian white noise with spectral density in current:

$$\frac{d\langle i_q^2 \rangle}{df} = 2qi$$

with i as the average current in the photodiode and q the electron charge.

This noise, whose power is proportional to the received optical power (whereas electric signal power is in P^2), constitutes the theoretical limit to the range of transmission systems. It is in fact due to the quantum nature of light, photons arriving randomly, following a Poisson distribution. The probability of detecting n photons during the time interval $\{t, t+\Delta t\}$ equals:

$$P(n) = \frac{N^n \cdot e^{-N}}{n!}$$

with N as average number of photons detected during a Δt period.

7.2.2.2. In avalanche photodiodes

In this case, multiplication is accompanied by an *excess noise*. In fact, each primary carrier produces m secondary carriers since m is a random variable with an average value M . Shot noise power is then multiplied by its quadratic mean value $\langle m^2 \rangle$, higher than M^2 , noted as:

$$\langle m^2 \rangle = M^2 \cdot F(M)$$

with $F(M)$ as the excess noise factor.

This factor depends on material, more precisely on the ratio k' between the electron ionization coefficient and the hole ionization coefficient, in the sense that $k' < 1$, again on the condition of injecting higher ionization carriers. Its law is:

$$F(M) = k'M + (2-1/M)(1-k')$$

that can be transformed into the approximate form:

$$F(M) = M^x$$

In the most unfavorable case where $\alpha^n = \alpha^p$, $x = 1$ (this is the case with germanium). In total, noise current in an avalanche photodiode has a quadratic mean value of:

$$\frac{d\langle i_q^2 \rangle}{df} = 2q(SP + i_D) \cdot M^{2+x} \text{ (approximate expression)}$$

7.2.3. Optical receiver modeling

From the point of view of the signal (and noise), the receiver can be modeled as in Figure 7.7 where we show:

- the photodiode modeled as a signal current source, in parallel with a capacitance C_{PD} (junction capacitance and distributed parasite capacitance) and the quantum noise source;
- bias resistance R_P and eventually feedback resistance R_C ($R_C = \infty$ if there is no feedback); these resistances are associated with sources of thermal noise current of general expression:

$$\frac{d\langle i_{th}^2 \rangle}{df} = 4 \frac{kT}{R}$$

with $k = 1.38 \cdot 10^{-23}$ J/K as the Boltzmann constant and T is the absolute temperature;

- the amplifying chain, classically modeled by a noiseless two-port-network, with input admittance modeled by a dipole R_A/C_A , preceded by a noise voltage source and a noise current source, which are independent and generally given in the amplifier notice.

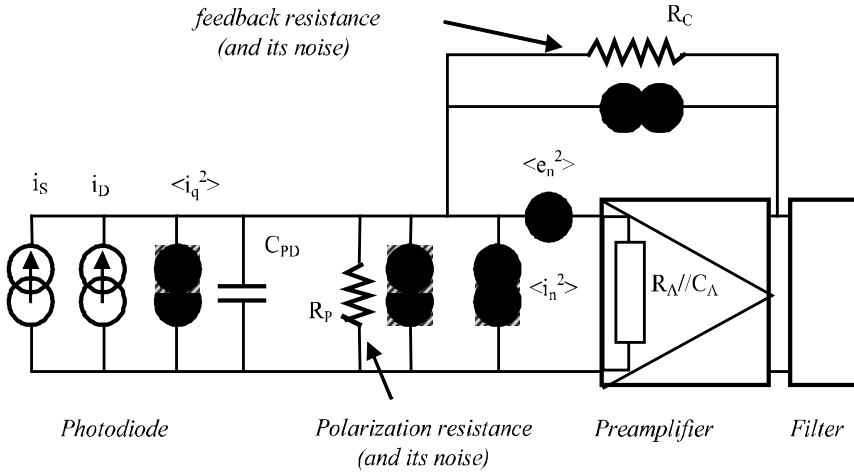


Figure 7.7. Optical receiver modeling

7.2.4. Noise current calculation

Since the signal is a current (i_s), the noise must be in the form of a current brought back to the circuit input. Its quadratic mean value is the sum of quadratic mean values of the different noise currents, or:

$$\langle i_B^2 \rangle = \langle i_q^2 \rangle + \langle i_{th}^2 \rangle + \langle i_A^2 \rangle$$

$\langle i_A^2 \rangle$, the amplifying chain noise, comes from the noise current source $\langle i_n^2 \rangle$ and noise voltage source $\langle e_n^2 \rangle$ which, flowing in an admittance Y , equals a current:

$$\langle i_n^2 \rangle = \langle e_n^2 \rangle \cdot |Y|^2$$

where:

$$Y = \frac{1}{R} + jC2\pi f$$

with:

$$\frac{1}{R} = \frac{1}{R_p} + \frac{1}{R_C} + \frac{1}{R_A}$$

and:

$$C = C_A + C_{PD}$$

In order for this contribution to not be excessive, R must be large and C must be small, i.e. global capacitance (photodiode – preamplifier – distributed capacitances of the circuit) must be as low as possible (in the order of pF).

Since Y depends on frequency f , we write in reality:

$$\langle i_A^2 \rangle = \int_0^{\Delta F} \left[\frac{d\langle i_n^2 \rangle}{df} + \frac{d\langle e_n^2 \rangle}{df} \left(\frac{1}{R^2} + (2\pi fC)^2 \right) \right] df$$

where ΔF is the noise bandwidth of the filter following the preamplifier. By integration, if noise sources of the amplifying chain are white, we obtain:

$$\langle i_A^2 \rangle = \left[\frac{d\langle i_n^2 \rangle}{df} + \frac{d\langle e_n^2 \rangle}{df} \left(\frac{1}{R^2} + \frac{(2\pi\Delta FC)^2}{3} \right) \right] \Delta F$$

This hypothesis is not always verified, notably at high frequencies where the noise spectral density has a tendency to increase, but also at very low frequencies because of noise in $1/f$ which is significant in III-V components; to avoid this, low frequencies are filtered (which is an additional reason to code the signal).

If a high impedance structure with a field effect transistor is used, R is very large and $\langle i_n^2 \rangle$ is negligible. Noise power then increases as ΔF^3 ; this structure is less noisy beyond a frequency of approximately 50 MHz (Figure 7.8).

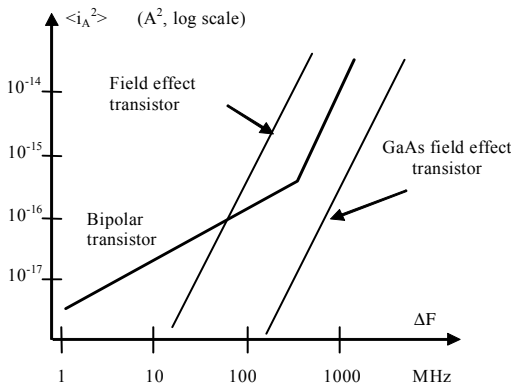


Figure 7.8. Comparison of preamplifier structures

Beyond this, a transimpedance amplifier with bipolar transistors is used, less noisy and of large bandwidth. This solution is limited by very high frequency stability problems, and integrated structures with field effect transistors InP are used integrating the photodiode. They reach bandwidths of more than 10 GHz for high throughput systems. Bandwidths over 40 GHz have recently been reached with edge-illuminated photodiode structures which minimize surface and therefore parasite capacitance.

7.2.5. Calculation of the signal-to-noise ratio

At preamplifier and filter output (Figure 7.7), this ratio in power is:

$$\text{SNR} = \frac{i_s^2}{\langle i_B^2 \rangle} = \frac{(\text{MSP})_2}{\langle i_q^2 \rangle + \langle i_F^2 \rangle + \langle i_L^2 \rangle}$$

with:

– i_s^2 is the electric signal power at the photodiode (that is why noise is considered at this level); if analog modulation is used (see Chapter 9), it is then the electric sub-carrier power;

– $\langle i_q^2 \rangle = 2q \cdot \text{SP} \cdot M^2 F(M) \Delta F$ is the *shot noise*; although it depends on the signal, we can consider its average value which is proportional to P_{mr} , the average optical power received;

$$- \langle i_F^2 \rangle = 4kT\Delta F \left(\frac{1}{R_p} + \frac{1}{R_c} \right) + \langle i_A^2 \rangle \text{ represents background noise, independent}$$

of the signal, caused by electronic circuits of the receiver, to which we can add the part of shot noise that is due to the photodiode's dark current if it is significant (because it is independent of the optical signal). This term is often, but incorrectly, called "thermal noise";

– $\langle i_L^2 \rangle = \text{RIN} \cdot i_s^2 \cdot \Delta F$, which comes from the source noise, transmitted and detected in the same way as the optical signal, this noise can be significant for laser diodes characterized by their relative intensity noise (RIN), in Hz^{-1} (see section 6.4.4). Since this noise power is proportional to the instant value of P^2 , its average value is then proportional to $\langle P^2 \rangle$, the quadratic mean value of P , and not to P_{mr}^2 .

These expressions are valid for an avalanche photodiode, as well as for a PIN photodiode by making $M=F(M) = 1$. We can reveal the noise term:

$$\frac{\sqrt{\langle i_B^2 \rangle}}{S}$$

which is equal to the optical power that would give, by photodetection, a current equal to the rms (*root mean square*) input noise current. Since this term is in $\sqrt{\Delta F}$ in the case of white noise, this power is measured in a 1 Hz band; it is called noise equivalent power or NEP, in $W/\sqrt{\text{Hz}}$. In order to intrinsically characterize the receiver, it is measured in the dark; the receiver background noise alone is involved. Thus:

$$\text{NEP} = \frac{\sqrt{\langle i_F^2 \rangle / \Delta F}}{S} \text{ in } W/\sqrt{\text{Hz}}$$

taking into account the order of magnitude, the usual unit is $\text{pW}/\sqrt{\text{Hz}}$.

Some receiving interface manufacturers, however, provide an NEP measured in the whole bandwidth and expressed in W (or even in dBm, logarithmic unit): what this bandwidth is must be verified.

7.2.6. Optimization of the signal-to-noise ratio

In practice, three cases are possible (Figure 7.9):

– if optical power P is low, and if gain M is small (or with a PIN photodiode), the receiver background noise is predominant and we can write:

$$\text{SNR} = \frac{(\text{MSP})^2}{\langle i_F^2 \rangle} = \frac{(\text{MP})^2}{\text{NEP}^2 \cdot \Delta F}$$

it increases in P^2 and in M^2 (hence the interest in APD);

– if P and/or M are high, the quantum noise is predominant, and we have:

$$\text{SNR} = \frac{SP}{2qF(M)\Delta F}$$

which this time increases as P , but decreases as M^{-x} when APD gain increases, because multiplication excess noise, which increases with the signal, becomes predominant;

– finally, if P is very high, the noise caused by the source can become predominant and:

$$\text{SNR} = \frac{1}{\text{RIN} \cdot \Delta F} \frac{P_{\text{mr}}^2}{\langle P^2 \rangle}$$

which is constant, the source demanding its own carrier-to-noise ratio, which can obviously not be exceeded. In practice, this equals at least 50 to 60 dB with laser diodes (much more with LEDs) and can only be awkward for high quality analog transmissions (see Chapter 8) or specific applications such as microwave antenna transfer.

Avalanche photodiodes thus present optimal gain, maximizing SNR for a given optical power, and which is deduced from:

$$\frac{d(\text{SNR})}{dM} = 0$$

from which:

$$M_{\text{opt}} = \left(\frac{\langle i_F^2 \rangle / \Delta F}{qx(SP + i_D)} \right)^{1/(2+x)}$$

This gain is all the higher as P is low, x is small (M_{opt} reaches high values in silicon), and the electronic background noise is strong, since the goal of using the avalanche photodiode is to partly mask it. This formula is pessimistic because it presumes that the dark current is completely multiplied.

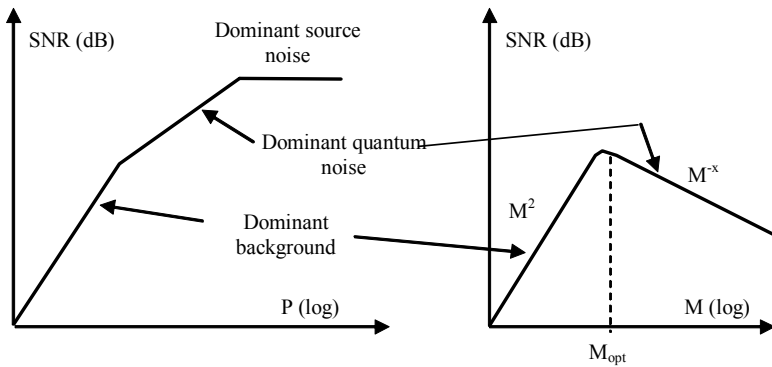


Figure 7.9. Signal-to-noise ratio at receiver output

7.3. Other photodetection schemas

7.3.1. Heterodyne detection

Direct detection in a photodiode delivers a current that is proportional to the optical power or to the field square; this is a quadratic detection. The photodiode acts as mixer. This property makes it possible to transpose to optics the heterodyne detection principle well known in radio. A beat is created between the optical wave received, of angular frequency ω_s , and a local oscillator which is a stabilized laser diode of angular frequency ω_L , in such a way to transpose the modulated signal at an intermediate frequency $|\omega_s - \omega_L|$ of several GHz, where it will later be demodulated. The advantage is to be able to perform phase or optical frequency modulations and to operate a coherent transmission (see section 9.1.5), whereas direct detection only authorizes amplitude modulation.

This frequency transposition is performed by mixing, in a single-mode fiber coupler, the electric field of the signal: $E_s(t) \cos \omega_s t$ where $E_s(t)$ is the complex amplitude of the received field, containing information, and of the local oscillator: $E_L \cos \omega_L t$ (Figure 7.10). In order for this to happen, their polarizations must be aligned, which is one of the main problems with this type of system. This signal is then detected by a photodiode which, because of quadratic detection, will produce a current that is proportional to $\langle E^2 \rangle$, where E is the sum of the fields; we then have:

$$E(t)^2 = E_s(t)^2 \cos^2 \omega_s t + E_L^2 \cos^2 \omega_L t + E_s(t) \cdot E_L \cos(\omega_s + \omega_L)t + E_s(t) \cdot E_L \cos(\omega_s - \omega_L)t$$

After photodetection (which corresponds to a low-pass filtering with a much lower cut-off frequency than light frequency), the first two terms have a constant average, the third one has a zero average and the fourth one is the signal transposed into intermediate frequency. This is amplified because its amplitude is multiplied by the local oscillator amplitude. This gain is limited however by shot noise generated from the photodiode where its power is almost proportional to E_L^2 , since the local oscillator is much more powerful than the signal received.

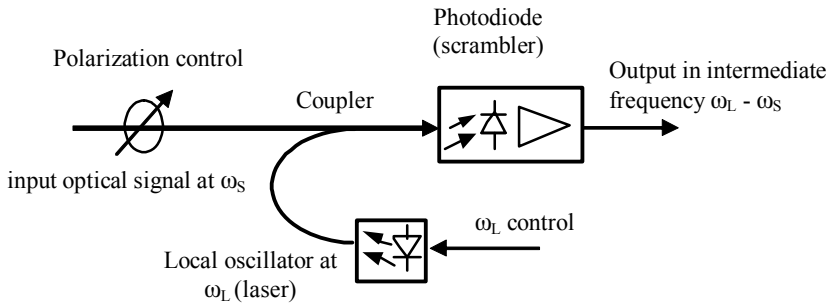


Figure 7.10. Heterodyne detection

It is theoretically possible to have $\omega_s = \omega_L$. It is the homodyne detection that makes it possible to gain 3 dB but it is even more complex to implement. The laser phase must in fact be controlled in addition to its frequency and polarization.

7.3.2. Balanced detection

This process uses two photodiodes receiving two optical powers modulated by signals opposed in phase (Figure 7.11). If photodiodes are identical, this differential mode cancels dark currents and the continuous component of the light signal, directly delivering the modulating signal $s(t)$ to the load. It mainly enables the cancellation of source noise (RIN of the laser – Chapter 6, amplified spontaneous emission (ASE) of an optical amplifier – Chapter 8) at the receiver, since these optical noises are a common mode term and the currents they generate cancel out in photodiodes, with only shot noises remaining in the photodiodes.

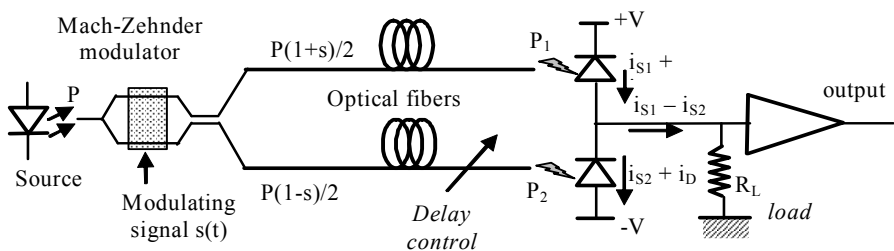


Figure 7.11. Balanced detection

This is a very complex process because the signal must be carried by two optical fibers of perfectly identical lengths and attenuations (the optical path difference must remain lower than the distance traveled by the light during a modulating signal period, which generally requires a controlled optical delay line) and an external modulation must be applied by a modified Mach-Zehnder modulator, delivering at two outputs two modulated signals with envelopes in phase opposition. This is possible by adding a matched guide coupler to the interferometer (section 2.4.3) and by using the optical phase quadrature effect on the coupled signal. It can be shown that the sum in one output and the difference in the other are obtained.

It is therefore used in very specific cases, notably for microwaves over optical fibers over short distances: The optical source noise problem can be solved, which is limiting for this type of application, and the use of two parallel fibers can be accepted over a short distance, even if in practice it is necessary to introduce a controllable delay line in a channel.

Developments made to date, for radar signal transfer for example, use in addition one (or more) integrated photodiode pair in order for them to have the most identical characteristics possible.

A balanced mixer is also interesting in heterodyne detection, because it eliminates continuous components and local oscillator laser noise (but not the quantum noise associated with photodiodes).

Chapter 8

Optical Amplification

8.1. Optical amplification in doped fiber

8.1.1. *Introduction*

Rare-earth-doped glasses make it possible to perform optical amplification, and therefore amplifiers, as well as lasers. In fact, rare earth atomic properties, similar to gas properties (particularly since energy levels are discrete), enable the development of 3 or 4 level optically pumped systems.

The general principle of optical amplification is as follows: an external light energy with a wavelength corresponding to the transition between levels n and $n + 2$ is absorbed and fills the higher level; emission is performed by radiative transition between levels $n + 2$ and $n + 1$; as this last level quickly empties by non-radiative transition toward stable state n , population inversion is thus obtained.

Several rare earth elements can be used: *erbium* (Er) as well as *neodymium* (Nd), the active element of YAG lasers radiating at $1.06\text{ }\mu\text{m}$, *praseodymium* (Pr) allowing us to design fiber amplifiers operating at $1.3\text{ }\mu\text{m}$, or even *thulium* (Tm) enabling the widening of amplifier gain to the band $1.45\text{-}1.5\text{ }\mu\text{m}$ (band S).

These elements take the form of ions doping a glass or crystal host matrix. In the case of fiber-optic amplifiers, this matrix is a single-mode fiber where the core has been erbium-doped during manufacturing. Amplifiers that are currently used are silica fibers where germanium oxide GeO_2 as well as alumina Al_2O_3 are added to the core. More efficient amplification in erbium-doped fluoride fibers has been the

subject of research studies, but is much more expensive and causes many more technological problems; because of this, they have remained unused.

Other research projects involve the development of integrated optics amplifiers in erbium-doped waveguide amplifiers (EDWA); applications are possible in signal processing or in photonic integrated circuits performing switching functions. Finally, laser sources using diode pumped Er^{+++} or Nd^{+++} doped crystals are currently available.

8.1.2. *Optical amplification principle in erbium-doped fibers*

The advantage of erbium in optical telecommunications is that one of its emission bands, around $1.54\ \mu\text{m}$, corresponds to the minimum attenuation in silica fibers. This band can be pumped to 1.48 or $0.98\ \mu\text{m}$, wavelengths where high power pump laser diodes can be developed (Figure 8.1).

In the case of pumping at $1.48\ \mu\text{m}$, it is the equivalent of a three level system, both lower levels corresponding in fact to two of the sublevels resulting from the widening of the fundamental level by the Stark effect. This effect is caused by the host crystal lattice influence on the ion. In the case of fibers, host matrix non-homogeneity leads to complex effects of non-homogenous widening and selective saturation. Because of level widening, wavelengths which can be radiated and amplified are contained inside a relatively large band.

Emission wavelengths, as well as the amplified bandwidth, slightly depend on the host matrix (the maximum is at $1,536\ \text{nm}$ in the aluminum co-doped silica, and at $1,540\ \text{nm}$ in fluoride fibers). They can be characterized by the fluorescence spectrum of the material corresponding to its spontaneous transmission after excitation by a wavelength contained in the absorption spectrum (see Figure 8.2).

In the case of pumping at $0.98\ \mu\text{m}$, it is a four level system, since the higher level is pumped through an even higher level with non-radiative transition between the two. The absorption and emission spectra are then well separated, which improves amplifier characteristics, in efficiency and noise.

On the other hand, $0.98\ \mu\text{m}$ laser diodes, developed in AlInAs over InP (or GaInAs over GaAs) in the form of constrained quantum wells, with lattice mismatching, became available later than those at $1.48\ \mu\text{m}$. For this reason linked to system reliability, $1.48\ \mu\text{m}$ pumping was chosen for the first optical amplification submarine links. Pumping is also possible at $0.80\ \mu\text{m}$ with low cost laser diodes, but it is not very efficient.

The excited state has a limited radiation lifetime of a dozen ms. This relatively high value provides efficiency and gain stability for signals with a frequency higher than a few kHz. It is a significant difference with semiconductor amplifiers where this lifetime is of the order of ns and where the gain is not stable for signals of less than a few GHz. In any case, there is a transient response effect at signal input.

Absorptions by excited states can occur and lead to emission at lower wavelengths than the pump.

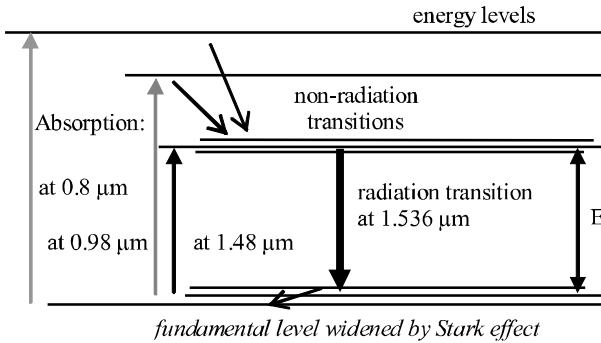


Figure 8.1. Principle of optical amplification in erbium

8.1.3. Optical amplification gain

The gain coefficient by unit of length, which depends on the optical frequency ν , is given by:

$$g(\nu) = \Gamma \cdot \sigma_e(\nu) \cdot N_2$$

with $\sigma_e(\nu)$ as the effective emission cross-section.

However, the absorption coefficient by unit of length is given by:

$$\alpha(\nu) = \Gamma \cdot \sigma_a(\nu) \cdot N_1$$

with $\sigma_a(\nu)$ effective absorption cross-section:

- $N_2 = x \cdot n_t$ and $N_1 = (1-x)n_t$ are the higher and lower level populations;
- n_t is the total erbium concentration (in m^{-3});

– x is the fraction of excited ions (included between 0 and 1), increasing with pump wave intensity, which increases amplifier gain;

– Γ is the overlap integral between its spatial distribution and its guided mode distribution. These distributions must coincide as much as possible, in order for Γ to be close to 1; actually, average gain on a cross-section is considered.

Cross-sections (called this because their dimension is the square of a length) are approximately 10^{-24} m^2 (Figure 8.2). They are tricky to measure directly.

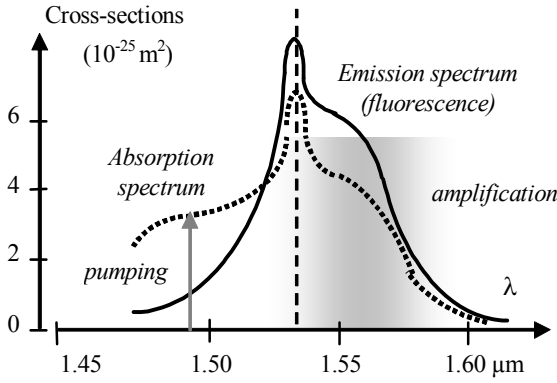


Figure 8.2. Absorption and transmission spectra in erbium

The spectra of these cross-sections depend on temperature and are related by:

$$\sigma_e(\nu) = \sigma_a(\nu) \exp \frac{E - h\nu}{kT}$$

where E is the transition energy.

The emission is shifted toward longer wavelengths than absorption; but there is spectrum overlap, therefore re-absorption, which decreases gain, all the more so as the temperature is high.

8.1.4. Amplified signal power

Signal power along the optical fiber, $P(z)$, is calculated by:

$$dP/dz = P(z) [g(z) - \alpha(z)]$$

which generally requires a complex numerical calculation, because it involves pump wave absorption and intermediate level depletion, accelerating when signal power increases, until a state is reached where there is no longer population inversion. These two effects decrease x , then the net gain, when z increases. Owing to this, gain goes through a maximum after a length L_{opt} , in the order of a dozen meters, which increases with pump power. In addition, gain depends on optical power at input, which can require stabilization, by AGC or by deliberately saturating the amplifier.

Gain spectrum at amplifier output has a strong resemblance to the emission spectrum, but is not identical because absorption is involved; its decrease when the wavelength increases in the $1.53 - 1.57 \mu\text{m}$ band, which is optimal for amplification (gray zone in Figure 8.2), makes the gain spectrum at amplifier output flatter than the emission spectrum.

Figure 8.3 gives power ranges of the signal and pump in the case of erbium-doped silica fibers (the optimal length is shorter with fluoride fibers). Pumping back reaches higher power (but not necessarily higher signal-to-noise ratios).

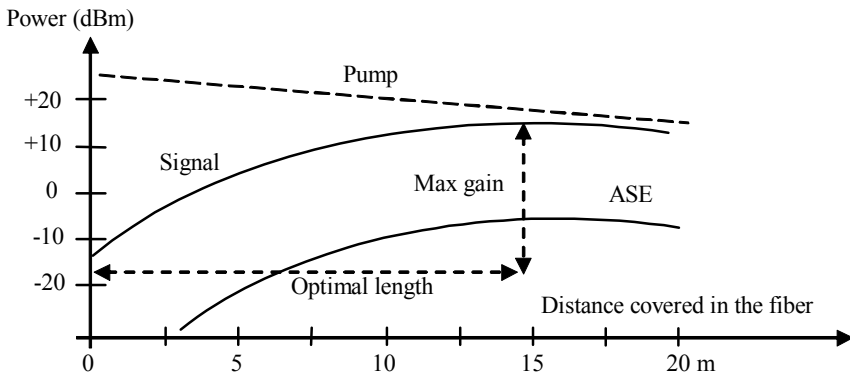


Figure 8.3. Evolution of power along the amplifying fiber

As erbium-doped wavelength amplifiers (EDWA) are very short, they operate under much more homogenous conditions and their gain is more stable, but the power obtained is not as high, and as with all integrated optical devices, they are penalized by connection losses with the fibers.

8.1.5. Optical amplification noise

The noise in an optical amplifier is caused by the amplified spontaneous emission (ASE), which is caused by the pump wave. It is an optical background noise propagating in both directions. It is expressed by its spectral density at amplifier output:

$$N_{\text{ase}} = 2 N_{\text{sp}} (G-1)h\nu$$

where G is the gain, and N_{sp} is the *population inversion factor* (factor 2 is due to spontaneous transmission in both polarizations). It is given by:

$$N_{\text{sp}} = \frac{N_2 \sigma_e}{N_2 \sigma_e - N_1 \sigma_a}$$

It decreases by ∞ (inversion appearance) to 1 (total inversion).

N_{sp} is only slightly higher than 1 if pumped at 980 nm, almost total population inversion ($N_1 \ll N_2$) can then be obtained. It is higher if pumped at 1,480 nm. As with gain, noise has quite a large spectrum (Figure 8.4a), and it must be filtered around the signal wavelength. Contrary to an electronic amplifier, this noise is not independent from the signal. It decreases in the presence of a signal because the stimulated transmission decreases spontaneous emission probability then noise (Figure 8.4b).

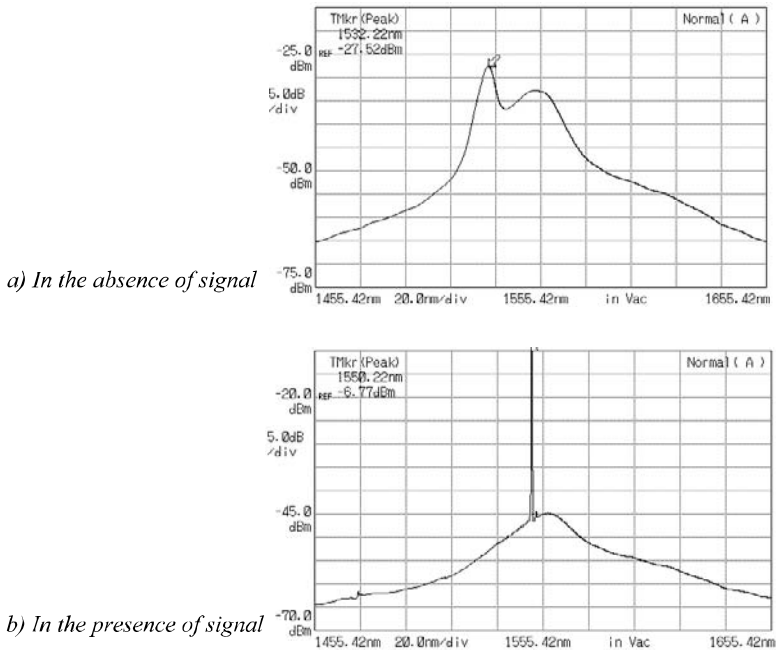


Figure 8.4. Amplified spontaneous emission spectrum

8.2. Erbium-doped fiber amplifiers

8.2.1. Description

The two main elements of an erbium-doped fiber amplifier (EDFA) are the erbium-doped amplifying fiber and the pump laser, which continuously emits a power of several dozen mW at 0.98 or 1.48 μm . Pumping can be injected in the same direction as the signal (forward pumping), or in the reverse direction (backward pumping). Some amplifiers use a pump in both directions. This is the case with amplifiers for submarine links, where these two pump lasers are shared between both directions in order to ensure security, as the system can continue to operate with only one pump (Figure 8.5).

The signal and pump are multiplexed by a wavelength division multiplexer in order to minimize losses. Isolators prevent the amplification of a signal that would arrive in the reverse direction from the fiber and therefore the occurrence of an oscillation by reflected wave amplification. In fact, the amplifier medium made up of the fiber is by nature bidirectional. They also stop amplified spontaneous

emission propagating in the opposite direction. Pump laser diodes are also equipped with isolators which are not represented in the figure.

In order to further reduce connection losses with line fibers, a mode-adapting fiber section is generally used. In fact, the diameter of the mode guided by the amplifying fiber is slightly lower than the line fiber. This allows us to increase the power density of the pump wave, therefore the gain and efficiency.

There is also at the repeater output an optical filter, intended for the elimination of pump wave residue and to reduce amplified spontaneous emission, as well as a photodiode for output level control and to possibly perform automatic gain control.

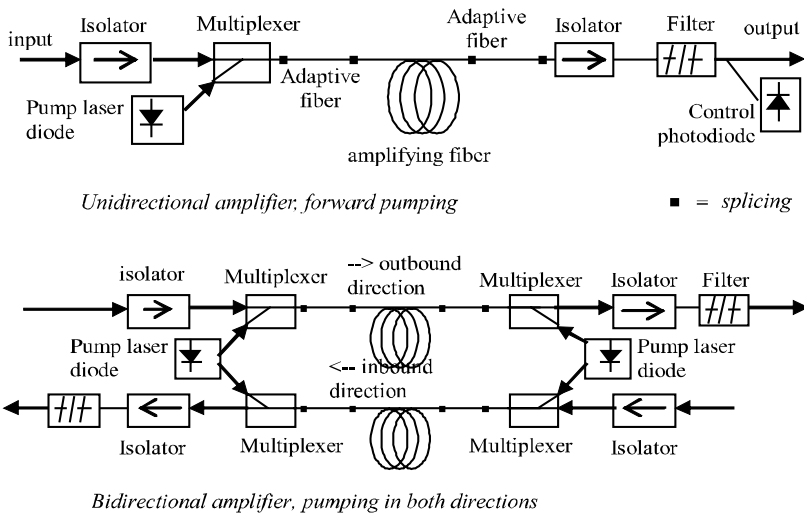


Figure 8.5. Erbium-doped fiber-optical amplifier schemas

8.2.2. Characteristics

An optical amplification repeater is much simpler than an electronic repeater-regenerator. It generally contains a monitoring electronic circuit, but it does not work at a high bitrate. It is actually only an amplifier with the following advantages:

- less complexity and cost;
- more reliability;
- transparence of transmitted signal, i.e. the bitrate may be changed without modifying amplifier operation (which is quite impossible in the case of the repeater-

regenerator, because of clock recovery); moreover, analog or digital signals can equally be amplified;

- gain has a very low dependence on polarization of the signal wave (it was a significant advantage compared to heterodyne detection);

- possibility of simultaneously amplifying a large number of multiplexed wavelengths. This advantage has been a determining factor because it has made it possible to use on a large scale, and in an economical way, wavelength division multiplexing.

In addition, amplification in a single-mode fiber can be obtained with a relatively low pump power (a few dozen mW) because of the high concentration of the pump wave, contrary to bulk crystals.

However, over a long link there are disadvantages caused by the absence of regeneration:

- accumulation of noise from one amplifier to another;
- accumulation of pulse broadening caused by chromatic dispersion;
- significant non-linear effects because of high output level.

8.2.3. *Gain parameters of an optical amplifier*

As with an electronic amplifier, an erbium-doped fiber amplifier is characterized by:

- its gain in small signal: $g = 10 \log G$; this is in the order of 20 to 30 dB for pumping at 1,480 nm, from 30 to 40 dB for pumping at 980 nm; an amplifier could theoretically compensate the attenuation of 150 to 200 km of optical fiber, but in practice this value is decreased because of noise;

- its saturation power, defined as in electronics by the power of the output signal when the gain is divided by 2 (or reduced by 3 dB): at output, it now reaches between 20 and 30 dBm for pumping at 980 nm. As it gets closer to saturation, quantum efficiency gets closer to its maximum (Figure 8.6). This power is becoming closer to power causing non-linear effects in the optical fiber (and even reaches it with the most powerful amplifiers exceeding 30 dBm, which requires laser security precautions);

- its quantum conversion efficiency (QCE) defined by:

$$\text{QCE} = \frac{\lambda_s}{\lambda_p} \frac{P_{s(s)} - P_{s(e)}}{P_p}$$

where p relates to the pump and s to the signal. It leans toward a maximum at saturation, whereas gain decreases (Figure 8.6). It exceeds 80% with forward pumping;

- its gain to pump power ratio: this ratio is relatively constant and goes by a maximum of approximately 4 dB/mW for pumping at 1,480 nm, and reaches 10 dB/mW for pumping at 980 nm. The amplifier gain can then easily be controlled by using the pump power.

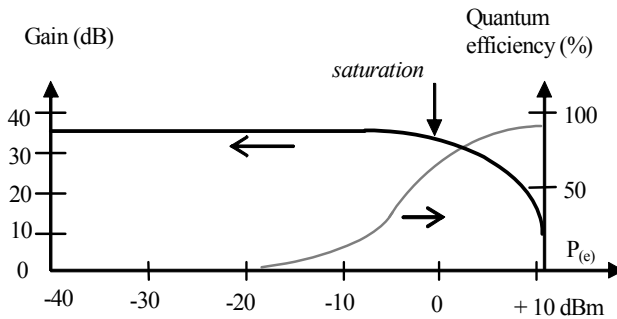


Figure 8.6. Gain and efficiency versus input $P_{(e)}$ power

8.2.4. Amplified bandwidth

Optical bandwidth is approximately 30 nm for erbium-doped fiber amplifiers; it covers “band C” from 1,530 to 1,565 nm, corresponding to the ITU grid for wavelength division multiplexing (WDM). However, it is necessary that the gain be as flat as possible in this band; but gain flatness depends on temperature, on input power and on the possible saturation of the amplifier with a signal from another wavelength (spectral hole burning phenomenon or appearance of “holes” in the gain spectrum). Gain equalization of erbium-doped fiber amplifiers is a tricky point, which for lack of anything better is performed by filters attenuating wavelengths with too much amplification. The use of photo-inscribed Bragg gratings is one of the most efficient methods.

Doped fluoride fibers allow a larger and flatter band, it was one of their main advantages compared to the first silica fiber amplifiers to have motivated a comeback in research studies for this material, but they have turned out to be too fragile.

8.2.5. Noise figure

As with an electronic amplifier, the noise figure is defined as (optical) signal-to-noise ratio degradation between input and output. At input, the optical “background noise” has a spectral density of $h\nu$, resulting from the Heisenberg uncertainty principle; at output, it is increased by the amplified spontaneous emission of spectral density N_{ase} . Input ($-10\log C_1$) and output ($-10\log C_2$) losses (Figure 8.7) must be taken into account.

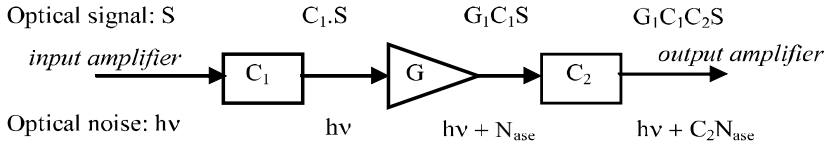


Figure 8.7. Model for noise figure calculation

The noise figure thus equals:

$$F = \frac{1}{G.C_1} \left[\frac{1}{C_2} + \frac{N_{ase}}{h\nu} \right] = \frac{1}{GC_1C_2} + 2 N_{sp} \cdot \frac{G-1}{GC_1}$$

If G is large and losses are low, then F leans toward a limit equaling $2 N_{sp}$; the theoretical minimum is 3 dB (in the absence of a particular action on polarization). If G is small, F becomes lower than 3 dB when G leans toward 1, which is no longer interesting from a practical point of view. The noise figure is a good indicator of amplifier quality, but for noise calculation on the link, it is preferable to use spectral density N_{ase} .

As with an electronic amplifier, input losses (low C_1) deteriorate noise figure. This is one of the reasons that it becomes high for semiconductor amplifiers.

8.3. Noise calculation in amplified links

8.3.1. Input noise in the presence of an optical amplifier

After photodetection, optical noise will create a *beat* with the signal of received optical power $P_{S(r)}$, as with itself, because of quadratic detection. A noise current then appears in the receiver which adds to the shot noise of photodetection and possibly to the source's relative intensity noise (see Chapter 6), which is generally

negligible at the receiver. The global noise current has an quadratic mean value which is the sum of:

– shot noise associated with the signal:

$$\langle i_{q(s)}^2 \rangle = 2q.S. P_{S(r)}. \Delta F$$

– shot noise associated with the spontaneous emission:

$$\langle i_{q(ase)}^2 \rangle = 2q.S. P_{ase(r)}. \Delta F = 2q.S. N_{ase(r)}. \Delta v. \Delta F$$

– the beat between signal and spontaneous emission:

$$\langle i_{b(ase)}^2 \rangle = 2S^2. P_{S(r)}. N_{ase(r)}. \Delta F$$

– the beat between the different components of spontaneous emission:

$$\langle i_{b(ase/ase)}^2 \rangle = 2S^2. N_{ase(r)}^2. \Delta v. \Delta F$$

The electric signal power after detection still equals:

$$i_s^2 = S^2. P_{S(r)}^2$$

$N_{ase(r)}$ is the spectral density of amplified spontaneous emission received at detector input. It is assumed to be constant within the optical filter of width Δv . The beat phenomenon, a consequence of quadratic detection, results in that all amplified spontaneous emission components far from each other (or from the optical carrier) at less than ΔF will create electric noise within band ΔF containing the signal.

ΔF is the electric filter bandwidth, determined by the signal bitrate, whereas Δv is the optical filter bandwidth, larger in practice, that should be made as small as possible (since the theoretical minimum, in intensity modulation, is $2\Delta F$). Otherwise, noise terms related to amplified spontaneous emission can become very high. The optical fiber offers some “self-filtering”, because of its spectral attenuation curve, but it is not sufficient.

We can develop these formulae by using:

$$P_{S(r)} = GC_1 C_2 A P_{(e)}$$

and:

$$N_{ase(r)} = 2 N_{sp} (G-1) h\nu C_2. A$$

in the case of a link with one amplifier, separated from the receiver by a total attenuation A (or $-10 \log A$ in dB) of the fiber section, since $P_{(e)}$ is the signal power at amplifier input. We note that quantum noise terms are as $A.G$, whereas beat terms are as $(A.G)^2$, as with electric signal power.

8.3.2. Case of an optical preamplifier receiver

In the case of use of a doped fiber preamplifier just before the detector, A is close to 1 and the beat terms are predominant. As long as they are lower than background noise of the receiver, the carrier-to-noise ratio at input is improved by $10 \log G$. When gain is high, and they dominate background noise, noise is in G^2 , and increasing gain does not improve the signal-to-noise ratio. It is possible to calculate the value of G for which these noises are equal (if the equivalent optical power of the receiver noise is known, Chapter 7), providing the value of “asymptotic gain” that is possible on the average power received which is necessary for a given signal-to-noise ratio (Figure 8.8). Its typical value is 15 to 20 dB.

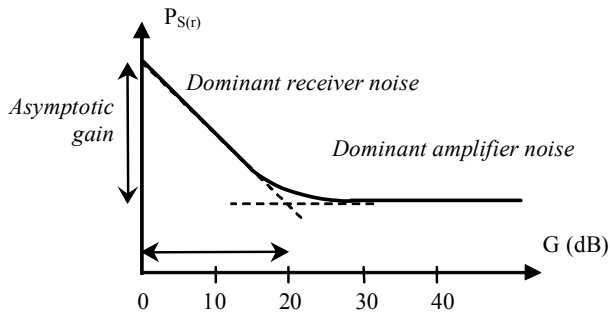


Figure 8.8. Input power required versus preamplifier gain

In instrumentation (notably in reflectometry), optical preamplifiers are beginning to be used to amplify very low optical signals and thus get closer to the quantum limit.

On the other hand, if the amplifier is far from the receiver, $A \ll 1$, which generally makes the beat terms negligible. The gain must then be strong since the dominating noise is quantum noise, in G , whereas (electric) signal power is in G^2 . Gain limit is then due to amplifier saturation.

In PON access networks (Chapter 10), the power of a single optically amplified transmitter (or of several, wavelength division multiplexed) can be distributed between a large number of receivers with star couplers. The limit to these systems'

capacity, in power and in number of channels, is due to the non-linear effects which will create intermodulation products between the different optical carriers.

8.3.3. Noise calculation over long links

Because of the absence of regeneration, noise accumulation occurs which limits the distance between optical amplifiers, at a value that is all the lower as the link is long. In fact, at the end of a length L , including M identical amplifying sections with length $d = L/M$, optical noise caused by amplified spontaneous emission accumulation equals, in spectral density:

$$N_{\text{ase(tot)}} = 2 M N_{\text{sp}} (G-1)h\nu$$

where:

$$g = 10 \log G = \alpha d$$

is the gain in dB for each amplifier which compensates the attenuation of the previous fiber section, of lineic attenuation α .

Hence:

$$M = \alpha L / g$$

and:

$$N_{\text{ase(tot)}} = 2 N_{\text{sp}} \alpha L \frac{G-1}{10 \log G} h\nu$$

which is all the lower the smaller G is.

This term occurs in the different noise components described previously. The link calculation will then allow us to determine its maximum value depending on the expected bit error rate, thus on the signal-to-noise ratio. The maximum G gain value, hence the minimum number of amplifiers to use, is deduced from it. Since G decreases when L increases, the number of repeaters increases faster than the link length (contrary to the case of a regenerated link where they are proportional). That is why if the distance between amplifiers is of 50 km for a 6,000 km link at 10 Gbit/s, it falls to 35 km for a 9,000 km link.

Reality is more complicated because amplifier saturation by optical noise accumulation has to be considered. Narrow optical filters must then be used in each amplifier to avoid the appearance of this phenomenon. As long as the amplified

spontaneous emission power is much lower than the signal, it can work by saturating the signal, providing some level control on the link. In a long link, the use of automatic gain control (AGC), by acting on pump power, is recommended, however, in order to compensate for the possible attenuation fluctuations.

The use of an error correction code at the receiver becomes very useful (and is easier than with a regenerated link where it would need to be used at each repeater).

In the case of a submarine link, since intermediate amplifiers are remotely powered, the goal is to optimize gain while limiting pump power. Ratio g/P_p must be maximized. It is possible to remotely pump an in-line amplifier from a terminal located several dozen kilometers away. In a submarine link, it is then possible to increase the distance between terminals, and avoid submerged active elements (distances of over 400 km have been reached).

8.4. Other types of optical amplifiers

8.4.1. *Semiconductor optical amplifiers (SCOA)*

It is possible to amplify light through a structure very similar to an edge-emitting laser diode (Chapter 6), whose faces are anti-reflection treated, to avoid the occurrence of a laser cavity (Figure 8.9). The operation is in progressive waves allowing us to use the total gain band of the material. The amplification threshold is then slightly lower than the laser emission threshold and this component can be used as semi-conductor optical amplifier (SCOA) with a gain band that is relatively large (30 to 40 nm).

For use in repeaters however, it presents the following drawbacks compared to erbium-doped fiber amplifiers:

- rather low saturation power (approximately 10 dBm for pump current of a hundred mA);
- relatively high noise (caused by amplified spontaneous emission);
- some sensitivity to incoming light polarization, but this drawback which is characteristic of the first SCOA's is less sensitive in more recent buried stripe structures;
- significant connection losses with the optical fiber is a major problem for line repeaters, but it is less so for amplifiers integrated with a laser source, a modulator or an integrated optical device;
- short carrier lifetime (in the range of a nanosecond), resulting in gain dependence on the signal for frequencies lower than 1 GHz, and a high-pass type

response. If there is wavelength division multiplexing, a variation of the signal at a wavelength can modify the gain for another wavelength.

SCOAs, however, present practical advantages compared to EDFAs (cost, size, consumption, integration with other optoelectronic functions) and are beginning to find other network applications.

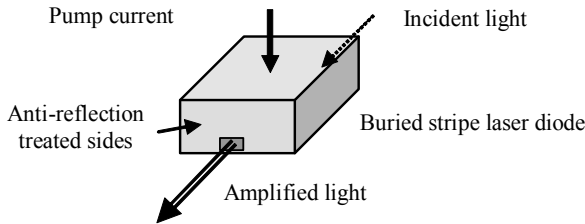


Figure 8.9. *Semi-conductor optical amplifiers*

8.4.2. Other SCOA applications

Their drawbacks can be used to create new functions (mixer, wavelength conversion, etc.). In fact, in order to transfer modulation from an arriving signal at a wavelength λ_1 to another wavelength λ_2 , a coupling is performed at amplifier input between the signal at λ_1 and a laser diode in continuous wave mode (cw) at λ_2 (Figure 8.10). When the level is low at input λ_1 , λ_2 sees the maximum gain and gives a high level at output λ_2 . When the level is high at input λ_1 , the amplifier is saturated and gives a low level at output λ_2 . It is then a transfer of modulation with logical inversion. This effect is only efficient below the frequency, in the range of GHz, beyond which the gain is stabilized.

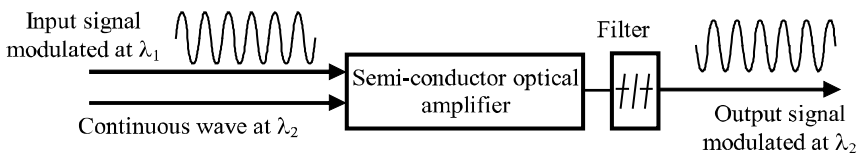


Figure 8.10. *Wavelength conversion*

Semi-conductor amplifiers can also be used as optical gates operating in on-off mode (switching from on to off state in a few hundred ps). Due to their integration capacity, they could be used as very fast (but with high consumption, even in the

absence of switching) switching matrix elements. They also enable optical regeneration experiments, being used as gates controlled by a clock, reshaping the signal.

8.4.3. Amplifier comparison

This is summarized in Table 8.1 where we compare EDFA and SCOA. In the first category, the best performances were obtained with silica fibers pumped at 980 nm, even if the pumps at 1,480 nm showed a reliability advantage with the first systems. Doped fluoride fibers are mentioned for reference, but due to their cost and brittleness they were abandoned.

8.4.4. Raman amplification

The Raman amplification (whose principle is explained in section 2.5.2) allowing the amplification of any band simply by choosing the pump wavelength, seemed like an interesting solution for long distances; it is in experimentation in some links (Figure 8.11). This is a “distributed amplification” because it occurs in the line fiber, caused by the Raman pump which is injected in the reverse direction from the signal just before the doped fiber amplifier, which is the configuration minimizing noise.

However, the efficiency of such an amplification is very low and all technical problems are not resolved. One of the few operational applications is to pump the fiber of a medium length submarine link (without submerged repeaters) from the receiving land terminal, thus gaining 10 to 20 dB.

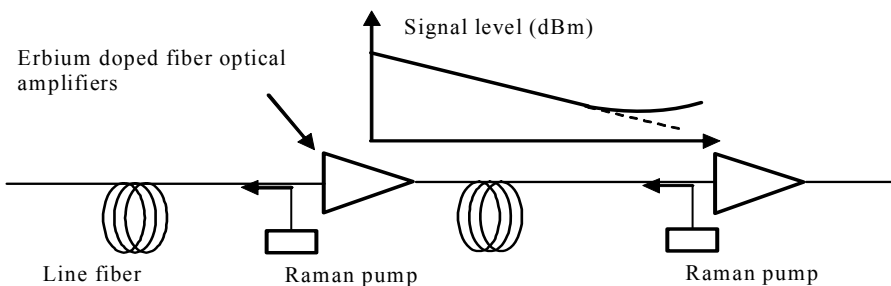


Figure 8.11. Principle of a link using distributed Raman amplification

Erbium-doped fiber	Silica	Silica	Fluoride fibers	Semi conductors
Pumping at	980 nm	1,480 nm	1,480 nm	
Gain	30 to 40 dB	20 to 30 dB	40 dB	20 to 30 dB
Gain to pump power ratio	10 dB/mW	4 dB/mW	6 dB/mW	
Saturation power	20 to 30 dBm	10 to 15 dBm	17 to 20 dBm	10 dBm
Quantum efficiency	80 %			
Amplified bandwidth	20 to 30 nm	10 to 20 nm	30 nm	30 to 40 nm
Noise figure	3 dB	6 to 9 dB	6 dB	12 dB

Table 8.1. *Optical amplifier characteristics comparison*

Chapter 9

Fiber-Optic Transmission Systems

9.1. Structure of a fiber-optic digital link

9.1.1. *Different systems*

The vast majority of fiber-optic links are naturally made up of digital links even though analog transmissions are still used in video or remote measurements. Fiber optics' low attenuation and large bandwidth take full advantage of digital transmissions, which became predominant in the telecommunications network when the first fiber-optic systems were being developed.

These systems can be classified into larger categories:

- wide area network (WAN) infrastructure, which first used plesiochronous digital hierarchy steps followed by massive deployment of the synchronous digital hierarchy SDH/SONET (see section 10.3). Fiber-optic links constitute the transmission infrastructure of the “optical transport network” (OTN) which carries SDH, ATM, IP, etc. frames. They are managed by “historical carriers” such as France Télécom, as well as by “carrier’s carriers”, often associated with traffic path companies (railroads, highways, riverways, electric networks, etc.) who re-lease transmission capabilities to telecom service providers in the form of “dark fibers” or channels materialized by one or more wavelengths;

- metropolitan area networks (MAN), for cities or for a very large business sites (airport, business district, etc.) often with a loop architecture and competition between SDH and Ethernet at 1 or 10 Gbit/s for the protocol. Contrary to WANs, this market is still growing in the recent fluctuating economy; this is in particular

where the most complex architectures are, and there is high demand for passive optical components;

- local computer and company networks, and internal local area networks (LAN); they can be made up of point-point links connected by electric nodes, as well as by passive optical networks; Ethernet dominates this market but more specific protocols exist (FDDI, Fiber Channel, fieldbus, IEEE 1394 called “firewire” for multimedia);

- distribution and subscriber access networks, designed at one time by FITL (fiber in the loop), and more commonly by FTTH (Fiber to the Home) or FTTx (Fiber to the ...) x designating an intermediate point where the fiber arrives, with several variations (see section 10.2).

For these last two categories, which require increasing throughputs, an important challenge has been equipment and installation cost reduction, in order to be more competitive with twisted pair, operating over short distances with relatively high throughputs (Ethernet and ADSL), and with WiFi wireless networks.

9.1.2. Long-haul links over optical fibers

They are organized according to the diagram in Figure 9.1, inherited from coax cable transmission systems. Up to 100 km long, they can operate without intermediate repeater. Beyond that, equipment must be inserted which, in the first generation of optical systems (approximately 1980–1995) were repeaters-regenerators including optoelectronic interfaces and logical circuits necessary for signal regeneration. This was an element of cost and a brake to throughput increase, especially in submarine systems.

Erbium-doped fiber amplification has enabled the implementation of optical amplifier repeaters (Chapter 8). The signal remains in the optical form, which makes it possible to amplify signals independently from their throughput, which can increase without modifying amplifier operation. In addition, these repeaters can simultaneously amplify several multiplexed (neighboring) wavelengths. On the other hand, they do not currently regenerate the digital signal and there is accumulation of noise and pulse broadening. These repeaters require electric power feeding, generally locally provided, except in submarine links (remote power feeding; a current of a few hundred mA is sent through a conductor integrated into the cable).

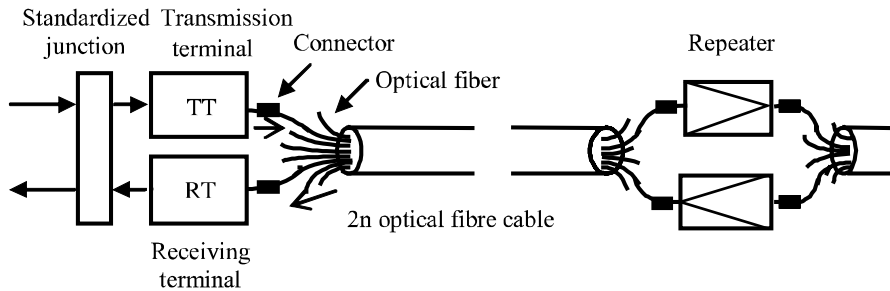


Figure 9.1. *Diagram of long-haul links over optical fibers*

9.1.3. Line terminals

These are pieces of end-of-line equipment which mainly contain (Figure 9.2):

- emission (EOI) and reception (ROI) optical interfaces; for long range systems, optical amplifiers can additionally be found behind the transmitter (booster) and in front of the receiver (preamplifier);

- at reception, clock recovery and *regeneration* circuits;

- *code conversion* circuits going from junction code to line code, and vice versa. This is often associated with scrambling. We recall that code conversion allows clock recovery at reception by introducing frequent transitions in the transmitted signal, and the elimination of continuous and low frequency components, generally not well transmitted, making transmitter control easier. Some codes allow us to measure the average error ratio (but they are not error correction codes at this level).

Finally, the terminal ensures a double function of *monitoring*:

- of itself: signal and clock presence (1), adequate interface operation (2), bit error rate at reception (3);

- and remote monitoring of repeaters, from which it receives information (4) and to which it sends commands such as looping (5), through specialized channels.

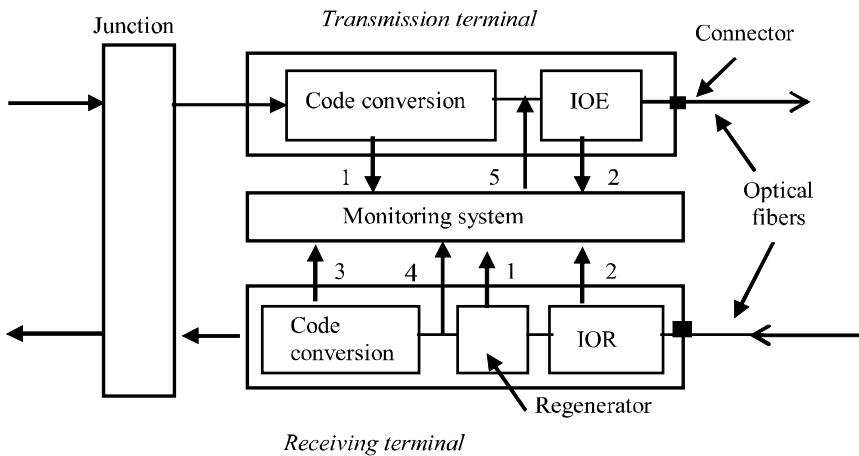


Figure 9.2. Line terminal for fiber optics transmissions

9.1.4. Line codes

In optical transmissions, binary codes are generally used, in which the low level corresponds to a zero light power (transmitter turned off, or external modulator on “off”):

- at rather low bitrates, *biphase* codes (also called *Manchester* codes) and differential Manchester codes (example: Ethernet 10 Mbit/s) or, up to 34 Mbit/s, CMI (*Code Mark Inversion*) codes, replacing one bit by a two bit sequence (Table 9.1);

- above this, in order to limit spectral widening, *nBmB block codes* which replace an n bit block by an m bit block, containing the maximum of transitions. For example, codes 4B5B or 8B9B are used. The line clock has a frequency that is multiplied by m/n . High bitrate systems (FDDI, Ethernet 100 Mbit/s and over, Fiber Channel) use it.

The RZ (return to zero) format is used in long-haul high bitrate links (especially submarine), allowing us to slightly push back the dispersion limit: as they are narrower at the source, pulses tolerate a slightly higher broadening.

In these links, the duobinary (or bipolar) format is starting to be used, in which bit 1 is alternatively coded by an amplitude of +1 and -1, which in optical terms means carrier phase inversion, obtained by an electro-optic modulator (see section 5.3.5). However, contrary to the systems described in section 9.1.5, this format does

not need coherent detection, because the absolute amplitude value still equals 1 (bit 0 is still coded by zero amplitude). The interest is that since the spectrum of such a signal cancels out at (optical) carrier frequency, it can be filtered (single-side band) and occupies half as much bandwidth (spectral efficiency is doubled). The effect of chromatic dispersion is decreased: a 0 between two 1 has a lower risk of being overlapped by the spread of neighboring bits, because optical signals will be in phase opposition and cancel out.

bit	RZ format	biphase phase	differential biphase code	CMI code	duobinary
0	00	01	sequence identical to the previous one	10	0
1	10	10	sequence reversed in relation to the previous one	00 or 11 alternated	1 or -1 (alternation of optical phase)

Table 9.1. *Line binary codes*

9.1.5. Coherent optical transmissions

In all operational systems, information modulates light intensity of a source without using coherence from the optical carrier. However, the signals can also be transmitted by frequency or phase modulation of a coherent optical carrier, and demodulated with the help of heterodyne reception (section 7.3.1). This applies classical radio frequency transmission processes to optical frequencies, with much larger technological problems. Even though they have been the subject of several research studies, these systems have not passed the experimental stage except for DPSK modulation.

The elements of a coherent transmission system are (Figure 9.3):

- a transmitter made up of a laser diode with very high spectral purity (better than the MHz, or a spectral width lower than $3 \cdot 10^{-6}$ nm) modulated in frequency (FSK) or most often in phase (PSK or DPSK), by an integrated external modulator (Mach-Zehnder);

- a receiver based on the principle of heterodyne detection explained in section 7.3.1, by a beat between the received optical wave of angular frequency ω_s , and a local oscillator of angular frequency ω_L , in a photodiode acting as mixer. The laser acting as local oscillator is controlled to transpose the modulated signal at an intermediate frequency $\omega_s - \omega_L$ controlled by a reference.

The signal transposed in intermediate frequency (IF) is amplified because its amplitude is multiplied by the amplitude of the local oscillator. This makes it possible to lower the detection threshold and to get closer to the quantum limit. Heterodyne detection is difficult to execute however because the local oscillator laser must be perfectly stabilized and polarization of the signal received must be controlled. Doped fiber-optical preamplification, which is not very sensitive to polarization of input signal, allows us to more easily obtain comparable results.

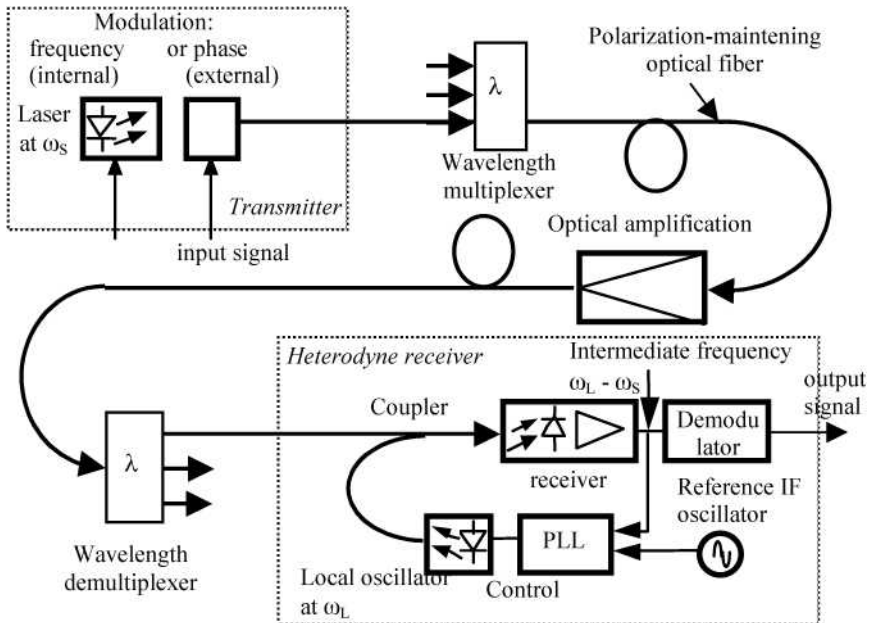


Figure 9.3. Coherent optical transmission system

The potential advantage of coherent transmissions was also its great selectivity: carriers spaced from less than 10 GHz, or 0.08 nm, can be separated in intermediate frequency. The spectacular progress of (optical) wavelength demultiplexers has greatly deflated this interest.

However interest has returned for differential phase shift keying (DPSK), a classical technique in modems, where optical carrier phase in a bit is reversed in relation to the previous bit if the bit equals 1, and retained if it equals 0. Mach-Zehnder electro-optic modulators are well suited for this modulation (see section 5.3.4). Demodulation is carried out in another Mach-Zehnder electro-optic interferometer by an interference between a bit and the previous bit delayed in a

delay line made up of a simple longer guide (at 40 Gbit/s, propagation over a guide of a few mm is enough to obtain a delay of one bit time), thus avoiding (as in radio) recovering the optical carrier phase. Demonstrations were performed at 2 and even at 4 phase states.

9.2. Digital link design

9.2.1. Filtering

In order to minimize noise while not creating inter-symbol interference, the signal must be filtered. It is known (Nyquist criteria) that the theoretical minimum width of this filter in the presence of Dirac pulses is $F_r/2$, where F_r is the clock frequency (calculated after line coding). In practice, a filter of frequency response $R(f)$ with a certain roll-off factor is used, for example a raised cosine filter. In the presence of pulses of format $s(t)$, and spectrum $S(f)$, a filter of response $G(f)$ must be used, such that:

$$R(f) = S(f).G(f).$$

In the presence of NRZ pulses, this filter resembles the illustration in Figure 9.4, with a noise bandwidth approximately equaling:

$$\Delta F = 0.7 F_r. \text{ This value will be used in noise calculations.}$$

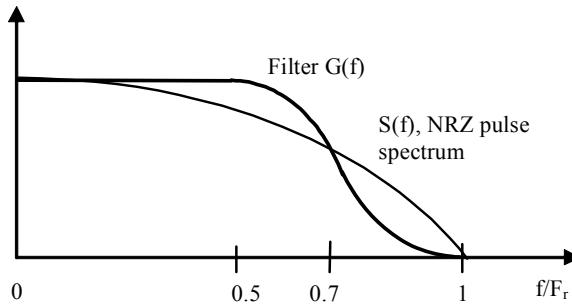


Figure 9.4. Filter for digital transmission in NRZ format

9.2.2. Choice of fiber bandwidth

The use of the Nyquist filter presumes that the optical fiber bandwidth BW is much larger than this value. Otherwise, an *equalization* is necessary in order for the

global fiber + equalizer + filter response to fulfill the Nyquist criteria. If the fiber bandwidth is unknown or liable to fluctuation, this equalization must be adaptive. This leads to additional noise and complexity. Thus, in practice, the following rule is adopted:

- if $BP > F_r$, equalization can be avoided; the inter-symbol interference effect will be negligible (as long as the adapted filter is used). This corresponds to a pulse broadening at half-maximum $\Delta\tau$ (due to global fiber dispersion – intermodal and chromatic; see Chapter 1) shorter than a half-bit:

$$\Delta\tau.D_B < 0.5 \text{ (} D_B \text{ is the bitrate); or}$$

- if BP is included between F_r and $0.7 F_r$, the pulse broadening effect is no longer negligible and leads to a *penalty* on the received level, in the range of 1 to 2 dB, that should be considered in the loss budget. This penalty can be calculated according to $\Delta\tau.D_B$, but it depends on the form of the received pulse, thus propagation conditions (it is approximately 2 dB if $\Delta\tau.D_B = 0.7$). If an equalization is made, a comparable penalty occurs, but its value depends on the signal-to-noise ratio: the equalization is interesting if the SNR is high;

- if $BP < 0.7 F_r$, the bandwidth is insufficient; the optical support must then be modified: move to another wavelength, replace a multimode fiber by a single-mode fiber, or a standard single-mode fiber by a shifted dispersion single-mode fiber, or as a last resort, introduce a chromatic dispersion compensating device, depending on the dominant cause of pulse broadening.

If possible, it is better to be in the first case, notably with multimode fibers whose bandwidth is too dependent on operating conditions. However, it can be necessary to work close to theoretical limits to increase throughput over a support that is already in place: that is why Gigabit Ethernet can run over several hundreds of meters of multimode fibers, or even over a kilometer, the strong signal-to-noise ratio allowing it to tolerate high penalty.

These semi-empirical rules do not apply as above to polarization mode dispersion (PMD, see Chapter 2), because of its random character: operators limit resulting pulse broadening to a quarter, sometimes 10% of bit time.

9.2.3. Calculation of the error probability

In the case where noise is white, additive and with Gaussian distribution, and where there is no inter-symbol interference, errors at regeneration of a binary symbol appear randomly, according to a Poisson distribution. The error probability equals:

$$P_E(Q) = \frac{1}{\sqrt{2\pi}} \int_Q^{\infty} \exp\left(-\frac{u^2}{2}\right) du \quad \text{with } Q = \frac{u_1 - u_0}{2\sigma_u} \text{ and:}$$

- u_1, u_0 voltages corresponding to levels 1 and 0 (presumed equiprobable);
- σ_u rms noise voltage.

Here are the most common numerical values:

Q	4.8	5	5.2	5.4	5.6	5.8	6.0	6.2	6.4	6.6	6.7
P_E	10^{-6}	3.10^{-7}	10^{-7}	3.10^{-8}	10^{-8}	3.10^{-9}	10^{-9}	3.10^{-10}	10^{-10}	3.10^{-11}	10^{-11}

Some publications use the error function:

$$\text{erfc}(x) = \frac{2}{\sqrt{\pi}} \int_x^{\infty} \exp(-t^2) dt \quad \text{which results in } P_E(Q) = \frac{1}{2} \text{erfc} \frac{Q}{\sqrt{2}}$$

with the same definition of Q .

Error probability can be calculated from the signal-to-noise ratio at receiver output (see Chapter 7) by assuming that the following amplifying chain no longer deteriorates this ratio, and that it is linear. Thus:

$$Q^2 = \left(\frac{u_1 - u_0}{2\sigma_u} \right)^2 = \text{SNR} = \frac{i_m^2}{\langle i_B^2 \rangle}$$

where i_m is the average current in the photodiode.

It is given by: $i_m = S.P_{mr}$ where P_{mr} is the average optical power received, by presuming that symbol 0 corresponds to a zero or negligible received power.

This result is somewhat simplified, because it presumes that noise is independent from the signal, which is not the case with shot noise. The approximation is correct however when the background noise is predominant, which is most often the case with a PIN photodiode.

We can trace curves connecting P_E and P_{mr} versus the bitrate (Figure 9.5 gives an example of the range). The penalty caused by dispersion, chromatic or intermodal, appears during measures in this type of curve.

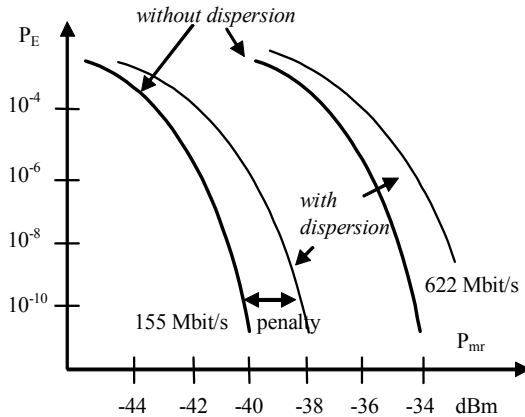


Figure 9.5. Error probability of P_E versus the average received power

9.2.4. Calculation of the average power required in reception

In reverse direction, using Q , it is possible to calculate the power P_{mr} corresponding to a given error probability (often 10^{-9}); knowledge of this value is necessary for optical link design.

Calculation is simple when the shot noise is negligible (that is generally the case in digital transmission when using a PIN photodiode); in fact, the noise is limited to receiver background noise, $\langle i_F^2 \rangle$, which does not depend on the received power, and the formula reversal results in:

$$Q^2 = \frac{(S \cdot P_{mr})^2}{\langle i_F^2 \rangle} \text{ hence } P_{mr} = \frac{Q}{S} \sqrt{\langle i_F^2 \rangle} = Q \cdot \text{NEP} \cdot \sqrt{\Delta F}$$

NEP is the noise equivalent power (in 1 Hz) of the receiver; one or the other expression is used depending on data available concerning the receiver.

With an avalanche photodiode, calculation is more complicated because its noise is significant and depends on the power received. When the dark current is negligible, calculation defines the optimum APD gain for the minimization of average received power for a given error probability (this is not the same definition as in Chapter 7): this gain equals:

$$M_{\text{opt}} = \left(\frac{\langle i_F^2 \rangle}{q^2 Q^2 \Delta F^2 x(2+x)} \right)^{1/(2+2x)}$$

and corresponding optical power equals:

$$P_{mr \text{ opt}} = \frac{\langle i_F^2 \rangle}{S \cdot q \cdot x \cdot \Delta F} \cdot M_{opt}^{(2+x)}.$$

If the dark current is significant, then this value is higher. Figure 9.6 shows numerical examples of P_{mr} versus bitrate and depending on the components used; we can see that avalanche photodiodes work with a much lower received power, and reduce the influence of the input transistor, but maintenance of their gain at a correct value must be ensured.

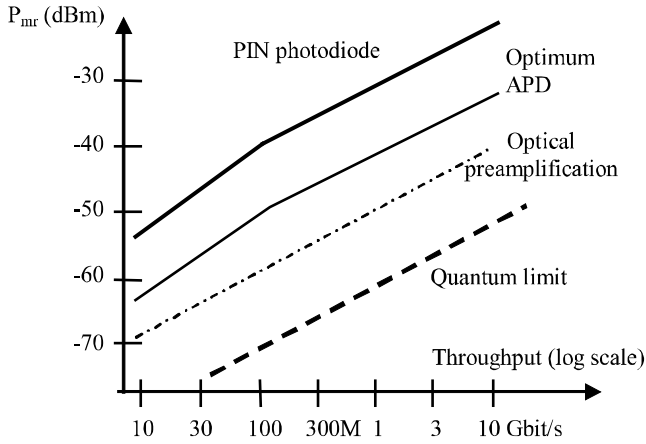


Figure 9.6. Average received power for $P_E = 10^{-9}$

On the other hand and in both cases, power P_{mr} increases with the bitrate, according to a law depending on spectral distribution of noise (and thus of components used); in a first approximation, it can be considered as proportional. In any case, the source noise effect can be ignored.

9.2.5. Quantum limit

The quantum limit is the theoretical P_{mr} value in the “ideal” case: in the absence of any noise from the source, amplifier, excess APD noise (then $F(M) = 1$), as well as photodiode dark current, we obtain:

$$Q^2 = \frac{(S \cdot P_{mr})^2}{2q \cdot S \cdot P_{mr} \cdot \Delta F} \text{ hence } P_{mr} = \frac{2q}{S} \cdot Q^2 \Delta F$$

This theoretical minimum, proportional to the bitrate, is lower by more than 30 dB to what a PIN photodiode receiver detects, by approximately 15 dB to what an APD detects (Figure 9.6); it corresponds to an average of 20 photons per bit to identify it with a probability of error of 10^{-9} (because of the Poisson photon statistic). Using heterodyne detection (section 9.1.5) or optical preamplification (Chapter 8) allows us to get closer, but these techniques also generate their own excess noise.

9.2.6. Loss budget

In order to design a link at a given bitrate, knowing performances of available components, the designer establishes a loss budget, a calculation that determines optical power distribution along the link (Table 9.2). These powers are usually expressed in dBm (10 log of the power in mW) often resulting in a negative dBm quantity, because powers are generally lower than mW (except at laser and optical amplifier output). Attenuations and margin in dB are subtracted from power in dBm (which in reality is a division of power by a dimensionless factor).

average power at emission, coupled in the fiber	$10 \log P_{me}$ (dBm)
- attenuation of connections	- A_R (dB)
- attenuation of possible multiplexers or couplers	- A_M (dB)
- margin for dispersions and protection against drifts	- m (dB)
- average received power	- $10 \log P_{mr}$ (dBm)
= available attenuation	A (dB)

Table 9.2. *Loss budget*

Average emission power is in principle equal to half of the peak power, but the power actually coupled in the fiber must be considered; it is given by the manufacturer if the transmitter is equipped with a pigtail. If the component is in a fixed connector, which is mostly the case with a multimode fiber, coupled power depends on parameters of the fiber and connector quality.

Since the bit error rate quickly deteriorates when received power decreases, it is necessary to plan for a margin at installation, and to consider a penalty of 1 or 2 dB when dispersion is not negligible. The margin is of 3 to 6 dB depending on operating conditions (component environment, risk of cable cut-off, frequency of uninstallation operations, etc.) and is generally known by experience.

The available attenuation allows us to calculate the maximum distance between transmitter and receiver, by dividing it by the average lineic attenuation of the

optical cable. It is slightly higher than that of the fiber, since line splice losses and the effect of constraints in the fiber are added. This last term is very low however with loose tube structure cables protecting fibers from constraints. In the case of a multi-terminal network, the available attenuation allows us to calculate the maximum number of these terminals.

After permitted distance calculation using the loss budget, bandwidth availability must be verified, as seen in section 9.2.2. Regardless of bandwidth limits, throughput increase decreases available attenuation because of increasing input noise (and it is barely possible to increase emitted power). That is one of the throughput limits.

When it is not immediately obvious, the choice of components can be made from available attenuation versus bitrate for different configurations (Figure 9.7). Obviously, the more reliable and less expensive components must be chosen to reach the expected ranges.

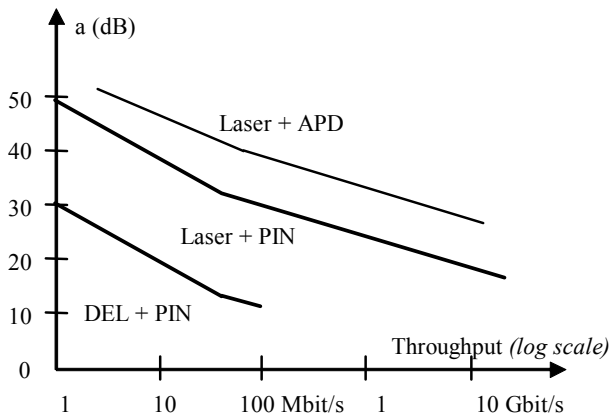


Figure 9.7. Available attenuation (examples of order of magnitude)

9.3. Digital link categories

9.3.1. Point-to-point, non-amplified lines

Figure 9.8 shows four large families of fiber-optic links, corresponding to wavelength windows used. Their spans are limited: on one hand by the attenuation (limit slowly decreasing when throughput D_B increases), on the other hand by (intermodal or chromatic) dispersion, giving an approximately $1/D_B$ limit. Operating at the dispersion limit is generally avoided.

The first category is plastic fiber transmissions at $0.67\text{ }\mu\text{m}$ for very short distance local industrial applications (cabling of workshops, computers links, internal to one machine, etc.) and up to 100 to 200 Mbit/s bitrate mainly for electric security reasons. This is now strongly developing in home automation, multimedia and automotive equipment fields.

The second category operates at $0.85\text{ }\mu\text{m}$ with LEDs and PIN photodiodes over multimode fibers. These relatively inexpensive systems are widely used in computer and industrial fields for distances in the km range: short distance transmission, local area networks (LAN), local distribution and mainly includes digital transmissions, as well as video or analog remote measurements. The decisive advantages are again electric security and insensitivity to parasites, but also savings in weight and size with optical fiber cabling. With LEDs however, bandwidth is limited by chromatic dispersion. A large market now addresses local area networks and short distance – high bitrate interconnections (1 Gbit/s and more), using VCSEL laser diodes at $0.85\text{ }\mu\text{m}$ over multimode fibers.

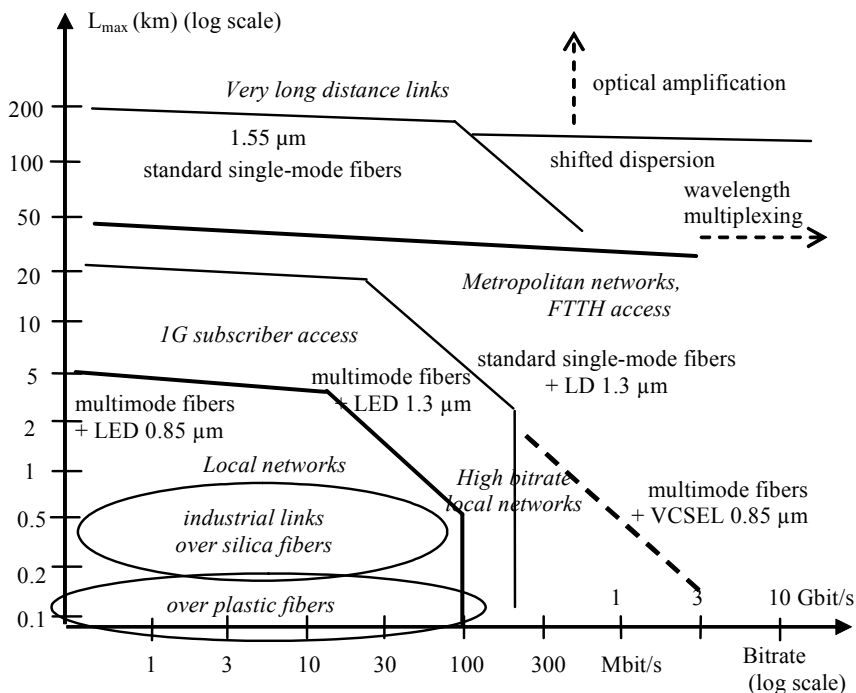


Figure 9.8. Digital line categories over fiber optics

The third category operates the window at 1.3 μm mainly with laser diodes and single-mode fibers. The low attenuation at 1.3 μm enables high bitrate metropolitan and long-haul links up to approximately 50 km, without repeaters, but the market for this window is currently focused on metropolitan area networks (MAN) and very high bitrate LANs (typically 1, and now up to 10 Gbit/s). The 1.3 μm window is also used over multimode fibers, with LEDs, for high bitrate local area networks (in the range of 100 Mbit/s). It can also operate multiplexed systems with two wavelengths over a single fiber (subscriber line for example).

The fourth category is long-haul links at 1.55 μm , requiring monochromatic laser diodes (of the DFB type). Without amplification, distances are limited by attenuation and can reach 150 km, at several Gbit/s. Standard single-mode fibers (G 652) can possibly be used with a chromatic dispersion compensation. For wide area networks (WAN), terrestrial as well as submarine, optical amplification repeaters and shifted dispersion single-mode fibers (G 655 type) must be used.

Subscriber access, which used to operate over multimode fibers in the first generation (1G), are now being deployed over single-mode fibers in passive optical network architecture, multiplexing the 2nd and 3rd window (see Chapter 10).

9.3.2. *Optically amplified links*

The quick progress achieved in the 1990s made it possible to introduce optical amplification in long distance transmission systems, and completely replace electric repeaters-regenerators. One of the main advantages of doped fiber-optical amplifiers is that they operate independently from the bitrate supported by the optical signal, and can amplify a large number of wavelengths, to easily increase the bitrate in an already installed link. Hence the explosion of throughputs which have gone from 280 Mbit/s to 640 Gbit/s per fiber in less than 10 years! The initial bitrate of the transatlantic TAT 12/13 link (first of this type installed in 1995) was of 5 Gbit/s, but it can be increased in an already installed link.

In point-to-point transmission (Figure 9.9), optical amplification can be used:

- as a line amplifier; total received noise must be minimized, as well as amplifier consumption, because they have to be remotely powered;
- as a preamplifier, just before detection; the goal is to achieve the lowest excess noise in order to get closer to the quantum limit;
- as a booster (power amplifier) right after the source; saturation power and quantum efficiency must then be maximized. It is then interesting to operate the amplifier at saturation, which stabilizes output power.

By associating a booster at transmitter and a preamplifier at receiver, links exceeding 350 km without intermediate amplifiers have been realized.

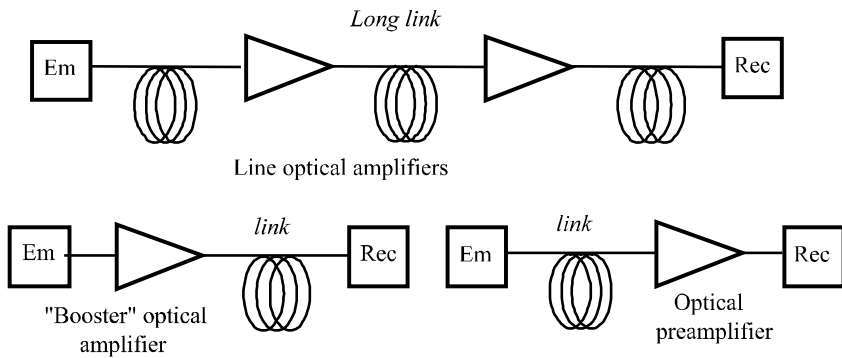


Figure 9.9. *Optically amplified links*

9.3.3. Wavelength division multiplexed links

Even though 40 Gbit/s systems are operational, 10 Gbit/s bitrate by wavelength is the highest generally used in networks. Increase of throughput is easily accomplished using wavelength division multiplexing (WDM) making it possible to reach hundreds of Gbit/s. Links with 4 to 64 multiplexed wavelengths, each modulated at 10 Gbit/s are operational in wide area networks, and are now appearing in metropolitan networks requiring increasingly high throughputs. Laboratory tests using hundreds of optical carriers have reached bitrates of over 10 Tbit/s per fiber!

The frequency plan or grid standardized by the ITU specifies wavelengths spaced from 100 GHz (or approximately 0.8 nm at 1.55 μm) between 1,528.8 and 1,560.6 nm (actually from 190 to 198 THz). There are derived plans spaced from 50 and 200 GHz, and the feasibility of an even denser grid at 25 GHz was demonstrated. Actually, the limit is caused by spectral widening of $2\Delta F$ created by optical intensity modulation. The use of WDM obviously requires laser diodes of great purity and spectral stability, and tunable if possible. Multiplexer selectivity is reinforced by the use of filters integrated in fibers. In order to increase capacities even more, the use of a widened band at higher ("L band" of 1,575 to 1,620 nm) and lower ("S band" of 1,500 to 1,525 nm) wavelengths is considered, even though erbium doped amplifiers are not as efficient in these bands (other rare earth elements such as thulium could be used).

Besides very high bitrates obtained more simply than with time-division multiplexing, wavelength division multiplexing allows us to progressively increase the capacity of links already in place. Dense wavelength division multiplexing (DWDM) helped in responding to the international traffic explosion, and adapting to this trend in a flexible way. This technique also allows us to build multi-terminal networks, which explains its increasing interest in architecture evolution.

Although wavelength division multiplexing has been possible for a long time, optical amplification is what has made it interesting. It is easy to perform, because erbium doped fiber amplifiers can simultaneously amplify several multiplexed wavelengths in the 3rd window. In addition, the very large length on which the signal remains optical (it can exceed 10,000 km) makes chromatic dispersion and polarization-mode dispersion problems critical. This limits bitrates by channel to values approximating 10 Gbit/s, or even 2.5 Gbit/s depending on fiber characteristics, and wavelength division multiplexing is currently the best solution in order to continue to increase link bitrates.

The use of optical amplifiers for wavelength division multiplexed systems does raise specific problems however:

- gain “flatness” (it must be identical from one channel to another); this can be reached in doped silica fiber amplifiers by using different gain equalizer optical devices (based on variable attenuators), adaptive if possible to follow link aging (still badly known);
- turning a channel on or off affects amplifier gain, therefore the level of other channels; this problem can be critical in packet networks where traffic is not constant;
- total output level must be limited to avoid non-linear mixing between channels. That is why a slight chromatic dispersion is recommended to limit the accumulation of non-linear mixing effects between optical carriers. The level of intermodulation products actually evolves as D_C^2 along the fiber. The use of higher mode diameter single-mode fibers, maybe with a photonic bandgap structure in the future, increases non-linear effect appearance thresholds.

Non-linear effects encourage the reduction of the number of multiplexed wavelengths, thus the increase of bitrate per channel (the goal is to deploy 40 Gbit/s), while the dispersion has a contradictory effect.

9.3.4. Dispersion effects

In a very long amplified link, and in the absence of regeneration, pulses broaden along the link. In order to limit chromatic dispersion, it is therefore necessary to use

a dispersion-shifted fiber (see Chapter 2). The first non-multiplexed systems considered the use of a zero dispersion fiber (G 653), which would have required perfectly monochromatic (and tunable) laser sources transmitting at the precise zero dispersion wavelength of the link.

In wavelength division multiplexed systems, this solution is too sensitive to non-linear effects and it was abandoned for NZ-DSF fibers (G 655), by compensating for the line fiber dispersion by a dispersion compensating fiber (DCF) which in the end leaves residual dispersion that can exceed 1000 ps/nm because it cannot simultaneously compensate for all wavelengths. After demultiplexing, a wavelength compensating device must be added (Figure 9.10). In submarine links, chromatic dispersion signs alternate from one section to another (the link is said to be dispersion managed, which requires custom design). Increasingly used is the RZ format which tolerates a slightly larger pulse broadening.

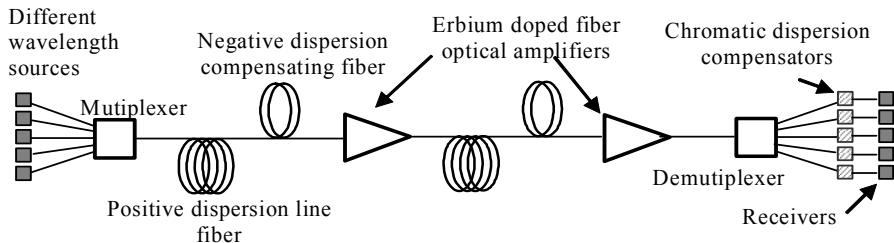


Figure 9.10. Dispersion compensation in long-haul links

At high throughput, external modulation must be used to avoid chirp effects (see Chapter 6) and the very low linewidths inherent to the laser ($\Delta\lambda$ less than 0.1 nm or approximately 12.5 GHz) is reached. In this case, intrinsic spectral widening caused by modulation, equaling $2\Delta F$ (or 0.15 nm at 10 Gbit/s), can no longer be ignored and when it is dominant $\Delta\lambda$ becomes proportional to the bitrate D_B . This phenomenon limits the product $D_B^2 \cdot L$ (where L is the total link length) since pulse broadening follows a law in $D_B \cdot D_C \cdot L$ and must remain lower than $1/2D_B$. It is one of the obstacles to the introduction of 40 Gbit/s in long links already installed because, according to the previous law, if the bitrate is multiplied by 4, the maximum distance is divided by 16 (instead of by 4 as at lower bitrates).

On the other hand, the fiber must have very low birefringence to avoid polarization mode dispersion (PMD) which spreads pulses over time even though it has very little influence on amplifier gain (see Chapter 2). This intermodal pulse broadening is proportional to \sqrt{L} because of the fiber birefringence random

character; this phenomenon also limits, for other reasons, the product $D_B^2 \cdot L$. It is all the more critical as it is difficult to compensate for it, and as a precaution, the designers generally limit the pulse widening to 10% of bit time. It is another obstacle to the development of high bitrate, long links over ancient fibers (if their PMD is in the range of $1 \text{ ps}/\sqrt{\text{km}}$, it is difficult to achieve more than 100 km at 10 Gbit/s!).

9.3.5. New modulation formats

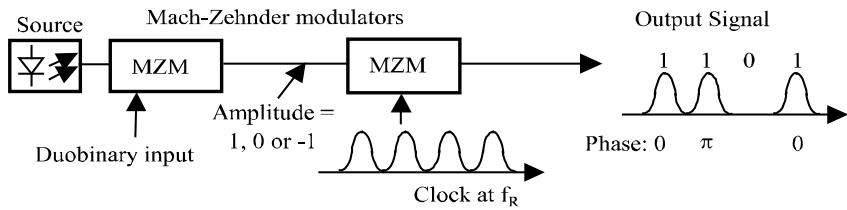
Even though systems currently in operation at least up to 10 Gbit/s use NRZ, sometimes even RZ format (see section 9.1.4), several links have experimented with new modulation formats to increase bitrates and have better resistance to chromatic dispersion.

9.3.5.1. Duobinary modulations

Duobinary modulation, as explained in section 9.1.4, associated with the RZ format, is an efficient and relatively simple way to reach these goals. A first Mach-Zehnder interferometric modulator (MZM, *Mach-Zehnder Modulator*, see section 5.3.4) creates the duobinary modulation (zero amplitude for 0, maximum amplitude with alternatively 0 and π phase for 1), followed by a second MZM that modulates intensity to create a return to zero once per bit (Figure 9.11a). The signal obtained can easily be decoded by direct detection since the intensity is enough to identify the bit, while the RZ format facilitates clock recovery. The signal envelope is not on-off modulated here as in RZ at lower bitrate; instead it is modulated by a sinusoidal clock frequency, hence the name intensity modulated (IM) that is also used.

In another set-up, a classical NRZ modulation is transformed into RZ duobinary by a 2nd MZM modulator controlled by a clock at half signal frequency, and a peak-to-peak amplitude from zero to twice the voltage giving a zero amplitude. The optical intensity goes through zero once per bit and the optical phase is reversed at each alternation, so from one bit to the next (Figure 9.11b) which creates the desired format, also called CS-RZ (Carrier Suppressed – Return to Zero) because there is no spectral component at the optical carrier frequency.

a) first method



b) second method (from NRZ input)

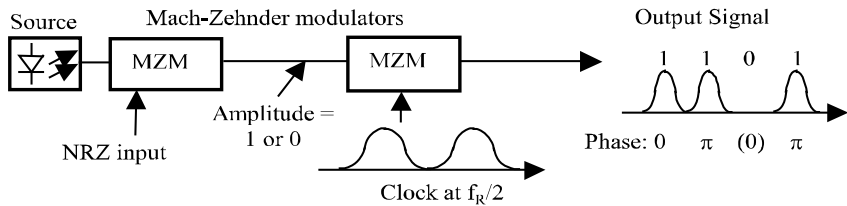


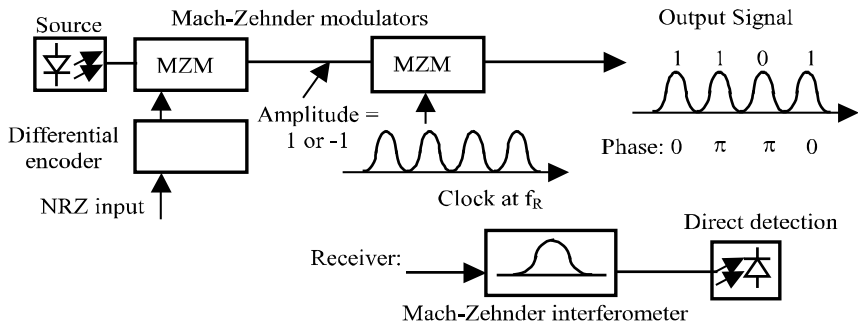
Figure 9.11. Duobinary type modulations

9.3.5.2. Phase modulations

The optical phase modulation is only currently used in the form of differential phase shift keying (DPSK) where information is contained in the phase change of a symbol compared to the previous one (see section 9.1.5). Demodulation is performed in an interferometer with one arm creating a delay of a symbol width compared to the other, and does not require phase recovery of the optical carrier, which is the advantage with this process. For modulation, the MZM modulator works at two phase states (0 and π) with the same amplitude, generally followed by a formatting RZ modulator controlled by the symbol clock, hence the name RZ-DPSK or IM-DPSK given to the process (Figure 9.12a). The intensity of the received optical signal reproduces exactly the symbol clock, regardless of the binary content.

It is possible to achieve differential quadrature phase shift keying (DQPSK) where odd and even bits modulate the in-phase and the quadrature carrier in two MZM, with one being followed by a $\pi/2$ phase shifter to obtain quadrature modulation in a single integrated circuit (Figure 9.12b). Bitrate is thus doubled, with identical spectral occupancy. A demonstration by Alcatel in 2007 transported a 107 Gbit/s signal in RZ-DQPSK (or a symbol rate of 53.5 Gbauds) over 2,000 km by using EDFAs and Raman amplifiers (Chapter 8), balanced detection (Chapter 7) and wavelength division multiplexing to obtain 10x107 Gbit/s per fiber.

a) IM-DPSK modulation



b) DQPSK modulation

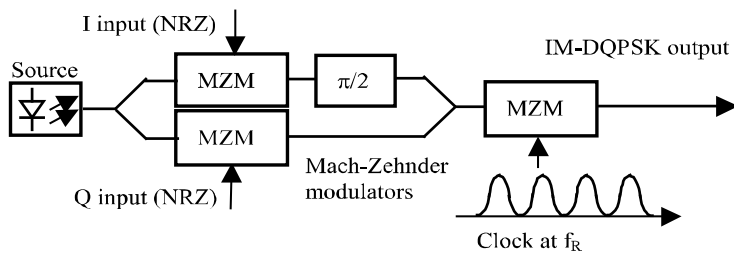


Figure 9.12. Differential phase modulations

9.3.6. Fiber-optic submarine links

Succeeding to coaxial cable analog links, the first submarine links were installed late in the 1980s (transatlantic TAT8 line in 1988) and used WDM and optical amplification as early as 1995. Although this market has suffered from the recent economic situation, submarine systems have always been at the leading edge of fiber-optic communications because they carry the longest distances, highest throughputs and strongest reliability requirements.

Currently, bitrates are in the range of hundreds of Gbit/s per fiber, with 4 to 6 fiber pairs per cable. Submarine cables (see Chapter 3) are laid at the bottom of the sea by large cable ships, and buried only close to shores. Their repair, after cable fishing if necessary by a submarine robot, is possible but tricky and expensive. Another difficult point is remote power feeding, since voltages can reach 12 to 25 kV at line extremities.

In addition to transoceanic lines (North Atlantic, now exceeded by the Pacific), there are several “coastal” links without repeaters, reaching over 300 km by using

optical amplifiers in on-shore terminals. They can connect islands or cross narrow seas (Baltic sea, Mediterranean, etc.). Several countries (Italy, Japan, Brazil, etc.) connect their major cities with submarine links along the coast. Most of the continents are thus surrounded by submarine cables; Africa is on its way to completion.

Submarine networks are increasingly becoming more prevalent, with several landing locations linked to the cable by branching units. The recent SEA-ME-WE 3 line (South East Asia–Middle East–Western Europe), since doubled by SEA-ME-WE 4, connects more than 30 countries with the same cable (Figure 9.13), using wavelength add/drop to multiplex the different destinations, multiplexers are submerged (names in boxes are names of the cable ships). Network architectures make it possible to apply security procedures by traffic rerouting.

The growth in international traffic driven recently by the Internet involves an increase in installed capacities (they – temporarily – exceed needs in the major routes) and undoubtedly surpass satellites, at ever decreasing cost. They also have better performance in terms of security and propagation delay, but satellites remain indispensable to directly connect a large number of users, especially if they are mobile or isolated. There is therefore much more complementarity than competition.

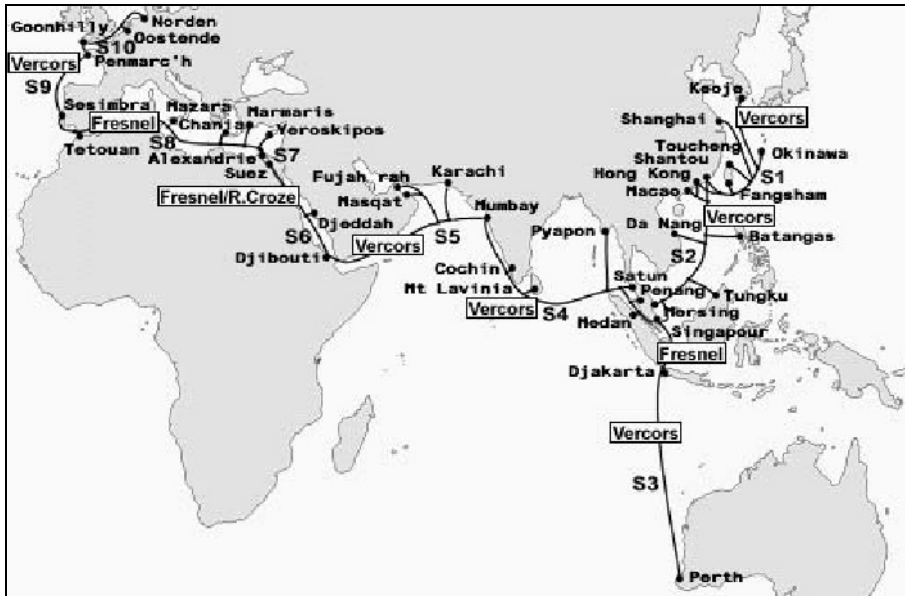


Figure 9.13. *SEA-ME-WE 3 link*

9.4. Fiber-optic analog transmissions

Although digital links constitute the major part of fiber-optic transmission systems, analog links in the field of measure or image transmissions also exist. They can be economically interesting for local use.

9.4.1. Analog baseband transmission

9.4.1.1. Principle

It is very simple: the analog signal directly modulates light intensity from the transmitter (see Figure 6.8). It uses linearity of the power-current characteristic of a LED (Figure 9.14). If the signal is alternative, an i_m bias current must be superimposed. In this case, as in radio amplitude modulation, the modulation index is defined as: $m = \Delta i / i_m$, where Δi is the signal amplitude. Because of the linearity of the transmission chain (fiber–receiver), this relation is the same at transmission and at reception.

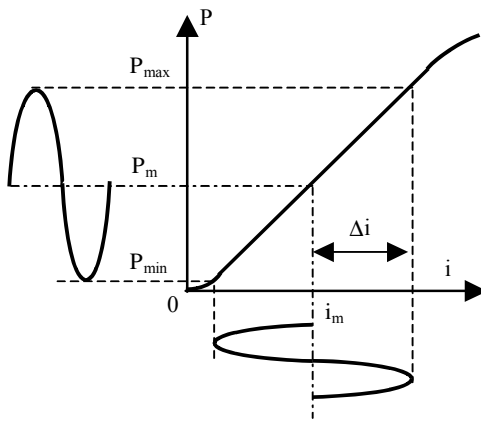


Figure 9.14. *Fiber-optic baseband transmission*

The modulation index is in the range of 90% as it is recommended to avoid characteristic extremities which are less linear. Linearity of the modulated signal is not perfect however (distortion of a few %). The use of a laser diode can cause linearity and noise problems, since the signal-to-noise ratio at laser output is not always sufficient for high quality analog applications. The main application for this technique is video monitoring in industrial sites or communication ways.

9.4.1.2. *Link calculation*

For a sinusoidal signal $i_m (1 + m \cdot \cos \omega t)$, the signal-to-noise ratio equals:

$$RSB_{\sin} = \frac{\Delta i^2}{2 \langle i_B^2 \rangle} = \frac{m^2}{2} \cdot \frac{i_m^2}{\langle i_B^2 \rangle}$$

where i_m is the average photocurrent value at reception, and $\langle i_B^2 \rangle$ is the total input noise measured in the signal bandwidth ΔF . Aside from receiving noise sources studied previously, this term can contain, in a significant part, source noise transmitted by the optical line. In fact, analog links require much higher signal-to-noise ratios than with digital, then lower signal attenuations, and therefore source noise.

As we have seen in Chapter 6, this noise leads to an input noise current of:

$$\langle i_L^2 \rangle = RIN \cdot \Delta F \cdot \langle i(t)^2 \rangle = RIN \cdot \Delta F \cdot i_m^2 (1 + m^2/2) \text{ for a sinusoidal signal.}$$

In the case where this noise is predominant, we then have:

$$RSB_{\sin} = \frac{m^2}{m^2 + 2} \frac{1}{RIN \cdot \Delta F} \text{ which is its maximum possible value.}$$

This case is less exceptional with analog links, which requires higher signal-to-noise ratios than with digital. Otherwise, the loss budget can be calculated with formulae from section 9.2 with:

$$Q = \frac{\sqrt{2}}{m} \sqrt{RSB_{\sin}}.$$

With video signals, since the signal-to-noise ratio is defined from the peak-to-peak signal:

$$RSB_{\text{video}} = 4m^2 \frac{i_m^2}{\langle i_B^2 \rangle} \text{ and: } Q = \frac{1}{2m} \sqrt{RSB_{\text{video}}}$$

must be used in formulae from section 9.2.

Since these formulae calculate average power P_{mr} at receiver input, we can then establish the loss budget and calculate range. Levels between - 20 and - 30 dBm are required for a standard high quality analog video signal of 6 MHz bandwidth ($RSB_{\text{video}} = 50$ to 60 dB). The designer should not forget to verify if a sufficient

bandwidth is available in the optical fiber (these systems are most often in multimode fiber).

9.4.2. *Transmission by frequency modulation of a sub-carrier*

The signal modulates in frequency, with a frequency deviation Δf , an electric sub-carrier, modulating light intensity itself (Figure 9.15). This much more efficient process has several advantages:

- improvement of signal-to-noise ratio by a theoretical factor of $1.5(\Delta f/\Delta F)^2$ compared to a 100% intensity modulation;
- insensitivity to non-linearities, leading to the possibility of using laser diodes and single-mode fibers and logical low cost links in squared frequency modulation;
- improved transmission of continuous components, especially using counting demodulation, that is important in video and remote measurements.

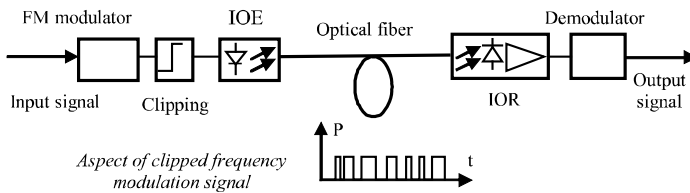


Figure 9.15. *Transmission by frequency modulation of a sub-carrier*

The modulated signal occupies a band $2(\Delta f + \Delta F)$ centered on the subcarrier. It is possible to frequency multiplex several signals (analog or data) in the same fiber by modulating them on different subcarriers. In this case, the transmitter must be perfectly linear to avoid intermodulation effects between the different channels. This solution was used for remote TV antenna transfer to cover shadow areas in distribution, in order to transmit several high quality signals sometimes over long distances, but now digital has taken over for television.

9.4.3. *Transmission of measurement signals*

Transmission of an electric signal over an optical fiber from a classical sensor has a quite specific implementation compared to the use of optical fibers in telecommunications (Figure 9.16) because the sensor and transmission optoelectronic interface can be in a “hostile” environment (pressure, temperature, high voltage, vibrations, radiation, etc.).

Due to this, it can be impossible to locally or remotely feed this device, since the cable must be isolated; it will need to have autonomous power feeding. Using optical power feeding consisting of transmitting the energy in light form and converting it into electric current by a photovoltaic receiver may be interesting: with a high power source and high efficiency photodiode, a few hundred electric mW can be obtained, enough to feed low consumption circuits.

Optical fibers improve transmission range and quality, especially in a disturbed environment. They do not occur in the measure itself, contrary to optical fiber sensors where the fiber is the sensitive element as well.

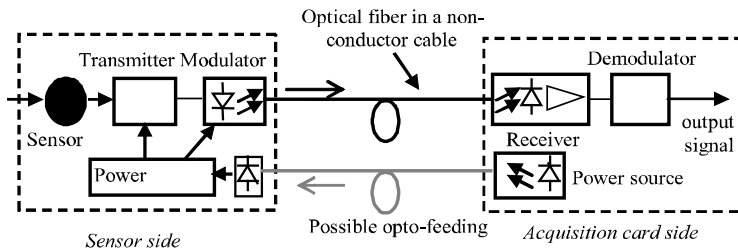


Figure 9.16. *Transmission of a measure over optical fiber*

9.5 Microwave over fiber optics links

9.5.1. Principle and applications

Even though most of the time information is digital, this technique consisting of transporting a microwave carrier (of frequency F_{mw} of a few GHz to several dozens of GHz) over an optical fiber, is similar to analog transmission concerning interfaces. In fact, the laser source must be able to be modulated with high linearity by a sinusoidal signal (or several multiplexed signals). In addition, if modulation with a large number of sub-carrier states (QAM, OFDM, etc.) is used, a strong signal-to-noise ratio at receiver is necessary, and the source noise (RIN, see section 9.4.2) may be a problem.

This technique already has ancient applications in antenna transfers, particularly active antennae where they can feed the many transmitters of the antenna array by controlling delay in each optical line and enabling electronic scanning. It now has new perspectives in subscriber or mobile station radio access from an optical infrastructure (Figure 9.17), notably for the development of wireless local area networks (of the WiFi hotspot type).

Fiberoptic transport of RF modulated signals (from 100 to 1,000 MHz), also called radio over fiber, can be assimilated to these techniques. It is used for wireless or cable television broadcasting, whether analog or digital; it is the main solution used in American coax networks for the migration of cable toward fiber optics (hybrid fiber-coax networks, see Chapter 10).

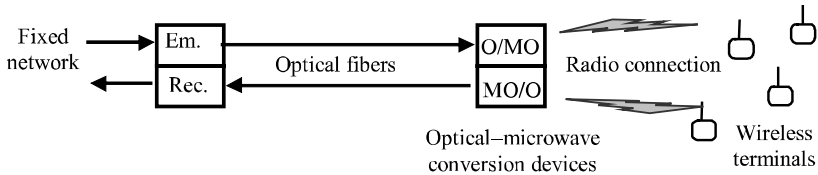


Figure 9.17. *Architecture of an optical – microwave link*

9.5.2. Different processes

In most experiments carried out, the fiber brings signals already modulated in microwave frequencies in order to make their conversion easier and control the transmission frequency. The main problems involve optoelectronic interfaces which must be able to operate at very high frequencies. External modulators can be used at 20, or even 30 GHz, beyond which very different processes must be used: harmonic generation, beat between two lasers or two lines of a laser spaced from F_{mw} ... Prototypes were developed but problems remain significant.

In addition, even though the chromatic dispersion effect of the fiber can be limited by the use of a single-side band (SSB, see section 9.5.3) modulation, polarization mode dispersion remains a critical problem.

Due to this, other processes are explored, such as transfer of a modulated signal in intermediate frequency over an optical fiber, or the direct conversion from baseband optical signal to microwave carrier (we can for example design a photo-oscillator whose frequency or phase is controlled by light intensity). Table 9.3 briefly compares these different techniques.

Process	Microwave carrier modulation	Intermediate frequency modulation	Baseband
Advantages	Centralized control of frequencies and modulations	Same with less constraints at interface level	Simplicity and compatibility with existing fiber networks
Disadvantages	Requires very high frequency interfaces; fiber dispersion (PMD)	Requires frequency transposition (ex. by heterodyning)	No centralized control resulting in operator reluctance

Table 9.3. *Microwave – optical transmission processes*

9.5.3. *Single-side band transmission*

SSB modulation is more simple and more efficient in the case of microwave optical fiber links than for digital systems. The reason is that after optical carrier modulation by the microwave signal at a frequency of F_{mw} , both side bands are spaced from $2F_{mw}$ making them quite easy to filter (wavelength gap is approximately 0.6 nm for $F_{mw} = 40$ GHz). They can also be separated in an interferometric device. Spectral widening of source $\Delta\lambda$, therefore pulse widening by chromatic dispersion, will not be proportional to F_{mw} , but will be to the clock frequency of the data modulating signal which is at a much lower rhythm.

On the other hand, for demodulation, this technique requires the transmission of the unmodulated carrier in the same fiber. The carrier is mixed in the receiving photodiode with the transmitted side band, thus recreating by beat the frequency F_{mw} . This process is called self-heterodyne (Figure 9.18). It can be implemented in different ways: for example, the unmodulated carrier and the carrier modulated by data (and not by microwave signal) can be two lines of a laser separated from F_{mw} , or lines from two slave lasers locked with a single master laser.

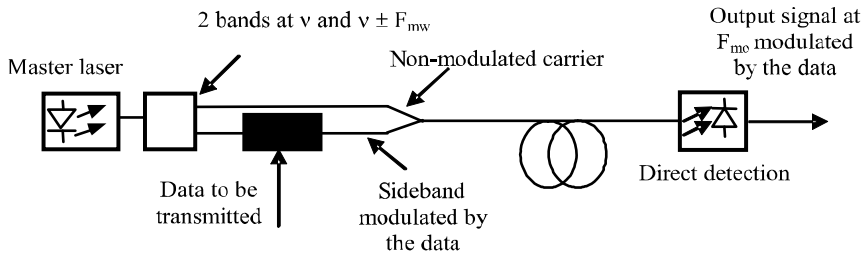


Figure 9.18. *Self-heterodyne microwave-optical line*

This page intentionally left blank

Chapter 10

Fiber-Optic Networks

10.1. Computer networks

10.1.1. *Introduction*

Even for short distance, the use of fiber optics in local area networks (LAN) has early on dominated the market, mainly because of their well known advantages in electric isolation and insensitivity to electromagnetic disruptions, often significant in local network environments.

Optical fibers were used very early on for point-to-point links compatible with classical standards (RS 232, IEEE 488, etc.), in token ring type networks or as network gateways. Low fiber attenuation enables us to extend these links: for example local area network sections can be extended over 2,000 m without repeaters. Bitrates have continuously increased, going from a few hundred kbit/s to several hundred Mbit/s, now reaching 4 to 10 Gbit/s with Fiber Channel or the latest Ethernet versions.

Optical fibers are also deployed in large scale backbones, constituting networks whose nodes (routers or switches) are still electrical. However, switching and optical routing have been the subject of several development projects in laboratories and should in the future revolutionize network operation.

On the other hand, field buses are used in the industry to connect machines, sensors, robots, embedded equipment, etc. Distances are short and throughputs are generally lower, but these networks must function with perfect reliability in disrupted environments. They are not as standardized as LANs and there are many

“proprietary” networks such as FIP (Field Information Protocol), based on a multi-star optical infrastructure. CAN and Flexray buses used in the automotive industry can also use fiber optics as support.

10.1.2. *Passive optical networks*

With the different passive optical components (couplers, splitters, wavelength division multiplexers, etc.) optical fibers have been able to constitute multi-terminal networks for a long time. They are mostly passive optical networks (PON) where multiplexing or access control can be operated; they are suitable for access networks (fiber sharing between several subscribers, see section 10.2) as well as for small local area networks.

Figure 10.1 shows examples of:

- broadcast networks, where a star coupler simultaneously broadcasts the same signal to many receivers; these can be a few dozen to several thousands with the use of an optical amplifier between source and coupler. Subscribers can possibly have a return channel by multiplexing or access control on the common support;
- point to multipoint networks where several stations share the same link with Y or star couplers, as addressing is contained in frames; slave stations communicate with the main station, but not between each other. In the graph, the return path uses the same optical fiber at another wavelength, but it is not necessarily the most economical for short distance; this solution is experiencing renewed interest in access networks with the FTTH/PON architecture;
- random access bus (Ethernet) or other standards with the same physical architecture (each station communicates directly with all others) but with different access protocols. Passive star topology developed around a star coupler with n branches is the most efficient as each station includes a transmitter and a receiver. Multiple star topologies can be used to increase its capacity.

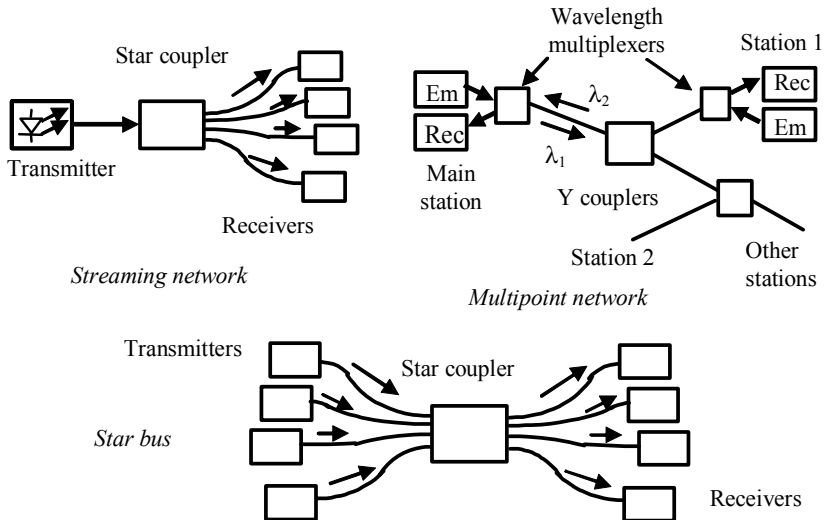


Figure 10.1. *Passive optical networks*

10.1.3. Design of a passive network

The loss budget is calculated as in section 9.2.6 taking into account insertion attenuations from couplers and/or multiplexers, and additional connections required by the passive network architecture. These terms are often larger than the fiber section attenuation, because distances are generally short. Due to this, it is often economically interesting to use the first transmission window, with LEDs and multimode fibers; as long as bitrates are low (10 to 50 Mbit/s) and as chromatic dispersion does not limit us.

The calculation must be performed on the worst case because attenuations are not necessarily the same for all transmitter-receiver pairs. The loss budget is advantageous for star structures, because the insertion loss of the coupler is in $\log n$, where n is the number of terminals, and differences between received levels at the different terminals are lower.

Such a multimode fiber network can be optimized by determining the maximum transmitter-receiver distance (equal to twice L , maximum station-star distance) authorized by the dispersion limit (by noting if a penalty is accepted or not), by deducing the maximum fiber attenuation and by rewriting the loss budget as follows (Table 10.1).

Average emitted power, coupled in the fiber	$10 \log P_{me}$ (dBm)
- attenuation of connections	- A_R (dB)
- attenuation of the fiber (with lineic attenuation α)	- $A_f = -2\alpha L$ (dB)
- margin	- m (typ. 3 dB)
- average received power	- $10 \log P_{mr}$ (dBm)
= available attenuation for the coupler	= a (dB)

Table 10.1. *Loss budget for a star network*

The unknown then becomes n , the maximum number of coupler branches, thus of terminals. If the theoretically possible value is higher than possible with the technology (star couplers are available up to 32 channels) then several must be cascaded, causing additional excess losses.

10.1.4. Ethernet local area networks

10.1.4.1. Introduction to Ethernet

Ethernet is by far the most widely used (and less costly) local area network. It uses random access mode with collision detection or CSMA/CD (Channel Sense Multiple Access/Collision Detection). Each station can transmit as soon as it has determined that the channel is idle after listening. There is collision probability when two stations start a transmission at the same time. This method is efficient for high bursty bitrates gone from 10 to 100 Mbit/s then at 1 and 10 Gbit/s. However, although efficiency is good for intermittent traffic, in the case of high traffic, collision risks increase very rapidly.

Historically, these networks are adapted to back office or computer applications with no real time requirements. Gigabit Ethernet, for high throughput interconnection of nodes with a routed protocol, is currently being deployed in backbones, and 10 Gbit/s, standardized in 2004 is growing in metropolitan area networks (MAN). A new IEEE workgroup is dedicated to 100 Gbit/s!

The Ethernet protocol (IEEE 802.3) accepts different physical supports. The oldest version (still used in industrial companies) operates over coax cable (thick or thin), a support on which stations are connected by shunting in "T".

For economical reasons, unshielded twisted pair (UTP) is the most widely used, at 10 Mbit/s (10 base T) and at shorter distance, at 100 Mbit/s (100 base T).

10.1.4.2. *Fiber optic Ethernet*

Optical fibers are increasingly being used to increase distances and can be used to interconnect stations using passive optical stars, when electric or electromagnetic security warrants it. For example, with multimode 62.5/125 fibers, 2,000 m are reached at 10 Mbit/s and 400 m at 100 Mbit/s, Gigabit Ethernet can reach 5 km over single-mode fibers with laser diodes (LD).

A major issue now is the reuse of multimode fibers which are not very expensive in connectivity, for Gigabit Ethernet: it is possible to reach several hundred meters and exceed a kilometer in certain conditions with fast and inexpensive VCSEL diodes at 0.85 μm . The attenuation is not a limit in local area networks, chromatic dispersion is insignificant because of the very low spectral width of the source, intermodal dispersion is the limiting factor. Modal filtering devices may improve bandwidth.

New 50/125 multimode fibers reaching 2 GHz.km and called OM3 have appeared on the market. They are much more expensive than single-mode fibers but provide global economy because of the low cost of connectors and interfaces. It is even possible to transmit 10 Gbit/s up to 300 m over a single wavelength and 1 km by distributing data over four wavelengths.

Table 10.2 indicates the main Ethernet versions; ranges are typical values and we can often find better.

10.1.4.3. *Ethernet architectures*

Risk of collision increases with frame propagation time, thus with distance, and with the number of users. Ethernet network architecture has evolved toward multi-level star topologies with the use of hubs or switches.

The economic optimum is often to link stations to 10/100 Mbit/s hubs with twisted pairs and to interconnect 100 Mbit/s hubs with twisted pairs (for short distance) or 1 Gbit/s hubs with optical fibers with the help of an active star. Thus the Ethernet network is extended, since the active star is in charge of detecting collision and possibly for routing data between the different network sections (Figure 10.2). This architecture must not be confused with the backbone, interconnecting local area networks with bridges or routers.

Name	Bitrate	Line code	Physical support	Topology	Range
10 base 2/5	10 Mbit/s	biphase (Manchester)	thin/thick coax	line bus	200/500 m
10 base T	10 Mbit/s		unshielded twisted pair	stations	100 m
10 base FL	10 Mbit/s		multimode 850 nm optical fiber (LED)	toward hubs	2,000 m
10 base FT	10 Mbit/s		same	passive star	500 m
100 base T	100 Mbit/s	bipolar	unshielded twisted pair	stations	50 m
100 base FX (Fast Ethernet)	100 Mbit/s	4B5B	multimode 1,310 nm optical fiber (LED)	toward hubs	400 m <i>2 km over 50/125</i>
1000 base SX	1 Gbit/s	8B10B	multimode 850 nm optical fiber (VCSEL)	active	250 m <i>550 m over 50/125</i>
1000 base LX	1 Gbit/s		multimode 1,310 nm optical fiber (LD)	star	5 km
10G base SX	10 Gbit/s		multimode OM 3 optical fiber at 850 nm (VCSEL)		300 m
10G base LX4	10 Gbit/s		4 wavelength multimode fiber, 1,310 nm window (LD)		300 m; <i>1 km over OM3 fiber</i>
10G base LX	10 Gbit/s		single-mode 1,310 nm optical fiber (LD)		10 km

Table 10.2. *Main Ethernet versions*

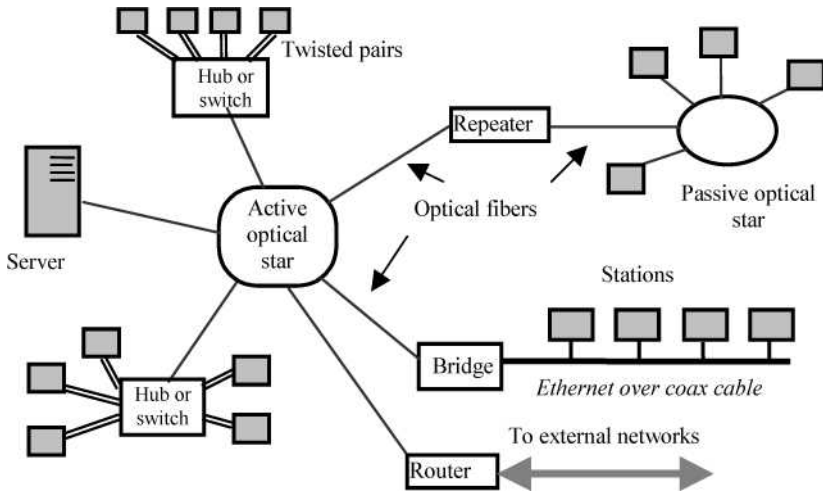


Figure 10.2. Possible uses of fiber optics in Ethernet networks

10.1.5. FDDI network

In order to increase bitrates and ranges, and to fulfill security requirements, a network was developed specifically over optical fibers in the 1990s: this is the FDDI (Fiber Distributed Data Interface) network, a ring network (with token access control, successor to the Token Ring), working at 100 Mbit/s with 4B5B code. This network mainly uses multimode 62.5/125 fibers (with LED at 1.3 μm) for distances under 2 km and connects up to 500 workstations. Twisted pairs can even be used for very short distance links. Single-mode fibers (with laser diodes at 1.3 μm) may cover long distances, but this version is not used much.

The ring is doubled and each “class A” station has double access ensuring securement (Figure 10.3): the traffic goes through the back-up ring in case of incident in one section of the main ring, which is then isolated. Smaller “class B” stations are connected through hubs and can be isolated from the network.

Standardized by ANSI, this network is well adapted for servers and workstations which must communicate in real time at high throughput with high security (industrial control, nuclear or medical facility monitoring, navigation systems). It can also be used as a local network backbone through bridges and routers. It is not competitive with Ethernet in the standard local area network market, but has retained a specific market with its security advantages. However, new industrial Ethernet versions which do take security requirements into consideration are competing with FDDI in this field.

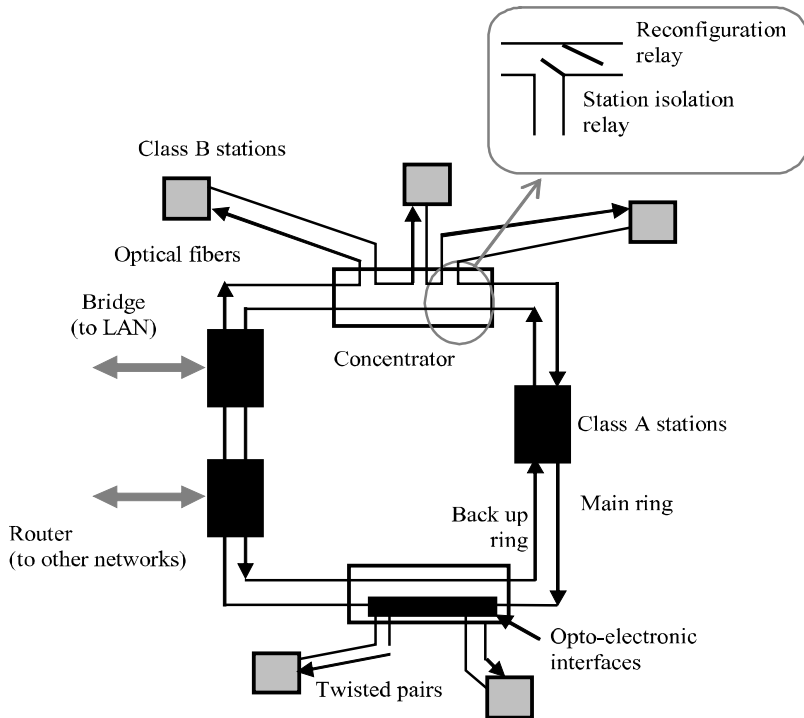


Figure 10.3. *FDDI network topology*

10.1.6. Fiber Channel

Also standardized by ANSI, the goal of this standard is to offer high bitrate interconnections over optical fibers which are compatible with all local area network protocols: Ethernet, SCSI (serial) or HIPPI (parallel) interfaces or wide area networks: TCP/IP, ATM, etc. It provides them with a lower layers service. This protocol is organized in layers:

- the FC0 layer corresponds to transmission/reception in the support (optical fiber, as well as twisted or coaxial pair for short distance) and to bit regeneration; each Fiber Channel (FC) station contains a transmitter/receiver with SC optical connector;
- the FC1 layer constitutes 2,168 byte frames coded 8B10B, of which 2,048 are error control and flow control words. Stuffing bytes allow us to tolerate some plesiochronism. Nominal useful symbol rate is 100 Mbytes/s or 1062.5 Mbauds (which can use the same interfaces as Gigabit Ethernet), but

multiple and sub-multiple bitrates are possible and widely used as illustrated in Table 10.3;

– the FC2 layer enabling different architectures: point-to-point, ring or switched star around a switching fabric operating in circuit, packet or datagram mode (Figure 10.4).

The main FC market is short distance storage area networks (SAN), requiring increasingly high throughputs, operating at up to 4 Gbit/s (the following 8 or 10 Gbit/s version, depending on coding used is announced). It is increasingly used in network securement over distances reaching 10 to 30 km.

	Transmitter	$\lambda(\text{nm})$	Maximum distance					
Name			1/8	1/4	1/2	1x	2x	4x
Useful throughput (Mbytes/s)			12.5	25	50	100	200	400
Twisted pair			100 m	50 m				
Coax			100 m	75 m	50 m	25 m		
Multi. fiber GI 62.5/125	LED	1,300	1.5 km	1.5 km				
Multi. fiber GI 50/125	VCSEL	850		2 km	1 km	500 m	300 m	150 m
Single-mode fiber	LD	1,300		10 km	10 km	10 km	4 to 10 km	2 to 10 km

Table 10.3. *Different FC versions*

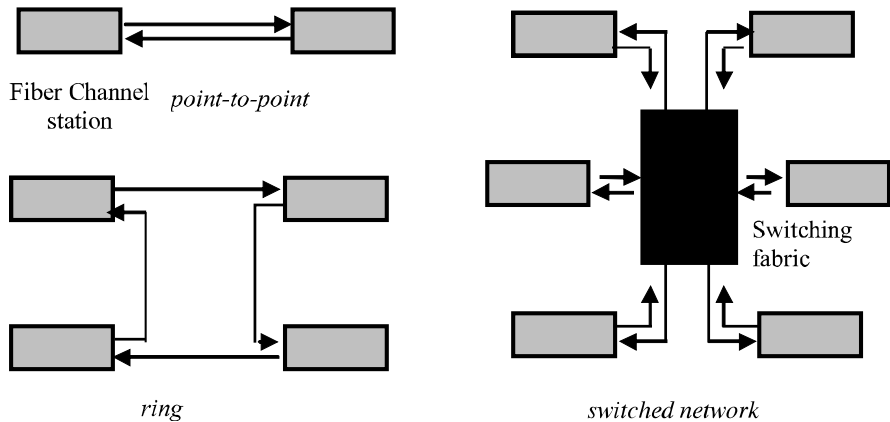


Figure 10.4. *FC architectures*

10.2. Access networks

10.2.1. Overview

When fiber optics first appeared, one of the main objectives was the deployment of access networks offering users phone, several television channels, sound channels and interactive services, even videophone, over fiber optics. What used to be called video communications networks, because of the importance of images in traffic, were being experimented in the 1980s (first French experiment in Biarritz in 1984) and deployed in a few operational networks. These first generation networks (1G) were based on a star structure enabled by the very small optical fiber size; each subscriber is connected with his (her) own fiber to the distribution center, but a second user can subsequently share this fiber with the help of wavelength division multiplexing.

The development of this type of “optical distribution” network remained marginal for economic reasons however (although fiber optics have quickly been used throughout the transport part of CATV distribution networks). Effort was concentrated on the development of “low cost” optoelectronic technologies competitive for mass-market distribution, but was blocked by the unexpected success of ADSL, providing bitrates exceeding 10 Mbit/s over already installed phone lines.

Only a few years ago, when ADSL had reached its limits, did high bitrate (10 to 100 Mbit/s per subscriber) optical access deployment restart mainly in Asia (Japan, Korea, China) and on a more modest scale in Europe (Sweden, Italy); the USA

prefers to use “hybrid fiber-coax” to take advantage of the massive availability of coax cable in television distribution.

France-Télécom and its competitors as well as several local communities (30,000 in Pau) have relaunched projects focusing on development of services (which were insufficient in 1G networks) and not only infrastructures.

For 2008, 20 million FTTH subscribers throughout the world are expected, among which 16 million are in Asia alone, and the market in Europe is also expected to take off.

10.2.2. *Different FTTx architectures*

Because of economic as well as historic (type of access network already installed) considerations, the choice is open among several architectures (Figure 10.5):

- FTTH (fiber to the home) where the fiber goes all the way to the subscriber’s home, with optical signal continuity, but involving possible cost and maintenance problems;

- FTTx (fiber to the...) where, to avoid these problems, the optical fiber stops at a point accessible to the operator, where an ONU (optical network unit) is implemented, less than 1 or 2 km away from the subscriber. It must be relayed for branching by a coax cable, a VDSL type link over a phone line, by a very short distance and high frequency (WiFi type) radio link, or even by an electric power line. Even though this terminology is not very standardized and there are redundancies, we speak of:

- FTTB (building) the fiber stops at the foot of the building,
- FTTC (curb) the fiber stops at the “curb” (for several homes),
- FTTN (node) the fiber stops at the dispatcher (extended by a VDSL connection for example),
- FTTP (premises) the fiber stops at the operator’s technical location.

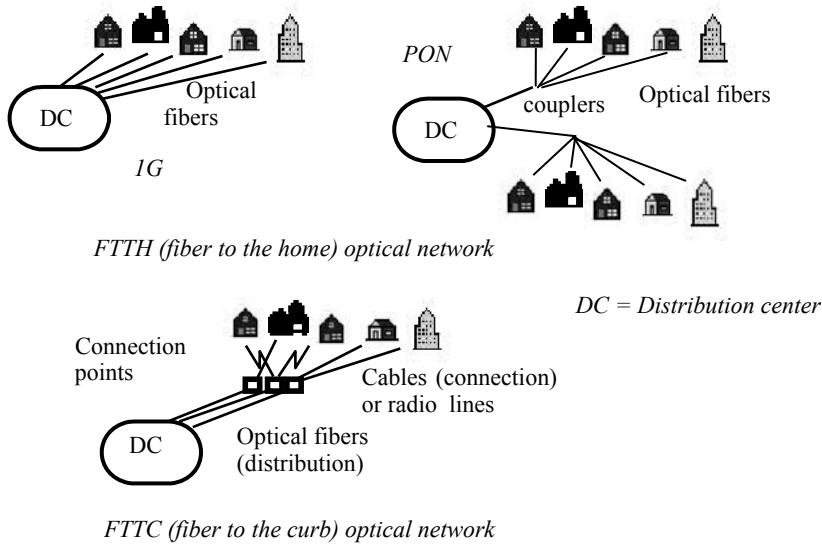


Figure 10.5. Different fiber-optic access architectures

With a rather similar principle, hybrid fiber-coax networks (HFC) use already installed coax networks in which the signal is provided by an optical fiber, interfaced with an ONU (optical network unit). They are mainly developed in countries with wide cable television network (CATV) installations such as the USA (Figure 10.6). One of their characteristics is to transmit RF signals from the cable with their modulation over a specific wavelength over the optical fiber in order to ensure interoperability.

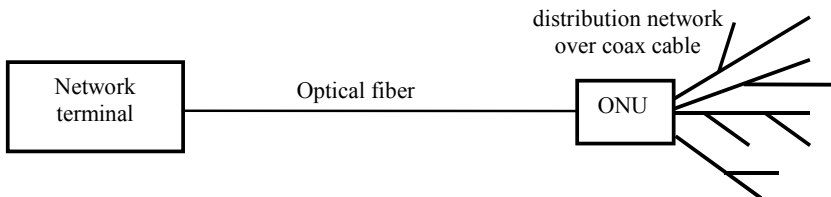


Figure 10.6. Hybrid fiber-coax (HFC) access

10.2.3. *Passive optical networks (PON)*

Whereas 1G networks were point-to-point (*PtoP*) with one multimode fiber by subscriber in a star architecture around the distribution center (DC), and despite several announcements of PtoP FTTH network deployments (Paris, Amsterdam, etc.), the architecture favored by operators is passive optical network (PON). With the help of passive couplers or splitters forming a tree topology, possibly with several levels (Figure 10.7), 32 subscribers (up to 64 in the 2nd phase) share the same standard single-mode fiber as well as a global bitrate of several Gbit/s. It provides several advantages:

- large reduction of the number of fibers from the network core, thus of the number of connections and cable size, enabling new cabling technologies (micro-cladding, micro-ribbons, etc.) and installation (blowing fiber into ducts), increasing density and decreasing installation costs;
- sharing of active equipment on the network side (OLT: Optical Line Termination) between a large number of subscribers;
- dynamic bitrate allocation in each direction between users of the same fiber with the help of ATM or Ethernet type protocols; statistically, 1 or 2.5 Gbit/s global bitrate can be shared between 32 subscribers at 100 Mbit/s, and the use of resources is optimized even though traffic can be very different between two users, peak throughputs much higher than the average throughput are even possible. The downlink frame contains information for the uplink bitrate allocation;
- reliability and upgradeability of passive components (bitrates can be increased simply by modifying terminals);
- possible cohabitation of several operators on the same passive infrastructure; a subject of some importance for regulation authorities (ARCEP in France).

Compared to point-to-point, PON also has constraints:

- subscriber terminals (called ONU if they are extended by a secondary link, or ONT (Optical Network Terminal), if they are located at the client site) operate at instant shared bitrate (1 to 2.5 Gbit/s) instead of at average subscriber bitrate; relatively inexpensive technologies must nevertheless be used, such as Fabry-Pérot laser diodes at 1.3 μm in uplink;
- TDMA (Time Division Multiple Access) access control in uplink is tricky to manage because of differences in levels and propagation delays (in downlink, ATM or Ethernet-type addressing is used without these problems); subscriber side transmitters must be synchronized with the help of the downlink frame;
- maintaining such a network is more complicated than with point-to-point. Notably, classical reflectometry does not directly apply (branch responses

superimpose and do not allow us to locate failures from the OLT) and must be adapted. This can be performed in a specific channel at 1,625 nm (monitoring). Reflections on connectors must also be very low (return loss lower than -50 dB), otherwise all subscribers in a single fiber are disturbed.

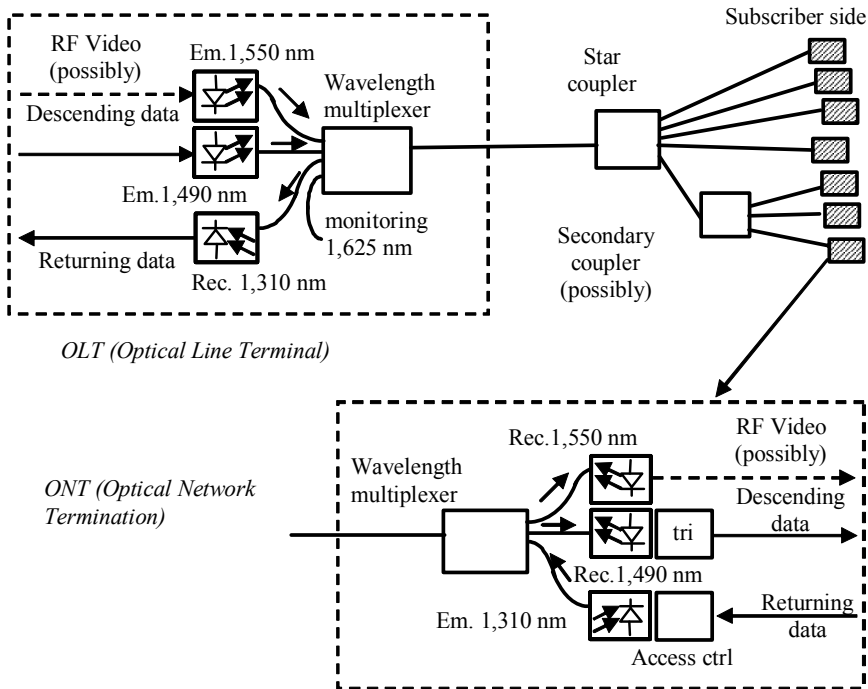


Figure 10.7. *PON architecture*

10.2.4. PON operation

Throughputs and protocols come from existing (local or long distance) networks, and three types of protocols are used in passive optical networks:

- BPON (Broadband PON) transporting ATM cells at 622 or 1,244 Mbit/s with time slot reservation in uplink (at 155 Mbit/s); derived from APON (*ATM over PON*), this solution is mostly deployed in the USA and its use is decreasing;
- EPON (Ethernet PON) standardized by IEEE (EFM (Ethernet in the First Mile) workgroup) uses dynamically shared frames, access protocols and 1 Gbit/s Ethernet interfaces; it is the most inexpensive solution, mostly deployed in Asia;

- GPON (Gigabit-capable PON) uses the SONET/SDH physical layer (section 10.3), currently with typical bitrates of 2.5 Gbit/s downlink and 1.25 Gbit/s uplink; this solution, standardized by ITU (G 984), seems to be prevalent in new deployments. The FSAN (full service access network) concept is also standardized by the ITU (G 983) and is compatible with all protocols (ATM, Ethernet, IP, etc.) with variable flows, and with all services: voice (traditional or over IP), data, images, video on demand (VoD) in downloading or streaming mode with guaranteed bandwidth, peer to peer interactive services, etc.

In most present deployments, as seen in Figure 10.7, wavelength division multiplexing is carried out between a downlink 1,490 nm channel, transmitting a 2.5 Gbit/s (STM-16) bitrate shared between subscribers by frame addressing (with specific encryption for each subscriber), and an uplink 1,310 nm channel, shared by time division multiple access (TDMA), allocation of time slots is controlled dynamically by the central station to avoid collisions. A 2nd descending channel at 1,550 nm can be used for video broadcasting over a RF sub-carrier (solution mostly used in the USA, as in HFC). For the subscriber, signals are distributed through Ethernet RJ 45 jacks or by WiFi to the different equipment, as is currently done with ADSL boxes; the ONT shares the received packets according to their overhead to only deliver those packets addressed to the subscriber.

The typical range is 20 km over standard single-mode fibers (G 652) and global attenuation, including couplers, is 20 to 30 dB. Current research projects are trying to bring these bitrates to 10 Gbit/s over the same fiber infrastructure in order to increase throughput per subscriber and/or the number of subscribers per coupler (which could reach 64, or even 128).

Later, wavelength division multiplexing generalization between services and/or users (DWDM/PON) will allow us to increase bitrates even more without modifying the infrastructure.

10.3. Wide area networks

10.3.1. SDH/SONET hierarchy systems

High throughput SDH (Synchronous Digital Hierarchy) was internationally standardized in the 1990s. It unifies the international telecommunications network while being compatible with pre-existing systems: older digital European, American and Japanese plesiochronous transmission hierarchies, as well as high bitrate data networks such as Ethernet, FDDI, etc. It has in fact been developed to become the transmission infrastructure of ATM networks, but can also transport IP frames.

The first SDH level is STM-1 at 155.52 Mbit/s (STM = Synchronous Transport Module). Levels of the hierarchy, called STM- n , are obtained by synchronous multiplexing byte by byte of n frames, with frame alignment (i.e. the n affluent frames start at the same time, which is not the case in plesiochronous multiplexing). The high bitrates obtained involve the choice of optical fiber as support; the STM-1 level however can also be transported by microwave link or satellite, or twisted pair over a very short distance (internally in operation centers).

Synchronous fiber optics transmission networks have been massively deployed these last years with link bitrates of:

- STM-1 at 155 Mbit/s (local access);
- STM-4 at 622 Mbit/s (regional networks);
- STM-16 at 2.5 Gbit/s (national links);
- STM-64 at 10 Gbit/s (international links);

and step STM-256 (40 Gbit/s) was recently industrialized but is technically difficult, with components (electronic and optoelectronic) as well as fibers (limitations caused by chromatic and polarization mode dispersion, not well known and highly dependent on the fiber PMD in the cable).

Very long links with amplifiers use additional online forward error control (FEC) which brings a symbol rate of STM-64 to 10.664 Gbauds. Note at this step the convergence with 10 Gbit/s Ethernet which makes optoelectronic interfaces compatible with both systems available on the market, but the protocols are not the same and neither are the frames, nor exactly the same bitrates because in SDH 10 Gbit/s is a rounded value.

In North America, transmission systems are defined by the SONET (Synchronous Optical NETWORK) standard, normalized by ANSI before SDH standardization by the ITU, explaining the number divergence: the first SONET level, at 52 Mbit/s (only used in America), does not correspond to the first SDH level (Table 10.4); OC-3 n then corresponds to STM- n .

SDH name	SONET name	Number of channels	Bitrate (Mbit/s)	Optical fiber	Wavelength (nm)	Max distances (km)
	OC-1	672	51.84	multimode	1310	2
STM-1	OC-3	2,016	155.52	multi/single-mode	1,310/1,550	2/15/60
STM-4	OC-12	8,064	622.08	standard single-mode	1,310/1,550	15/60
STM-16	OC-48	33,256	2,488.32	standard single-mode/ shifted dispersion	1,550	60/120
STM-64	OC-192	129,024	9,953.28	shifted dispersion single-mode	1,550	60
STM-256	OC-768	516,096	39,813.12	single-mode shifted dispersion and very low PMD	1,550	?

Table 10.4. *Major SDH/SONET systems*

In order to increase bitrates even more, wavelength division multiplexing (WDM) allows bitrates of $n \times 2.5$ Gbit/s (which is the most adapted to chromatic and polarization mode dispersion performance of previously installed G 652 optical fibers) and $n \times 10$ Gbit/s for more recent G 655 type fibers. Bitrates of approximately 640 Gbit/s can operate on the major links, and the theoretical limit is far from being reached.

10.3.2. Constitution of synchronous digital hierarchy frames

In STM-1, the basic frame of 125 μ s length (the voice sampling period in digital telephony), contains a total of 2,430 bytes organized in a table with 9 rows and 270 columns (Figure 10.8). The first 9 header columns constitute a section overhead (SOH) containing synchronization, auxiliary data channels, parity check bytes for

error detection, as well as transmission quality supervisory and network security management information. Apart from a few overhead functions, SONET OC-3 frames are identical to STM-1 frames.

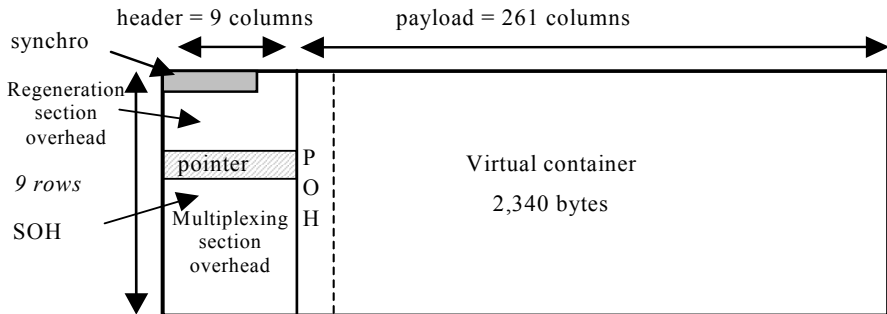


Figure 10.8. *SDH frame*

This overhead is structured into two levels: multiplexing section (between 2 multiplexers) and regeneration section (between 2 regenerators). These devices can also communicate with the control network by adding or dropping information at reserved locations in the frame (even though in paradox optical amplifier repeaters cannot use this possibility, since they do not process the digital signal). Data is transmitted in NRZ format after scrambling (scrambled NRZ), the first 6 bytes are the only ones not scrambled because they are frame synchronizing bytes.

The other bytes constitute the payload, in the form of a “virtual container” (VC) with actual bitrate of 149.76 kbit/s, or 260 columns of 9 bytes in addition to the 1st column of each VC, called POH (Path OverHead), which contains information on the container and which is transmitted end to end with its contents, contrary to SOH. The beginning position of a virtual container, located by its POH, can vary in the STM-1 frame in case the clocks are not perfectly synchronized, which is called plesiochronism.

The virtual container is a very flexible concept, it can be made up of primary frames (24 or 30 phone channels at 64 kbit/s), frames from older plesiochronous hierarchies (European and American), 44 ATM cells, local area network frames (Ethernet, FDDI) or IP frames, contained in different levels of virtual containers. A specific POH byte indicates the type of contents.

This data can be synchronous or asynchronous since the actual position in the container is indicated by a pointer in the 4th overhead row. This position can vary because of a justification mechanism which increments the pointer (positive justification if throughput is too low: the VC is delayed by one byte) or decrements it (negative justification if throughput is too high: the VC is advanced of one byte). This allows us to know the exact position of each channel at anytime and thus to directly add or drop any channel in the SDH frame, including a basic 64 kbit/s channel instead of demultiplexing all levels one by one as in plesiochronous multiplexing.

10.3.3. SDH rings

The SDH is not only a point-to-point transmission protocol, it involves multipoint ring architectures and enables securement (Figure 10.9).

The simplest scheme is a two fiber ring; the main fiber transmits unidirectional traffic whereas the second one acts as back up fiber. When used (in case of interface failure or fiber cut-off), the securement protocol transmits the signal in the reverse direction. In the second scheme, a fiber pair ensures normal bidirectional traffic; there is here a back up fiber in each direction, transmitting in case of securement by the same arc and in the same direction. This concept extends to $2(n + 1)$ fibers (seurement 1: n) where one back up pair secures n traffic pairs. If A – D (major path) is completely cut off, A – D traffic restoration can be performed by BC (minor path).

In the ring, the traffic can use several possible paths: for example A – B, A – C by B, D – B by A, which will then be multiplexed (electrically or by wavelength) in the same arc (AB here). Each node uses an add-drop multiplexer which enables it to connect one or several users (individual terminal, PABX, LAN access point, etc.) and becomes the key component of these rings, which explains the increased importance of OADM (Optical Add-Drop Multiplexers, see Chapter 5) and the advantage of making them reconfigurable.

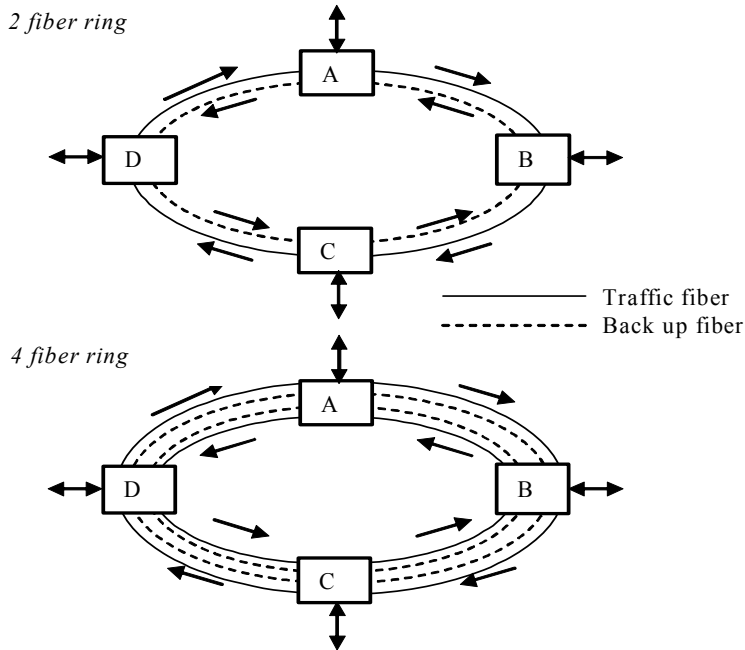
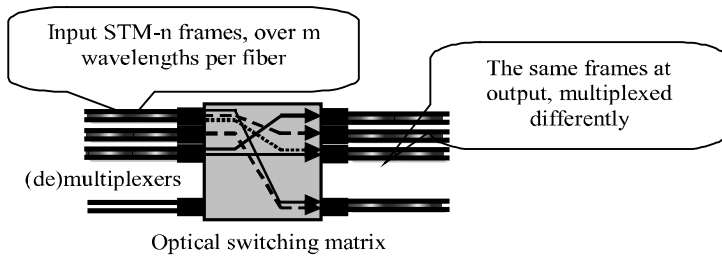
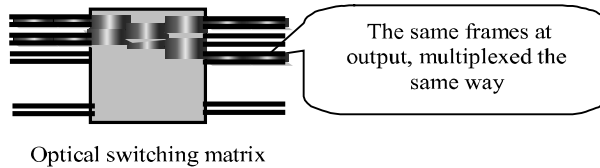


Figure 10.9. SDH rings over fiber optics

Rings can be interconnected by electric or optical cross-connects. Currently, the SDH ring architecture is mainly used in MANs (metropolitan area networks) where reconfiguration can be performed in less than 50 ms; it is less adapted to wide area networks because of propagation delay which varies significantly during reconfigurations.

10.3.4. Optical cross-connect

Cross-connecting consists of modifying the distribution of the different affluent multiplexed units within higher level units between cross-connect (OXC: Optical Cross-Connect) input and output. In SDH, cross-connect is carried out at all levels: between lower or higher level VC, between STM-1 or STM-n frames, with electronic switching matrices. It can also be carried out in the optical layer between wavelengths or between fibers (Figure 10.10). In the first case, the different input wavelengths are demultiplexed, separately switched and remultiplexed differently at output; in the second case, all wavelengths of an input fiber are switched together to a single output fiber.

Wavelength cross-connect*Optical fiber cross-connect***Figure 10.10.** *Different types of optical cross-connects*

In both cases, (de)multiplexing and switching are completely optical, there is an electronic control signal but no signal at the data bitrate, which can reach 10 or even 40 Gbit/s without limiting speed. There is transparency: electric signals, overheads in particular are not modified. Cross-connecting is currently used for network reconfiguration in case of incident or congestion (switching all channels from one fiber to another) and not for real time channel switching. Mechanical or micro electro-mechanical structure (MEMS) switching technologies are therefore the most adapted (see Chapter 5).

10.3.5. Optical transport network (OTN)

The evolution of SONET/SDH networks, which in their design remain marked by telephone circuit transport, is taking the form of the optical transport network (OTN) whose standardization by the ITU started in 2002 (G 709). It allows us to directly and transparently transport Ethernet, IP, Fiber Channel, SDH/SONET or ATM frames, for a convergence that avoids stacking of protocol layers.

In charge of transport, multiplexing, routing, network security and control, the OTN protocol is organized in electric layers and optical layer (section 10.3.6).

The electric frame is organized into a 4 row and 4,080 column matrix (Figure 10.11), is called OTU (Optical Transport Unit) and includes the client payload and:

- framing;
- a three part overhead:
 - the OPU (Optical Payload Unit) overhead containing information on the type of client, and is in charge of adaptation,
 - the ODU (Optical Data Unit) overhead containing end to end channel supervisory information,
 - the OTU overhead containing supervisory information for a section (between a transmitter and an optical receiver);
- forward error control (FEC) based on a Reed-Solomon code (255, 239)¹, allowing the same error ratio with 5.8 dB less power, for a bitrate increase of 7%; an interleaving technique allows us to correct bursts. The major SDH functions are present, with more usage flexibility.

The OTN hierarchy includes 3 levels, obtained either directly or by multiplexing of the lower level frame by frame and not byte by byte as in SDH; frames then remain complete and their duration is reduced whereas it remains constant (at 125 μ s) in SDH. These levels are:

- OTU1 at 2.7 Gbit/s (which can transport an STM-16);
- OTU2 at 10.7 Gbit/s (which can transport an STM-64, Ethernet 10G, etc.);
- OTU3 at 43 Gbit/s (which can transport an STM-256), while being introduced.

Bitrate increase compared to SDH comes from overhead and error control bytes. There is no coincidence between a SDH frame and the payload.

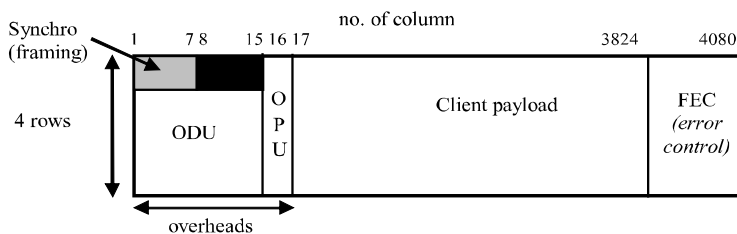


Figure 10.11. OTU frame

¹ Which means that 16 control bytes are added to a block of 239 data bytes for a total of 255 bytes.

10.3.6. The optical OTN layer

The optical layer constitutes the main OTN enhancement. It ensures dense wavelength division multiplexing (DWDM) of several OTU frames in the same fiber. The number of wavelengths and the bitrate per wavelength can be adapted in a flexible way. High grooming can thus be reached, which means that the bitrate can vary over a very large range with a fine pitch (2.5 Gbit/s).

An optical supervisory channel (OSC), at a specific wavelength of 1,510 nm, transports tracking and control information for data channels, to multiplexers, routers, etc., constituting a distinct signaling network, such as the signaling network in telephony.

This information is transmitted as packets and structured on three levels:

- optical channel (OCh) tracking an end to end optical signal at a given wavelength, information corresponding to the different wavelengths is temporally multiplexed;
- optical multiplex section (OMS) which controls multiplexers and cross-connects; this information is common to all multiplexed channels in the same fiber;
- optical transport section (OTS) controlling a regeneration section.

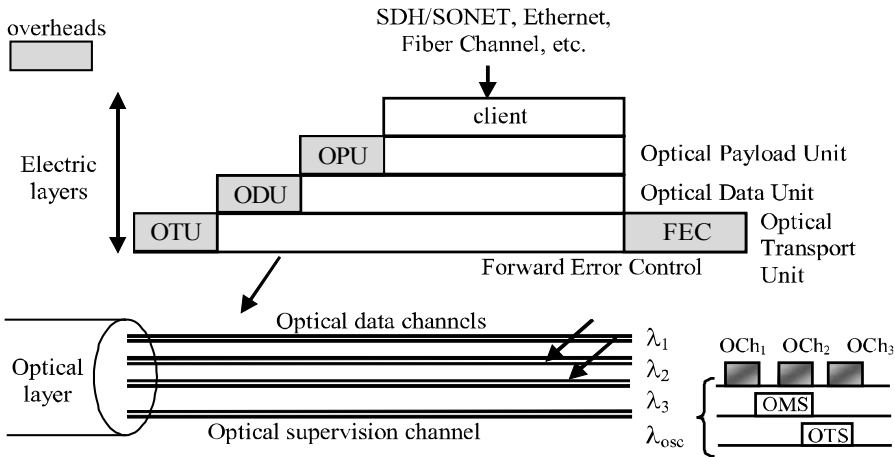


Figure 10.12. Optical transport network (OTN) layers

This channel communicates with the network management and control plane which controls active network components without having to convert data channels. The supervisory channel is the only one that needs to be converted into electric signals and processed in network nodes as its bitrate is much lower (currently 100 or 155 Mbit/s). Data channels can be multiplexed and switched optically; it is not necessary to detect and process signals at 10 or 40 Gbit/s, which is a significant difference with SDH. This is one of the impediments to bitrate increase, the relative slowness of electronic processing in nodes, which disappears.

The OSC in particular can transmit GMPLS signaling (section 10.4.4) and control all-optical switches. The optical transport network is not completely established yet, but it is a significant step toward next generation networks (NGN).

10.4. Toward all optical networks

10.4.1. Wavelength division multiplexed networks

It is easy to multiplex signals coming from geographically distant sources in the same fiber because the multiplexer is passive and requires no synchronization, contrary to time-division multiplexing. Add-drop multiplexers (ADM, see Chapter 5) are used to connect intermediate terminals (Figure 10.13). This method is largely used in wide area networks, submarine notably (SEA-ME-WE link example, see Figure 9.11), but is also developed in metropolitan area networks or in company backbones. A different wavelength is affected at each path, in a fixed way.

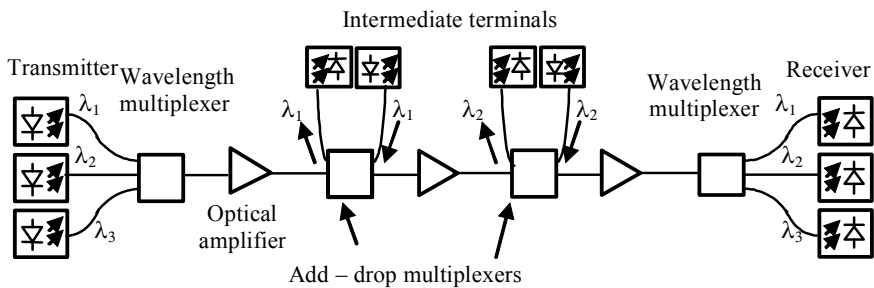


Figure 10.13. Connection using wavelength division multiplexing

10.4.2. Wavelength routing

In order for the network to be more flexible, wavelength routing can be performed: each terminal can emit at several wavelengths (generally using tunable

laser diodes) corresponding to as many receivers: it selects its wavelength according to the receiver. These wavelengths can be separated in a passive demultiplexer, or by a filter in each receiver. In this case, routing is performed at the source because it is tunable.

It is also possible to route at receiver level using a filter or a tunable ADM which matches with the source wavelength, but this method is not as advanced. The wavelength allocation can be reconfigured dynamically, but it is always the same one used end to end in a given path.

To optimize the use of wavelengths and be able to massively reuse them, as with frequencies in a radio network, it is helpful to change wavelengths at each node. This can be done with the help of an optical-electric-optical interface receiving the signal in a wavelength and retransmits it in another, possibly tunable wavelength.

However, to remain optical from end to end, wavelength conversion done by devices derived from semi-conductor optical amplifiers (see section 8.4.2) transposing a signal from one wavelength to another at each node, must be achieved (Figure 10.14).

These nodes will become real optical routers but still need electronics to process signaling information and establish connections. However, this information, which is transported by the optical supervision channel, has a much lower throughput than data.

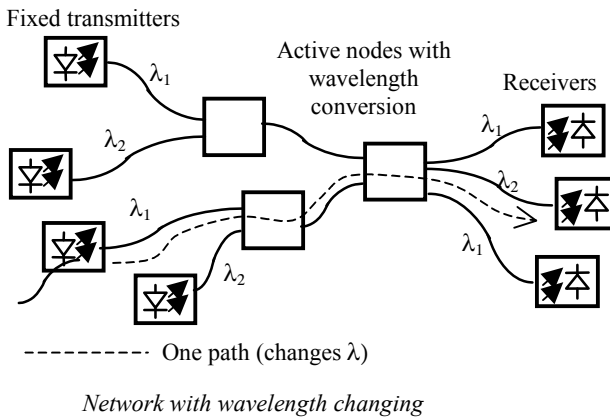
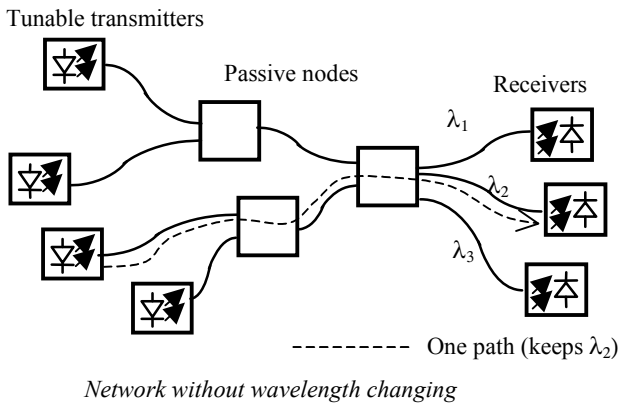


Figure 10.14. Two types of wavelength routing

10.4.3. All optical network architectures

The combination of optical cross-connecting and wavelength division multiplexing is very interesting in metropolitan area networks or in large company backbones. The architecture of these systems is evolving toward rings making securement and reconfiguration easier (Figure 10.15); it is inspired by the SDH architecture, but these rings are interconnected by optical cross-connects (OXC) to establish back up routes by other paths.

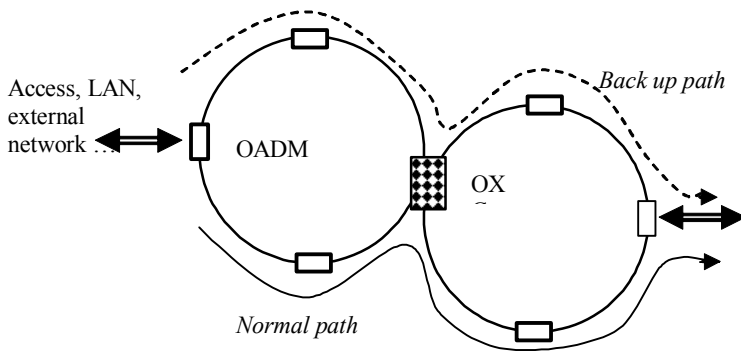


Figure 10.15. *All optical network, ring architecture*

Introduced by OTN, the optical layer concept plays an important part under SDH, ATM or IP layers. It includes the main optical components which are optical add-drop multiplexers (OADM) and optical cross-connects (OXC). The former are used at the network access (most often through a local area network) whereas the latter interconnect rings or switch to back up routes.

In this architecture, the signal remains optical from end to end. This is the concept of a transparent network contrary to an opaque network where signal is converted into electronic at each node. Whereas in the current state of technology, the signal keeps its wavelength, wavelength conversion will make the network intelligent by dynamically affecting wavelengths taking into account the traffic and by optimizing the use of resources (section 10.4.2). A specific protocol must then control the optical layer.

10.4.4. MPLS protocols

MPLS (multi protocol label switching) is a label routing protocol standardized by IETF (the organization which standardizes the Internet), initially introduced at the end of the 1990s to optimize IP frame transport in different types of switched networks. It is packet-transport oriented and has OAM (Operating, Administration and Maintenance) tools.

Containing a label and switched in the form of ATM cells, data is separated from signaling which is routed in IP. Data follows a path called LSP (Label Switched Path) established beforehand, labels (or “references”) are processed and modified in the routers through routing tables updated by signaling. This method comes from the

ATM virtual path concept. MPLS signaling establishes, controls and deletes these paths, according to traffic, and ensures circuit securement.

There are label edge routers (LER) and label switching routers (LSR). The reference is inserted in the overhead of only 32 bits, which is added to frame and packet headers. There are several reference distribution protocols. Flow aggregation toward the same destination simplifies routing. Virtual private networks (VPN) can be established.

Generalization of this protocol led to GMPLS (generalized MPLS) where the role of reference can also be played by the number of a time slot in a synchronous time-division frame (TDMC: Time Division Multiplexing Capable), the wavelength number in a fiber (LSC: Lambda Switching Capable), or the number of a fiber in the cable (FSC: Fiber Switching Capable). A hierarchy of the supports can be carried out (Figure 10.16), which the protocol must respect when establishing connections between routers.

Flows transmitted over the fiber wavelengths, which can be of high bitrate SONET/SDH format, can be switched by their optical label without electric processing. Signaling information for implementing virtual circuits is transmitted by a control plane separate from the user plane transferring data. The control plane, which is in real time, controls connections and dynamic reconfigurations (via optical cross-connects or wavelengths switches) and uses an IP protocol over Ethernet. It must not be confused with the management plane which has much longer time constants and plans for the network evolution.

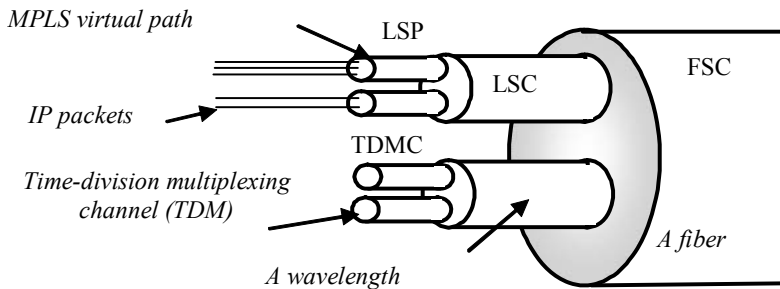


Figure 10.16. *MPLS hierarchy*

In the optical transport network OTN, signaling is transported by the optical supervision channel, at a specific wavelength (section 10.3.6) and not in SDH frame overheads, data can then remain all-optical and at very high bitrates. GMPLS can

quickly be reconfigured, and also offer quality of service (QoS). In the future, it must allow the installation of the automatically switched transport network (ASTN).

10.4.5. Trends

In parallel, access control techniques such as optical CDMA (Code Division Multiple Access, widely used in radio) are the subject of research projects focusing on access networks, they require the development of an optical spread-spectrum technique, with the help of photo-inscribed fiber Bragg gratings for example.

Completely optical packet switching is even more futuristic because it would require optical memory, which only exists in experimental form and is very expensive.

This page intentionally left blank

Chapter 11

Fiber-Optic Sensors and Instrumentation

11.1. Fiber optics in instrumentation

11.1.1. *Introduction*

Parallel to the development of fiber optics in telecommunications in the last 20 years, several studies focused on their use in instrumentation and sensors. Their specific advantages come from:

- low disruption caused by lightweight, small and insulating fiber optics;
- their intrinsic security (absence of electric current) and their insensitivity to electromagnetic parasites;
- the possibility they offer for remote analysis with high spatial resolution of environments that are difficult or dangerous to access;
- and finally, the possibility of using the optical fiber itself as a sensitive element for a certain number of physical dimensions. It is possible to build distributed sensors or sensor networks in which the optical fiber can be used as a sensitive element and transmission support simultaneously.

However, fiber-optic sensors having reached their technological maturity are rare. This is especially the case with those where the optical fiber improves an existing measurement system without modifying its principle. Large perspectives exist for when the optical fiber can instrument a complete system, a structure or material by integration. It then is no longer a sensor in the sense of an isolated component, but an element of a real intelligent system.

In addition, the development of silicon integrated optics helps in the design of microsystems integrating an optical sensor, optoelectronic interfaces and processing circuits (the reading head of magneto-optical disks developed at LETI for example).

11.1.2. *Use of fiber optics in instrumentation*

The use of fiber optics in measurement can have 3 forms:

- fiber-optic transmission of a measurement, generally electric and analog; this application is described in Chapter 9;
- optical instrumentation using fibers for light propagation;
- actual optical fiber sensors.

At the chapter instrumentation, we can add the use of fiber optics to transmit light beams of various powers:

- low power: display (direct observation of the light at fiber output); this can be the transmission of the colored emission of an LED by a plastic optical fiber;
- intermediate power: lighting (white light transmission, clear of infrared light, by a bundle of glass fiber, or at short distance, plastic fiber); this is one of the oldest optical fiber applications;
- high power: particularly the YAG laser beam transfer, emitting at $1.06\text{ }\mu\text{m}$ (wavelength well transmitted by silica, even in the form of very strong pulses). These are new applications developed in mechanical industries and surgery notably.

11.1.3. *Fiber-optic measurement instrumentation*

In this case, measurement is completely optical; it is performed remotely with the help of one (or more) optical fiber(s) playing a passive role, but offers significant implementation advantages: accessibility, high spatial resolution, cartography possibility by moving the test point, security, etc.

Some of these concepts are relatively old, but they have benefited from technological advances and decreased cost of optoelectronics.

Today, several operational applications exist in fields such as:

- physical chemistry: pH measurement, colorimetry, refractometry, infrared and Raman spectroscopy;

– temperature measure by pyrometry (black body radiation analysis): because of this radiation's spectrum, which is mainly in infrared (Figure 11.1), it can be transmitted by silica optical fibers if the temperature is higher than 300°C, and by fluoride fibers when temperature becomes ambient;

– near field microscopy;

– robotics and computer-integrated manufacturing (Figure 11.2): proximity detection, optical barriers, pattern recognition, laser telemetry;

– endoscopy (transmission of an image by a fiber optics bundle), used in medicine as well as in manufacturing, civil engineering, archeology, etc., which is one of the most well known fiber optics applications. Since each fiber (with a diameter of a few micrometers) transports a pixel, placement must be exactly the same at both extremities (coherent bundle) explaining its high cost. Camera miniaturization makes its market decrease.

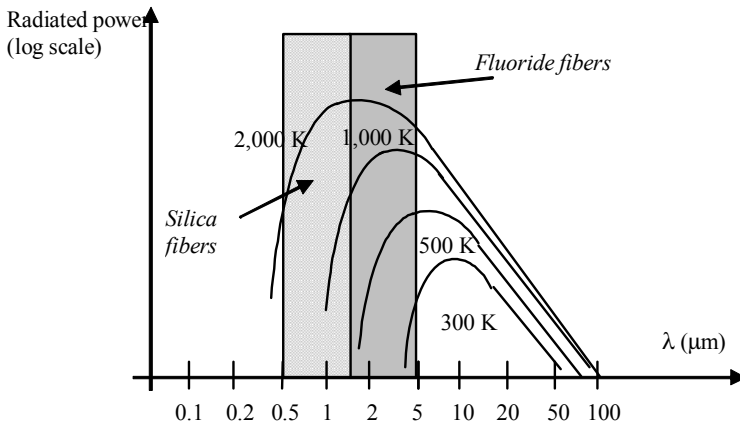


Figure 11.1. Black body radiation transmission

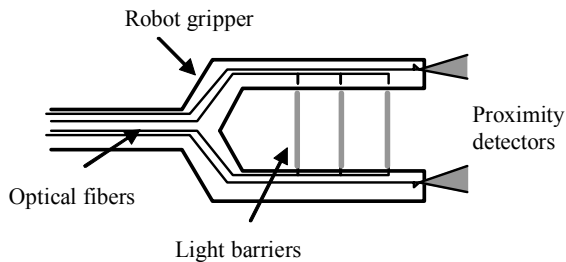


Figure 11.2. Examples of fiber optic uses in robotics

11.1.4. *Fiber-optic sensor classification*

In the strict sense, sensors use the light propagation modification in an optical fiber by the phenomenon to measure.

They can be classified according to several criteria:

- extrinsic sensors (effects at fiber extremities or connections) versus intrinsic sensors (modification of internal guide properties or of its material);
- non-coherent sensors (only based on light power; they are simple but not always very precise or reliable) versus coherent sensors (based on light phase or polarization, they are much more sensitive, but a lot more difficult to use);
- punctual sensors versus distributed sensors; in the second case, the fiber is sensitive throughout; it is then useful to distinguish whether the installation enables localization of the phenomenon to be measured or not.

11.2. Non-coherent fiber-optic sensors

11.2.1. *Geometric and mechanical size sensors*

Very simple in principle, these sensors have multiple applications in industrial or security systems, insofar as high precision is not required. They are used in analog measurements as well as go-no go applications (detection, counting, etc.).

Following are a few examples:

- micro-movement sensors (longitudinal or angular) using techniques such as spatial filtering at the connection of both fibers, or by extremity reflection (Figure 11.3); they can also be used as force or vibration sensors;

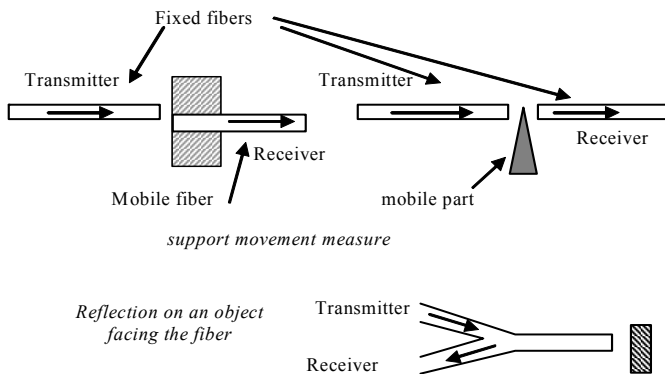


Figure 11.3. *Micro-movement sensors using spatial filtering*

– external medium refraction index measure with the help of the Fresnel reflection coefficient at fiber extremity (or, more rarely, bending losses); the most common applications are level detection (Figure 11.4) or bubble counting, but it can be used to find out a temperature or chemical composition;

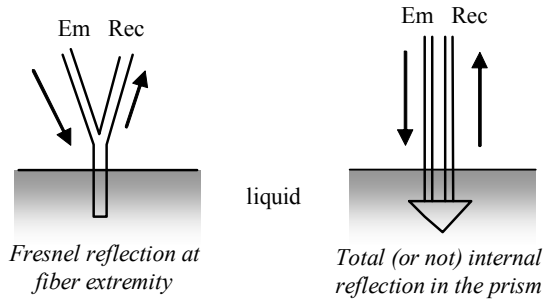


Figure 11.4. *Level sensors*

– velocity measurement and vibration analysis by laser-Doppler velocimetry, which can favorably use fiber optics (Figure 11.5). It is known that the reflection of a wave of frequency ν on an object moving at speed v causes a frequency shift of the reflected wave of:

$$\Delta\nu = \frac{2v}{c} \cdot \nu$$

By beat with the wave reflecting on the fiber extremity, a frequency $\Delta\nu$ is measured after detection, which has a range from kHz to MHz for movement velocities from mm/s to m/s.

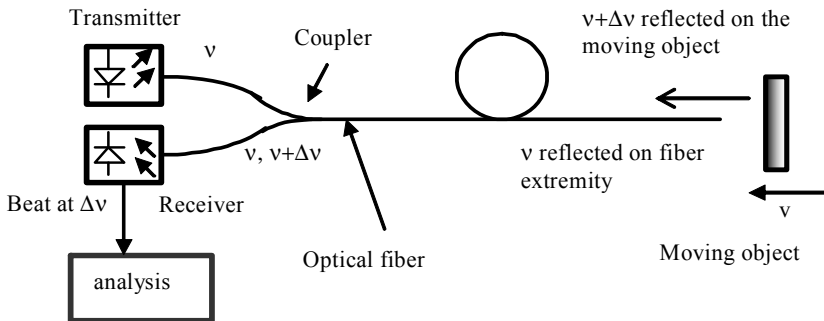


Figure 11.5. *Doppler velocimetry by fiber optics*

11.2.2. Bending or micro-bending sensors

Sensors using losses in strong bending of an optical fiber were experienced. Since these losses quickly vary with bending radius as well as with numerical aperture, it is possible to achieve geometric measures as well as an index of the medium surrounding the core (cladding with an index which depends on a dimension to measure, or fiber without cladding sensitive to external medium index).

There are also different types of micro-bending constraint sensors (Figure 11.6); their main advantage is the ability to be integrated in structures (mechanical, aeronautical, bridges, etc.) and to locate constraints by reflectometry. Micro-bending loss measure can be sensitive, particularly with graded-index fibers, when the spatial distortion period corresponds to the mode coupling period.

However, bending or micro-bending measures are not very accurate, and they require fibers of strong mechanical resistance.

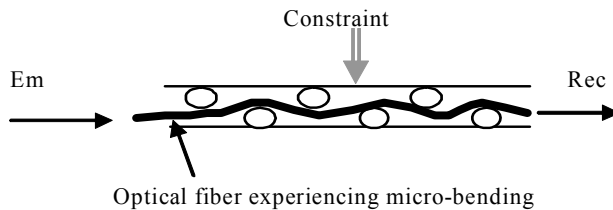


Figure 11.6. *Micro-bending constraints sensor*

11.2.3. Temperature extrinsic sensors

These sensors detect an optical property of material placed at the end of the optical fiber (in the form of a thin layer deposit for example). The general scheme is illustrated in Figure 11.7. The optical property depending on temperature can be:

- photoluminescence: the material retransmits a light with a spectrum that depends on temperature when it is lit;
- fluorescence: decrease in time of the re-emitted light depends on temperature;
- absorption of a semiconductor close to its cut off wavelength which greatly varies with temperature;
- reflectivity of a material whose index depends on temperature, etc.

There are also on-off sensors indicating threshold temperature overshoot, using the liquid crystal state for example.

Some applications corresponding to different sensitivity and precision ranges were commercialized. The major advantages with these sensors is their small size and electric insulation, and it is very convenient to place them in a reflection-based network (see section 11.4).

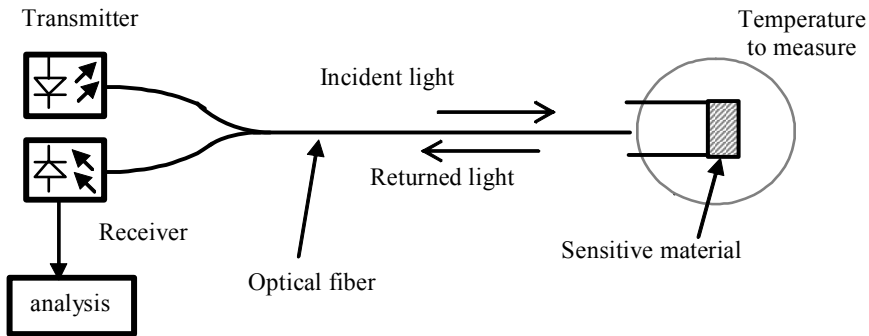


Figure 11.7. Principle of temperature extrinsic fiber-optic sensors

11.2.4. Intrinsic non-coherent sensors

These are sensors using light intensity variations appearing in the optical fiber matter.

In this way, intrinsic temperature sensors, contrary to the previous ones, use the variation of the fiber material property with temperature. It can be the core-cladding index difference, measured with the help of the numerical aperture variation (more simple than with interferometry). Other sensors use the Raman scattering of the fiber matter, or scattering or fluorescence variations in doped fiber. These measures make it possible to obtain a temperature profile along the fiber by backscattering, but these methods are very complicated, and only installed in certain sensitive sites (high power electric lines, gas pipelines, etc.) for locating abnormally hot or cold spots.

Intrinsic chemical sensors were also realized. Their general principle (Figure 11.8) is the use of optical cladding for absorbing the matter to be detected (methane for example). Through the evanescent field, the light is then attenuated where this matter is absorbed; they can then be located with an OTDR. In the same principle, interferometric sensors were developed which use index variation with absorption of the matter to be detected.

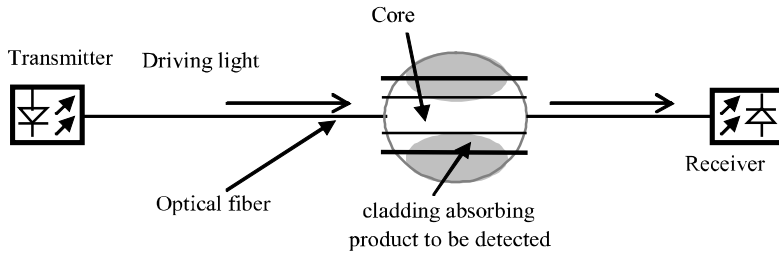


Figure 11.8. *Chemical fiber-optic sensor*

Finally, fiber-optic radiation sensors use a specific type of optical fiber, generally made of plastic (doped polystyrene) presenting a fluorescence property (light radiation caused by external illumination at a shorter wavelength). The fiber guides (over a short distance) the light it has emitted. A spectral, spatial and temporal radiation analysis can then be achieved. Fluorescent (sensitive to visible or ultraviolet light) and scintillating (sensitive to nuclear radiations) fibers are on the market; they have applications in visualization and display.

11.3. Interferometric sensors

11.3.1. Overview

These sensors are based on coherent techniques: analysis of the phase or polarization of light in a single-mode optical fiber, or at a more experimental step, interferometry between modes in a multimode fiber. They are extremely sensitive and do not affect optical fiber reliability. They are less easy to implement and often require signal processing to obtain absolute (and not relative) measures and separate the effects of different physical influential parameters (notably temperature). We will give some examples.

11.3.2. Two arm interferometers

11.3.2.1. Mach-Zehnder interferometer

In this interferometer (Figure 11.9), both arms are made up of two single-mode fibers (or two guides in integrated optics) with identical lengths L . Phase shift between the measurement and reference arm is caused by a stretching ΔL or by an index variation Δn , which is most often due to variation in temperature ΔT or in differential pressure ΔP (by photo-elasticity). Chemical sensors of this type were also developed, mainly in integrated optics, by using effective index variation in the measure arm, due to the contact of a chemical matter.

In the set-up using fibers and two couplers, the receiver receives an intensity modulated by $\cos^2 \Delta\phi$; the phase is measured within π and we must delete the ambiguity (by a two wavelength measurement for example). The second set-up which can be carried out in integrated optics, creates interference fringes between beam output coming from both guides that move and can be counted.

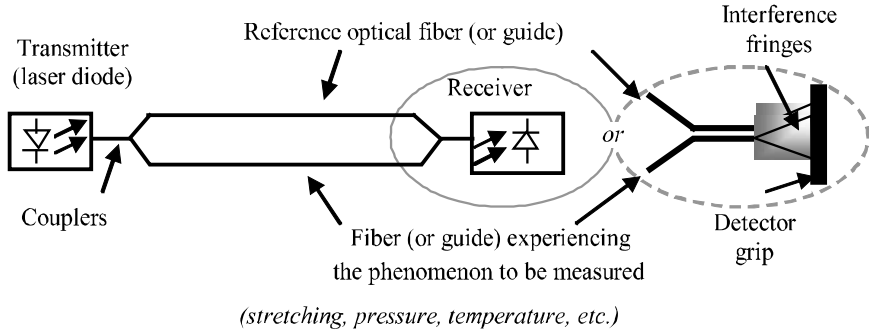


Figure 11.9. Fiber or optical guide Mach-Zehnder interferometer

Phase shift equals:

$$\Delta\phi = k_0 n \cdot \Delta L + k_0 L \left[\frac{dn}{dT} \Delta T + \frac{dn}{dP} \Delta P + \frac{dn}{dX} \Delta X \right]$$

These different parameters (X is another parameter liable to influence the index, chemical for example) can therefore simultaneously be measured, but they are difficult to separate. This is possible by using several wavelengths whose relative sensitivities from n to P , T , X , etc. are not the same at each wavelength.

The main application is the acoustic sensor, with large bandwidth, used in hydrophones. This is a dynamic and differential measure. For absolute and static measures, the main problem remains sensitivity to the difference in temperature between both arms; it is attenuated but not cancelled by the realization in integrated optics.

11.3.2.2. Michelson interferometer

Based on a single-mode fiber coupler X (Figure 11.10), it provides the same measures, but is mainly interesting for relative micrometric movement measures, using interferometry in non-coherent light (from an LED).

This type of sensor can also be developed in silicon integrated optics.

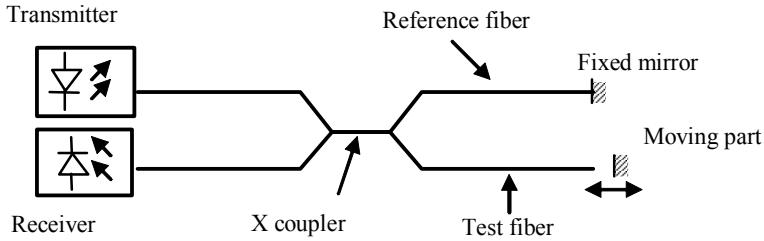


Figure 11.10. *Fiber-optic Michelson interferometer*

11.3.3. Intermodal interferometry

We have experimented with sensors based on intermodal interferometry in multimode fibers through coherent light. The phase shift between guided modes is very sensitive to index variations, even very low ones, caused by mechanical perturbations (photo-elasticity).

These phase fluctuations are converted into amplitude fluctuations in case of spatial filtering, intentional or not (it can be a bad connector). The modal noise phenomenon discourages the use of laser diodes with multimode fibers.

The main advantage with this type of sensor is that it only has one fiber and is thus easily integrated, and that optical installation is very simple, since spatial filtering can be carried out by connecting two different fibers (Figure 11.11). It easily detects vibrations of the structure in which the fiber is integrated, but the signal obtained is complex.

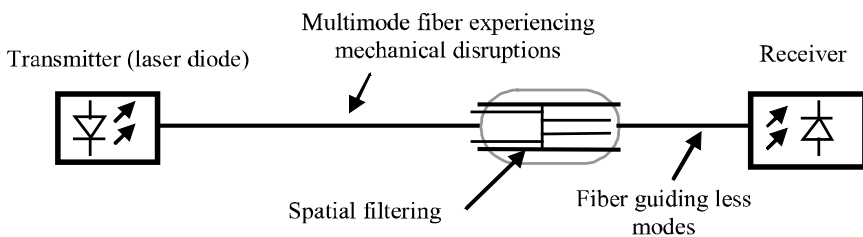


Figure 11.11. *Vibration sensor by intermodal interferometry*

11.3.4. One fiber interferometers

Other constraint measurement methods through stretching of a single optical fiber were developed. Their main advantage is easy integration of the sensor in material (for aeronautic, civil engineering and other structures).

11.3.4.1. Fabry-Pérot interferometer

This is made up of two parallel mirrors spaced from Λ integrated in an optical fiber or between two optical fibers (Figure 11.12). By interferometer resonance, power transmitted is at its maximum for wavelengths with:

$$\lambda = 2 n \Lambda / p \quad (p \text{ is an integer, } n \text{ is the fiber index})$$

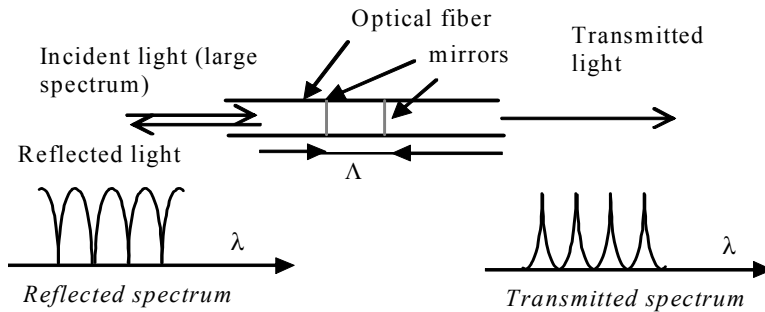


Figure 11.12. Fabry-Pérot interferometer sensor

11.3.4.2. Bragg grating sensor

This more recent technology uses a Bragg grating photo-inscribed in the fiber core matter (Figure 11.13). It is a periodic and longitudinal variation of the refractive index (Chapter 4), with step Λ , causing reflection of the wavelength λ following the phase matching relation:

$$\lambda = 2 \Lambda n \quad (n \text{ is the average fiber index})$$

In both cases, by increasing Λ , fiber stretching will induce a variation of the transmitted or reflected wavelength which can be remotely measured with perfect reliability: the light wavelength, contrary to its intensity or its polarization, cannot be modified by its propagation in the optical fiber. In addition, these sensors are usable in reflection and are well adapted for serial implementation and reflectometry interrogation.

However, these techniques are expensive and complicated to implement and the problem of sensitivity to temperature (which influences the index) remains.

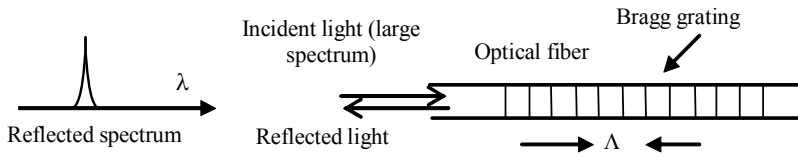


Figure 11.13. *Stretching sensor using a Bragg grating*

11.3.5. Ring (or Sagnac) interferometers

11.3.5.1. Optical fiber gyroscope

This is one of the oldest optical fiber sensors, at the source of intense scientific and industrial activity. The principle is identical to the laser or acoustic wave gyroscope principle and consists of measuring by interferometry the phase shift between both propagation directions in the same ring-based optical fiber (Figure 11.14). The influence of temperature then auto-compensates. If the set-up turns around an axis that is perpendicular to the fiber plane, phase shift $\Delta\phi$ is proportional to the speed of rotation Ω :

$$\Delta\phi = \frac{8\pi NS\Omega}{\lambda c}$$

where S is the loop surface; N is the number of turns, which can be quite large, for precision and accuracy better than one degree per day. The device represented, which is exactly a gyrometer (rotation speed measure), enables the realization of gyroscopes (measure and conservation of a direction) much simpler than inertial gyroscopes. It is starting to be used in ground or aerial navigation.

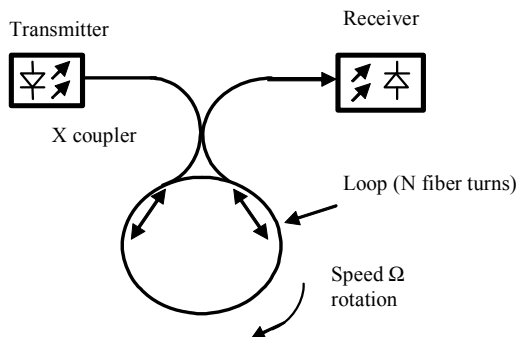


Figure 11.14. *Fiber-optic gyroscope*

11.3.5.2. Fiber-optic current sensor

It uses the same ring set-up (Figure 11.15), but this time measures polarization rotation θ caused by the magnetic field \vec{H} created by current I to be measured (Faraday effect):

$$\theta = 2N.V_F.I$$

with V_F as Verdet constant = $4,6.10^{-6}$ rd/A in silica.

This is proportional to the current as well as to the number N of fiber turns around the conductor, but it does not depend on the fiber path, temperature or mechanical constraints.

This sensor is therefore precise, accurate and securely measures very high currents at very high voltages. However, it is expensive and must be installed permanently on a high voltage power line for example; this type of sensor has remained experimental and integrated sensors made from glass with a high Verdet constant are being developed.

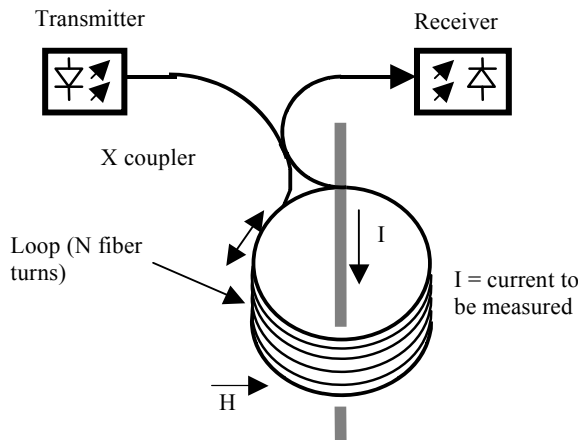


Figure 11.15. *Fiber-optic current sensor*

11.3.6. Polarimetric sensors

These are interferometric sensors as well (requiring a coherent source), but both orthogonal polarizations guided by the fiber play the role of the two interferometer arms. This allows a better integration of the sensor and lower sensitivity to temperature.

The major application is the constraint sensor by birefringence (Figure 11.16): it uses created (or modified) birefringence in a single-mode fiber by a non-isotropic constraint. The polarization state analysis gives the constraint direction and value. For a remote sensor, the main problem is to correctly transmit the state of polarization from the sensitive point to the analysis point; high birefringence fibers are then used (see Chapter 2) in which the constraint will couple light in the polarization orthogonal to initial polarization. Light can also be injected into both polarizations; the constraint then creates a phase shift between them. The resulting polarization state, preserved by the following birefringent fiber, is determined by the constraint applied and allows us to analyze it (in direction and intensity).

This measure is quite complex, but it has the advantage of only using one fiber; the effect of temperature is theoretically neutralized and it enables the creation of a distributed constraint sensor. Location of the constraint is possible by rather complicated coherence multiplexing techniques (see section 11.4.4). Birefringent fibers are tricky to use, however.

Finally, there are optical sensors where the fiber remotely measures the transmission of a crystal placed between two polarizers, and experiencing constraints making it birefringent; it is then an extrinsic sensor.

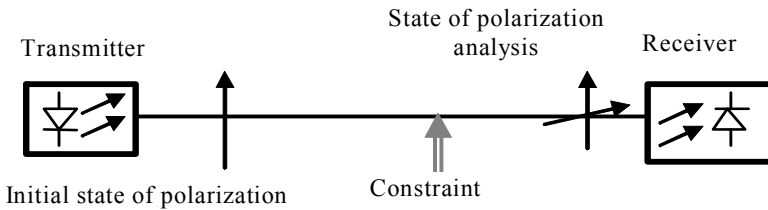


Figure 11.16. *Measurement of constraints by birefringence (principle)*

11.4. Fiber-optic sensor networks

11.4.1. Distributed sensors

The location of a phenomenon in a continuously sensitive fiber is classically performed by reflectometry (OTDR), which is possible if this phenomenon occurs by an attenuation or reflection in the optical fiber. This corresponds to using non-coherent sensor techniques.

Specific methods were developed for sensors such as POTDR (OTDR with polarization analysis) or OFDR (Optical Frequency Domain Reflectometry) which is a frequency-domain reflectometry. The set-up is similar to temporal reflectometry,

for locating attenuating or reflecting events in the fiber, but the laser is wavelength modulated (in the form of a ramp or chirp) instead of transmitting pulses (Figure 11.17).

Distance z of the point measured is proportional to beat frequency f_b between the signal received and the signal transmitted (returned by the mirror):

$$f_b = \frac{2z \Delta f}{v_g T}$$

where Δf is the optical frequency deviation (several GHz) and T is the ramp period. By spectrally analyzing the signal received, it is possible to separate responses from the different sensitive points; very high spatial resolutions can be reached. This method however requires laser diodes which can be wavelength modulated with high spectral purity as well as polarization control; this remains experimental to this day.

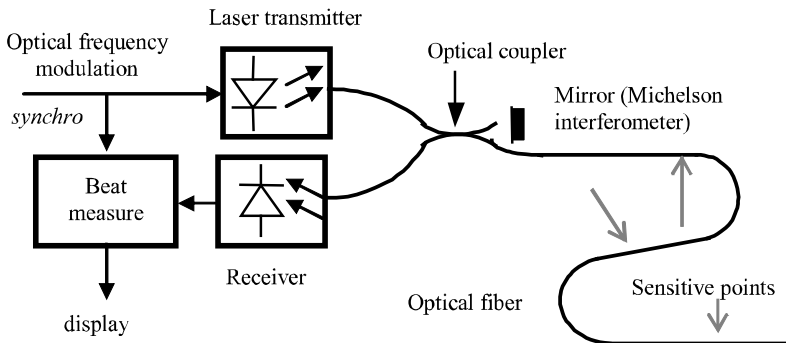


Figure 11.17. *Optical frequency domain reflectometry (OFDR) measurement*

In addition to these completely distributed sensors (in which the optical fiber can be continuously sensitive), it is possible to design multipoint sensor networks, used with a common optoelectronic transmitter and receiver thanks to multiplexing.

11.4.2. Time-division multiplexing

The different sensors respond by more or less attenuating (or reflecting) a pulse sent by a single source. Responses are shifted over time by optical paths with different lengths (Figure 11.18). A time-domain (or possibly frequency-domain) reflectometry demultiplexes sensors.

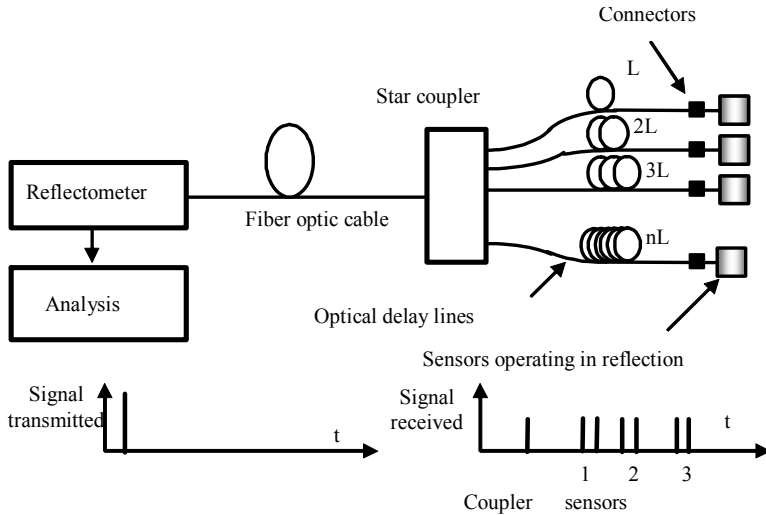


Figure 11.18. Time-division multiplexing sensor network

11.4.3. Wavelength division multiplexing

In this technique, also called chromatic multiplexing, each sensor continuously works at its own wavelength obtained from a unique LED spectrum (Figure 11.19). This has the advantage of working with an LED in continuous wave mode (or low frequency modulated for synchronous detection), and showing correct sensitivity; but wavelength division multiplexers are expensive.

11.4.4. Coherence multiplexing

This specific method applies to polarimetric sensors distributed along a high birefringent fiber. Since the propagation constants of these two polarizations are different, the delay between them at receiver is proportional to the coupling point distance, thus to the sensor. This delay can be measured by a Michelson interferometer placed at the end of the fiber, as each polarization is injected in each arm (Figure 11.20).

The interferometer operates in non-coherent light (from an LED or a superluminescent diode): a beat can only be observed between both polarizations when the measurement arm delay exactly compensates for the slow polarization delay. It is thus possible to spatially separate with high resolution several measurement points distributed along the fiber (the separating power corresponding to source coherence, which is short). However, this is a very complicated technique.

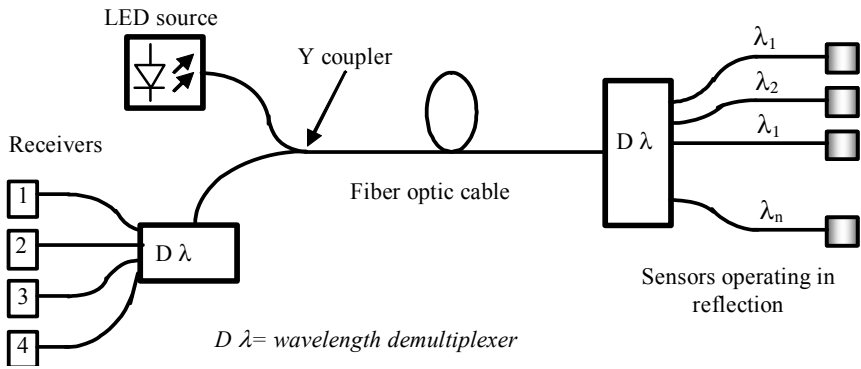


Figure 11.19. Chromatic multiplexing sensor network

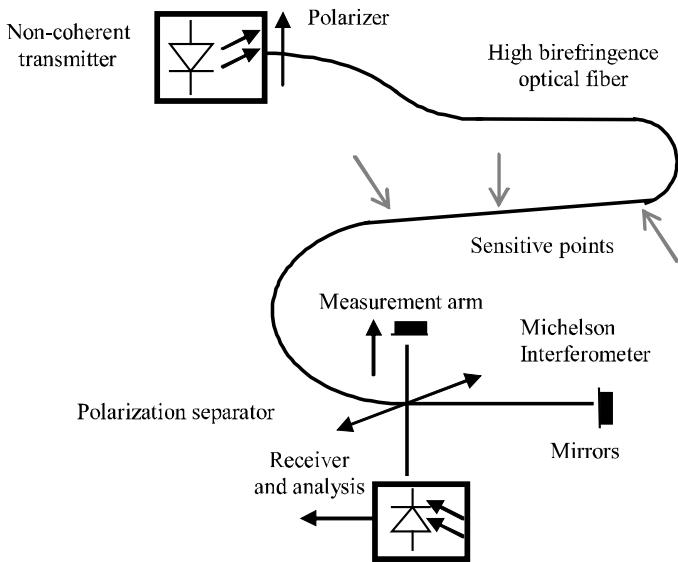


Figure 11.20. Coherence multiplexing sensor network

This page intentionally left blank

Exercises

Part 1: fiber optics, propagation and technology

Exercise 1.1. *Propagation in a graded-index optical fiber*

An optical fiber with an index in cylindrical coordinates, given by:

$$n(r) = n_1 \sqrt{1 - 2\Delta(r/a)^2} \quad \text{if } r < a \text{ (in the core);}$$

$$n(r) = n_2 \quad \text{if } r > a \text{ (in cladding)}$$

with:

$$\Delta = \frac{n_1^2 - n_2^2}{2n_1^2}$$

and:

$$\Delta \ll 1$$

Calculate the trajectory of a light ray injected at the extremity of the fiber in its center, making an angle of θ_a with the axis (see Figure 1.10). On what condition is it guided?

Exercise 1.2. *Intermodal dispersion in a step-index fiber*

Establish a simple relation between the total pulse broadening by unit of length, $\Delta\tau_{im}$, and the numerical aperture NA of a step-index fiber.

Give numerical values for $NA = 0.2$ then 0.4 , with a cladding index of 1.46 . In practice, where is the actual pulse width at half maximum?

Exercise 1.3. Graded-index multimode fiber bandwidth

The bandwidth BW in a multimode fiber was measured according to the distance traveled L .

L (km)	0.5	1	1.5	2	3	4	5	6
BP (MHz)	1,200	600	405	310	240	195	165	143

Estimate factor γ (from the law in $L^{-\gamma}$) and equilibrium distance.

Exercise 1.4. Link bandwidth

Calculate the bandwidth over a 2 km link using:

- a light-emitting diode (LED) of central wavelength: 850 nm , and spectral width: 50 nm ;
- a $62.5/125$ optical fiber (graded-index multimode) with a bandwidth of 300 MHz.km , and a chromatic dispersion coefficient: 100 ps/nm/km (at source wavelength). By what type of dispersion is the bandwidth limited?

Redo the same calculation with an LED emitting at $1,300 \text{ nm}$, a wavelength where the chromatic dispersion coefficient equals 3 ps/nm/km . What conclusion(s) can be made about applications?

Exercise 1.5. Injection of light in a single-mode fiber

A $1.3 \text{ }\mu\text{m}$ laser delivers a Gaussian and parallel beam, with a mode diameter of: $2w_{0l} = 1 \text{ mm}$.

Which lens should be used to perfectly couple this beam to a single-mode fiber with a mode diameter of: $2w_{0f} = 10 \text{ }\mu\text{m}$ at $1.3 \text{ }\mu\text{m}$?

Exercise 1.6. Single-mode fiber parameters

A step-index optical fiber has the parameters:

- absolute index difference: $n_1 - n_2 = 4 \cdot 10^{-3}$;
- core index: $n_1 = 1.47$;
- core diameter: $2a = 9 \mu\text{m}$;
- optical cladding diameter: $2b = 125 \mu\text{m}$.

Under what condition over the wavelength is this fiber single-mode?

Using the material dispersion curve in Figure 2.6, calculate the chromatic dispersion coefficient of this fiber at 1.3 and 1.55 μm . At which wavelength will it be preferable to use it, and why?

Exercise 1.7. *Single-mode fiber design*

An optical fiber will be used at 1.55 μm and must be single-mode from 1.2 μm .

It is a silica fiber such that:

$$n_1 = 1.47 \text{ core index}$$

$$\Delta = 2.7 \cdot 10^{-3} \text{ relative index difference}$$

- 1) Calculate the fiber core radius.
- 2) Calculate its chromatic dispersion coefficient, knowing that material dispersion at 1.55 μm equals: $D_M = 20 \text{ ps/nm/km}$.
- 3) There are 3 causes of attenuation, when the fiber is used in a cable:
 - intrinsic attenuation, which will be determined by calculating the Rayleigh scattering, and by taking into account a residual infrared absorption of 0.02 dB/km at 1.55 μm ;
 - micro-bending losses, equaling 0.05 dB/km;
 - connection losses, knowing that there is a splice every 20 km, and that:
 - the off-centering error is of: $e_t < 1 \mu\text{m}$,
 - the misalignment error is of: $D_\alpha < 0.2$,
 - the mode diameter tolerance is $\pm 5\%$.

Calculate the average lineic attenuation of the cabled and connected fiber.

4) This optical fiber is replaced by another with a relative index difference of: $\Delta = 4.10^{-3}$. Is it possible to cancel chromatic dispersion? If not, calculate optical fiber parameters for taking the dispersion below 10 ps/nm/km.

Without recalculating, is it possible to predict how the different losses will evolve? What conclusion(s) can be reached?

Exercise 1.8. *Depressed inner cladding single-mode fiber*

A depressed inner cladding single-mode fiber has:

- absolute index differences: $\Delta n^+ = 4.10^{-3}$ and $\Delta n^- = 2.10^{-3}$;
- a core diameter: 7 μm ;
- an inner cladding diameter: 50 μm ;
- an outer cladding diameter: 125 μm .

1) Calculate its cut-off wavelength. Can this fiber be used at both wavelengths, $\lambda_1 = 1.3 \mu\text{m}$ and $\lambda_2 = 1.54 \mu\text{m}$?

2) For usable wavelength(s), calculate:

- mode diameter;
- attenuation by Rayleigh scattering;
- total intrinsic attenuation, knowing that absorption loss equals 0.03 dB/km at 1.3 μm and 0.02 dB/km at 1.54 μm ;
- guide dispersion and chromatic dispersion.

Deduce the zero chromatic dispersion wavelength (approximately).

Exercise 1.9. *Single-mode fiber dispersion*

Calculate pulse broadening over 1,000 km of a link using optical amplifiers, a laser diode transmitting at 1.54 μm with spectral width of 0.1 nm, and a single-mode optical fiber with:

- a 3 ps/nm/km chromatic dispersion coefficient (at source wavelength);
- a PMD of 0.5 ps/ $\sqrt{\text{km}}$.

What is the maximum theoretical bitrate of this link?

To increase this, a chromatic dispersion compensator is used. What must its slope be? What then is the maximum theoretical bitrate?

Exercise 1.10. Graded-index plastic fibers

Several laboratories are working toward the development of graded-index plastic fibers for Ethernet Gbit. Supposing that an available attenuation of 30 dB is needed, with the use of VCSEL laser diodes, calculate the maximum corresponding distance based on the attenuation of the best current plastic fibers which is 150 dB/km.

Deduce the kilometer bandwidth in MHz.km that this new fiber must have. Could chromatic dispersion become a problem?

Exercise 1.11. Connector for multimode fibers

A connector for multimode fibers with optical cladding diameter of 125 μm has the following characteristics:

- off-centering: $e_t < 2 \mu\text{m}$;
- angular misalignment: $D_\alpha < 1$;
- longitudinal spacing: $D_e < 5 \mu\text{m}$.

Calculate the maximum loss of this connector, with and without index matching, for two types of graded-index optical fibers, with an index on axis $n_1 = 1.47$.

Fiber	Core diameter	Numerical aperture
50/125	50 $\mu\text{m} \pm 2 \mu\text{m}$	0.20 \pm 0.01
62.5/125	62.5 $\mu\text{m} \pm 2 \mu\text{m}$	0.27 \pm 0.01

Compare results for both fibers.

Exercise 1.12. Reflectometry

An OTDR for multimode fibers operates at 850 nm. The goal is to characterize links over 50/125 fiber to (OM1 ITU specifications) up to a length of 5 km, with a

resolution of distant defects of 50 cm and a signal-to-noise ratio higher than 10 dB. What must the pulse time and minimum unidirectional dynamics of the device be?

Exercise 1.13. *Design of a reflectometer*

The goal is to establish the specifications of a reflectometer for the characterization of links over graded index all silica optical fiber of 62.5/125 type, with a numerical aperture of 0.27. The core index equals 1.48.

The transmitter is a pulsed laser diode at 850 nm, delivering rectangular pulses of peak power equaling 5 W. Calculate pulse width $\delta\tau$ in order for the reflectometer resolution to be 1 m.

The receiver has a noise equivalent power of $5 \text{ pW}/\sqrt{\text{Hz}}$, and its bandwidth is set at $1/\delta\tau$. The constant bidirectional losses (coupler, connector) are 8 dB.

Calculate the dynamic of this reflectometer, defined at the point where the backscattered signal to receiver noise ratio is 1 (or 0 dB). Deduce its theoretical range knowing that optical fiber attenuation is 2.7 dB/km at the wavelength used.

At this point, the reflection peak would exceed the backscattered signal by how much?

What can be done to improve the signal-to-noise ratio by 10 dB?

Part 2: fiber-optic system components

Exercise 2.1. *Light coupling in a planar dielectric wave guide*

A single-mode planar guide is made up of a thin layer of index n_1 , deposited on a substrate of index n_2 (see Figure 4.7). It guides a mode of propagation constant β .

Demonstrate total coupling conditions of a plane wave with an incidence angle of θ_i , depending on if it is injected through:

- a prism of index n_p ;
- a diffraction grating with a step Λ .

Exercise 2.2. *Chromatic dispersion compensator*

The device in Figure 4.11 contains a circulator and a “chirped” Bragg grating photo-inscribed in a single-mode optical fiber, meaning that its step is not constant; it varies along the fiber according to a law:

$$\Lambda = \Lambda_0 - z.d\Lambda/dz$$

What is the effect of this device on an input light pulse? How can it serve to compensate chromatic dispersion at the end of a very long distance link? Determine the slope of this compensator (in ps/nm) to compensate the chromatic dispersion at the end of a 200 km fiber link at 3 ps/nm/km. In which wavelength range does it need to function if 4 wavelengths spaced from 100 GHz are multiplexed in the 3rd window? Deduce Bragg grating parameters by taking into account an average fiber index equal to 1.5.

Exercise 2.3. *Star coupler*

Calculate total insertion loss of an optical signal through a 7 branch star coupler with excess loss equal to 1 dB. Take into account a loss of 0.2 dB per connection.

Exercise 2.4. *Y coupler*

We buy a Y optical fiber non-symmetric coupler: power is distributed between both outputs in a $\frac{1}{4}$ (path 2) – $\frac{3}{4}$ (path 3) ratio with notations from Figure E.1. The provider also indicates an excess loss of 1 dB. Give transmission factors in dB:

- from 1 to 2 and from 2 to 1;
- from 1 to 3 and from 3 to 1.

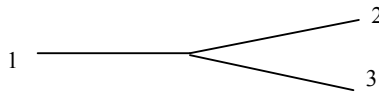


Figure E.1. *Asymmetric Y coupler*

Exercise 2.5. *Number of longitudinal modes of a laser diode*

A Fabry-Pérot cavity laser diode has the following characteristics:

- central wavelength: $\lambda = 1.3 \mu\text{m}$;

- material index: $n = 3.5$ (do $n = N$, group index);
- length $L = 0.5$ mm.

Transition energies are contained in a 10 meV range. Calculate the spacing between longitudinal modes as well as their total number.

Exercise 2.6. Calculation of a DFB laser diode

Calculate the diffraction grating step (used at first order) of a DFB laser diode transmitting at $\lambda = 1.55$ μm , the material index being 3.5.

When the current is modulated in the laser diode, an optical frequency modulation of 1 GHz/mA is observed. What will the laser spectrum widening be if the modulation amplitude is 10 mA? What would the pulse broadening be after 100 km of propagation in a single-mode fiber of chromatic dispersion coefficient: 15 ps/nm/km?

Exercise 2.7. Laser diode noise at emission

A laser diode is modulated sinusoidally by a sub-carrier, which is frequency modulated. We know:

- the average emitted optical power: 3 mW;
- the modulation index of the optical carrier: 80%;
- the central sub-carrier frequency: 50 MHz;
- the modulating signal bandwidth: 12 MHz;
- the relative intensity noise (RIN) of the laser: 10^{-14} Hz^{-1} .

Calculate the carrier-to-noise ratio at transmitter.

Exercise 2.8. Noise equivalent power of a receiver

Consider the optical receiver of Figure E.2.

The photodiode is a silicon PIN photodiode, with a responsivity of: $S = 0.5$ A/W, and a dark current of: $i_D = 0.5$ nA. The preamplifier (inverter) has very high gain and input impedance, and a rms input noise current (it is a white noise) of $2 \text{ pA}/\sqrt{\text{Hz}}$, in set-up conditions.

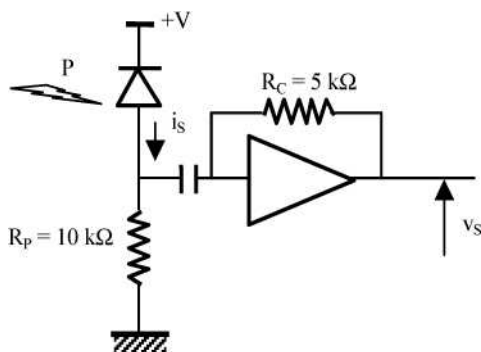


Figure E.2. Transimpedance receiver

- 1) Calculate the noise equivalent optical power of this set-up. Up to which value of optical power P will it be possible to neglect the shot noise?
- 2) Calculate v_s/P ratio.

Exercise 2.9. Optical preamplification

An NRZ 2.5 Gbit/s link at $1.54 \mu\text{m}$ uses a GaInAs photodiode receiver with a sensitivity of $S = 0.8 \text{ A/W}$. The average received signal power corresponding to a bit error probability of 10^{-11} is -26 dBm (without margin).

In order to lower this power, an optical amplifier pumped at 980 nm is placed just before the receiver, it has the following characteristics:

- maximum gain: 30 dB ;
- input and output losses: 0.5 dB each;
- almost total population inversion.

- 1) Calculate the noise current spectral density of the electronic amplifier, as well as the noise figure of the optical amplifier.
- 2) Assuming that an optical filter of 0.5 nm spectral width is used, calculate the values of the different noise sources according to optical amplifier gain. In what sense must it be changed in order to maximize carrier-to-noise ratio? What will the optimum gain be?

3) Determine the new average power value at the optical amplifier input. Deduce the link extension that it authorizes as the optical fiber has an attenuation of 0.2 dB/km.

Part 3: fiber-optic systems and networks

Exercise 3.1. *Link between micro-computers over plastic optical fibers*

A piece of equipment is connected to a computer by a serial connection over plastic fiber with a maximum bitrate of 2 Mbit/s.

The component characteristics are:

- transmitter: red LED ($\lambda = 670$ nm), coupled power in the fiber: $P_e = 150 \mu\text{W}$ for a 60 mA current;
- plastic optical fiber, 1mm diameter, attenuation = 200 dB/km;
- receiver: it is a logical receiver with a threshold of -39 dBm.

Interfaces (transmitter-receiver) are in fixed connectors, and there is no intermediate connection.

Write the loss budget taking into account a margin of 3 dB. Calculate transmission power that would enable a 100 m link, and deduce the corresponding current in the LED.

What is the advantage of this type of link?

Exercise 3.2. *Data link at 2 Mbit/s, differential Manchester coded*

Calculate the range of such a link if it uses:

- an LED transmitting at $0.85 \mu\text{m}$ with an average power of $50 \mu\text{W}$ in the optical fiber;
- an optical fiber with a lineic attenuation $\alpha = 2.5$ dB/km;
- a silicon photodiode receiver with a sensitivity of: $S = 0.5$ A/W, and a preamplifier with a spectral current density of background noise equaling $10^{-24} \text{ A}^2/\text{Hz}$;
- a connector of 0.5 dB maximum loss, at each extremity.

An error rate of 10^{-8} with a margin of 3 dB is required.

Which kilometer bandwidth will be necessary for correct link operation? Is it possible to obtain it easily with currently available optical fibers?

Exercise 3.3. Multimode fiber link

A digital signal at STM1 level of the synchronous hierarchy (155 Mbit/s), is transmitted over a 62.5/125 optical fiber with ITU specifications (OM2).

The wavelength is $1.3\ \mu\text{m}$ and we use:

- an LED coupling a peak power of $50\ \mu\text{W}$ in the optical fiber;
- connectors with each 0.5 dB loss;
- a receiver with noise equivalent power $3\ \text{pW}/\sqrt{\text{Hz}}$.

Establish loss budget and calculate the distance that it is possible to cover for an error probability of 10^{-9} with a margin of 3 dB. Specify if this distance is limited by attenuation or by dispersion.

Exercise 3.4. Single-mode fiber link at $1.3\ \mu\text{m}$

Which average optical power is needed to receive a 622 Mbit/s signal in NRZ code, with an error probability of 10^{-10} , and a receiver whose NEP is $5\ \text{pW}/\sqrt{\text{Hz}}$?

What distance can be reached in a standard single-mode fiber, at $1.3\ \mu\text{m}$, with a laser diode with peak power at 1 mW at the source, and a margin of 3 dB? Connectors of 0.2 dB attenuation are used. Can chromatic dispersion limit it?

Exercise 3.5. Baseband video transmission

A classical baseband analog video signal ($\Delta F = 6\ \text{MHz}$) is transmitted over an optical fiber at $0.85\ \mu\text{m}$. The modulation index is 90%.

The transmitter (light-emitting diode) couples an average power of -16 dBm in the optical fiber. The optical fiber is a graded index 62.5/125 fiber, whose attenuation is 2.6 dB/km. At each extremity, a connector of maximum 0.5 dB attenuation is used.

The receiver has a noise equivalent power of $1\ \text{pW}/\sqrt{\text{Hz}}$.

Calculate the maximum link length allowing in reception a video signal-to-noise ratio of at least 40 dB with a margin of 3 dB. Deduce the required kilometer bandwidth. Will the bandwidth from the fiber used be sufficient?

Exercise 3.6. *Wavelength division multiplexed link*

A transmission system uses wavelength division multiplexing of optical channels with frequencies separated by 100 GHz. The link uses optical amplifiers operating in band 1,535 to 1,565 nm with output saturation level at 23 dBm.

Calculate the number of channels and power of each channel as well as the global bitrate if each channel is modulated at 10 Gbit/s.

Exercise 3.7. *Amplified link*

A submarine cable uses a shifted dispersion single-mode fiber at 1.54 μm . Its attenuation equals 0.2 dB/km and its chromatic dispersion coefficient equals 2 ps/nm/km maximum. The source is a DFB laser diode with spectral width of 0.1 nm and 1 mW of peak power. It transmits a bitrate of 10 Gbit/s over a distance of 300 km. As specified by the receiver manufacturer, the average received power required is -29 dBm. According to the loss budget and with a margin of 3 dB, should optical amplifiers be used?

Optical amplifiers with the following characteristics are available:

- small signal gain = 40 dB;
- saturation power = 25 dBm.

Can the desired distance be attained with only one amplifier? Where should it be placed?

Exercise 3.8. *Fiber-optic data bus*

A passive star optical network uses:

- a 1.3 μm LED coupling peak power 50 μW in the optical fiber;
- a graded-index multimode optical fiber, with 0.9 dB/km attenuation, knowing that maximum distance between a station and the star is 1 km;
- a star coupler with an excess loss of 2 dB;
- connectors with 0.5 dB unit loss;

– a receiver with noise equivalent power $3 \text{ pW}/\sqrt{\text{Hz}}$.

Establish the loss budget and calculate the number of terminals that can be connected, for a bitrate of 100 Mbit/s in block code 4B5B, an error probability of 10^{-9} and a margin of 3 dB.

What will the minimum bandwidth of 1 km of optical fiber be in order for the link to work? Do you think it is possible to reach it with the components used?

Exercise 3.9. Ring network

Along a circular highway that is 30 km long, 10 base transceiver stations (BTS) of a mobile telephone network must be linked, where each one supports a bitrate of 155 Mbit/s in each direction. Each BTS must communicate with the base station controller (BSC) but the BTSs do not communicate with each other.

Indicate the most appropriate type of optical fiber and wavelength and propose a solution to link all stations in both directions with only one optical fiber, explaining the architecture and optical components to use.

Exercise 3.10. Access network

In a FTTH/PON type access network, 32 branch star couplers are used in order to reach the maximum number of receivers in a radius of 20 km with a single transmitter. These couplers have an excess loss of 3 dB, including connection losses.

A digital signal at 1 Gbit/s coded 8B9B is distributed at a wavelength of $1.54 \text{ }\mu\text{m}$. A single-mode optical fiber with the following characteristics is used:

- intrinsic attenuation = 0.2 dB/km ;
- unit length = 10 km ;
- loss by connector $< 0.3 \text{ dB}$;
- chromatic dispersion = 10 ps/nm/km .

The source is a DFB laser diode with peak power of 1 mW and spectral width of 0.1 nm. The receiver uses a GaInAs photodiode of responsivity 0.8 A/W and a preamplifier with noise current spectral density of $2 \cdot 10^{-23} \text{ A}^2/\text{Hz}$. Calculate the average received power for an error probability of 10^{-10} and a margin of 3 dB.

1) Calculate the maximum number of receivers which can be covered without optical amplification.

2) To increase this number, an optical amplifier is placed behind the sources with the following characteristics:

- small signal gain = 30 dB;
- noise figure = 3 dB;
- saturation power = 20 dBm.

Input and output losses are negligible.

Calculate the total noise at reception, if a 1 nm wide optical filter is placed, for the same power received as before. What should be concluded?

Redo the loss budget and calculate the new number of receivers.

Exercise 3.11. *Multimode fiber multiplexed link*

A digital signal at 50 Mbit/s (coded 4B5B) downlink and 10 Mbit/s (Manchester coded) uplink must be transmitted over 4 km between a terminal and the network. In order to do this, the following are used:

- 62.5/125 optical fibers;
- 1.3 μm LED coupling 50 μW peak power in the optical fiber;
- 0.85 μm LED coupling 40 μW peak power in the optical fiber;
- connectors with each 0.5 dB loss;
- Si photodiode receivers with noise equivalent power 4 $\text{pW}/\sqrt{\text{Hz}}$;
- GaInAs photodiode receivers with noise equivalent power 3 $\text{pW}/\sqrt{\text{Hz}}$;
- wavelength division multiplexers separating both windows, with a loss of 0.5 dB at transmitted wavelength.

With the help of loss budgets, compare the solution using a single fiber and the solution using one fiber per direction. In each case, specify the components used (and why). Verify that the link is not limited by dispersion (by explaining what is the dominating dispersion) knowing that LEDs have a spectral width of 50 nm and that the fiber chromatic dispersion is approximately 100 ps/km/nm at 0.85 μm .

Which solution seems the best at first glance? Why?

Exercise 3.12. *Very high bitrate single-mode fiber link*

A long distance link is established at 10 Gbit/s, in NRZ code, over a dispersion shifted optical fiber. At the source, a DFB laser diode with a peak power of 2 mW, and spectral width of 0.1 nm is used, followed by an electro-optic modulator attenuating by 1 dB at *on* and by 25 dB at *off*. The fiber chromatic dispersion coefficient is 3 ps/nm/km and it has a polarization mode dispersion of 0.5 ps/ $\sqrt{\text{km}}$. At the link end, a receiver with a NEP of 10 pW/ $\sqrt{\text{Hz}}$ is used.

1) Calculate possible maximum distance between transmitter and receiver without intermediate optical amplifiers. An error probability of 10^{-11} with a margin of 3 dB is required. Fiber attenuation is 0.2 dB/km and at every 20 km there is a 0.1 dB loss splice.

2) What distance can be reached with optical amplifiers? What will it be limited by? What global gain must these amplifiers have? If each amplifier has a maximum gain of 32 dB, what will the minimum number of amplifiers be? Will the actual number be higher than this theoretical minimum or not, and why?

3) Is it possible to eliminate the chromatic dispersion effect? With what device? Calculate the maximum possible distance after chromatic dispersion compensation, by supposing that widening caused by polarization mode dispersion must not exceed 20% of a bit time.

Exercise 3.13. *Time-division multiplexing sensor network*

We use optical fiber sensors operating in all or nothing reflection, with the help of a temporal multiplexing network (according to Figure 11.18).

Pulses transmitted have a power of 10 W and a 5 ns duration, and are repeated with a frequency of 10 kHz. We require the minimum L value, unit length of the line with optical delay.

Final problem: design of fiber-optic links

Objective

Technical solutions for the different fiber-optic link requirements listed below must be proposed. For each one of them, propose the choice of the most appropriate components in the tables and justify these choices; indicating, when appropriate, what other solutions could have been retained. Establish the loss budget

and verify that bandwidth is sufficient in each case (by specifying if dispersion compensation or equalization is necessary). Prices are given as examples to compare different possible solutions, they have no commercial value.

These links are:

- 1) a 100 Mbit/s (code 4B5B) Ethernet link over 100 m, inside a building (maximum 100 m), with a margin of 3 dB and error probability of 10^{-9} ;
- 2) a computer network made up of 1 Gbit/s (8B10B code) links, of 500 m maximum length, with a margin of 3 dB and error probability of 10^{-10} ;
- 3) an FTTH subscriber network at 100 Mbit/s (4B5B code) downlink (network → subscriber) and at 50 Mbit/s (4B5B code) uplink (subscriber → network), distances between 5 and 10 km according to subscriber locations, with a margin of 3 dB and error probability of 10^{-9} ;
- 4) a link at STM-16 SDH hierarchy level, over 20 km, with a margin of 3 dB and error probability of 10^{-11} , enabling evolution to STM-64 with very few modifications;
- 5) a long distance link over 800 km, for a global bitrate of 40 Gbit/s, with a margin of 3 dB and error probability of 10^{-11} ;
- 6) a broadcasting network of 100 digital video channels time-division multiplexed (1.5 Mbit/s per channel) to about a hundred receivers located less than 500 m with an error probability of 10^{-9} and a margin of 3 dB;
- 7) a ring network linking 10 access points with a bitrate of 622 Mbit/s each, a few km between them, using only one fiber per direction, with a margin of 3 dB and error probability of 10^{-9} .

Characteristics of components

Fiber optics

Type	Core-cladding diameter (μm)	Wavelength	Attenuation (dB/km)	Bandwidth (MHz.km)	Chromatic dispersion (ps/nm/km)	Price (€/m)
Plastic (multi. SI)	980/1,000	at 0.67 μm	150	50	negligible	0.10
Multimode GI	50/125	at 0.85 μm at 1.3 μm	3 0.7	500 500	100 negligible	0.10
Multimode GI	62.5/125	at 0.85 μm at 1.3 μm	2.6 0.7	200 300	100 negligible	0.10
Standard single-mode	9/125	at 1.3 μm at 1.55 μm	0.5 0.18		1 16	0.08
Dispersion -shifted single-mode	7/125	at 1.55 μm	0.2		3	0.10

Connections

Type	On fiber	Loss (dB)	Cost (€)
connector	Plastic	1	1
connector	50/125	1	10
connector	62.5/125	0.5	10
connector	9/125	0.5	40
connector	7/125	0.7	40
splice	multimode	0.1	1
splice	single-mode	0.1	2

External modulator

Type: Mach Zehnder; max speed: 10 Gbauds; price: 1,000 €.

Transmitters

Type	Wavelength (μm)	Spectral width (nm)	Average power (dBm)	Coupled in fiber	Max speed (Mbauds)	Price (€)
LED	0.67	50	-10	plastic	125	5
LED	0.85	50	-16 -13	50/125 62.5/125	50	10
LED	1.3	50	-15 -12	50/125 62.5/125	125	15
VCSEL laser diode	0.85	0.1	+2 0	50/125 9/125	1,500	40
FP laser diode	1.3	5	0	9/125	2,500	100
DFB laser diode	1.3	0.1	-1	9/125	2,500	300
DFB laser diode	1.55	0.1	-1 0	7/125 9/125	2,500	300

Receivers

Type	Photodiode	Bandwidth (MHz)	NEP (pW/√Hz)	Price (€)
High impedance	Si	6	2	10
High impedance	Si	20	3	20
High impedance	GaInAs	20	2	40
Trans-impedance	Si	100	5	30
Trans-impedance	GaInAs	100	4	60
Trans-impedance	Si	1,000	8	80
Trans-impedance	GaInAs	1,000	6	120
Photodiode + integrated preampl	GaInAs	2,500	8	200
Photodiode + integrated preampl	GaInAs	10,000	10	800

Wavelength division multiplexers

1) Type: two windows (0.85 and 1.3 μm). Loss at transmitted wavelength: 2 dB over 50/125 fiber and 1 dB over 62.5/125 fiber; price: 100 €.

2) Type: two windows (1.3 and 1.55 μm). Loss at transmitted wavelength: 2 dB over 7/125 fiber; 1 dB over 9/125 fiber; price: 250 €.

3) Type: 4 paths located in the 3rd window and spaced from 200 GHz; loss: 2 dB over single-mode fibers; price: 300 €.

4) Type: 16 paths located in the 3rd window and spaced from 100 GHz; loss: 3 dB over single-mode fibers; price: 500 €.

5) Type: add – drop (OADM) in the 3rd window, 10 channels; loss: 1 dB transmission at 2 dB access; price 400 €.

Star coupler

10 branches, excess loss: 3 dB over 50/125 fiber and 2 dB over 62.5/125 fiber; price: 150 €.

Optical amplifier

- Small signal gain: 30 dB.
- Saturation power: + 20 dBm.
- Noise figure: 3 dB.
- Amplified bandwidth: 30 nm (from 1,535 to 1,565 nm).
- Price: 2,000 €.

Chromatic dispersion compensator

- Dispersion which can be compensated: max 10 ns/nm.
- Compensation range: 20 nm (from 1,540 to 1,560 nm).
- Price: 1,500 €.

This page intentionally left blank

Exercise Answers

Part 1: fiber optics, propagation and technology

Exercise 1.1. *Propagation in a graded-index optical fiber*

Light ray path follows the $r(z)$ law, with:

$$n(r) \cdot \cos \theta = c^{te} = n_1 \cos \theta_a \text{ and } r(0) = 0 \text{ as initial condition}$$

By writing $\tan \theta_a = dr/dz$, and using $\cos^2 \theta = 1/(1+\tan^2 \theta)$ and $n(r)$ law, we obtain the differential equation:

$$\cos^2 \theta_a [1 + (dr/dz)^2] + 2 \Delta (r/a)^2 = 1$$

and its solution is written:

$$r(z) = \frac{a}{\sqrt{2\Delta}} \sin \theta_a \cdot \sin \left[\frac{\sqrt{2\Delta}}{a \cdot \cos \theta_a} \cdot z \right]$$

This ray remains guided in the core if:

$$\sin \theta_a < \sqrt{2\Delta}$$

or:

$$n_1 \sin \theta_a < \sqrt{n_1^2 - n_2^2}$$

corresponding to the numerical aperture of the graded index fiber for a center injected ray. The ray path is of the sine type with a spatial period of:

$$L = a.2\pi. \frac{\cos\theta_a}{\sqrt{2\Delta}}$$

which depends very little on θ_a , because $\cos \theta_a$ is still very close to 1.

Exercise 1.2. *Intermodal dispersion in a step-index fiber*

Propagation time, by unit of length, of the ray of angle θ_a equals:

$$\tau(\theta_a) = \frac{n_1}{c.\cos\theta_a}$$

hence the total pulse broadening by unit of length:

$$\Delta\tau_{im} = \tau(\theta_0) - \tau(0)$$

with:

$$\cos \theta_0 = n_2/n_1$$

where:

$$\Delta\tau_{im} = \frac{n_1}{c} [n_2/n_1 - 1] \approx \frac{n_1}{c} \Delta$$

Numerical values:

ON	Δ	θ_0	$\Delta\tau_{im}$ (ns/km)
0.2	0.9%	11.5°	45
0.4	3.6%	23.5°	181

Broadening at half-maximum is obviously lower than this value.

Exercise 1.3. *Graded-index multimode fiber bandwidth*

We are looking for a $BP = 600.L^{-\gamma}$ law; we calculate:

$$\gamma = \frac{\text{Ln} [600/BP(L)]}{\text{Ln } L}$$

converging toward $\gamma = 0.8$ for $L < 4$ km (equilibrium distance).

Exercise 1.4. Link bandwidth

Over 1 km, pulse broadening caused by intermodal dispersion equals:

$$\Delta\tau_{\text{im}} = 1.6 \text{ ns/km (deduced from the bandwidth of 300 MHz.km)}$$

and pulse broadening caused by chromatic dispersion equals:

$$\Delta\tau_c = 5 \text{ ns/km for 850 nm LED, thus globally } \Delta\tau = 5.25 \text{ ns/km}$$

Over 2 km, we then have 10.5 ns thus a bandwidth of slightly less than 50 MHz, limited by chromatic dispersion.

On the other hand, at 1,300 nm, the chromatic dispersion effect is negligible and the bandwidth is thus 150 MHz (approximate but not exact value, because of mode coupling).

Exercise 1.5. Injection of light in a single-mode fiber

Transformation of the Gaussian beam by the lens is represented below (Figure E.3).

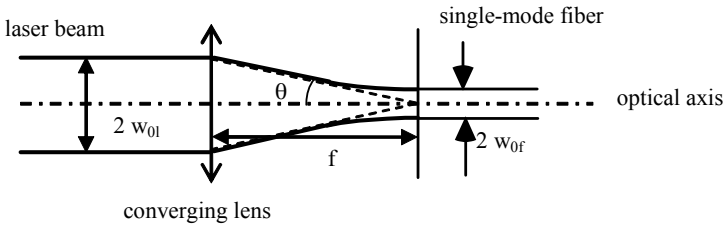


Figure E.3. Gaussian beam coupling

In order to perfectly couple this beam to a single-mode fiber, the angle of convergence must obey:

$$\theta = \lambda/\pi w_{0f} \text{ with } \text{tg } \theta = w_{0l}/f$$

f being the lens focal distance. θ is small therefore $\theta \approx \text{tg } \theta$.

We then obtain:

$$f = \pi w_{0f} w_{0l} / \lambda = 6 \text{ mm}$$

and, of course, the alignments must be perfect.

Exercise 1.6. *Single-mode fiber parameters*

The cut-off wavelength (formula in section 2.2.3) equals $1.27 \text{ } \mu\text{m}$. This fiber must then be used at a higher wavelength.

At $1.3 \text{ } \mu\text{m}$, we have:

$$V = 2.35 \text{ (deduced from } V/2.4 = \lambda_c/\lambda \text{)}$$

hence a guide dispersion equaling -3.6 ps/nm/km and total dispersion that is almost zero (material dispersion has approximately the same absolute value).

At $1.55 \text{ } \mu\text{m}$, we have:

$$V = 1.98$$

from which we deduce a guide dispersion of -4.3 ps/nm/km and a total dispersion of slightly less than 16 ps/nm/km (material dispersion approximately equals 20 ps/nm/km).

Exercise 1.7. *Single-mode fiber design*

1) Since the cut-off wavelength is $1.2 \text{ } \mu\text{m}$, the core fiber radius equals $4.2 \text{ } \mu\text{m}$.

2) At $1.55 \text{ } \mu\text{m}$, we have $V = 1.85$ (quickly deduced from $V/2.4 = \lambda_c/\lambda$) hence:

$$V \cdot \frac{d^2(VB)}{dV^2} = 0.57$$

from which a guide dispersion of 4.9 ps/nm/km and a total dispersion of 15.1 ps/nm/km are deduced. In order to avoid unit errors, in D_G expression, use: λ in nm and $c = 3 \cdot 10^7 \text{ km/ps}$.

3) Connection losses depend on w_0 which equals $1.26a = 5.7 \text{ } \mu\text{m}$.

We find:

- by off-centering: 0.13 dB;
- by misalignment: 0.01 dB;
- by tolerance over w_0 : 0.04 dB;

in total 0.18 dB at each splice, thus 0.009 dB/km (if the fiber is long) adding to:

- Rayleigh scattering = 0.176 dB/km;
- infrared absorption = 0.02 dB/km;
- micro-bending losses = 0.05 dB/km;

in total 0.255 dB/km.

4) To cancel chromatic dispersion, D_G would have to equal 20 ps/nm/km, thus:

$$V \cdot \frac{d^2(VB)}{dV^2} = 1.55$$

a value that this function never reaches. It is therefore not possible.

By settling for $D_G = 10$ ps/nm/km, V must be such that:

$$V \cdot \frac{d^2(VB)}{dV^2} = 0.77$$

or:

$$V = 1.72$$

We deduce that $a = 3.2 \mu\text{m}$ and $w_0 = 1.48 a = 4.7 \mu\text{m}$.

Splicing losses increase because w_0 decreases, and Rayleigh scattering increases because Δ increases. On the other hand, micro-bending losses decrease. Globally, this fiber has better performance than the previous one, but the depressed inner cladding fiber is the only one that is optimal.

Exercise 1.8. Depressed inner cladding single-mode fiber

1) The cut-off wavelength is calculated with Δn (absolute) = $6 \cdot 10^{-3}$, by using $n_1 = 1.47$ we find $1.2 \mu\text{m}$. It is therefore possible to use this fiber for both $\lambda_1 = 1.3 \mu\text{m}$ and $\lambda_2 = 1.54 \mu\text{m}$ wavelengths.

2) At these two wavelengths we calculate the normalized V frequency, the mode diameter from w_0/a , and Rayleigh scattering by:

$$\alpha_d = (0.75 + 66 \Delta n^+) \lambda^{-4} = 1.01 \lambda^{-4}$$

for guide dispersion we use Δn and not Δn^+ . Dispersions are in ps/nm/km.

$\lambda(\mu\text{m})$	V	$w_0(\mu\text{m})$	$\alpha_d(\text{dB/km})$	α total	D_G	D_M	D_c
1.3	2.2	8	0.36	0.39	-6.2	3	-3.2
1.54	1.87	10	0.18	0.20	-7.3	20	12.7

The zero chromatic dispersion wavelength is deduced (approximately) from linear interpolation between both wavelengths, resulting in $1.35 \mu\text{m}$.

Exercise 1.9. Single-mode fiber dispersion

Pulse broadening caused by chromatic dispersion equals 300 ps over 1,000 km. The one caused by polarization dispersion (in \sqrt{L}) equals 16 ps, insignificant compared to the other (because of the quadratic law). The global pulse broadening is of approximately 300 ps, and the bitrate will necessarily be lower than 3.3 Gbit/s (2.5 Gbit/s should work).

The compensator must have a slope equal to $D_C \cdot L$ thus 3,000 ps/nm (it is calculated to compensate for dispersion of 1,000 km of fiber regardless of the source width). If chromatic dispersion is compensated, polarization dispersion leaves a broadening of 16 ps and the bitrate will be slightly lower than 60 Gbit/s (10 Gbit/s but probably not 40 Gbit/s, because of its random character, a margin larger for polarization dispersion than for chromatic dispersion is needed).

Exercise 1.10. Graded-index plastic fibers

The available 30 dB attenuation corresponds to a maximum 200 m distance. Assuming that we need a 1 GHz bandwidth over this distance, 200 MHz.km will therefore be needed (which is beyond reach for step-index fibers). Chromatic

dispersion should not be a problem because laser diodes with very small spectral width must be used to achieve this throughput.

Exercise 1.11. *Connector for multimode fibers*

The different causes provide the following losses (in dB), calculated or indicated in the diagram (Figure 3.11).

Optical fiber	50/125	50/125	62.5/125	62.5/125
Index adaptation	with	without	with	without
Off-centering	0.20	0.20	0.15	0.15
Angular misalignment	0.15	0.10	0.12	0.07
Longitudinal spacing	0.20	0.30	0.20	0.30
Diameter tolerance	0.70	0.70	0.55	0.55
ON tolerance	0.87	0.87	0.64	0.64
Reflection	0	0.35	0	0.35
Maximum loss	2.12	2.52	1.66	2.06

These maximum losses correspond to worst cases, average loss is much lower. These results show the advantage of the 62.5/125 fiber from this point of view.

Exercise 1.12. *Reflectometry*

Reflectometer pulses width: $\delta\tau = 5$ ns for 50 cm resolution.

The dynamic will have to be higher than the attenuation of 5 km of 50/125 fiber, thus 5 dB at 1.3 μm (see Table 3.1), increased with the signal-to-noise ratio (10 dB in this case) at the farthest point of the fiber, thus a dynamic of at least 15 dB.

Exercise 1.13. *Design of a reflectometer*

Reflectometer pulses width: $\delta\tau = 10$ ns for 1 m resolution.

Receiver bandwidth then equals 100 MHz, hence:

$$P_{\text{rmin}} = 50 \text{ nW } (-43 \text{ dBm})$$

We set the signal-to-noise ratio = 1 at limit, so:

$$P_{\min} = P_r$$

The dynamic equals:

$$D = P_e - P_r - A + S$$

with:

$$P_e = +37 \text{ dBm}$$

$$A = 8 \text{ dB}$$

and:

$$S \text{ (dB)} = 10 \log (\alpha_D v_g / 2 \cdot \delta \tau \cdot \kappa)$$

calculated with:

$$v_g / 2 \cdot \delta \tau = 1 \text{ m}$$

$$\alpha_D = 2.2 \cdot 10^{-4} \cdot \lambda^{-4} \text{ m}^{-1} = 4.2 \cdot 10^{-4} \text{ m}^{-1}$$

$$\kappa = 1/4 (ON/n_1)^2 = 8.3 \cdot 10^{-3} \text{ (graded-index fiber)}$$

where:

$$S = -54.5 \text{ dB}$$

and:

$$D = 17.5 \text{ dB both ways}$$

dividing by 2α , we obtain range, equaling 3.24 km.

Reflection peak: $S = -14 \text{ dB}$, it then exceeds the backscattered signal by 40.5 dB.

To improve the signal-to-noise ratio (and therefore the dynamic) by 10 dB, 100 measures have to be averaged.

Part 2: fiber-optic system components

Exercise 2.1. *Light coupling in a planar dielectric wave guide*

The beam refracted (by the prism) or diffracted (by the grating) must be injected in the guide with an angle θ such that the propagation constant β is equal to:

$$k_0 n_1 \cos\theta \text{ (see Figure 4.7)}$$

Under this condition, there is total coupling.

In the case of the prism:

$$n_p \sin \theta_i = n_1 \cos\theta$$

then:

$$\beta = k_0 n_p \sin \theta_i$$

In the case of the diffraction grating: there must be a $2\pi m$ phase shift between waves diffracted by two close patterns.

For the path in the guide:

$$\Phi = \Lambda k_0 n_1 \cos\theta$$

for the path in the air (optically shorter):

$$\Phi = \Lambda k_0 \sin\theta_i$$

from which we deduce:

$$\beta = k_0 \sin \theta_i + m \frac{2\pi}{\Lambda}$$

Exercise 2.2. *Chromatic dispersion compensator*

A “chirped” Bragg grating will reflect a wavelength band and not a single wavelength. However, short wavelengths, reflected at the grating far end, will be more delayed than long wavelengths, reflected at the near end. However, in the case of positive chromatic dispersion in the fiber, long wavelengths arrived later. Therefore, there is a possibility of compensation. The device slope must be of

600 ps/nm (propagation time difference between two wavelengths spaced from 1 nm) to compensate total chromatic dispersion of the link (equal to $D_c L$).

Then $d\Lambda/dz = \Delta\Lambda/L$ (constant, as the law is linear) $= 1/(c \cdot D) = 5.5$ nm/m.

The gap $\Delta\lambda$ between two wavelengths is deduced from $\Delta\lambda/\lambda = \Delta v/v$ with $v = c/\lambda$: it equals 0.8 nm for $\lambda = 1.55$ μm and $\Delta v = 100$ GHz.

There will be 3 intervals, the compensator must therefore operate over a 2.4 nm range. By using:

$$\Delta\Lambda = \frac{\Delta\lambda}{2n_a} = 0.8 \text{ nm}$$

we deduce that the photo-inscribed zone must be 14.5 cm long (which shows that it is difficult to realize these devices for a large wavelength range).

Exercise 2.3. *Star coupler*

Adding the different loss causes:

- sharing between 7 branches: $10 \log 7 = 8.4$ dB;
- excess loss = 1 dB;
- 2 connection losses = 0.4 dB;

resulting in 9.8 dB of total loss.

Exercise 2.4. *Y coupler*

From 1 to 2 the transmission coefficient is 0.25 thus an insertion attenuation - $10\log(0.25) = 6$ dB, giving a total of 7 dB with excess loss. From 2 to 1, because of reciprocity; the attenuation is the same.

From 1 to 3 (and from 3 to 1) the insertion attenuation is of $-10\log(0.75) = 1.2$ dB giving a total of 2.2 dB with excess loss.

Exercise 2.5. Number of longitudinal modes of a laser diode

Spacing between longitudinal modes equals:

$$\delta\lambda = \lambda^2/2nL = 0.48 \text{ nm}$$

The spectral width is given by $\Delta\lambda/\lambda = \Delta E_g / E_g$ with $E_g = hc/\lambda$ where $\Delta\lambda = 13.6 \text{ nm}$ (using $hc = 1.24 \text{ eV}$) or approximately 30 modes in the spectrum.

Exercise 2.6. Calculation of a DFB laser diode

The diffraction grating step equals $\Lambda = \lambda/2n = 221 \text{ nm}$.

Laser line widening is deduced from $\Delta\lambda/\lambda = \Delta v/v$: it equals 0.08 nm (for $\Delta v = 10 \text{ GHz}$).

Pulse broadening equals $\Delta\lambda.D_c.L = 120 \text{ ps}$ over 100 km .

Exercise 2.7. Laser diode noise at emission

If we note as P_{em} the average emitted optical power, the optical signal is intensity modulated by a sub-carrier at 50 MHz with an amplitude equaling $m.P_{em}$ (m modulation index), therefore electric signal power after photodetection will be proportional to $(m.P_{em})^2/2$.

The average electric power of noise at receiver input is proportional to:

$$(1 + m^2/2) P_{em}^2 . RIN . \Delta F$$

with RIN = relative laser intensity noise and $\Delta F = 24 \text{ MHz}$ (twice the baseband). As proportionality factors are the same, we deduce carrier-to-noise ratio (identical at transmission and reception):

$$CNR = \frac{m^2}{m^2+2} \frac{1}{RIN . \Delta F} = 1.10^6 \text{ or } 60 \text{ dB}$$

Due to this value, source noise should be much lower than receiver noises.

Exercise 2.8. Noise equivalent power of a receiver

1) Since noise sources are white, we calculate spectral density of the receiver background noise:

$$\frac{d\langle i_F^2 \rangle}{df} = 4 kT \left[\frac{1}{R_p} + \frac{1}{R_c} \right] + \frac{d\langle i_A^2 \rangle}{df} = 9 \cdot 10^{-24} \text{ A}^2/\text{Hz}$$

with:

$$\frac{d\langle i_A^2 \rangle}{df} = 5 \cdot 10^{-24} \text{ A}^2/\text{Hz}$$

The noise equivalent optical power of this set-up is given by:

$$\text{NEP} = 1/S \cdot \sqrt{\frac{d\langle i_F^2 \rangle}{df}} = 6 \text{ pW}/\sqrt{\text{Hz}}$$

The shot noise has a spectral density of $2q \cdot \text{SP}$ which is equal to background noise for approximately $30 \text{ } \mu\text{W}$; for much lower received powers, we can then neglect this. The shot noise associated with the dark current is also negligible.

2) The v_S/P ratio equals $-R_c \cdot S$ or $-2.5 \text{ mV}/\mu\text{W}$ (inverting amplifier).

Exercise 2.9. Optical preamplification

1) The average signal power in reception enabling error probability of 10^{-11} ($Q = 6.7$) being of -26 dBm ($2.5 \text{ } \mu\text{W}$), we deduce the spectral density of background noise current:

$$\frac{d\langle i_F^2 \rangle}{df} = \left(\frac{S \cdot P_{mr}}{Q} \right)^2 / 0.7 \cdot F_r = 5,1 \cdot 10^{-23} \text{ A}^2/\text{Hz}$$

On the other hand, the optical amplifier noise figure practically equals:

$$F = \frac{2N_{sp}}{C_1} \text{ because } G \text{ is large}$$

with $C_1 = 0.9$ (0.5 dB) and $N_{sp} = 1$ (almost total population inversion when pumped at 980 nm) hence $F = 2.2$ (3.5 dB).

2) Consider spectral densities of the different noise sources at receiver input, for the same optical power as previously received:

– shot noise associated with the signal:

$$\frac{d\langle i_{q(s)}^2 \rangle}{df} = 2q.S.P_{S(r)} = 6,4.10^{-25} \text{ A}^2/\text{Hz}$$

which is independent from optical gain, and much lower than background noise;

– shot noise associated with spontaneous emission:

$$\frac{d\langle i_{q(ase)}^2 \rangle}{df} = 2q.S.N_{ase(r)}.\Delta\nu \text{ with } N_{ase(r)} = 2 N_{sp} (G-1)h\nu.C_2.A$$

$N_{sp} = 1$ and $A = 1$ if the optical amplifier is just before the detector (since the connection loss is counted in C_2). The optical filter has a width of 0.5 nm or 65 GHz at 1.54 μm , wavelength where $h\nu = 1,32.10^{-19}$ J. Supposing that G is large, this results in:

$$N_{ase(r)} = G.2,34.10^{-19} \text{ J hence } \frac{d\langle i_{q(ase)}^2 \rangle}{df} = G.3,9.10^{-27} \text{ A}^2/\text{Hz}$$

which, for $G = 1,000$ (30 dB), is higher than the previous noise, while remaining below the background noise;

– beat between signal and spontaneous emission:

$$\frac{d\langle i_{b(s/ase)}^2 \rangle}{df} = 2S^2.P_{S(r)} N_{ase(r)} = G.7,5.10^{-25} \text{ A}^2/\text{Hz}$$

which is not only much larger than the previous noises, but will become higher than the background noise for $G > 68$ (18 dB). In order to keep the same error probability, i.e. the carrier-to-noise ratio, power received $P_{S(r)}$ will have to be increased as G . In fact, the noise will then increase as G^2 , just like electric signal power which then is in $P_{S(r)}^2$. Increasing $P_{S(r)}$ as G means that power at optical amplifier input remains constant. Consequently, optical gain increase no longer allows us to lower the detection threshold;

– beat between the different components of spontaneous emission:

$$\frac{d\langle i_{b(ase/ase)}^2 \rangle}{df} = 2S^2 \cdot N_{ase(r)}^2 \Delta\nu = G^2 \cdot 4,5 \cdot 10^{-27} \text{ A}^2/\text{Hz}$$

which becomes higher than the previous noise for $G > 166$ (22 dB). At identical input power, this noise term is in G^2 , as electric signal power, and the conclusion is the same as for spontaneous emission/signal beat noise. Note that because of narrow optical filtering, the threshold for this last phenomenon is lower. This means that the filter was well chosen and that it is not necessary to make it narrower.

3) The previous study shows that in the best case, we win 18 dB, thus a power of -44 dBm at optical amplifier input. However, its gain must be at least 21dB, in order to compensate for noise at receiver caused by its own noise. The link extension that it authorizes is therefore 90 km.

Part 3: fiber-optic systems and networks

Exercise 3.1. *Link between micro-computers over plastic optical fibers*

Optical fiber attenuation is 20 dB over 100 m, adding a margin of 3 dB, transmission power must therefore be $-39 + 23 = -16$ dBm or 25 μ W.

Since it is proportional to the current, we deduce that a current of 10 mA in the LED allows this power. A twisted pair could be used for this distance, but the optical fiber brings insulation and electromagnetic immunity.

Exercise 3.2. *Data link at 2 Mbit/s, differential Manchester coded*

The noise equivalent power equals:

$$NEP = 1/S \cdot \sqrt{\frac{d\langle i_F^2 \rangle}{df}} = 2 \text{ pW}/\sqrt{\text{Hz}}$$

From which we deduce average received power with $Q = 5.6$ and $\Delta F = 0.7F_r = 2.8$ MHz: $P_{mr} = 17.8$ nW.

The loss budget is written as:

Average emitted power, coupled in the fiber ($10 \log P_{me}$)	- 13 dBm
- attenuation of connections	- 1 dB
- margin	- 3 dB
- average received power ($10 \log P_{mr}$)	- (-47.2 dBm)
= available attenuation	= 30.2 dB

hence a 12 km range considering the lineic attenuation of the optical fiber. A bandwidth equal to $F_r = 4$ MHz (because of Manchester code) over 12 km is sufficient therefore 48 MHz.km, widely available with commercial multimode fibers (typically 62.5/125 GI) even when taking into account chromatic dispersion (see the answer to exercise 1.4).

Exercise 3.3. Multimode fiber link

We can write the loss budget as:

Average emitted power, coupled in the fiber ($10 \log 25 \mu W$)	- 16 dBm
- attenuation of connections	- 1 dB
- margin	- 3 dB
- average received power ($10 \log P_{mr}$)	- (-37.3 dBm)
= available attenuation	= 17.3 dB

The average input power is calculated with $Q = 6$ and $\Delta F = 0.7 F_r = 108$ MHz: we find $P_{mr} = 187$ nW.

A distance of 19.2 km could be reach with a 0.9 dB/km fiber¹ but it will obviously be limited by intermodal dispersion, since the fiber is specified at 300 MHz.km, not much more than 15 MHz will be available at this distance!

With the criterion $BW \text{ (fiber)} > F_r$ or 155 MHz, approximately 2 km can be reached.

With the criterion $BW \text{ (fiber)} > 0.7 F_r$ or 108 MHz, close to 3 km can be reached, as long as a penalty is accepted, as at this distance we will obtain an additional

¹ In this exercise as with the following exercises, fiber characteristics are taken from Table 3.1.

14 dB in the loss budget (the attenuation for the 16 km that cannot be reached) there is therefore no problem.

Exercise 3.4. *Single-mode fiber link at 1.3 μm*

Average received power equals 0.67 μW , which is calculated with $Q = 6.4$ and $\Delta F = 0.7F_r = 435 \text{ MHz}$. The loss budget is written as:

Average emitted power, coupled in the fiber ($10 \log 0.5 \text{ mW}$)	- 3 dBm
- attenuation of connections (splices in this case)	- 0.4 dB
- margin	- 3 dB
- average received power ($10 \log P_{\text{mr}}$)	- (-31.8 dBm)
= available attenuation	= 25.4 dB

The range equals 59.8 km taking into account 0.5 dB/km optical fiber attenuation. The effect of chromatic dispersion is negligible at this wavelength.

Exercise 3.5. *Baseband video transmission*

For a baseband video signal, average received power must be at least:

$$P_{\text{mr}} = \frac{1}{2m} \sqrt{\text{SNR}_{\text{video}}} \cdot \text{NEP} \sqrt{\Delta F}$$

with $\text{SNR}_{\text{video}} = 10^4$ or -38.6 dBm in log.

With an average transmitted power of -16 dBm and two connectors with total attenuation of 1 dB, we find an available attenuation of 18.6 dB thus a maximum length of 7.15 km (with the margin).

A kilometer bandwidth of at least 43 MHz.km will be needed. The bandwidth of the fiber used is much larger even considering chromatic dispersion.

Exercise 3.6. Wavelength division multiplexed link

Around 1.55 μm , a frequency spacing of 100 GHz corresponds to a 0.8 nm wavelength spacing (using $\Delta v/v = \Delta\lambda/\lambda$). In the amplifier bandwidth of 30 nm, there is room for 38 channels.

The amplifier saturation power is 23 dBm thus 200 mW, therefore 5.2 mW per channel.

Exercise 3.7. Amplified link

The loss budget is written as:

Average emitted power, coupled in the fiber ($10 \log 0.5 \text{ mW}$)	- 3 dBm
- attenuation of connections (splices)	- 0.4 dB
- margin	- 3 dB
- average received power ($10 \log P_{\text{mr}}$)	- (-29 dBm)
= available attenuation	= 22.6 dB

which is not enough for the 300 km of fiber representing 60 dB.

For the missing 32.4 dB, one amplifier is sufficient but it must be placed in the middle of the link under the sea. Actually, if we place it behind the source, it will work at saturation power (+25 dBm peak thus +22 dBm average) and that will not be sufficient, an optical preamplifier in the receiver will also be required. However, this may be less expensive than a submarine repeater.

Exercise 3.8. Fiber-optic data bus

The loss budget is presented in the following form where the unknown is N, number of stations. Line symbol rate is 125 Mbauds from which we calculate an average received power of 168 nW (with $Q = 6$).

The number of connectors and the fiber length on a link between a transmitter and receiver must be taken into account.

Average emitted power ($10 \log 25 \mu\text{W}$)	- 16 dBm
- attenuation of connection (4 connectors in a link)	- 2 dB
- coupler attenuation	- $(10 \log N + 2)$ dB
- margin	- 3 dB
- fiber attenuation (2 km in a link)	- 1.8 dB
= average received power ($10 \log P_{mr}$)	= (- 37.7 dBm)

from which $10 \log N = 12.9$ thus $N = 19$ (rounded to lower integer).

Over 2 km, because of intermodal dispersion (dominating at this wavelength) the available bandwidth is approximately 150 MHz, which is sufficient.

Exercise 3.9. Ring network

The network topology (circular highway) and its operation (each BTS only communicates with the base station controller or BSC) allow us to use a single-fiber ring network with wavelength division multiplexing (Figure E.4). Each BTS has its own wavelength at which it receives (from the BSC) and retransmits (toward the BSC over the other arc), which corresponds perfectly to the operation of optical add-drop multiplexers (OADM, see section 5.2.5). At BSC level, all wavelengths are multiplexed and demultiplexed.

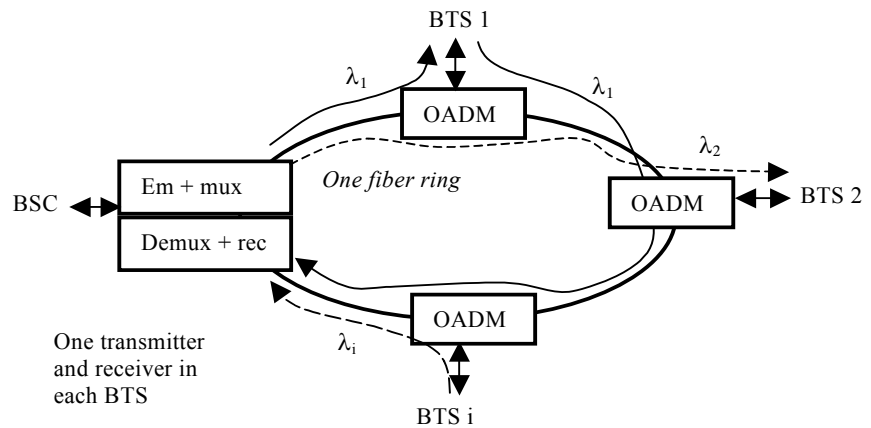


Figure E.4. Base station controller network (BSC)

The bitrate x distance product demands a single-mode fiber, but the standard single-mode fiber is sufficient. The 1.3 μm wavelength could be appropriate but the availability of multiplexers will probably involve the use of the 3rd window.

Exercise 3.10. Access network

1) The average received power equals 800 nW or -31dBm, with $Q = 6.4$.

The loss budget is written differently because we do not know the number of couplers. The available attenuation will be allocated to couplers and their splices.

Average emitted power ($10 \log 0.5 \text{ mW}$)	-3 dBm
- attenuation of connections (2 connectors at extremity)	-0.6 dB
- fiber attenuation (20 km all in one section)	-4 dB
- margin	-3 dB
- average received power ($10 \log P_{mr}$)	- (-31 dBm)
= available attenuation	20.4 dB

Attenuation of 32 branch star couplers is $10 \log(32) + \text{excess loss}$ therefore 18 dB: we can only use one with the available attenuation. The maximum number of receivers which can be covered without optical amplification is 32.

2) With an optical amplifier behind the source, it will operate at saturation power (+17 dBm in average power). With the same received power of -30 dBm, the attenuation between this amplifier and the receivers is 47 dB or $A = 2.10^{-5}$. In these conditions its noise at receiver is much lower than background noise: the total noise at receiver will not be increased by the presence of an optical amplifier at transmitter.

The average power at transmission has been increased by 20 dB without changing the rest of the loss budget; the available attenuation is now 40.4 dB enabling the serial placement of two couplers, then one 32 branch coupler in each of the first coupler's 32 branches, for a total of 1,024 receivers with a single amplified transmitter (and even 2,048 because it is possible use an additional Y coupler).

Exercise 3.11. Multimode fiber multiplexed link

First, take a single fiber. It will use 2 window wavelength division multiplexing, attributing $1.3\ \mu\text{m}$ to the direction with the highest throughput. We therefore have 2 loss budgets, where we must take into consideration 2 multiplexers.

Average received powers are calculated with $Q = 6$ for the different configurations. A Si photodiode must be used at $0.85\ \mu\text{m}$ and a GaInAs at $1.3\ \mu\text{m}$.

Direction	uplink	downlink
- wavelength	$0.85\ \mu\text{m}$	$1.3\ \mu\text{m}$
- average emitted power	-17 dBm	-16 dBm
- attenuation of connectors (6)	-3 dB	-3 dB
- multiplexers (2)	-1 dB	-1 dB
- margin:	-3 dB	-3 dB
- average received power ($10 \log P_{\text{mr}}$)	- (-40.4 dBm)	- (-39.2 dBm)
= available attenuation	= 16.4 dB	= 16.2 dB

Since attenuation of 4 km of fiber is 10.8 dB at $0.85\ \mu\text{m}$ and 3.6 dB at $1.3\ \mu\text{m}$, technically this choice is correct. Available bandwidths over 4 km (75 MHz at $1.3\ \mu\text{m}$ and close to 25 MHz at $0.85\ \mu\text{m}$ because of chromatic dispersion) are sufficient even if they do not offer much possibility of increasing throughput.

If we take a fiber in each direction: we must use the same wavelengths because at $0.85\ \mu\text{m}$ (which would be more economical) there is not enough bandwidth in downlink.

Loss budgets are naturally verified (we take out multiplexers and their connectors) but despite saving the cost of multiplexers, it is probable that over 4 km, the cost of the 2nd fiber and its installation will be higher (this would not be the case for short distance, in a company network for example).

The first solution is preferable.

Exercise 3.12. Very high bitrate single-mode fiber link

1) $P_{mr} = 5.6 \mu W$, thus -22.6 dBm (with $Q = 6.7$). The external modulator attenuates by 1 dB at on and totally cuts off at off (it lets 0.3% of the power leak through which is negligible) from which we find the following loss budget:

Average emitted power (10 log 1 mW)	0 dBm
- loss of modulator at on	-1 dB
- attenuation of connections (2 splices at extremities)	-0.2 dB
- margin	-3 dB
- average received power (10 log P_{mr})	- (-22.6 dBm)
= available attenuation	= 18.4 dB

allowing 90 km (lineic attenuation of 0.2 dB/km + 0.005 dB/km caused by splices).

2) With amplifiers, the chromatic dispersion will limit distance. In addition, very high bitrate modulation (this is an amplitude modulation at 10 Gbit/s) will widen the laser line by 20 GHz, or 0.16 nm. Supposing a quadratic combination with natural laser line width of 0.1 nm, we obtain $\Delta\lambda = 0.2$ nm hence $\Delta\lambda \cdot D_c = 0.6$ ps/km. In order for the pulse broadening to remain lower than 70 ps (limit with equalization and penalty) we cannot exceed 117 km. We only have an additional 27 km, or 5.5 dB for which a single amplifier is sufficient, even with penalty. It will either be placed at transmission or at reception according to practical and economic constraints.

3) It is possible to optically compensate for chromatic dispersion with the help of a fiber or a Bragg grating optical device (exercise 2.2) with opposite sign dispersion. It is then polarization mode dispersion (PMD) that will limit us: the 20 ps are reached at the end of 1,600 km. Optical compensation is much more difficult because of coupling between polarizations. For the additional 1,510 km or close to 310 dB, at least 10 amplifiers will be needed but their cumulative noise may not remain much lower than the NEP of the optoelectronic receiver. If not, it will be necessary to decrease their gain and increase their number.

Exercise 3.13. Time-division multiplexing sensor network

The reflectometer used has a pulse width of 5 ns and therefore a resolution of 50 cm. In order to correctly observe the responses from the consecutive sensors, the elementary length L will need to be slightly higher at this value. On the other hand

the repetition period is of 100 μs enabling the analysis of 10 km of fiber, much more than is needed for this application.

Engineering department: fiber-optic link design

Procedure to follow

For each application, select in the proper order:

- the type of fiber (plastic or silica, multimode or single-mode, etc.) according to bitrate and distance (Figure 9.8 can provide a starting guide);
- the wavelength (choices are few, but for certain fibers 2 wavelengths are possible);
- the transmitter (generally imposed by the fiber/wavelength pair, but at 1.3 μm in single-mode fiber we still have a choice);
- the photodiode: imposed by the wavelength (silicon below 1 μm , GaInAs over);
- the preamplifier: determined by the bitrate (its bandwidth must be at least $0.7 F_r$). If it is not directly given (in the case of an integrated receiver), the NEP is then deduced from the preamplifier noise current and photodiode sensitivity.

Do not forget the network architecture when it is not a simple point-to-point connection, but when couplers or multiplexers are used.

Subsequently, make a loss budget based on real component characteristics to verify if it is technically possible or not. Do not forget to calculate global dispersion which will need to remain lower than a half-bit time (after line coding) or $0.7 T$ (T is a bit time) only in the cases where a penalty is acceptable. If that is not possible, go to a combination with better performance.

Obviously the less expensive solution should be chosen, however you must also consider the network's future evolution, notably its throughput increase.

Typical solutions

1) Except when indicated otherwise (environment constraints), use a plastic fiber at 0.67 μm ; the choice of the rest follows. The available attenuation, taking the margin into account, is higher than actual fiber attenuation over 100 m.

2) A choice must be made between the multimode 50/125 fiber with a bandwidth that authorizes 1.25 Gbauds over 500 m (with a penalty that causes no problem, because VCSEL diodes have to be used to achieve the bitrate, and give a large power margin), and the standard single-mode fiber used at 1.3 μm with FP laser diodes. The first solution is less expensive but the second one is more evolutive (it will allow us to upgrade to 10 Gbit/s).

3) We have a choice between using 2 fibers and only one with wavelength division multiplexing. In both cases, because of the bitrate \times distance product (higher than in exercise 3.11) a single-mode fiber is needed; the standard fiber will be convenient.

- 1st choice (2 fibers): both directions are at 1.3 μm (attenuation remains low);
- 2nd choice (one fiber): one direction will be at 1.55 μm for multiplexing. Logically, it will be a downlink (the highest bitrate).

The cost will be the determining factor. Over 5 km, the additional cost of 2 multiplexers and components at 1.55 μm will not compensate for the economy made on the fiber, but it is the opposite over 10 km, and there are other arguments (cable size in a subscriber network, number of splices to make, etc.) in favor of the one fiber solution. Nevertheless, the cost of this solution encourages fiber sharing between several subscribers (this is the principle of PON/FTTH networks).

4) It is 2.5 Gbit/s. The standard single-mode fiber is suitable once more and can be used at 1.3 μm (10 dB of attenuation over 20 km will not be a problem). This choice will enable the increase of bitrate to 10 Gbit/s since a very large bandwidth is available, only transceivers modules will need to be modified.

5) The very high bitrate demands shifted dispersion single-mode fiber (except if a standard fiber is already installed, then it can be used again with a chromatic dispersion compensator). The distance demands the use of 1.55 μm (with DFB laser diode) and optical amplifiers. Total attenuation is 160 dB, and since available attenuation without amplifiers is approximately 25 dB, 135 dB remain to be compensated, requiring at least 5 amplifiers set at (approximately) 27 dB of gain. This presumes that their noise remains much lower than that of the receiver, which only a simulation software can verify (it is probable however).

On the other hand, currently, the bitrate can only be reached through wavelength division multiplexing. We have a choice between 4 \times 10 Gbit/s and 16 \times 2.5 Gbit/s. In the first case, there are not as many transmitters but globally they are more expensive (because they need an external modulator); in addition chromatic dispersion compensation (equaling 240 ps over 800 km) is necessary at 10 Gbit/s

and can be avoided at 2.5 Gbit/s. It is therefore possible that the 2nd solution is less expensive, which only a market survey will enable us to find out.

6) It is broadcasting network architecture, for 100 lines, 10 couplers of 10 branches each must be used with an 11th one for grouping them. Distance and bitrate (150 Mbit/s in total) allow the use of a GI fiber at 1.3 μm (preferably a 62.5/125 one for fewer losses) with an LED at the central station, and in each station a GaInAs photodiode trans-impedance 100 MHz receiver.

7) The most recommended architecture, as in exercise 3.9, is to use a single fiber ring (standard single-mode) and wavelength division multiplexing in the 3rd window with OADMs at each station and a multiplexer/demultiplexer at each extremity (only 10 out of the 16 lines will be used). Each station uses a wavelength and communicates with end stations (but not directly with the other stations). The return fiber is not necessary to the normal operation but brings added security.

Bibliography

Theoretical optics and fiber propagation

- [AGR 04] AGRAWAL G., *Lightwave Technology – Components and Devices*, Wiley, New York, 2004.
- [DEF 98] DE FORNEL F., *Les ondes évanescentes*, Eyrolles, Paris, 1998.
- [HUA 94] HUARD S., *Polarisation de la lumière*, Masson, Paris, 1994.
- [JEU 93] JEUNHOMME L., *Single Mode Fiber Optics*, Dekker, New York, 1993.
- [LOU 03] LOURTIOZ J.M., *Les cristaux photoniques ou la lumière en cage*, Hermes, Paris, 2003.
- [SAL 91] SALEH B., TEICH M.C., *Fundamentals of Photonics*, John Wiley & Sons, New York, 1991.
- [SAN 99] SANCHEZ F., *Optique non linéaire*, Ellipses, Paris, 1999.
- [SHA 05] SHARMA A., *Guided Waves Optics*, Anshan, 2005.
- [THO 85] THOMSON-CSF, *L'optique guidée monomode et ses applications*, Masson, Paris, 1985.

Fiber-optic technology

- [CLU 94] CLUB FIBRES OPTIQUES PLASTIQUES, *Les fibres optiques plastiques*, Masson, Paris, 1994.
- [DER 98] DERICKSON D., *Fiber Optic Test and Measurement*, Prentice Hall, Upper Saddle River, NJ, 1998.
- [KUZ 06] KUZIK M., *Polymer Fiber Optics*, Taylor & Francis Books, 2006.
- [MEN 07] MENDEZ A., MORSE T.F., *Specialty Optical Fibers Handbook*, Academic Press, New York, 2007.
- [MEU 03a] MEUNIER J.P., *Physique et technologie des fibres optiques*, Hermes, Paris, 2003.

Optic and optoelectronic components

- [AGR 06] AGRAWAL G., *Nonlinear Fiber Optics*, Academic Press, Fribourg, 2006.
- [BJA 93] BJARKLEV A., *Optical Fiber Amplifiers*, Artech, Boston, 1993.
- [BUU 05] BUUS J. *et al.*, *Tunable Laser Diodes and Related Optical Sources*, Wiley, New York, 2005.
- [CHA 92] CHAIMOVICS J.P., *Introduction à l'optoélectronique*, Dunod, Paris, 1992.
- [DES 94] DESURVIRE E., *Erbium Doped Fiber Amplifiers*, John Wiley & Sons, New York, 1994.
- [DUT 03] DUTTA A. *et al.*, *WDM Technologies – Passive Optical Components*, Academic Press, New York, 2003.
- [GRO 01] GROTE N., VENGHAUS H., *Fiber Optic Communications Devices*, Artech, Boston, 2001.
- [HUN 02] HUNSPERGER R., TAMIR T., *Integrated Optics*, Springer, Paris, 2002.
- [LAU 02] LAUDE J.P., *Dense Wavelength Division Multiplexing*, Artech, Boston, 2002.
- [PAL 05] PAL B., *Guided Wave Optical Components and Devices*, Academic Press, San Diego, 2005.
- [ROS 02] ROSENCHER E., VINTER B., *Optoélectronique*, Dunod, Paris, 2002.
- [TOF 01] TOFFANO Z., *Optoélectronique*, Ellipses, Paris, 2001.

Transmission systems and networks

- [BEN 01] BENNER A., *Fiber Channel for SANs*, McGraw-Hill, London, 2001.
- [BOR 98] BORELLA. A *et al.*, *Wavelength Division Multiple Access Networks*, Artech, Boston, 1998.
- [BOU 04] BOUCHET O. *et al.*, *Optique sans fil*, Hermes, Paris, 2004.
- [FRA 02] FRANCE TELECOM., Les communications optiques du futur, Technical note no. 19, 2002.
- [GOW 93] GOWAR J., *Optical Communication Systems*, Prentice Hall, Upper Saddle River, NJ, 1993.
- [ILY 03] ILYAS M., MOUFTAH H., *Optical Communication Networks*, CRC Press, 2003.
- [JOI 96] JOINDOT I. ET M., *Les télécommunications par fibres optiques*, Dunod, Paris, 1996.
- [KAZ 06] KAZI K., *Optical Network Standards*, Springer, Paris, 2006.
- [LIN 06] LIN C., *Broadband Optical Access Networks and Fiber-to-the-Home*, Wiley, New York, 2006.

- [LEC 05] LECOY P., *Principes et technologies des télécoms*, Hermes, Paris, 2005.
- [MEU 03b] MEUNIER J.P., *Télécoms optiques*, Hermes, Paris, 2003.
- [RAM 98] RAMSHWAMI R., SIVARAJAN K.N., *Optical Networks*, Morgan-Kaufmann, San Francisco, 1998.

Sensors and applications

- [DAK 97] DAKIN J., CULSHAW B., *Optical Fiber Sensors*, Artech, Boston, 1997.
- [FER 92] FERDINAND P., *Capteurs à fibres optiques*, Lavoisier, Paris, 1992.
- [LEF 93] LEFÈVRE H., *The Fiber-Optic Gyroscope*, Artech, Boston, 1993.
- [UDD 06] UDD E., *Fiber Optic Sensors*, Wiley, New York, 2006.
- [VAL 02] VALETTE S., *Applications de l'optoélectronique*, Hermes, Paris, 2002.

Conferences (generally annual)

ECOC, EFOC/LAN, Europnet, JNOG, MWP, OFC, OFS, OPTO, Photon, SPIE.

Journals

Applied Optics

Electronics letters

Electro-optics

Europhotonics

Fiber Systems

IEEE Journal on Lightwave Technology

IEEE Photonics Technology Letters

Journal of Optics

Lightwave

Microwave and Optical Technology Letters

Optical Networks magazine

Opto & Laser Europe

Photonics Spectra

Photoniques (revue de la SFO)

Proceedings of IEEE

Réseaux et Télécom

Some non-commercial websites

[ARCEP] <http://www.arcep.fr>

[CERCLE] <http://www.cercle-credo.com>

[FIBERS] <http://fibers.org>

[FRANCE] <http://www.france-optique.org>

[FTTH] <http://www.ftthcouncil.org>

[ITU] <http://www.itu.int>

[JOUR] <http://www.jouraldunet.com>

[OPTIC1] <http://optics.org>

[OPTIC2] <http://www.opticsvalley.org>

[OPTICA] <http://www.optical-networks.com>

[PHOTO] <http://www.photonics.com>

[RES 01] <http://01reseaux.com>

[SONET] <http://www.sonet.com>

[TELE] <http://www.telecom.gouv.fr>

Index

III-V semiconductors, 104, 143, 149, 171
1G network, 242

A

absorption, 71, 107, 145, 268
acousto-optic modulators, 116
active layer, 146
add-drop multiplexer, 251, 256
aerial cables, 83
amplification, 153
amplified spontaneous emission, 190
amplifier, 149
angled cleavage, 86
antenna transfers, 228
apodization, 119
apparent index, 116
architecture, 237, 241, 243, 245, 251
asymmetric guide, 13
ATM, 203, 246, 247, 250
attenuation, 30, 48, 53, 66, 69, 81, 95, 98, 186, 215
attenuators, 125
available attenuation, 214
avalanche photodiode, 169, 175, 181, 212
azimuthal order, 22, 34

B

background noise, 195, 212
backscattering, 71, 95, 269
balanced detection, 183
bandwidth, 28, 30, 99, 179, 194, 209, 215
baseband, 225, 229
beat, 182, 195

bending, 88, 107, 268
Bessel function, 35, 38
birefringence, 51, 54, 123, 276
bitrate, 49, 60, 72, 75, 101, 206, 210, 216, 217, 218, 223, 233, 236, 239, 241, 242, 245, 248, 254, 260
blind zone, 98
blue diodes, 144, 148
Boltzmann constant, 176
booster, 217
Bragg grating, 51, 116, 155, 158, 273
Bragg mirror, 62, 159
Brewster angle, 7
Brillouin scattering, 56
buried stripe, 106
bus, 234

C

cable, 215
caustic, 22
chemical sensors, 269, 270
chirp, 135, 156, 162
chirped gratings, 119
chromatic dispersion, 14, 26, 44, 51, 59, 66, 26, 75, 100, 154, 207, 216, 219
circulators, 125, 129
cladding, 15, 18, 78
coating, 16, 79
code conversion, 205
codes, 206
chromatic dispersion coefficient, 45, 46
coherent transmission, 57, 182, 207
collapsing, 77

dispersion compensation, 51, 119
 compression, 59
 confinement, 147
 connectors, 85, 98
 constraints, 52, 81, 97, 273
 control loop, 163
 convolution product, 99
 cooler, 164
 couplers, 234, 271
 coupling, 107, 114, 117, 160, 163
 cross-connects, 252, 258
 cross-phase modulation, 58
 cross-sections, 188
 cut-back, 95
 cut-off frequency, 12, 39, 105
 cut-off wavelength, 12, 42, 44, 71, 94

D

dark current, 168
 data transmission, 72
 DBR, 157
 depressed inner cladding, 48, 71, 77
 DFB, 155
 diffraction, 43, 94, 112, 163
 diffraction grating, 108, 112, 115, 128, 157
 digital transmissions, 203, 247
 diopter, 4
 direct semiconductors, 141
 dispersion, 215
 dispersion diagram, 40, 63
 dispersion-shifted fiber, 50, 220
 distributed reflection, 117, 155
 DPSK, 134, 208
 drawing, 77, 79
 duobinary, 133, 206, 221
 dynamics, 98

E

EDFA, 150
 effective index, 10, 65
 efficiency, 201
 electro-absorption, 134, 146
 electroluminescence, 141
 electro-optic effect, 129, 131, 158
 emission, 142, 186
 emission diagram, 151, 163
 endoscopy, 265
 equalization, 139, 194, 209

erbium, 149, 185
 error control, 248, 254
 error probability, 210
 Ethernet, 236, 245, 246
 evanescent field, 9, 10, 21, 48, 106, 269
 evanescent wave, 9
 excess loss, 121
 excess noise, 175, 180
 external modulator, 132, 133, 156, 162, 220

F

Fabry-Pérot, 154, 245, 273
 far field, 44, 114
 Faraday effect, 52, 124, 275
 FDDI, 87, 239
 Fiber Channel, 240
 fiber dispersion, 217, 220
 field bus, 233
 filters, 125, 126, 178, 192, 196, 209
 fluorescence, 186, 268
 fluoride fiber, 71, 73, 185, 194
 four wave mixing, 58
 frame, 249, 254
 frequency modulation, 227
 Fresnel reflection, 8, 66, 86, 89, 267
 FTTH, 243
 FTTx, 243
 fused splice, 85

G

gain, 153, 159, 187, 193
 gain band, 153, 199
 Gaussian beam, 43
 geometric optics, 1, 3, 10, 13, 15
 germanium, 48, 71, 118, 143, 170, 172
 Gigabit Ethernet, 18, 29, 73, 210, 236
 glued splice, 85
 GMPLS, 260
 Goos-Hanchen effect, 11, 117
 GPON, 75, 247
 graded-index, 73
 grid, 127, 218
 grooming, 255
 group delay, 14, 46, 100
 group index, 24, 45
 guide dispersion, 26, 46
 gyroscope, 274

H

heterodyne detection, 182, 207
heterojunction, 146, 150, 154, 171, 174
heterostructures, 144
hierachy, 247, 254, 260
high input impedance, 174, 178
hollow core, 66
holographic gratings, 112, 137
hybrid fiber-coax, 229, 244
hybrid mode, 37
hydrophone, 271

I, J, K

index gradient, 4, 17, 25
index profile, 17
instrumentation, 44, 71, 98, 157, 197, 264
integrated optics, 64, 104, 107, 123, 136, 147, 186, 264, 271
interferometry, 152, 270, 272
interleavers, 111, 127
intermodal dispersion, 14, 16, 23, 237
International Telecommunications Union, 49, 127
intrinsic spectral widening, 220
isolator, 53, 124, 164, 191
jitter, 61
justification, 251
Kerr effect, 58, 59, 60, 131

L

laser-Doppler velocimetry, 267
lasers, 66, 149, 185, 264
lateral guiding, 106, 156
lattice matching, 144
leaking, 21, 49
lifetime, 144, 187, 199
light-emitting diode, 26, 150
light ray, 1, 3
lighting, 72, 264
limit refraction, 8, 13, 38
linearity, 161, 225
liquid crystal, 137, 269
lithium niobate, 104, 130
local area network, 18, 74, 125, 204, 216, 233
long link, 75, 83, 198, 203, 217

loose tube, 82
loss budget, 214, 235
losses, 85, 88, 89, 107, 121, 150, 192, 199

M

Mach-Zehnder electro-optic interferometer, 208
Mach-Zehnder interferometer, 133, 270
margin, 214
matched guides, 110
material dispersion, 26, 46
matrices, 135, 137, 139
Maxwell equation, 33
measurements, 93, 227, 264
mechanical resistance, 73, 80, 84, 268
MEMS, 136, 138, 139, 159
meridional rays, 18, 20, 37
metropolitan area networks, 203, 217, 236, 258
Michelson interferometer, 271, 278
micro-bending, 88, 94, 268
micro-movement, 266
microwave optical fiber, 135, 184, 228
modal noise, 31, 272
mode coupling, 30, 107
mode diameter, 43, 44
mode equilibrium, 30
mode field diameter, 94
modulation, 161
modulation index, 225
MPLS, 259
multimode fiber, 15, 90, 93, 122, 216, 237, 272
multiplication, 170, 175

N

near field, 9, 44, 265
networks, 215, 224, 259
noise equivalent power, 180, 212
noise figure, 195
noise, 155, 174, 177, 190, 198, 199, 210
non-linear effects, 50, 54, 66, 193, 219
non-linear index, 57
normalized frequency, 11, 23, 38
number of modes, 22
numerical aperture, 16, 18, 72, 73, 89, 93
Nyquist criteria, 209

O

optical add-drop multiplexers (OADM),
129, 139, 259
optical amplification, 56, 61, 148, 185, 217,
219
optical cross-connects, 138
optical head, 163
optical interconnections, 160
optical layer, 252, 255, 259
optical power feeding, 73, 228
optical receiving interface, 174
optical regeneration, 61, 201
optical supervisory channel, 255
optical switches, 135
optical transmitter interface, 160
optical transport network, 253, 260
optoelectronic, 104, 141, 160, 165
oxidation, 77

P

passive optical networks, 234, 245
passive star, 234
penalty, 210, 211, 214
phasars, 128
phase delay, 14
phonon, 55, 141
photocurrent, 168, 170, 173, 226
photodetection, 142, 145, 146, 167, 182
photodiode, 167, 176
photo-elasticity, 52, 270
photo-inscription, 118
photon, 55, 141, 148, 153, 167, 175
photonic bandgap, 62
photonic crystals, 62, 104
phototransistor, 173
photovoltaic, 146, 169, 228
pigtail, 163
PIN diode, 167
Planck constant, 141
planar guide, 10, 64, 105
plane wave, 1, 51
plasma, 78
plastic fiber, 72, 74, 81, 216
Pockels effect, 130
point-to-point, 245
polarization, 7, 13, 35, 37, 38, 41, 51, 124,
150, 193, 199, 208
polarization dispersion, 53

polarization maintenance, 53, 66
polarization mode dispersion, 210, 220
population inversion, 149, 153, 190
power, 3, 54, 96, 151, 160, 188, 212
Poynting vector, 3
preamplifier, 174, 178, 197, 217
preform, 77, 79
propagation constant, 10, 19, 37
propagation equation, 2, 31
propagation mode, 11
protocol, 236, 259
pseudo-modes, 40
pulse broadening, 24, 27, 33, 34, 44, 53, 210
pump laser, 148, 191
pump wave, 55
pumping, 149, 186

Q

quadratic detection, 182, 195
quantum efficiency, 142, 145, 148, 160,
168, 193
quantum limit, 213
quantum noise, 175, 179, 196, 211
quantum well, 147, 159, 186

R

radiations, 49, 71, 73
Raman amplification, 201
Raman scattering, 55, 269
random access mode, 236
ray equation, 3, 18
Rayleigh scattering, 71, 96, 97
receiver, 176
reflection, 97, 122, 164, 246
reflection coefficient, 7, 109, 154
reflectometry, 95, 245, 268, 273, 276
refraction, 4, 13
refraction index, 2, 130, 147
regeneration, 205, 210
relative index difference, 17, 44
relative intensity noise (RIN), 162
remote monitoring, 205
remote power feeding, 204, 223
repeater, 192
repeater remote power feeding, 84
resolution, 96, 99, 114
response time, 151, 158, 162, 169
responsivity, 168

retroreflections, 85
 ribbon, 83
 RIN, 162, 179, 226, 228
 ring, 239, 241, 251, 258, 274
 routers, 257, 259
 routing, 129, 158, 256
 RZ format, 60, 206

S

satellites, 224
 saturation, 193, 197, 199, 217
 scrambling, 205, 250
 SDH, 203, 247, 253
 secondary parameters, 44, 94
 section overhead, 249
 security, 193, 216, 237, 239, 263
 self-focusing, 58
 self-phase modulation, 58
 semiconductor optical amplifier, 149, 199
 sensors, 31, 52, 53, 72, 88, 98, 118, 227, 263, 266
 SiGe, 172, 174
 signal-to-noise ratio, 180, 197, 211, 226
 signaling, 255, 260
 silica, 49, 57, 69, 74, 77
 silicon, 104, 136, 143, 171, 181
 single-mode fiber, 42, 44, 49, 91, 94, 127, 151, 217, 245
 Snell-Descartes law, 5, 16
 soliton, 58, 59, 133
 SONET, 248, 250
 spectral widening, 156, 218
 spectrum, 55, 142, 151, 154, 155, 188
 splitters, 117, 121, 122, 127, 245
 spontaneous emission, 142, 151
 standard fiber, 49
 star, 235, 237, 241, 242
 star coupler, 122, 234
 step-index, 15, 24, 65, 78
 stimulated emission, 148, 153
 Stokes wave, 55
 storage area networks, 241
 stretching, 273
 submarine cables, 84, 223
 submarine links, 61, 83, 93, 186, 191, 199, 223
 subscriber access, 75
 superluminescent diodes, 152
 surveillance, 249
 switching, 131, 132, 201

switching fabric, 241
 synchronous multiplexing, 248

T

temperature, 73, 80, 130, 146, 161, 164, 168, 176, 188, 194, 265, 268, 270
 temperature coefficient, 161
 temporal switching, 61
 threshold current, 148, 149, 155, 160, 163
 tight structures, 82
 time-division multiplexing, 132, 277
 time-domain response, 27, 28, 99
 token, 239
 total reflection, 8, 10, 11
 transimpedance, 174, 179
 transmission window, 74
 transmission, 225, 228
 transmitters, 152, 166, 225
 transverse mode, 37
 tube, 77
 tunable laser diodes, 257
 tunnel effect, 21

V

VCSEL, 74, 159, 216, 237
 vertical cavity, 159
 vibrations, 56, 266, 272
 video, 226
 video communications, 242
 virtual container, 250
 visible LEDs, 72

W

waveguide, 10
 wavelength, 1, 2, 144, 150, 186
 wavelength conversion, 200, 257
 wavelength division multiplexing, 42, 50, 74, 111, 114, 125, 139, 191, 193, 218, 247, 249, 278
 wavelength laser diodes, 100
 wavelength-tunable laser diodes, 157
 wavenumber, 2, 34, 63
 white LED, 144

Y, Z

Yablonivite, 62
 zero dispersion, 47, 66